FTD-HT-23-927-68

FOREIGN TECHNOLOGY DIVISION

COMBUSTION OF HEAVY LIQUID FUELS

by

L. V. Kulagin and S. S. Okhotnikov

FTD-HT-23-927-68

UNEDITED ROUGH DRAFT TRANSLATION

COMBUSTION OF HEAVY LIQUID FUELS

By: L. V. Kulagin and S. S. Okhotnikov

English Pages: 279

Source: Szhiganiye Tyazhelykh Zhidkikh Topliv, Izd-vo "Nedra," Moscow, pp. 1-280.

Translated under: Contract No. F33657-68-D-0865 P002

TABLE OF CONTENTS

Table of Contents (Continued)

UDC 662.75:621.182

NOTE

This book examines the basic relationships for the processes of liquid fuel atomization and combustion, on the basis of which analysis and selection of optimum combustion conditions are carried out.

Combustion characteristics of single drops as functions of external conditions and fuel properties are examined, as are the combustion processes of drops in a flame and the relation between flame length and atomization efficiency; requirements for atomization efficiency are formulated and the spary nozzle designs and arrangements analyzed on this basis. Methods of calculating centrifugal and pneumatic spray nozzles are presented and also methods of controlling the degree of atomization and combustion efficiency.

The book is intended for engineers engaged in organization of the processes of liquid fuel combustion and also for students of advanced courses in the corresponding special field.

INTRODUCTION

Improvement of old and introduction of new technological processes in petroleum refining have given rise to a large assortment of cheap residual fuels of the petroleum residue and cracking residue type, the use of which in furnaces requires the overcoming of various technical difficulties. This circumstance has given rise to a large number of arrangements and designs for various assemblies of combustion devices for the efficient combustion of fuel. Thus, for example, more than five thousand different atomizer designs have been proposed to date. An analogous pattern is observed with respect to furnace designs.

Scientific research work on the combustion of liquid fuels is mostly limited to the study of the laws of combustion of light liquids which evaporate completely. Under these conditions, the creation of new or the modernization of old combustion engineering installations are now beset with considerable difficulties. On the one hand, it is necessary to select from the great diversity of proposed and utilized schemes of organization of the combustion process precisely the one satisfying in the highest degree the requirements of each specific case. On the other hand, the theoretical solution of even individual partial problems of liquid-fuel flame combustion, on the basis of which this selection could be made, involves the laws of combustion of fuels with properties which differ considerably from the properties of industrial fuels.

All this compels us to include in the design of a combustion device such highly general concepts as the actually attained values for the specific thermal stress of the furnace space and the total excess of air. Based on these values, the generally accepted method of heat calculation for furnaces allows us to determine only the final composition of the products of combustion and their parameters, without indicating, however, how to achieve this. As G.F. Knorre remarked "...from the point of view of building up a rational technology and distribution of the limits of stable or economic furnace operating conditions, excessive use of these indices – averaged for the whole furnace – is futile at the least. Frequently, this only obscures the true pattern of the process and the degree of effectiveness of the factors which really determine the efficiency of the combustion center." The design of an efficient scheme for the combustion of any liquid fuel, including heavy fuel, is obviously possible only by ascertaining the basic physical laws of the combustion process, taking into account the physicochemical properties of the fuel used in any particular case. Only then is it possible to design a furnace which permits efficient combustion of all heavy liquid boiler or furnace fuels, including the high-sulfur petroleum

residues [mazuts].

In all cases the efficiency of the combustion process is defined by the combustion time for each fuel particle which must burn completely during its stay time in the furnace space. Accordingly, the practical measures of organizing the combustion process should be directed toward achieving optimum combustion conditions for each separate fuel particle. Consequently, it is essential above all to ascertain the features of the progress in the combustion of heavy fuels as an entire process and in its separate stages.

The fact that the combustion of a liquid fuel is the combustion of the vapors of this fuel permits us to visualize this process in the form of separate elementary stages successively changing from one to the other.

Since intense evaporation from the drop surface begins only at a certain minimum temperature which is typical for each grade of fuel (equilibrium evaporation temperature), each fuel particle should first be heated to this temperature. Obviously, the higher this temperature, the more time (all other conditions equal) required forthe preheating of the particle.

Ignition of the fuel drop takes place only when a combustible mixture of fuel vapor and air is formed on the surface and the parameters (concentration and temperature) correspond to the ignition conditions for any given fuel.

The nature of the development and the characteristics of the combustion process for the fuel drop depend greatly on external conditions (temperature and relative speed) and on the physicochemical properties of the fuel. High content of asphalt-tar substances and high distillation temperatures are responsible for the development of tar and asphaltene polymerization processes taking place simultaneously with the evaporation process within the drop, leading to the formation of a coke residue whose combustion takes place at a considerably slower rate than the combustion of the vapors.

Initial data and format used in the literature for the description of physical fuel combustion processes in GTU (ГТУ) [gas turbine installation] chambers are used in this book in several cases because in our opinion this makes it possible to ascertain more clearly the effect of the physicochemical fuel properties on the elementary process characteristics and those of the total combustion effect.

Chapters 1 and 2, Sections 14 and 16 of Chapter 4, Section 23 of Chapter 5 and Section 26 of Chapter 6 were written by S.S. Okhotnikov; Chapter 3, Section 15 of Chapter 4, Sections 17, 18, 19, 20, 21 and 22 of Chapter 5 and Sections 24 and 25 of Chapter 6 were written by L.V. Kulagin.

The authors deem it their duty to express their profound gratitude to the honored scientist and engineer Doctor of Technical Sciences, Professor N.I. Belokon', to Doctor of Technical Sciences, Professor S.N. Grigor'yev and also to the co-workers at Laboratory of Thermal Power Engineering of the TsNII MPS [Central Scientific

Research Institute of the Ministry of Railroads], of Candidate of Technical Sciences L.K. Kist'yants, Candidate of Technical Sciences Ye.M. Yudayeva, Senior Engineers B.M. Morosov, E.R. Tozha, N.D. Rybchenkov, A.P. Koroleva, Z.A. Pravdina and others for their great assistance in the preparation and writing of the book. The authors declare themselves indebted to Doctor of Technical Sciences Professor Z.I. Geller for various valuable comments which have improved the book.

The authors request that any comments and wishes concerning the contents of the book be directed to Moscow, K-12, Tret'yakovskiy Proyezd, 1/19.

Chapter 1

COMBUSTION OF SINGLE DROPS

1. PROCESS OF COMBUSTION FOR A SINGLE DROP

In discussing the basic laws of combustion for a single fuel drop we shall start with the fact that under real conditions this process is bounded by two extremes: the heating of a drop which is at rest relative to the ambient medium and the heating of a moving drop.

We assume that the immobile fuel drop has the form of a sphere and is homogeneous in composition. At the initial instant of time the entire drop mass has the same temperature t_0. The drop enters a medium with temperature t_{sr} and is subjected to surface heating. The temperature of the medium remains constant. Under these conditions, the temperature distribution in the sphere at any instant of time can be described by the differential equation for the non-steady thermal regime of a sphere [1, 2]

$$\frac{\partial \theta}{\partial \tau} = a\left(\frac{\partial^2 \theta}{\partial r^2} + \frac{2}{r}\frac{\partial \theta}{\partial r}\right), \tag{1.1}$$

where θ is the temperature difference between the medium and the subject point on the sphere; τ is time; r is the instantaneous drop radius; a is the thermal diffusivity of the drop substance.

The general solution of this equation for the sphere surface after determination of the constants of integration from the given temperature distribution at the initial instant of time is written in the form of the infinite series

$$\theta_{r,\tau} = \theta_0 \sum_{i=1}^{i=\infty} 2\,\frac{\sin n_i - n_i \cos n_i}{n_i - \sin n_i \cos n_i} \cdot \frac{\sin n_i}{n_i} \exp\left(-n_i^2 F_0\right), \tag{1.2}$$

where $\theta_{r,\tau}$ is the sought temperature difference at the instant of time τ at a point on the sphere a distance r from the center; θ_0 is the initial temperature difference between the medium and this point on the sphere; n_i is the ith root of the transcebdental equation

$$n \operatorname{ctg} n = 1 - \mathrm{Bi}, \tag{1.3}$$

where Bi is the Biot number,

$$\mathrm{Bi} = \frac{\alpha r_k}{\lambda_1}, \tag{1.4}$$

α is the coefficient of heat transfer from the medium to the drop surface; r_k is the external radius of the drop; λ_t is the thermal conductivity of the drop substance; and Fo in the Fourier criterion

$$Fo = \frac{a\tau}{R^2}, \tag{1.5}$$

where τ is the time on expiration of which temperature distribution is considered.

Expressing the quantities $\theta_{F,\tau}$ and θ_0 in terms of the medium temperature t_{sr} and the surface temperature t_p with the appropriate subscripts and carrying out the necessary transformations, we obtain an expression which enables us to determine the surface temperature of the drop at any instant of time:

$$t_{F,\tau} = t_{cp} - A\,(t_{cp} - t_{F,0}). \tag{1.6}$$

where

$$A = \sum_{i=1}^{i=\infty} 2\,\frac{\sin n_i - n_i \cos n_i}{n_i - \sin n_i \cos n_i} \cdot \frac{\sin n_i}{n_i} \exp\left(-n_i^2 Fo\right). \tag{1.7}$$

The magnitude of A is determined only from the Bi and Fo parameters which in turn depend on heat transfer conditions, time, dimensions and physical properties of the drop substance.

In the general case, this solution is valid only when heat transfer from the outer drop surface to the center takes place by heat conduction without participation of convection in the drop. The possibility of internal convection in fact is quite real. The possible influence of natural convection may be evaluated by comparing the imaginary and real thermal conductivity coefficients

$$\varepsilon = \frac{\lambda_\phi}{\lambda_T}. \tag{1.8}$$

This ratio should be determined [3] from the expression

$$\varepsilon = \frac{\lambda_\phi}{\lambda_T} = 0{,}18\delta \left[\frac{\beta g\,(t_n - t_n)\,Pr_T}{\nu^2 \delta}\right]^{0.25}. \tag{1.9}$$

where t_p and t_{ts}, respectively, are the drop surface temperature and the drop center temperature; β is the thermal expansion ratio of the drop substance; Pr is the Prandtl number for the drop substance; ν is the liquid viscosity; δ is the thickness of the layer across which we have the temperature drop $t_p - t_{ts}$.

As calculations according to Eq. (1.9) show, convective mixing must be allowed for in kerosene when the drop diameter is equal to or greater than 2000 μm. For drops with a diameter close to or less than 200 μm at a temperature difference of 50°C across a layer 50 μm thick, natural convection does not occur [3]. In heavy fuels for which Pr and ν are known to be larger than for kerosene, natural

convection will take place in any case under analogous conditions. If one takes into account, however, that the viscosity of the heavy fuels is considerably greater than that of kerosene and its effect on the magnitude of ε is much greater, for example, than on the Pr parameter, it can be stated that for a fuel drop not exceeding 1000 μm, the effect of natural convection can be neglected.

For heating of a sphere stationary relative to the medium, the heat transfer coefficient α in Expression (1.4) can be determined from the limit value of the Nusselt number Nu, equal to ~2.

$$Nu = \frac{\alpha d_к}{\lambda_т} \approx 2 \qquad (1.10)$$

Hence,

$$\alpha = \frac{2\lambda_т}{d_к}, \qquad (1.10a)$$

where λ_t is the thermal conductivity of the medium surrounding the drop.

Substituting the value of α into the expression for Bi (1.4), we obtain

$$Bi = \frac{\lambda_т}{\lambda_т}. \qquad (1.11)$$

Thus, the Bi number is one of the parameters which determine the temperature of a drop heated under conditions of natural convection, and can be expressed as the thermal conductivity ratio of the medium and the drop substance.

Using data on thermal conductivities for various liquid fuels [4] and also the numerical values of λ_g, the value of the Bi number can be determined for each specific case of drop heating (Table 1).

As follows from the data of Table 1, light fuels of the kerosene type exhibit the greatest variation in Bi ($0.35 < Bi < 1.00$); this range narrows considerably as the density of the fuel increses, and for cracking residues it falls within limits of 0.30 and 0.70.

Under the actual conditions of heating an immobile drop, a certain fraction of the heat can be acquired by the drop through radiation from heated surfaces and the flame. The effect of tne radiative component in the heat transfer between the drop and the medium can be evaluated approximately in the following way.

As is well known [4], the total heat transfer coefficient in complex heat transfer can be represented the form of the sum

$$\alpha = \alpha_к + \alpha_л \qquad (1.12)$$

where α_K is the coefficient of heat conduction; α_l is the coefficient of radiative heat transfer.

TABLE 1

Values of the Bi Number as a Function of Fuel Grade, Fuel Temperature and Ambient Temperature

1 Топливо	2 Температура среды, °С							
	300	400	500	600	800	1000	1200	1400
	3 Теплопроводность среды, ккал/м·ч·°С							
	0,369	0,417	0,456	0,500	0,575	0,655	0,737	0,810
4 Керосин $t = 100°C$	0,465	0,521	0,580	0,628	0,720	0,819	0,910	1,00
5 Мазуты М40, М60								
$t = 20°C$	0,315	0,357	0,397	0,428	0,491	0,560	0,621	0,685
$t = 100°C$	0,336	0,379	0,421	0,455	0,523	0,595	0,661	0,728
6 Крекинг-остаток								
$t = 20°C$	0,264	0,298	0,331	0,358	0,410	0,465	0,520	0,573
$t = 100°C$	0,307	0,348	0,386	0,417	0,480	0,545	0,606	0,668

1) Fuel; 2) temperature of medium, °C; 3) thermal conductivity of the medium, kcal/m·h °C; 4) kerosene; 5) petroleum residues [mazuts]; 6) cracking residue.

The quantity α_1 in turn is defined as

$$\alpha_1 = \varepsilon_f \varphi_k T_{sr}^3 \sigma \vartheta, \qquad (1.13)$$

where $\vartheta = 10^{-8} \frac{T_{sr}^4 - T_k^4}{T_{sr} - T_k}$; ε_f is the emissivity of the radiating body; ε_k is the us the emissivity of the drop surface; φ_k is the emittance to the drop from the radiating medium; $\sigma = 4.92$ kcal/m^2·h·deg is the universal constant for black-body radiation; T_{sr} is the temperature of the emitting medium in °K; T_k is the surface temperature of the drop in °K.

Under flame conditions in boilers in which the drop is irradiated mainly by the burning flame, the average emissivities of the emitting body can be assumed to be $\varepsilon_f \approx 0.4$.

The drop surface emissivity is still very uncertain. Thus in Reference [5] it is estimated as $\varepsilon_k \approx 0.05$. However, taking into account the specific properties of heavy fuels, we estimate this value as $\varepsilon_k \approx 0.3$. The value of φ_k we assume equal to unity.

In this case the expression for α_1 assumes the form

$$\alpha_1 = 0{,}59\vartheta. \qquad (1.14)$$

With Eqs. (1.10a) and (1.14), the ratio of α_1 and α_k can be written in the form

$$\frac{\alpha_1}{\alpha_k} = \frac{0{,}59\vartheta_1}{2\lambda_1}. \qquad (1.15)$$

It follows from Eq. (1.15) that the role of radiative heat ex-

change increases as the parameter θ and the drop size increase. The numerical values of the fraction of the heat transfer coefficient at different ambient temperatures, of the drop radii and of the drop surface temperature, calculated with Eq. (1.15), are given in Table 2.

TABLE 2

Radiation and Conduction Heat Transfer Coefficient Ratio α_l/α_k (in %) for Drop Surface Temperatures of t_k = 100°C and t_k = 300°C

r_k, μm	Температура среды, °C											
	600		800		1000		1200		1400		1600	
	t_k=100	300	100	300	100	300	100	300	100	300	100	t_k=300
50	0,115	0,189	0,172	0,259	0,240	0,334	0,323	0,423	0,42	0,521	0,53	0,645
100	0,230	0,378	0,344	0,519	0,480	0,650	0,647	0,845	0,84	1,040	1,06	1,290
200	0,460	0,756	0,690	1,030	0,960	1,330	1,290	1,690	1,68	2,080	2,12	2,580
300	0,690	1,130	1,030	1,550	1,440	2,000	1,940	2,540	2,52	3,030	3,18	3,870
500	1,150	1,890	1,720	2,600	2,400	3,340	3,230	4,230	4,20	5,210	5,30	6,450
1000	2,30	3,780	3,440	5,190	4,860	6,590	6,470	8,450	8,40	10,400	10,50	12,900

1) Temperature of the medium, °C; 2) micrometers [microns].

It follows directly from the data of Table 2 that the fraction of radiative heat exchange in the total process of heating a stationary drop is generally negligibly small. Only for very large drops ($d_k \geq 1000$ μm) can a marked increase in the fraction of radiation be observed at temperatures above 1000°C (~5% and over).

The range of variation for the Fo criterion, which also deliver the drop surface temperature, is bounded on the one hand at Fo = 0, since at the initial instant of time (τ = 0) the drop surface temperature is equal to the initial temperature of the fuel ($t_{F,\ \tau} = t_{F,\ 0}$), and on the other hand, Fo exhibits a limit at the value at which the drop surface temperature, as a result of heating, attains values to form a sufficient quantity of vapor for the development of a flammable fuel-air mixture around the drop.

This temperature is generally the equilibrium evaporation temperature, since during drop heating an instant inevitably arrives when the rate of heat supply to the drop is equal to the rate of heat removed with the evaporating fuel, when thermal equilibrium of the drop ensues (although only temporarily) and its temperature remains constant for some time. This temperature is conventionally known as the equilibrium evaporation temperature. Special investigations have shown that this temperature is not a uniquely defined characteristic of the fuel but depends in turn on the fuel properties and the pressure and temperature of the ambient medium. Thus, for example, at t_{sr} = 100°C and a pressure of 1 kg/cm², the equilibrium evaporation temperature of gasoline is ≈40°C, but at 400°C it increases to ≈70°C, coming close to the gasoline boiling point of ~75-80°C. With heavier fuels and higher ambient temperatures,

the equilibrium evaporation temperature increases more rapidly, also tending toward its maximum -- the temperature of onset of boiling. Thus, for kerosene at a 500°C temperature for the medium, the equilibrium evaporation temperature is approximately 140°C [3], whereas the temperature of onset of boiling (distillation), according to GOST 10227-62, does not exceed 150°C. An analogous pattern is observed with diesel fuel. If one takes these data into account and also the almost complete lack of information on the equilibrium evaporation temperature for heavy liquid fuels of the petroleum residue and cracking residue type, it seems reasonable to take the temperature of onset of boiling as the maximum equilibrium evaporation temperature. This assumption is justified also by the fact that the process of drop heating under the conditions of various types of furnaces takes place in a medium with fairly high temperature (~600-1000°C).

Another quantity which defines the limits of variation for the Fo criterion andwhich depends only on the physical properties of the fuel is the thermal diffusivity a.

A third quantity which defines the value of the Fo criterion and, consequently, the time required to heat the drop surface to the required temperature is the drop diameter. Evaluation of the real drop size formed in atomization of a fuel by various types of spray nozzles shows that the range of drop size variation falls within limits of ~10-500 μm.

The use of all these extreme values and also consideration of the actual drop heating conditions make possible the conclusion that the limit value for the Fo criterion is Fo = 1.0.

Thus, having the boundary values of both criteria, we can estimate the range of variation in A for different values of the Bi and Fo criteria (Fig. 1) obtained as a result of solving Eq. (1.7).

Of greatest significance for practical purposes is the problem of determining the time required to heat the drop surface to a given temperature under specific conditions. The problem is reduced here to determination of the Fo criterion on the basis of given values of A and Bi, after which the required time is determined by means of Eq. (1.6).

As an example, let us consider the problem of heating drops of various fuels -- with equal diameters under the same conditions -- to the temperature of onset of boiling (Table 3).

The data of Table 3 show that increasing density of fuel under otherwise equal conditions leads to marked increase in the heating in comparison to a light-fuel drop of equal size. From the data of Table 3 also follows directly that a combination of preheating the fuel and a considerable increase in the temperature of the medium is a very effective method of shortening the heating time and increasing the time of complete combustion of the drop.

As pointed out above, the heating of a drop which is stationary relative to the medium is an extreme case of the heating of a fuel

drop which is emitted from the spray nozzle. In reality, the fuel drops which issue from the spray nozzle retain their velocity relative to the medium for some time. During this period, or most of it, the drops successively pass through regions with various temperatures and densities. All this determines the continuous variation of the conditions of heat transfer from the medium to the drop.

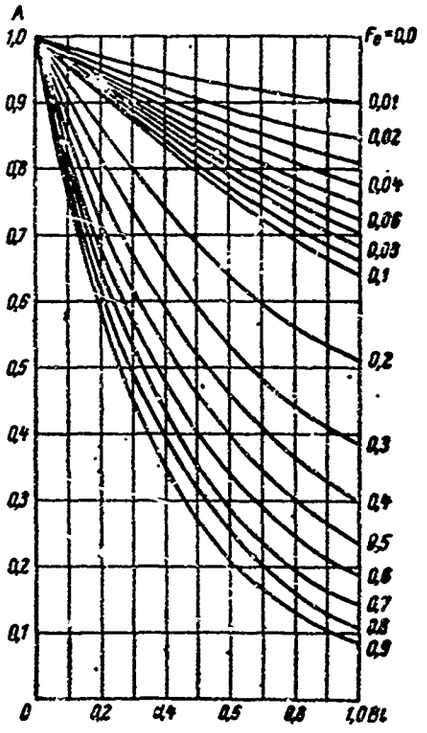

Fig. 1. Coefficient A in Eq. (1.6) as a function of the parameters Bi and Fo.

Nonetheless, these features permit the assumption that the nature of the temperature distribution within the drop itself corresponds as before to the conditions of nonsteady heat transfer. Since the above-indicated differences mainly concern the conditions of heat transfer from the medium to the drop and are characterized by the Bi parameter, let us examine the variation of this parameter as a function of the external conditions of heat transfer.

For the Re range of variations, between Re = 20 and Re = 150,000, the following relationship is most widely used [1]

$$Nu = 0{,}37Re^{0.6}Pr^{0.33}. \qquad (1.16)$$

TABLE 3

Heating Time for Stationary Drops d_k = 200 μm of Various Grades of Fuel

1 Показатели	2 Керосин		3 Мазуты				4 Крекинг-остаток			
			М40		М60					
5 Начальная температура капли, °С	20		20		100		20		100	
6 Коэффициент температуропроводности вещества капли, м²/ч 10^3	0,22		0,22		0,22		0,25			
7 Температура среды, °С	600	1000	600	1000	600	1000	600	1000	600	1000
8 Конечная температура поверхности капли, °С	120	120	180	180	180	180	250	250	250	250
9 Безразмерная разность температур	0,828	0,899	0,725	0,837	0,840	0,911	0,604	0,765	0,700	0,834
10 Критерий Bi	0,500	0,655	0,428	0,560	0,460	0,600	0,358	0,468	0,417	0,560
11 Критерий Fo	0,070	0,015	0,200	0,000	0,080	0,015	0,450	0,150	0,250	0,060
12 Время, необходимое для прогрева поверхности капли до $t_{F,\tau}$, мсек	13,5	3,0	32,8	9,85	13,2	2,5	55,0	21,5	39,6	8,6

1) Indices; 2) kerosene; 3) petroleum residues; 4) cracking residue; 5) initial drop temperature, °C; 6) coefficient of thermal diffusivity of the drop substance, m^2/h 10^3; 7) temperature of medium, °C; 8) final temperature of the drop surface, °C; 9) dimensionless temperature difference; 10) Bi number; 11) Fo criterion; 12) time required for the heating of the drop surface to $t_{F,\tau}$, ms.

For normal combustion conditions where atmospheric air is used as the oxidizer, the Pr number is fairly stable and within the temperature range of 50-1200°C it can be assumed to be equal to 0.723. In this case Eq. (1.16) can be transformed to

$$Nu = 0{,}33Re^{0.6}. \tag{1.17}$$

Substituting Expression (1.17) into Eq. (1.10), the coefficient of heat transfer from the medium to the drop can be defined as

$$\alpha = \frac{0{,}33}{d_k}\lambda_r Re^{0.6}. \tag{1.18}$$

The equation shows that the numerical value of the heat transfer coefficient α can be determined at any given instant of time if the conditions of drop motion are known. Correspondingly, the Bi* criterion can also be determined at any given instant of time if Expression (1.18) is substituted into (1.4), the original equation for Bi. Thus the characteristic of the external heat transfer in the presence of a realtive drop velocity can be written in the form

$$Bi^* = \frac{\alpha d_k}{2\lambda_r} = \frac{0{,}33\lambda_r Re^{0.6}}{2\lambda_r} = 0{,}165\,Bi\,Re^{0.6}, \tag{1.19}$$

where $Bi = \lambda_g/\lambda_t$ is the Biot parameter for the heating condition of a stationary drop in a medium with the same parameters.

The value of the Bi* parameter differs from that for the stationary drop by a coefficient which is numerically equal to half the Nu parameter. The extreme value of this coefficient, equal to unity, corresponds to the limit value Re = 20. An estimate of the real drop sizes formed by atomization, of the conditions of their motion and of the parameters of the medium in which drop heating takes place shows that the other extreme of the Re parameter which limits the range of its variation is Re $\simeq$ 1000.

Accordingly Fig. 2 shows the nature of the variation in the numerical values of Bi in Eq. (1.19) as a function of the instantaneous value of the parameter Re. A marked effect of the relative velocity begins to show up at Re $\simeq$ 40 when the heat transfer from the medium to the drop increases 1.5 times.

In connection with the fact that the motion of the fuel drop relative to the medium is characterized by a continuous velocity decrease owing to the force of aerodynamic drag the problem of the variation of the parameter Re with time is of interest.

The parameter Re is defined by the following expression:

$$Re = \frac{w_k d_k}{\nu}, \tag{1.20}$$

where w_k is the relative velocity of the drop; ν is the kinematic viscosity of the medium.

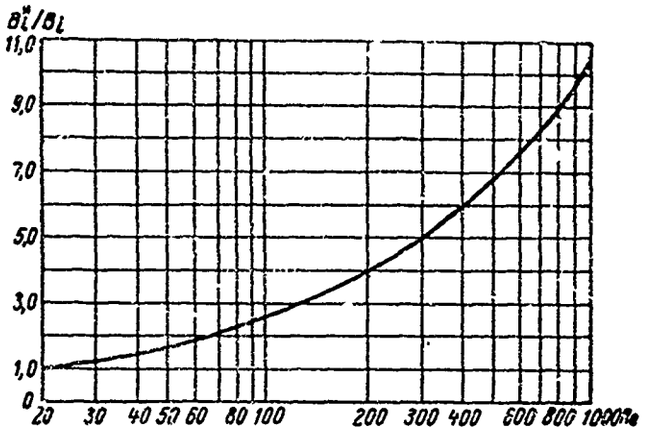

Fig. 2. Ratio Bi*/Bi as a function of the parameter Re.

In Expression (1.20), the drop velocity is the determining quantity because the drop diameter d_k can be regarded as constant and the viscosity characteristics of the medium vary only slightly. The relative velocity at any given instant of time is determined from the condition of equilibrium for the forces acting on the moving drop. In this case

$$m\frac{dw}{d\tau} = -R, \tag{1.21}$$

where m is the mass of the drop; w the instantaneous value of the relative drop velocity; τ is time; and R is the resistance.

The expression for resistance to the motion of the drop, in analogy with a moving sphere, can be written in the form

$$R = \Phi\frac{w^2}{2g}\gamma_в F_к, \tag{1.22}$$

where Φ is the aerodynamic resistance of the drop; g is the acceleration of gravity; γ_v is the specific weight of the medium; F_k is the cross sectional area of the drop.

Considering that

$$m = \frac{\pi d^3}{6g}\gamma_п, \tag{1.23}$$

$$F_к = \frac{\pi d^2}{4}. \tag{1.24}$$

and substituting (1.22) and (1.23) into the original Eq. (1.21),

after transformation we obtain

$$\frac{dw}{w^3} = \frac{3}{4}\frac{\varphi\gamma_в}{d_к\gamma_т}d\tau. \qquad (1.25)$$

The coefficient φ of the aerodynamic resistance in turn is a function of velocity and, within the variation range of Re = 50-1000, it is determined in accordance with the expression

$$\varphi = \frac{a}{\sqrt{Re}}, \qquad (1.26)$$

where a is some constant factor characterizing the shape of a body. For a sphere, we assume $a = 14$.

Substituting (1.26) into (1.25) and carrying out the necessary transformations, we obtain

$$\frac{dw}{w^{1.5}} = \frac{3}{4}\frac{a\nu^{0.5}\gamma_в}{d_к^{1.5}\gamma_т}d\tau. \qquad (1.27)$$

We denote by φ_k' the complex of quantities which characterize the physical properties of the medium and of the drop substance

$$\varphi_к' = \frac{3}{4}\frac{a\nu^{0.5}\gamma_в}{\gamma_т}. \qquad (1.28)$$

Equation (1.27) can be written in the form

$$\frac{dw}{w^{1.5}} = \varphi_к'\frac{d\tau}{d_к^{1.5}}. \qquad (1.29)$$

We integrate Eq. (1.29) under the condition that at the initial instant of time ($\tau = 0$) the drop velocity is equal to $w = w_0$

$$w_к = \frac{4d_к^2 w_0}{(2d_к^{1.5} + \varphi_к'\tau\sqrt{w_0})^2}. \qquad (1.30)$$

Substituting (1.30) into (1.20), we obtain an expression which allows us to determine the value of the parameter Re at any instant of time

$$Re = \frac{4d_к^2 w_0}{\nu(2d_к^{1.5} + \varphi_к'\tau\sqrt{w_0})^2}. \qquad (1.31)$$

Figure 3 shows curves characterizing the variation of the parameter Re in time for drops with diameters of 200, 100 and 50 μm, moving at an initial velocity w_0 = 180 m/s in air, the temperature and pressure of which are 1000°C and 1 kgf/cm^2, respectively. It follows from Re = $f(\tau)$ that the magnitude of Re decreases rapidly with time. This decrease is particularly marked for drops with

small diameter. Thus, for example, for a drop with a diameter of 50 μm Re becomes ~10 within 1 ms after it has left the spray nozzle, while the corresponding figure for a drop with a diameter of 100 μm is attained after approximately 7.5 ms. For lighter fuels, the process of deceleration is somewhat more rapid since higher values of φ_k' correspond to these fuels.

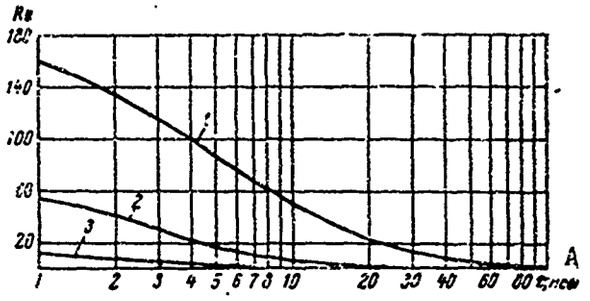

Fig. 3. Variation of Re with time for drops of various diameters (ω_0 = 180 m/sec, D_{sr} = 1000°C): 1) d_k = 200 μm; 2) d_k = 100 μm; 3) d_k = 50 μm. A) τ/ms.

According to the change in Re, the intensity of heat transfer from the medium to the drop decreases with time, as shown by the curves of Fig. 2. The maximum intensity of heat transfer is observed only during the initial period of drop motion. However, during this time interval under real conditions the drops move in the field of lowest temperatures, comparable to the temperature of the supplied air. As the drop penetrates into regions with higher temperature, its velocity begins to decrease rapidly because the viscosity characteristics of the medium increase considerably with temperature. Accordingly, the intensity of heat transfer to the surface of the drop decreases. For drops with small diameters (20-100 μm) this process is most pronounced.

The effect of the radiation component on the heating of a moving drop can also be analyzed by means of the method described. However, there is no need for this, since the heating fraction in this case will be less than in the case of a stationary drop because the coefficient of convective heat transfer during relative motion of the drop generally increases while α_1 is independent of the rate of motion.

Thus, analysis of the data shows that for comparable conditions of heating stationary drops of various liquid-fuel grades and equal size, the heating time increases continually in proportion to the reduction in fuel quality. For a fuel of the cracking residue type, it exceeds the corresponding time for kerosene by a factor of 5-7. Increasing the temperature of the medium and preheating the fuel decreases the surface heating time. Drop size has the strongest effect on heating time. Thus, discussion of the process of drop heating when stationary relative to the medium allows the conclusion that considerable shortening of the fuel-preparation time when

different grades of heavy fuel are used is made possible above all by improving the fineness of atomization and by increasing the temperature of the medium. Preheating the fuel also shortens the heating time of the drop somewhat. These measures, as a result of shortening the pre-ignition segment of the flame, permit an increase in the stay time for the drop in the nucleus of the flame, i.e., to improve considerably the conditions for the combustion process.

Having examined the conditions of motion for the fuel drop and its heating conditions, we can conclude that the process of heating small moving drops occurs in the range of small values of Re, i.e., under conditions which differ only slightly from the heating conditions for stationary drops. Large drops with diameters of 200 μm and more retain their relative velocity for a longer time, so that the intensity of their heating increases 2-4 times, compared with a stationary drop of the same diameter.

2. IGNITION OF THE DROP

A vapor cloud is formed around the drop by the heating of the fuel and the beginning pronounced vaporization. Owing to diffusion and turbulent pulsations, the fuel vapors formed on the drop surface will be removed from the drop to the ambient medium. Owing to the mixing of the fuel vapors with air, their concentration decreases as their distance from the drop surface and the temperature of the formed fuel-air mixture increase because of the continued heating of the fuel vapors. Thus, at some distance from the drop, local mixture foci in which the fuel concentration corresponds to the lower (concentration) ignition limit may be formed. According to the theory of the combustion of homogeneous fuel-air mixtures [6, 7] their ignition is possible only after a certain defined time interval – the "induction period" – which depends on the fuel concentration in the mixture and its physical characteristics, as well as on the temperature of the mixture. Accordingly, the ignition time of the fuel drop can be defined approximately as the sum of the time required for preheating, initial vaporization and further heating of the mixture to the ignition temperature. The last two processes (vaporization and heating of the vapor) occur virtually at the same time. The fuel-drop quantity vaporization process is usually analyzed in the assumption that the fuel vaporizing from the drop surface during preheating is negligible. This corresponds fairly well to the real preheating and vaporizing conditions for heavy fuel grades (Fig. 4).

Initial data for calcudation of drop vaporization is given by

$$dG = \beta_p F_к (p_п - p_{п.о})\, d\tau, \qquad (1.32)$$

where dG is the quantity of vaporized fuel; β_p is the vaporization coefficient referred to the partial vapor pressure difference between the drop surface (p_p) and the ambient medium ($p_{p.o}$); $F_к$ is the drop surface; τ the vaporization time.

With rapid drop deceleration and the main part of the vaporization process occurring without relative velocity, the vaporization coefficient β_p is determined from the condition $Nu_D = 2$.

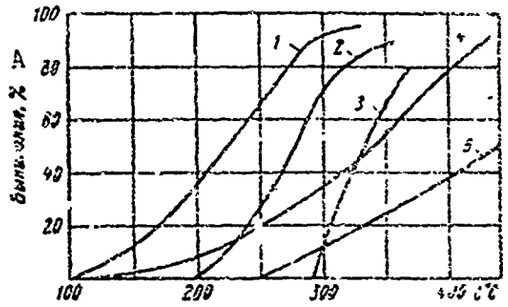

Fig. 4. Vaporization properties of fuels as a function of temperature: 1) Kerosene; 2) gas oil; 3) heavy diesel oil; 4) slow-coking distillate; 5) naval petroleum residue 12. A) Boil-off, %.

In this case

$$\mathrm{Nu}_D = \frac{d_к \beta_p}{D_p} \simeq 2, \tag{1.33}$$

whence

$$\beta_p = 2\frac{D_p}{d_к}, \tag{1.34}$$

where Nu_D is the Nusselt number for the vaporization process; D_p is the diffusion coefficient referred to the difference between the fuel vapor concentration on the drop surface and in the ambient medium; $d_к$ is the drop diameter.

On the other hand, the quantity of vaporized fuel can be expressed as

$$dG = F_к \gamma_т \, dd_к = \pi d_к^2 \gamma_т \, dd_к, \tag{1.35}$$

where γ_t is the specific gravity of the fuel.

Substituting the values of β_p and dG into the original equation (1.32), integrating and defining

$$k = \frac{8D_p(c_п - p_{п.п})}{\gamma_т}, \tag{1.36}$$

we obtain an expression which defines the change in drop diameter with time

$$d_0^2 - d_т^2 = k\tau, \tag{1.37}$$

where d_0 and d_τ, respectively, are the initial drop diameter and the drop diameter after the time τ.

On the assumption that in the ambient medium (at a rather

great distance from the drop surface) the partial vapor pressure is zero, we can write

$$p_n - p_{n.s} \simeq p_n \tag{1.38}$$

The pressure of the saturated vapors near the drop is usually described by an equation of the form [8]

$$p_n = A\exp\left(-\frac{B}{T_k}\right), \tag{1.39}$$

where A and B are constants characterizing the properties of the fuel; T_k is the absolute temperature of the drop surface.

Under these conditions, the vaporization characteristic k is usually known as the vaporization constant and is described in the form of the following relation:

$$k = c\left(\frac{T}{273}\right)^q \exp\left(-\frac{B}{T_k}\right), \tag{1.40}$$

$$c = \frac{8AD_{p.o}}{p_0\gamma_T}, \tag{1.41}$$

where p_0 is the pressure of the medium; T the absolute temperatue of the medium; $D_{p.o}$ the diffusion coefficient referred to the difference between the partial pressures at 0°C and atmospheric pressure.

The numerical values of the exponent q normally fall within the range 0.5-1.0.

An analysis of the expression for the vaporization characteristic k shows that under otherwise equal conditions it should decrease with deterioration in fuel quality. For heavy fuels, the diffusion coefficient $D_{p.o}$ has lower values than for light fuels and the values of the constants A and B are also lower.

Equation (1.37) makes it possible to determine the time during which the quantity of fuel required for the formation of the flammable fuel-air mixture around the drop vaporizes from the drop surface. The quantity of vaporized fuel is equal to

$$\Delta G = G_0 - G_\tau = \gamma_T \frac{\pi d_0^3}{6}\left(1 - \frac{d_\tau^3}{d_0^3}\right), \tag{1.42}$$

where G_0 is the drop weight at the initial instant of time; G_τ is the drop weight after time τ.

Having determined from Eq. (1.37) the value of d_τ and having substituted this into Eq. (1.42), after transformation we obtain

$$\Delta G = \gamma_т \frac{\pi d_0^3}{6}\left[1 - \left(1 - \frac{k\tau}{d_0^2}\right)^{3/2}\right]. \qquad (1.43)$$

Referring ΔG to the initial weight of the drop and with Ω denoting the vaporization of the drop, we have

$$\Omega = \frac{\Delta G}{G_0} = 1 - \left(1 - \frac{k\tau}{d_0^2}\right)^{3/2}. \qquad (1.44)$$

Hence the time required for the development of a flammable fuel-air mixture around a drop with a known vaporization characteristic k is defined by

$$\tau_{исп} = \frac{d_0^2\left(1 - \sqrt[3]{(1-\Omega)^2}\right)}{k}. \qquad (1.45)$$

In this equation, the degree of the initial vaporization Ω is undetermined. In the ideal case, in the absence of convection currents and with spherically-symmetric distribution of the fuel vapor relative to the drop surface and also with a constant vaporization rate, the variation in fuel vapor concentration and temperature along the radius can be approximately described by equations of the form [9]:

$$C_t = C_{т.к}\frac{r_к}{r}, \qquad (1.46)$$

$$T = T_{ср} - (T_{ср} - T_F)\frac{r_к}{r}, \qquad (1.47)$$

where C_t and T, respectively, are the fuel concentration and temperature of the mixture at a point r distant from the center; $C_{t.k}$ $\cdot T_F$ is the concentration and temperature of the vapors at the surface of a drop with radius r_k; T_{sr} is the temperature of the medium.

If we consider the fuel vapor at the drop surface as an ideal gas, the weight concentration of the fuel vapors will be numerically equal to their specific gravity at the saturation temperature and partial pressure

$$C_{т.к} = \gamma_п, \qquad (1.48)$$

$$\gamma_п = \frac{\mu_п p_п}{848 T_F}, \qquad (1.49)$$

where γ_p is the specific gravity of the fuel vapors; p_p is the vapor pressure at the saturation temperature, assumed equal to the drop surface temperature; μ_p is the molecular weight of the fuel vapors.

The degree of the initial vaporization can be determined in the following manner. We choose in the space around the drop a sphere with radius r and thickness dr. Accordingly the quantity of fuel

vapor enclosed in this spherical envelope will be

$$dG = 4\pi r^2 C_т\, dr. \tag{1.50}$$

The quantity of fuel vapor contained in the space bounded by the surface of the drop and the sphere with radius r can be determined by integrating Eq. (1.50) within the limits r and r_k.

$$\Delta G' = \int dG = 4\pi C_{т.к} r_к \int_{r_к}^{r} r\, dr = 2\pi C_{т.к} r_к (r^2 - r_к^2). \tag{1.51}$$

For practical calculations, the values of Ω are entirely sufficient to limit r to the value r_v at which the vapor concentration corresponds to the lower concentration limit of ignition, i.e., the leanest mixture, characterized by an air excess α_v and the temperature T_v of the vapor-air mixture will be equal to the ignition temperature.

From Eq. (1.47) we obtain

$$r_в = r_к \theta, \tag{1.52}$$

$$\theta = \frac{T_{ср} - T_F}{T_{ср} - T_в}. \tag{1.52a}$$

Substituting (1.52) into the expression for $\Delta G'$, we find

$$\Delta G' = 2\pi C_{т.к} r_к^3 (\theta^2 - 1), \tag{1.53}$$

or

$$\Delta G' = \frac{2\pi\mu_п p_п}{848 T_F} r_к^3 (\theta^2 - 1). \tag{1.53a}$$

Hence the degree of initial vaporization is

$$\Omega = \frac{\Delta G'}{G_к} = \frac{3}{2} \frac{\mu_п p_п}{848 T_F \gamma_T} (\theta^2 - 1), \tag{1.54}$$

where γ_T is the specific gravity of the drop substance.

The fuel vapor weight concentration in a layer of thickness dr can be defined as

$$C_т = \gamma_{см} g_п, \tag{1.55}$$

where γ_{sm} is the specific gravity of the mixture; g_p is the weight fraction of the fuel vapors.

The specific gravity of the mixture is determined by the equation

$$\gamma_{см} = \frac{\gamma_в \gamma_п}{g_в \gamma_п + g_п \gamma_в}, \tag{1.56}$$

where g_v; and γ_v are the weight fraction and specific weight of the

air in the mixture, respectively.

Considering that

$$g_n = \frac{\alpha_v L_0}{1+\alpha_v L_0}, \quad g_a = \frac{1}{1+\alpha_v L_0}, \tag{1.57}$$

we can write Eq. (1.56) in the form

$$\gamma_{cm} = \frac{\gamma_a (1+\alpha_v L_0)}{\alpha_v L_0 + \frac{\gamma_a}{\gamma_n}}. \tag{1.58}$$

Replacing the ratio of the specific weights of the air and vapor with the ratio of their molecular weights, we can conclude that this ratio is negligibly small compared with the quantity $\alpha_v L_0$, so that it can be neglected in the subsequent calculations.

Substituting the expression for the specific weight of the mixture and the weight fraction of the fuel vapors into Expression (1.46), we find

$$\frac{\gamma_n}{\alpha_v L_0} = \frac{\mu_n \rho_n}{848 T_F} \frac{r_k}{r}. \tag{1.59}$$

After having substituted into Eq. (1.59) the value of γ_j expressed in terms of the appropriate parameters, and having eliminated the partial fuel vapor pressures at a point with radius r_v, the magnitude of radius r_v can be defined as

$$r_v = r_k \alpha_v L_0 \frac{\mu_n}{\mu_a} \frac{\rho_n}{\rho_0} \frac{T_a}{T_F}, \tag{1.60}$$

where T_v is the temperature at the ignition point.

Substituting the ignition radius (1.60) together with the fuel vapor concentration near the drop surface into (1.51), the equation for the quantity of evaporated fuel, we obtain

$$\Delta G = 2\pi r_k \frac{\mu_n \rho_n}{848 T_F} \left[r_k^2 \left(\frac{\rho_n}{\rho_0} \frac{\mu_n}{\mu_a} \frac{T_a}{T_F} \alpha L_0 \right)^2 - r_k^2 \right] = \tag{1.61}$$

and

$$= 2\pi r_k^3 \frac{\mu_n \rho_n}{848 T_F} \left[\left(\alpha L_0 \frac{\rho_n}{\rho_0} \frac{\mu_n}{\mu_a} \frac{T_a}{T_F} \right)^2 - 1 \right] \tag{1.62}$$

$$\Omega = \frac{3}{2} \frac{\mu_n \rho_n}{848 T_F \gamma_T} \left[\left(\alpha L_0 \frac{\rho_n}{\rho_0} \frac{\mu_n}{\mu_a} \frac{T_a}{T_F} \right)^2 - 1 \right].$$

As follows from Eq. (1.60), the relative radius of the ignition zone can be expressed as

$$\bar{r}_0 = \frac{r_a}{r_k} = \alpha_v L_0 \frac{\rho_n}{\rho_0} \frac{T_a}{T_F} \frac{\mu_n}{\mu_a}. \tag{1.63}$$

Considering this, the expression for the degree of the initial

vaporization can be written in the form

$$\Omega = \frac{3}{2} \frac{\mu_n \rho_n}{848 T_F \gamma_T} (\bar{r}_p^2 - 1). \qquad (1.64)$$

For the instant of ignition which is possible only when two conditions are realized simultaneously at the ignition point, and namely, the necessary fuel vapor concentration and a temperature equal to the spontaneous ignition temperature, the two values of the degree of initial vaporization (1.64) and (1.54) are numerically equal. In this case, the ignition condition can be written in the form

$$\theta = \bar{r}_p, \qquad (1.65)$$

or in expanded form

$$\frac{T_F (T_{cp} - T_F)}{T_s (T_{cp} - T_s)} = \frac{\mu_n}{\mu_s} \frac{\rho_n}{\rho_s} \alpha_s L_0. \qquad (1.66)$$

It is readily seen from Eq. (1.64) that Ω, the degree of initial vaporization, is independent of the drop size but is entirely determined by the physical properties of the drop substance. Light fuels with high vapor pressure have relatively large values of Ω; ignition of their vapors occurs at considerable distances from the drop surface. With increasing fuel-vapor molecular weight, the degree of initial vaporization is reduced and the ignition zone is closer to the drop surface. Increasing the temperature of the medium considerably reduces these quantities, whereas ignition may become virtually impossible when the difference $T_{sr} - T_v$ is large.

TABLE 4

Relative Radius $\bar{r}_r$ and Degree of Initial Vaproization Ω for Some Liquid Fuels

1 Показатели	2 Керосин	3 Соляровое масло	4 Мазут
5 Средний молекулярный вес	160	200	340
6 Температура поверхности капли, °K	373	473	573
7 Удельный вес топлива, кг/м³	800	850	920
8 Предельное значение избытка воздуха	1,5	1,75	1,9
9 Температура самовоспламенения, °K	673	653	653
10 Упругость паров, кг/м²	370	160	80
11 Относительный радиус зоны воспламенения	6,31	3,80	2,48
12 Степень предварительного испарения	0,0238	0,0019	0,000415

1) Indices; 2) kerosene; 3) solar oil; 4) petroleum residue; 5) average molecular weight; 6) drop surface temperature, °K; 7) specific gravity of fuel, kg/m³; 8) maximum excess of air; 9) spontaneous ignition temperature, °K; 10) vapor pressure, kg/m²; 11) relative radius of the ignition zone; 12) degree of initial vaporization.

Table 4 gives tentative values for Ω and $\bar{r}_r$, calculated by means of the above described method, using the data on the maximum air excess (α_v) corresponding to the lower concentration limit of ignition, taken from Reference [10].

Thus, having determined Ω, it is possible to calculate the time required for the initial vaporization.

If the term "ignition lag" is applied to a single drop of liquid fuel, meaning the time interval between the instant of its introduction into the heated medium and the instant of the appearance of a visible flame, the ignition lag can be represented approximately in the form

$$\tau_з = \tau_{пр} + \tau_{исп} + \tau_{инд}. \qquad (1.67)$$

where τ_{pr} is the heating time of the drop; τ_{isp} is the time of initial vaporization; τ_{ind} is the period of "chemical induction."

All other conditions equal, the quantities τ_{pr} and τ_{isp} are defined by the square of the initial drop diameter. The chemical induction period τ_{ind} is determined only by the chemical nature and properties of the fuel and is independent of drop size. The generally accepted form of the expression for the chemical induction period as a function of various conditions is an expression of the form

$$\tau_{инд} = A \exp\left(\frac{E}{RT}\right), \qquad (1.68)$$

where A is a factor typical for each fuel; E is the activation energy; R is the gas constant of the mixture; T is the temperature of the mixture.

The activation energy for hydrocarbon fuels [6, 7] falls within the range of 36,000-46,000 kcal/mole. Thus, in the most general form, the total ignition lag of the fuel drop can be expressed in the form of the binomial function

$$\tau_з = \tau_{инд} + \frac{d_0^2}{k_v}, \qquad (1.69)$$

where k_v is a coefficient, conventionally called the ignition characteristic

$$k_v = \frac{k_{пр} k_{исп}}{k_{пр} + k_{исп}}. \qquad (1.70)$$

This characteristic is determined by the properties of the fuel as well as the heating conditions of the drop.

This form of notation for the ignition lag is also convenient because direct determination of ignition time components under real

conditions presents great technical and methodological difficulties. The total ignition lag is much more easily and accurately determined.

According to Eq. (1.69), the square of the drop diameter and the total ignition lag are related by a linear function, in which the graph of this function never passes through the origin of the coordinates, even for drops with vanishingly small diameters. The curve slope $\tau_v = f(d_0^2)$ is determined by the properties of the fuel and the heating conditions. Since the heating time for drops of heavy fuel considerably exceeds the heating time for drops of light fuel, the total ignition lag will also be greater.

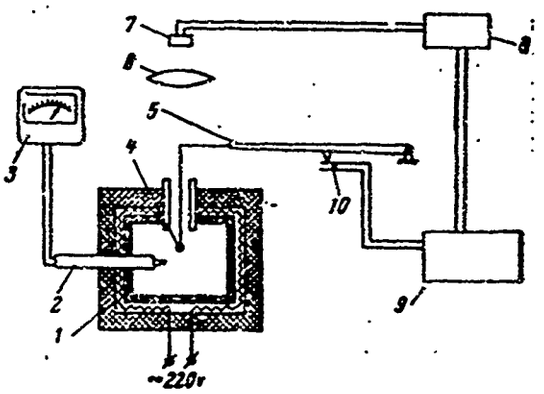

Fig. 5. Diagram of apparatus for investigating processes of ignition and combustion of a single drop in a stationary medium: 1) Electrid muffle furnace; 2) thermocouple; 3) galvanometer; 4) drop; 5) lever for introduction of the drop; 6) lens; 7) photoresistance; 8) photocurrent amplifier; 9) loop oscillograph; 10) marker of instant of drop introduction.

Figure 5 shows a diagram of an apparatus for the study of the ignition and combustion processes of single drops of liquid fuel, which is used at the All-Union Research Institute of Railway Transport.[1] A fuel drop with a diameter of 150 to 700 μm at the end of a fine wire (0.03 mm) was introduced through a small orifice into the furnace in which the temperature was varied in the range from 700 to 950°C and monitored with a special thermocouple. The instant of introduction of the drop into the furnace was fixed by means of a loop oscillograph. The instant of ignition of the drop was determined from the appearance of a luminous flame around the drop, which was recorded on the motion-picture film of the oscillograph by means of a photoresistance. Thus, the ignition lag was defined as the difference between two pulses on the oscillogram.

The experimental data showed that a linear relation really exists between the ignition time and the square of the initial drop diameter and, moreover, that this relation applies to a wide range of liquid fuels, from kerosene to heavy petroleum residues of the M60 type.

1/57

The data in Fig. 6 indicate that the slope of the straight-line curves corresponding to the proportionality factor k_v in Eq. (1.69) depends on the fuel grade. Generally, the heavier the fuel, the greater the slope of the corresponding line and, consequently, the smaller the value of k_v. Accordingly, the time required for the ignition of the drop is increased.

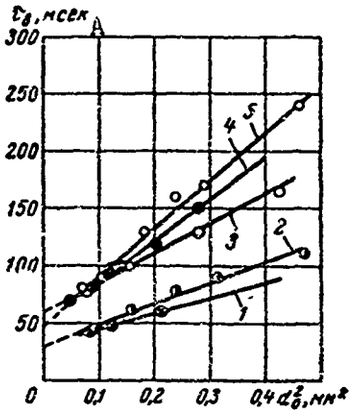

Fig. 6. Ignition time of a single drop of various fuel grades as a function of the square of the initial drop diameter (t_{sr} = 850°C): 1) Kerosene; 2) diesel oil; 3) naval petroleum residue 12; 4) fuel oil 20; 5) fuel oil 60. A) τ_v, ms.

The general trend of the relation $\tau_v = f(d_0^2)$, as follows from Fig. 6, is in complete agreement with Eq. (1.69) according to which the ignition time of drops of very small size will be considerably limited by the "chemical induction" time. All the straight lines at $d_0^2 = 0$ do not pass through the coordinate origin. In accordance with Eq. (1.69), the segments on the τ-axis can be represented as the "chemical induction" time of the respective fuel grade. For diesel oil and kerosene, the values of τ_{ind} differ only slightly and under experimental conditions amount to 25-30 ms. Heavy fuels (petroleum residues F-12, M20, M60 and cracking residues) are characterized by somewhat larger values of τ_{ind} (45-60 ms) and a greater difference in these values for various grades of petroleum residue.

Lowering the temperature of the medium increased the ignition lag considerably (Fig. 7).

The nature of the dependence and the slope of the curves corresponding to various air temperatures remained approximately the same, while the "chemical induction" time increased sharply with decrease in temperature.

The proportionality factor k_v (ignition characteristic) from

Eq. (1.69) can be defined as

$$k_v = \frac{d_0^2}{\tau_в - \tau_{инд}}. \qquad (1.71)$$

Table 5 shows the ignition characteristics of various fuels, determined by means of Eq. (1.71).

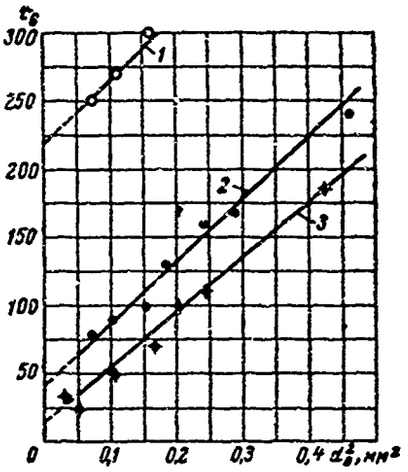

Fig. 7. Ignition time of a single drop of petroleum residue M60 as a function of the square of the initial drop diameter and gas temperature: 1) t_{sr} = 700°C; 2) t_{sr} = 850°C; 3) t_{sr} = 950°C.

TABLE 5

Average Ignition Characteristics of Some Liquid Fuels (t_{sr} = 850°C)

Топливо 1	$\tau_в$, 2 сек	$k_в$, 3 см²/сек
4 Керосин	0,025	0,0541
5 Дизельное топливо . . .	0,030	0,0555
6 Мазут Ф-12	0,060	0,0412
Мазут М20	0,055	0,0257
Мазут М60	0,045	0,0242
7 Крекинг-остаток	0,055	0,0355
8 Цилиндровое масло . .	0,080	0,0128

1) Fuel; 2) τ_v, s; 3) k_v, cm²/s; 4) kerosene; 5) diesel oil; 6) petroleum residue F-12; 7) cracking residue; 8) cylinder oil.

Comparison of the k_v values in Table 5 shows that this coefficient within the investigated temperature range (700-950°C) varies considerably as the fuel gets heavier. The "chemical induction" time drops markedly with increase in temperature, as shown by the curve $\tau_{ind} = f(t_{sr})$ for the petroleum residue M60, as shown in Fig. 8.

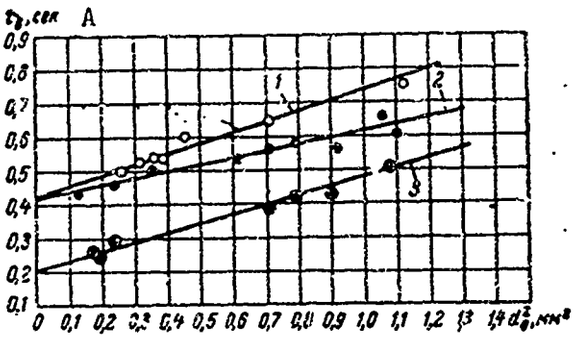

Fig. 8. Ignition time of a fuel drop in a stream of hot air as a function of the square of the drop diameter (t_{sr} = 700°C, w = = 2.63 m/s): 1) Cracking residue; 2) petroleum residue M60; 3) diesel oil. A) s.

Thus, examination of ignition process features for a single fuel drop, stationary relative to the air, and corresponding experimental data, demonstrated that the duration of this process is determined mainly by the heating time, the initial vaporization time and the time of chemical induction. For the heavy fuels, the main factors are the heating time of the drop and τ_{ind}, since the initial vaporization is of relatively less importance. With decrease in drop size, the effect of τ_{ind} predominates. Hence, a radical method of accelerating the process of drop preparation for combustion is an increase in gas temperature, simultaneously with an improvement in atomization efficiency.

Considerably more complex is the ignition process of a moving fuel drop. In this case, the fuel vapors will be removed to the ambient medium, which interferes with the formation of a flammable mixture at the drop surface. It can be assumed that the instant of ignition for the moving drop occurs somewhat later than for a stationary drop, since a much greater vaporization intensity is then required.

Direct observation of the ignition process of a fuel drop entrained in the stream made it possible to establish that at low air spreads drop ignition takes place close to the surface, the flame immediately enveloping the entire drop surface. With increase in the air speed, the fuel vapors coming off the drop surface are ignited at a certain distance from the drop in its wake. This distance increases in proportion to the increase in the airstream speed and at certain values of the relative drop velocity vapor ignition did not take place. This velocity is determined by the temperature of the stream. The higher the temperature of the air stream, the greater the velocity at which the flame is cut off. An analogous phenomenon has been described in Reference [9], where some data are given on the ignition and combustion of liquid fuel drops (kerosene, isooctane, ethyl alcohol).

In ignition of drops moving relative to a medium at a certain constant velocity, a linear relation between the square of the initial drop diameter and the ignition time is also observed (Fig. 9). As in the case of the ignition of these fuels in quiescent air, we observe here a fairly clear separation of the fuels with regard to their physicochemical properties, on deterioration of which the time required for drop ignition under these conditions increases.

The shape of the function $\tau_v = f(d_0^2)$ makes it possible to isolate a certain period of chemical induction, different for various fuels. In this case the chemical induction period for diesel oil

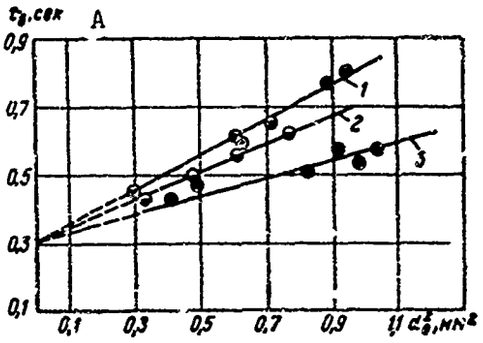

Fig. 9. Ignition time of a fuel drop in a stream as a function of the drop size and the relative velocity (t_{sr} = 850°C): 1) w = = 6.5 m/s; 2) w = 3.9 m/s; 3) w = 2.63 m/s. A) s.

as for other fuels) is of the same order as in the case of a stationary drop. The average value of the ignition characteristic for given conditions, determined in accordance with Fig. 9, amounted to k_v = 0.038 cm²/s for diesel oil, 0.020 cm²/s for petroleum residue M80 and to 0.031 cm²/s for cracking residue. At airstream speeds over 0.263 m/s, fuel drop ignition occurred only at a stream temperature of not less than 850°C. With increasing airstream speed, the average value of the ignition characteristic decreased (see Fig. 9) and, accordingly, the time required for the ignition of the fuel drop increased. At the same time, the chemical induction period remained virtually constant. The increase in the ignition time, determined from the reduction in the ignition characteristic k_v, is apparently explained by the presence of a relative velocity, as indicated earlier.

Examination of ignition conditions for a fuel drop, stationary as well as moving at relative velocity, enables us to conclude that the total duration of the ignition process (regarding this process from the instant of drop entry into the medium until the instant of the appearance of a visible flame) is generally determined by three components: the heating time, the initial vaporization time and the chemical induction period. The preheating time and the chemical induction period are the longest and play the most important part. With increase in the molecular weight of the

fuel, the role of the initial vaporization is considerably reduced in importance. Simultaneously, the relative radius of the ignition zone is reduced.

The presence of a relative drop velocity does not introduce any significant changes into the general nature of the ignition process. However, the total duration of the process increases because of the more intense removal of vapor from the drop surface. Although the presence of a relative velocity somewhat increases the vaporization rate owing to the intensification of the preheating process and the lowering of the partial vapor pressure near the drop surface, the maximum concentration of the fuel vapor is attained somewhat later. An increase in the relative velocity can have the consequence that ignition of the drop becomes impossible even if the stream temperature exceeds the spontaneous ignition temperature. Depending on drop size and the properties of the fuel (molecular weight, activation energy, etc.), in real flames, where drops of different size are present, small drops (to ~50-100 μm) are ignited much earlier than larger ones. The ignition of the latter, however, should take place only under conditions of an already formed flame. This will be most clearly manifest in a flame of heavy fuel.

3. COMBUSTION OF THE DROP

The analysis of the combustion process of a fuel drop should be based on consideration of the mutual influence of the factors which determine the chemical kinetics, heat and mass transfer, vaporization and other phenomena accompanying combustion and caused by it. Evidently, the building up of a complete theoretical scheme of the combustion process involves extremely great difficulties. Hence, the theoretical works discuss idealized schemes, using nervous simplifying assumptions. Removed from the real conditions of drop combustion, the process is considered as quasi-stationary under assumption of spherical symmetry of the temperature and concentration fields relative to the drop surface and also of a predominating influence of the diffusion, compared with the kinetic processes.

Based on these simplifying assumptions [11], the process of combustion of a spherical drop can be described by a system of differential equations in accordance with the following scheme (Fig. 10). The diffuse fuel vapors from the drop surface to the combustion zone and oxygen diffuses from the ambient medium. A chemical reaction of the combination of the fuel with oxygen takes place in the combustion zone, in consequence of which heat is evolved and combustion products are formed, which are carried away into the surrounding medium by diffusion. The heat evolved during the reaction is partly transferred to the drop by heat conduction and is partly given off to the surrounding medium.

The diffusion theory of combustion of single drops in absence of convection makes it possible to calculate the mass rate of combustion of a fuel drop, the drop temperature and the temperature of the combustion zone and also the relative distance of the combustion zone from the drop surface when the variation of the physical characteristics of the drop substance and its vapor as a function of temperature is known. The combustion time of a stationary drop of fuel, according to diffusion theory, is defined as

$$\tau_r = \frac{r_0^2}{k_r}, \tag{1.72}$$

$$k_r = \frac{2\lambda T_s \int_{x_k}^{x_r} \frac{\varphi(x)\,dx}{f(x_1 x_k)}}{\lambda_r \left(1 - \frac{r_k}{r_r}\right)}, \tag{1.73}$$

where r_0 is the initial radius of the fuel drop; r_g is the radius of the combustion zone: γ_t is the specific gravity of the fuel; x_1, x_k, respectively, are the dimensionless temperature (T/T_0), the dimensionless temperature of the drop (T_k/T_0), and $\varphi(x)$ is a function, defining the dependence of the heat transfer coefficient on temperature; $f(x_1, x_k)$ is a function, defining the dependence of the variation of the heat content of the fuel vapors on x and x_k.

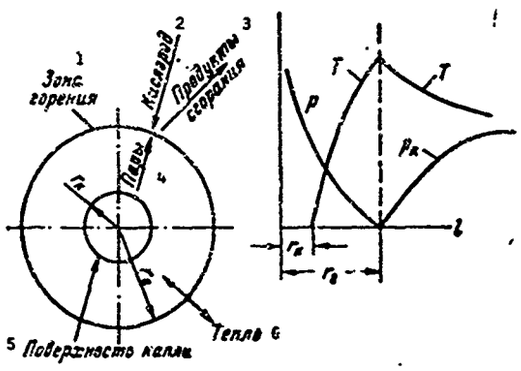

Fig. 10. Scheme of the combustion of a single drop. 1) Combustion zone; 2) oxygen; 3) combustion products; 4) vapor; 5) drop surface; 6) heat.

Thus, according to diffusion theory, the combustion time of the fuel drop is proportional to the square of the initial drop radius on condition that the quantity k_g, often referred to as the "combustion constant," does not vary during the combustion of the fuel drop.

The later works [12, 13, 14] on the study of the laws of combustion of single drop on the whole, are analogous to Reference [11] with regard to the calculation scheme and method. However, in some details they use simpler assumptions; for example, the independence of the heat transfer coefficient from temperature and also the equality of the drop temperature and the boiling point. Although these assumptions do not introduce great errors into the calculation results, they nevertheless make the whole calculation system less exact. Common to all these theoretical works is the fact that they lead in principle to the same conclusions concerning the laws of

combustion of a single-component fuel drop in a stationary medium:

1) the mass rate of combustion of the drop is proportional to the first power of the drop radius;

2) the relative radius of the combustion zone (ratio of the combustion zone radius to the drop radius) is independent of drop size and the temperature of the combustion zone;

3) the combustion time of the preheated drop of single-component fuel is proportional to the square of its initial diameter. The experimental studies of the combustion of a single drop [15, 16, 17, 18] basically confirm the conclusions derived on the basis of the diffusion theory. In most of these works, a study was made of the process of variation in drop size during combustion in quiescent air as well as in the presence of a relative velocity for the drop. The data obtained in these works, mainly carried out on light or generally single-component fuels, made it possible to formulate the basic law of the combustion of single drops in the form of a linear relation between the combustion time of the drop and the square of its initial diameter in accordance with diffusion theory. The drop diameters during intermediate instants of time are determined fairly accurately from the expression

$$d_\tau^2 = d_0^2 - k_r \tau, \qquad (1.74)$$

where d_τ is the diameter of the fuel drop after time τ from the beginning of combustion; d_0 is the drop diameter at the initial instant; k_g is the proportionality factor.

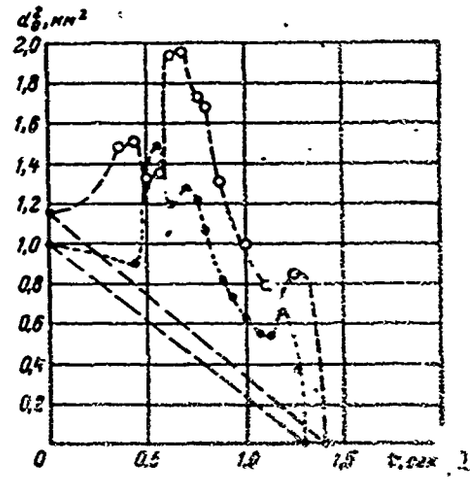

Fig. 11. Variation of the square of the instantaneous drop diameter d_τ as a function of time in the combustion of a single drop in stationary air (γ = 0.864; t_{sr} = 800°C). 1) s.

The validity of this relation (Sreznevskiy law) is confirmed, for example, by the experimental curves of the variation in the square of the drop diameter of *n*-heptane, isooctane and kerosene, burning in a medium with a temperature of 860°C [19]. However, when real and particularly multifraction fuels were used, a certain deviation of the combustion relationships for single drops from the law described by Eq. (1.74) was observed. We note that even in the combustion of a single drop of benzene, the relation between the initial drop diameter and the time of its complete combustion in a stationary medium is described by a broken line consisting of segments of two straight lines, the intersection of which corresponds to the instant of drop ignition. An analogous pattern is observed in the combustion of single drops of solar oil.

Consequently, Eq. (1.74) applies only during the period of the actual combustion of the fuel drop, with exclusion of the period of preparation of the drop for combustion. In this case, the value of k_g will be the true value in contrast to the "apparent" value of k_g', defined as the ratio of the square of the drop diameter to the total combustion time, also including the preparation period

$$k_r' = \frac{d_0^2}{\tau}. \qquad (1.75)$$

Accordingly, k_g' will be somewhat smaller than the true value of k_g.

The need to transform Eq. (1.74) into Eq. (1.75) becomes even more obvious from the data on the time dependence of the square of the instantaneous drop diameter of liquid fuel with a specific gravity of 864 kg/m^3 (Fig. 11) [20]. Thus, the concept of a *combustion constant* which is usually related to the proportionality factor k_g and k_g' in Eqs. (1.74) and (1.75), and is fairly frequently encountered in the literature, is not quite accurate if one has in mind the real industrial fuels. From our point of view, the most suitable term is *combustion characteristic*, because the quantity k_g' characterizes only the total duration of the combustion of a fuel drop without providing any possibility of determining the drop size during intermediate instants of time. In one of the first works on the verification of the applicability of diffusion theory to the case of combustion of a single drop of heavy multicomponent fuels it was found that in drops of petroleum residue, entering a stream of air heated to 900-1100°C, two stages can be fairly clearly distinguished. During the first stage the rate of vaporization is quite low, in consequence of which a certain increase in the drop diameter is observed due to the thermal expansion of the petroleum residue. After the ignition of the vapor thus formed, the vaporization intensity increases rapidly, resulting in a decrease in the drop diameter in proportion to its combusion. In some experiments, spark formation was observed toward the end of the combustion process, corresponding to a certain increase in the size of the drop which subsequently again decreased until its complete dissappearance. Such a phenomenon was not observed in the combustion of a drop of solar oil. The spark formation toward the end of the combustion process of a drop of petroleum residue is explained

by the formation of a coke envelope at the drop surface [17] which prevents the fuel vapor from leaving the internal regions of the drop, in consequence of which they are overheated and their pressure is correspondingly increased. As a result of this, the envelope swells and then is ruptured with scattering of the overheated vapor to the surrounding medium, which then ignite. Based on this it is concluded [17] that the drop of heavy fuel may explode, in consequence of which the combustion time can be considerably shortened.

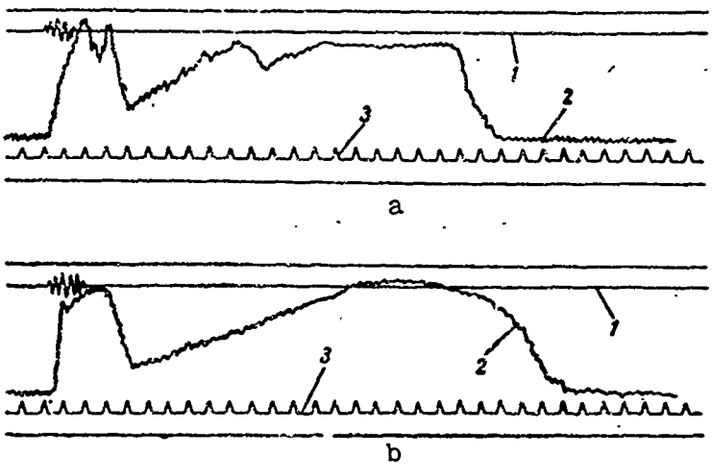

Fig. 12. Typical oscillograms of the combustion of a single drop in quiescent "cold" air on ignition by a spark discharge: a) For diesel oil; b) for petroleum residue M80. 1) Duration of ignition discharge; 2) luminosity trace of the drop combustion zone; 3) time mark.

The explosion of drops of heavy fuels during heating was observed during the vaporization and combustion of fuels with high water content and specially prepared fuel-water emulsions [21]. In this case, the explosion of the fuel drop takes place, not toward the end of the combustion of the drop, but much earlier, because the boiling point of a fine water particle inside the fuel drop is much lower than the normally observed temperatures of a drop of "dry" petroleum residue. The water in the drop is overheated and vaporizes, forming steam which ruptures the drop, the fragments of which burned at a high rate in the presence of steam.

Despite the general nature of the mechanism and the final effect (drop explosion), the phenomenon pointed out in Reference [17] is essentially determined by other causes, namely: the continuous coke formation on the drop surface. To some degree this contradicts the hypothesis that all fractions vaporize simultaneously from the top surface while the fuel in the internal regions of the drop retains virtually the initial composition [17]. The formation of a coke layer evidently indicates selective vaporization in which the light components are preferentially vaporized. The heavy components are heated and form a coke layer on the surface, which then ruptures at different points. In this case, a highly porous residue should form at the end of the combustion period,

consisting of particularly heavy fractions of either fuel or solid coke residues from the pyrolysis of the drop substance and there may be no explosion of the drop. However, it is not possible at present to derive any final conclusions from the fact of the explosion of drops, sometimes observed during the combustion of single, fairly large drops of heavy fuels, because of the clearly insufficient quantity of experimental material.

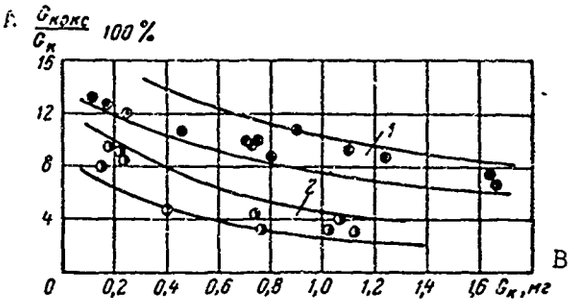

Fig. 13. Relative weight of the coke residue as a function of the initial weight of the drop: 1) Cracking residue; 2) naval petroleum residue 12. A) Coke; B) mg.

To exclude the effect of the drop combustion preparation period (preheating and ignition) in studies on the drop combustion process [22], drop ignition was effected by a brief high-voltage arc discharge and the actual drop combustion was carried out in quiescent cold air. The duration of the igniting discharge was recorded by means of a loop oscillograph. The drop combustion time was determined from the duration of its luminosity. The oscillograms thus obtained (Fig. 12) show that during the initial period (during the igniting discharge) the flame luminosity for both fuels is approximately of equal intensity. After discharge ceases, combustion intensity drops sharply for diesel oil as well as for petroleum residue. The luminosity trace begins to rise comparatively slowly. During this period the difference between the properties of the fuels is fairly clearly manifested, since for petroleum residue the duration of the luminosity-increase period is approximately twice that of diesel oil. This period corresponds to a nonsteady thermal state of the drop because the intensity of heat transfer to the drop surface is considerably reduced and heat comes only from the combustion zone.

For diesel oil less heat is required to obtain a sufficient quantity of vapor than for petroleum residues, so that the attainment of equilibrium conditions takes place within a shorter interval. The light emission of a diesel oil flame is terminated considerably sooner than that of a petroleum residue flame. Simultaneously, it was found by direct observation that drops of certain grades of petroleum residue do not burn completely. During some stage of the process, the combustion of the petroleum residue is terminated and a coke residue remains on the quartz suspension in the form of a porous body, the dimensions and relative weight of which are different for different grades of petroleum residue and drop sizes

(Fig. 13). The larger the drops, the greater the size of the coke residue, but its relative weight is reduced at the same time. This is explained by the porosity of the coke residue.

The formation of the coke residue during the combustion of a drop of heavy fuel introduces even greater ambiguity into the concept of "combustion characteristic."

The quantity of unburned fuel in the form of a coke residue for most heavy fuels is relatively small, and the relation between the drop combustion time and its initial size can be written in the form

$$k_t' = \frac{d_0^2 - d_{ост}^2}{\tau}, \qquad (1.76)$$

where d_0 is the initial drop diameter; d_{ost} is the calculated drop diameter at the end of the combustion;

$$d_{ост} = \sqrt[3]{\frac{6\gamma_t G_{кокс} Q_{кокс}}{\pi Q_т}}. \qquad (1.77)$$

where γ_t is the specific gravity of the original fuel; G_{koks} is the weight of the coke residue; Q_{koks} and Q_t are the specific heating values of the coke residue and the original fuel, respectively.

The experimental data, processed with consideration of the reduced combustion characteristic, show that in this case the fuel drop combustion time is also a linear function of the square of th initial drop diameter and that the mass rate of combustion is independent of size and is determined entirely by the physical characteristics of the fuel. Figure 14 shows a graph plotted from experimental data for the M60 and M80 petroleum residues and Table 6 gives the combustion characteristics calculated on the basis of the experimental data.

The combustion characteristics for various grades of petroleum residue, given in Table 6, differ only slightly, whereas the relative weights of the coke residue have a certain tendency to increase as the original fuel gets heavier. The slight difference in the value of k_g'' for different grades of petroleum residue can be accounted for by the fact that in this case the combustion process of the drop was in fact the process of combustion of its liquid component or the products of internal gasification which are not strongly dependent on the difference in properties or group composition. The total combustion time, taking into account the combustion time of the coke residue, differs with the grade of fuel.

Of greatest interest from a practical point of view is the case of fuel drop combustion in presence of a relative velocity (combustion of a moving drop). Using the basic assumptions of diffusion theory [9], we can represent the functional dependence between drop size and time in the form of the equation

$$d_0^{3/2} - d_\tau^{3/2} = k_r \tau, \tag{1.78}$$

$$k_r = 4{,}5 \frac{\lambda_0 T_0 (1 + \omega)\, w^{1/2}}{L q_0 \gamma_r \nu^{1/2}} \int_{x_{вп}}^{x_r} \varphi(x)\, dx, \tag{1.78a}$$

$$\omega = q_0 L \int_{x_к}^{x_r} \frac{\varphi(x)\, dx}{f(x_r, x_к)} \left[\int_{x_{вп}}^{x_r} \varphi(x)\, dx \right]^{-1}, \tag{1.78b}$$

where ω is the relative velocity of the drop; ν is the kinematic viscosity of the medium; x_{vn} is the dimensionless temperature at the outer surface of the combustion zone (T_{vn}/T_0).

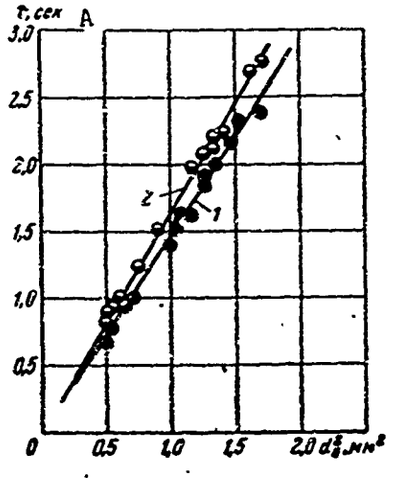

Fig. 14. Combustion time of a drop in quiescent cold air with ignition by means of an electric discharge as a function of the square of initial diameter: 1) Petroleum residue M60; 2) petroleum residue M80. A) s.

TABLE 6

Standard Characteristics and Combustion Characteristics of Stationary Drops of Heavy Liquid Fuels

1 Топливо	Характеристики топлива 2					
	ν_4^{20}	ВУ$_{50}$ 3	$t_{всп}$, °C	коксуемость 4	k_r^*	$G_{кокс}$, %
5 Дизельное	—	—	—	—	0,71—0,72	
6 Мазут ФС-5	907	4,0	103	5,1	0,65	—
Мазут Ф-12	952	8,3	124	6,6	0,62	6,5
Мазут М-20	913	4,0	—	5,5	0,65	5,5
Мазут М-60	—	55,0	160	—	0,68	6,0
Мазут М-80	—	77,0	152	—	0,62	6,5
7 Крекинг-остаток	—	110,0	—	18,7	0,64	11,5
8 Гудрон	—	—	—	19,3	0,65	—
9 Цилиндровое масло	—	—	Выше 300 10		0,57	0

1) Fuel; 2) fuel characteristics; 3) VU; 4) coking capacity; 5) diesel; 6) petroleum residue; 7) cracking residue; 8) petroleum asphalt; 9) cylinder oil; 10) over.

The experimental data obtained by filming a drop during combustion of virtually single-component fuels (isooctane, alcohol and kerosene) in a stream of preheated air in the form of the curves of the function $d^{5/3} = f(\tau)$ are shown in Fig. 15 [9]. Simultaneously, it is pointed out [9] that when a drop is introduced into a stream with sufficiently high temperature, the ignition of the drop takes place after some delay. The primary ignition focus appears in the wake of the drop at a certain distance from its surface and then the flame the flame envelops the entire drop. The liquid drop is then within the combustion zone until its complete disappearance. This pattern is observed only when the velocity of the impinging stream is less than a certain critical value which depends on the temperature of the stream. With increase in the airstream speed, at constant temperature, the flame focus does not approach closer to the drop but is located in its wake. A further increase in airstream speed causes detachment of the flame.

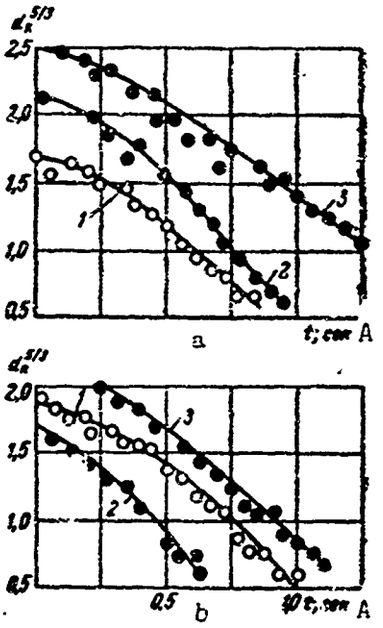

Fig. 15. Instantaneous drop diameter as a function of time for various flow conditions: a) w = 5.7 m/s; t_{sr} = 700-710°C (with flame breakaway); b) w = 1.5 m/s; t_{sr} 700-710°C (the drop burns). 1) kerosene; 2) isooctane; 3) ethyl alcohol. A) s.

As in the combustion of a stationary drop of heavy fuel, the calculations of the drop combustion time in a stream of heated air are usually based on the relation between initial drop size and the time of its complete combustion in the stream:

$$d^n = k_t^* \tau. \qquad (1.79)$$

Usually, n = 2, which yields a slight difference relative to n = 5/3. The experimental data - plotted in coordinates of d_0^2, τ -

obtained during combustion of cracking residue in a stream of hot air which has a relative speed of w = 1.8-2.6 m/s [22] show that in this case there is again a linear relation between the square of the drop diameter and the combustion time.

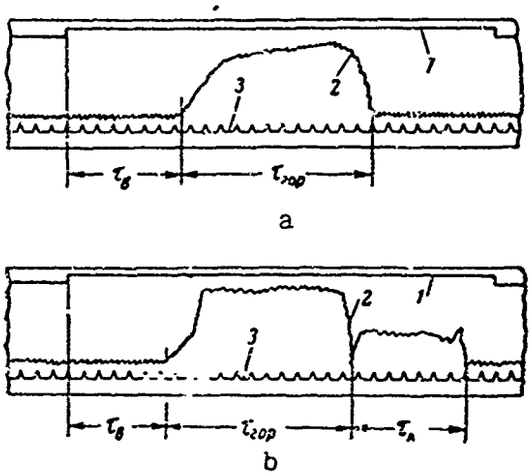

Fig. 16. Typical oscillograms of drop combustion in a stream of hot air. a) Diesel fuel; b) petroleum residue. 1) Time mark process start; 2) luminosity trace of drop combustion zone; 3) time mark.

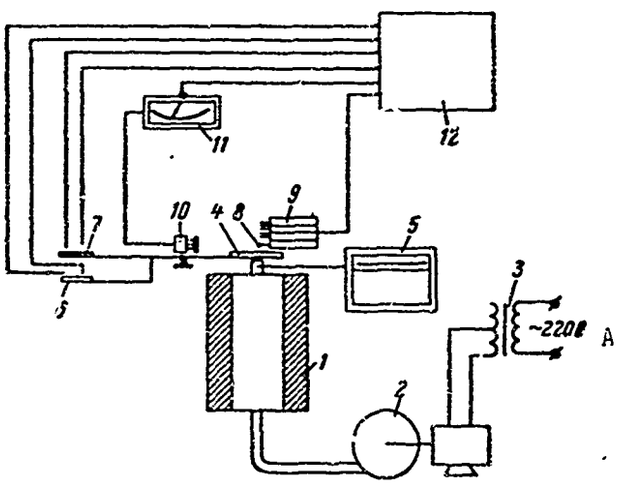

Fig. 17. Diagram of the testing device for the study of the fuel drop combustion process in a stream of hot air: 1) Heating furnace; 2) fan with electric motor; 3) control transformer; 4) watercooled screen; 5) thermocouple with potentiometer; 6) contact group to actuate transformer; 7) contact group for initial time mark; 8) fuel drop; 9) thermocouple block and ionization sensors; 10) photometer sensor; 11) photometer; 12) loop oscillograph. A) V.

The experimental investigations carried out at the TsNII MPS [22] make it possible to obtain a more complete idea of the nature of the combustion process for single heavy fuel drops in a stream of hot air. A distinctive feature of this method of investigation is the separate determination of the combustion process stages. Following the introduction of the fuel drop into the hot air stream, there is a certain preheating period (Fig. 16, 1). The ignition of the fuel drop (diesel oil or petroleum residue) does not take place instantly but fairly smoothly. Compared with petroleum residue, the rate of increase in flame luminosity for diesel oil is greater, which is in agreement with the nature of the vapor pressure increase for these fuels with temperature increase. Flame stabilization around the drop is characterized by a rather clearly distinguishable section of the oscillogram with the maximum of the luminosity curve. The length of this section amounts to a considerable portion of the total combustion time for a drop of diesel fuel (~50%), and to 30% for petroleum residue. The practically abrupt cessation of flame luminosity observed with these fuels attests to the cessation of the combustion process for the main liquid phase of the drop, which corresponds to the complete combustion of diesel oil. With petroleum residue, this instant is followed by luminosity with considerably less intensity. This period of heavy-fuel drop combustion corresponds to combustion of the coke residue which forms during the combustion period of the liquid drop phase.

Further investigations of residue fuel single drop combustion features in petroleum residues were carried out by the authors under slightly modified conditions. At the instant of drop suspension the airstream was covered by a large horizontal watercooled screen to prevent heating of the drop during its introduction and measurement. Three low-lag thermocouples were placed in succession at different heights above the drop. The first thermocouple, which was in the immediate vicinity of the drop surface (~5 mm), was located in the interelectrode space of the flame ionization sensor. Flame luminosity was recorded by a photoelectric photometer (the diagram of the test equipment is shown in Fig. 17).

Typical examples of oscillograms of the combustion process of diesel oil and petroleum residue, obtained under identical conditions, are presented in Fig. 18. If one examines these oscillograms, we find that the luminosity curves for a drop of petroleum residue and diesel oil differ considerably in character. The luminosity curve for petroleum residue has three clearly distinguished sections, whereas the luminosity curve of diesel oil is a smooth curve with a maximum situated approximately in the middle. The shape of the luminosity curve generally approximates fairly closely the curve of the flame ionizaton level which, for petroleum residue, also has an inflection which coincides in time with the first inflection of the luminosity curve. The second section of the luminosity curve for a drop of petroleum residue is characterized by a much greater loop deviation amplitude which corresponds to greater flame luminosity. The ionization level in the second section is also considerably higher than in the first. The third section of the luminosity curve is characterized by zero ionization and low brightness. The virtual coincidence in time of the characteristic points of the process as recorded by all the utilized measurement methods indicates the reliability of the pattern found for the combustion process of a single

drop. Analysis of the oscillograms makes possible the conclusion that the difference between the properties of the diesel oil and the petroleum residue are primarily reflected in the unequal number of stages in the process of their combustion. While the combustion of a drop of diesel oil proceeds in two stages – preheating and combustion proper – the combustion of a drop of petroleum residue takes place in four stages – preheating, two combustion phases

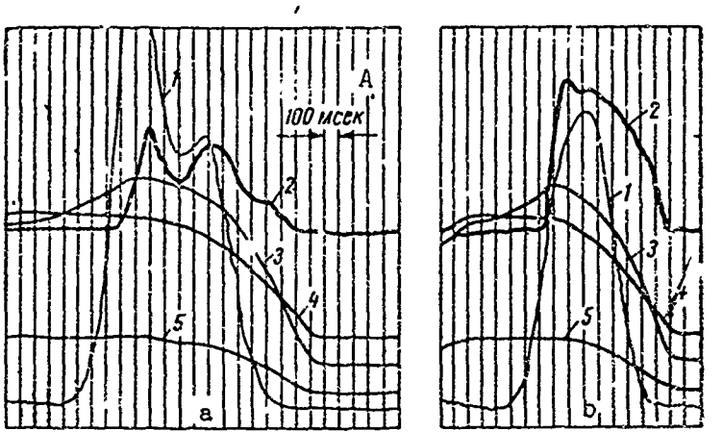

Fig. 18. Typical oscillograms for the combustion of a fuel drop in a stream of hot air: a) Petroleum residue M20; b) diesel oil. 1) Flame luminosity; 2) flame ionization in zone of 1st thermocouple; 3, 4, 5) thermoelectromotiv force curves for thermocouples 1, 2, 3. A) ms.

and the combustion of the coke residue. The second stage of the combustion of a drop of petroleum residue, corresponding to an increase in flame luminosity and ionization, evidently also determines the formation of the coke residue, the combustion of which forms the concluding stage. Examination of the curves for changes in the thermoelectromotiv force of the thermocouples situated in the flame zone of the drop reveals that they are essentially similar for the two fuels. Typical for all three curves is the existence of three sections most clearly evident for the thermocouple located near the drop, obviously in the zone of the highest temperatures. The first section represents the preheating period of the drop during which the thermocouple junctions are in contact only with the hot air whose temperature corresponds to the slope of the trace. The inflection point which is the boundary between the first and second section corresponds to the instant of drop ignition when the thermocouple junctions are subjected to the action of high-temperature combustion products. The third characteristic point of the thermoelectromotiv force curve corresponds to the termination of the combustion process in the liquid phase of the drop, shown by the change in the nature of the curve. Processing these curves and taking into account the statistical and dynamic characteristics of the thermocouples employed, we were able to build in first approximation the variation pattern for local temperatures with time (Fig. 19). As follows from Fig. 19 which also shows the luminosity and ionization curves, the highest tempera-

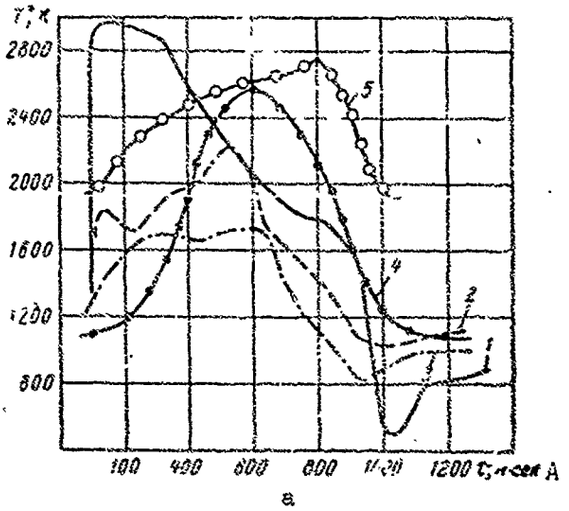

a

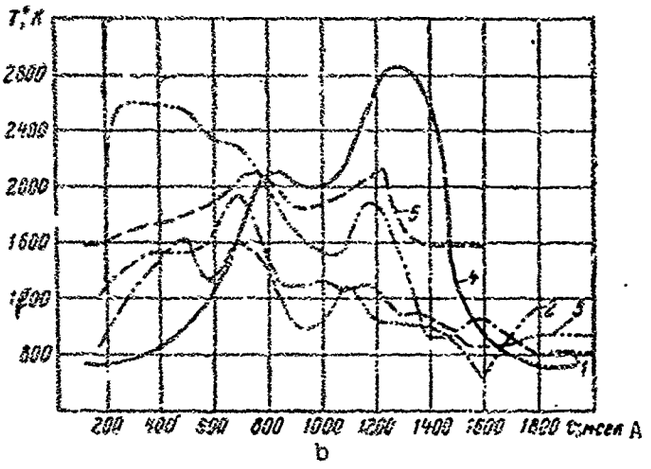

b

Fig. 19. Time variations in flame temperature for a single drop in a stream of air (t_{air} = 835°C): a) Diesel oil; b) petroleum residue. 1, 2, 3) Flame temperatures in the zones of the first, second and third thermocouples, respectively; 4) flame luminosity; 5) flame ionization in the zone of the first thermocouple. A) ms.

tures develop during the initial combustion period in a drop of petroleum residue, in the immediate vicinity of the drop, which apparently corresponds to the position of the ignition front. The subsequent development of the combustion process is characterized by continuous lowering of the temperature of this zone, to the instant at which the second combustion stage begins. From this instant on, simultaneous with the increase in flame luminosity and ionization, the temperature also begins to rise, without, however, attaining its previous maximum. This is followed by a sharp drop in temperature to values approximately corresponding to the airstream temperature. The two other thermocouples, located higher, show an

analogous variation, but with smaller absolute values.

The curves of flame temperature variation in a drop of diesel oil are qualitatively of a different nature (see Fig. 19, b). Instead of the dip in the temperature curve, in this case we have a general tendency to decrease after passing the maximum. The flame temperature maximum differs for diesel oil and petroleum residue by 500-600°C and also by position. The maximum flame temperature during the combustion of a drop of solar oil is attained slightly earlier than for petroleum residue. The numerical values of the maximum flame temperatures coincide fairly well with the calculated combustion zone temperatures given in [23, 24] and amount, respectively, for benzene, to 3400°K, for n-heptane, to 3230°K, for ethyl alcohol, to 3100°K, for toluene, to 3370°K, and for ethylbenzene, to 3470°K. The average maximum temperature which we found is ~2900°K for diesel oil and ~2500°K for petroleum residue.

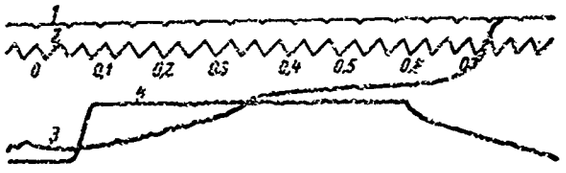

Fig. 20. Oscillogram of the combustion of a single drop in a stream of air: 1) Marks for the instants of recording; 2) time marks; 3) drop temperature; 4) temperature of the drop flame.

At the same time, the general law time variation in flame temperature and the numerical values of the maximum temperatures are in definite contradiction to the data published in [17] where it is stated that "the drop (flame) temperature in the combustion zone remains constant and is the same for petroleum residue and solar oil, amounting to 1800°K." As an illustration of this, an oscillogram is presented (Fig. 20) showing a trace of the flame temperature measured by means of a specially designed photoelectric pyrometer. Reference [25] presents data on the flame temperature variation for a single drop from which follows that the flame temperature toward the end of the combustion process of a drop of kerosene increases slightly, in the same manner as the decrease of the initial drop diameter. From our standpoint, the difference between the data obtained by us and those given in [17, 25] is explained mainly by the difference in the method of measurement.

The fact that the flame of a single drop contains a large number of incandescent carbon particles, i.e., particles whose temperature is, strictly speaking, measured by optical and photoelectric pyrometers, does not signify by any means that their number remains constant during the entire combustion process. It is highly probable that the number of such incandescent soot particles varies with time, for example, increasing toward the end of the process, as indicated by the luminosity and ionization curves. It is also quite probable that the quantity of hydrogen formed as a result of the decomposition of the fuel vapor in the pre-flame zone will reach

a maximum during the initial combustion period and will decrease toward the end of the process. These circumstances can have the result that at the initial instant of combustion, despite the high temperature, flame luminosity and, consequently, color and brightness temperatures of the drop flame will be comparatively low, whereas toward the end of the process the reverse pattern will be found, i.e., high flame luminosity at a relatively low temperature. In this case, the photoelectric or optical pyrometers which pick up the radiation of the entire flame record a temperature which differs from that of the thermocouple.

Certain errors are naturally involved in the measurement of flame temperature with low-lag thermocouples. However, these errors mainly concern the absolute temperatures and much less the nature of its time variation, as confirmed by the entire set of oscillogram curves.

Comparison of the temperatures averaged for the entire combustion period of a fuel drop as given in [17] shows that the differences here are no longer significant. Thus, for example, the flame temperature of a drop of diesel oil, averaged over the entire flame and the whole combustion period, is about 1900°K and for a drop of petroleum residue ~1850°K, whereas according to the data of [17] this temperature is about 1800°K. Thus, the research results permit the combustion process for a single drop to be described in first approximation as follows.

At the end of the drop surface preheating period the vapor cloud formed around the drop is ignited, the ignition process taking place at a very high rate. Under the influence of the high combustion-zone temperature, the fractional vaporization of the fuel from the drop surface continues and is apparently accompanied by processes of fuel decomposition on the drop surface. As a result, fuel vapors greatly enriched with hydrogen arrive in the combustion zone. Hence, high temperatures develop in the combustion zone and the combustion zone itself is now located at a rather great distance from the drop surface.

The flame temperature then decreases in proportion to the consumption of the light fractions and the combustion zone moves nearer to the drop. When the flame front is fairly close, the surface temperature of the drop beings to increase rapidly, apparently leading to an intensification of the fuel decomposition process, changing into a pyrolysis process with formation of aromatic gaseous hydrocarbons and coke. The combustion of these hydrocarbons in the flame zone obviously entails a temporary temperature increase and high luminosity for the combustion products because of the higher concentration of incandescent soot particles.

Coke and polymerization products of tars and asphaltenes gradually accumulate within the drop. Hence, drop surface coking will set in and ejection of flammable components from the internal regions of the drop way occur. The development of these processes causes the quantity of gaseous hydrocarbons given off at the drop surface to become insufficient to maintain combustion in the gas phase. From this instant on, coke residue combustion stage begins if the parameters (temperature and oxygen content) of the ambient

medium correspond to the combustion conditions.

The foregoing scheme of combustion process development is also applicable to the combustion process of a diesel oil drop. It can be concluded from Fig. 19b that here too the combustion of the relatively light fractions with relatively low carbon content takes place during the initial period of the combustion process. During this period the highest temperatures develop but flame luminosity and ionization are relatively slight. In proportion to the increase in molecular weight of the fuel vapor and its enrichment with carbon, flame luminosity and ionization increase and temperature decreases monotonically. It can be assumed that a coke residue is again formed, but in such small quantity that its combustion virtually coincides with the final period of drop combustion.

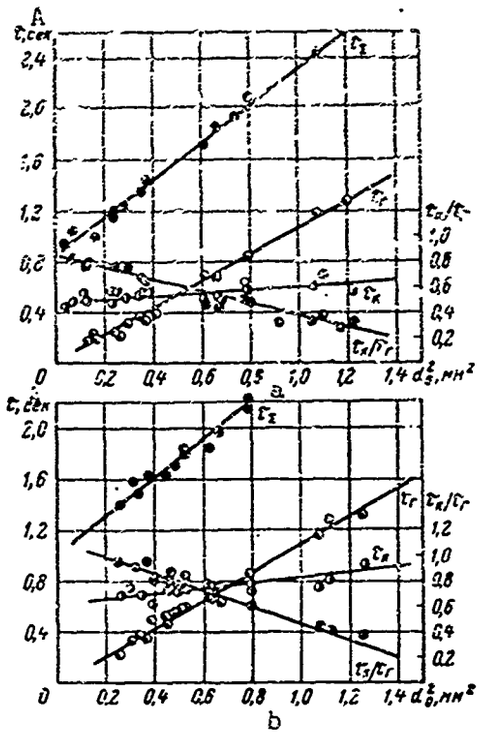

Fig. 21. Total combustion time and duration of individual stages of single drop combustion in a stream of hot air as a function of the square of the initial drop diameter (w = 1.18 m/s; t_{sr} = 700°C): a) Petroleum residue M80; b) cracking residue. τ_ε) Total combustion time of a drop (including ignition period); τ_g) combustion time of the liquid phase (without ignition period); τ_k) combustion time forthe coke residue; τ_k/τ_g) ratio of coke residue combustion time to the total combustion time of the drop liquid phase (including ignition period). A) s.

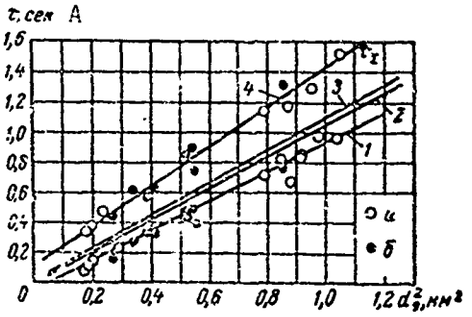

Fig. 22. Liquid phase combustion time for a drop of heavy fuel as a function of the square of its initial diameter (w = 1.18 m/s): a) t_{sr} = 700°C; b) t_{sr} = 850°C. 1) Combustion time of a drop of diesel oil without taking into account the ignition period; 2) the same, for a drop of petroleum residue M80; 3) the same, for a drop of cracking residue; 4) total time of combustion for a drop of diesel oil. A) s.

Sufficient experimental material has not yet been accumulated to explain the basic quantitative relationships of the development of the intermediate stage of combustion of heavy liquid fuel drops, although the fact of its existence itself can be considered as established. Also taking into account that the transition of the basic phase to the intermediate stage takes place fairly smoothly, it now appears expedient to combine it with the basic stage, normally called stationary combustion stage or the liquid phase combustion stage. Accordingly, the total combustion time of such a drop will be determined by the total duration of the preheating and ignition processes, steady combustion and combustion of the coke residue.

According to the data of [22], the total combustion time τ_Σ, including drop ignition time in an airstream (w = 0.3-3 m/s; t_{sr} = 700°C) as well as the combustion time of the main liquid phase of the drop are described adequately by a linear relation of the (1.75) type. The combustion time for the coke residue in first approximation can also be represented in the form of a linear function of the square of the initial drop diameter. The ratio of the combustion time of the coke residue to the time of combustion for the main liquid phase of the drop, including the ignition period, does not remain constant with variation of drop size, since for drops with small diameter the combustion time of the coke residue is comparable to τ_Σ and fro cracking residues may even exceed it. With increase in the initial drop size, the relative combustion time for the coke residue decreases, although the absolute value of τ_K increases, as is clearly evident from Fig. 21. The curve representing the combustion time of the liquid phase (without taking into account the ignition period) as a function of the square of the diameter for petroleum residue and cracking residue

is virtually the same and differs only slightly from the analogous relations for diesel oil (Fig. 22).

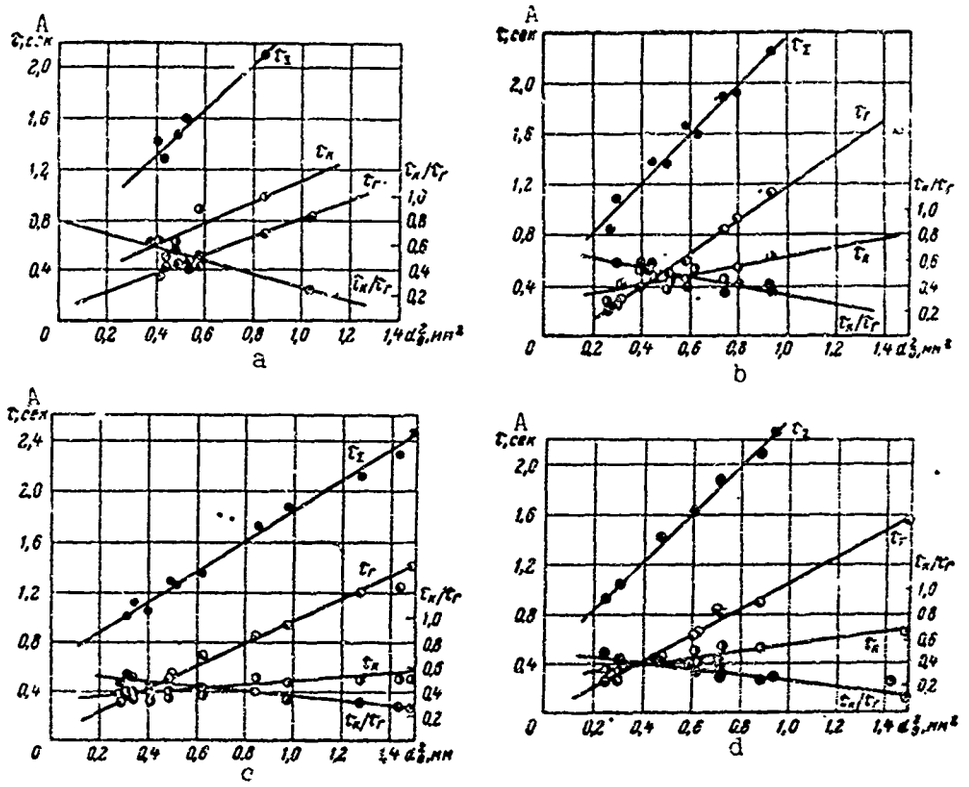

Fig. 23. Total combustion time and duration of individual stages of combustion for a single drop of petroleum residue M80 at a stream temperature of t_{str} = 850°C as a function of the airstream speed: a) w = 0.8 m/s; b) w = 1.18 m/s; c) w = 1.58 m/s; d) w = = 1.98 m/s. A) s.

For diesel oil, variation of the temperature conditions (airstream temperature) within the investigated range has virtually no effect on the total duration of the combustion process or on the duration of the combustion proper. This circumstance permits the conclusion that the total duration of the combustion process for heavy residual fuels, as compared with light fuels, is determined by the duration of the preparation of the fuel and the combustion of the coke residue. Variation of the flow conditions around the drop, expressed in a variation of temperature and velocity, did not modify the general sequence and nature of the development of the combustion process (Fig. 23). The airstream speed was varied in the range of 3.3-6.5 m/s. In this case, comparison of the corresponding total combustion times for a single drop of petroleum residue (τ_Σ) under different airstream conditions shows that the value of τ_Σ is approximately constant. At the same time, the combustion time of the liquid phase increases with increase in the relative velocity. This phenomenon is a result of the fact that

with increase in airstream speed the flame is displaced relative to the drop and the principal combustion focus is located in the wake of the drop.

Flame displacement in turn disrupts the heat balance of the drop through a lower heat flux in consequence of which the vaporization intensity is reduced. An increase in the rate of combustion of the coke residue compensates to a considerable degree for the increased combustion time of the liquid phase.

TABLE 7

Average Values of the Reduced Combustion Characteristic k''_g for Some Grades of Heavy Fuel

1 Топливо	2 Условия горения: $t_{ср}$, °C	2 Условия горения: w, м/сек 3	k''_g, мм²/сек 4
5 Дизельное топливо	700	0,388	0,642
6 То же	850	0,388	0,652
7 Мазут М20	700	0,388	0,496
8 Цилиндровое масло	700	0,388	0,415
Мазут М80	700	0,388	0,445
» М80	850	0,330	0,505
» М80	850	0,388	0,514
» М80	850	0,520	0,626
» М80	850	0,550	0,565
9 Крекинг-остаток	700	0,388	0,435

1) Fuel; 2) combustion conditions; 3) ms; 4) mm²/s; 5) diesel oil; 6) the same; 7) petroleum residue M20; 8) cylinder oil; 9) cracking residue.

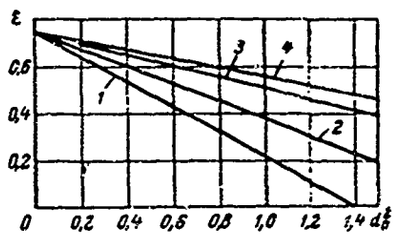

Fig. 24. Relative combustion time of the coke residue as a function of the square of the initial diameter of a drop of petroleum residue M80: 1) w = 3.3 m/s; 2) w = 5.2 m/s; 3) w = 6.5 m/s; 4) cracking residue w = 3.88 m/s, t_{sr} = 700°C.

The total duration of the combustion process of a single drop of heavy fuel remains virtually constant on variation of the temperature and relative velocity of the stream within certain limits, whereas the duration of the coke residue combustion is considerably shortened. A study of the combustion of individual components of naval petroleum residue from the Novo-Ufa petroleum Refinery, undertaken to ascertain their role in the process of coke residue

formation, has shown that only the tars and polycyclic aromatic compounds burn with formation of such a residue.

Thus, the total combustion time of a single drop of most residual heavy fuels can be represented as

$$\tau_{\Sigma} = \tau_{з} + \tau_{т} + \tau_{к}. \qquad (1.80)$$

In analogy with the light, completely vaporizing fuels, the sum of the ignition and combustion times of the liquid phase can be represented as the time τ related to the initial drop diameter by a function of the form (1.75). Taking into account that the combustion time for the coke residue (τ_k) can be expressed in first approximation by the relation

$$\tau_{к} = \chi\tau, \qquad (1.81)$$

the total combustion time of a drop of heavy fuel is described by

$$\tau_{\Sigma} = \tau(1 + \chi). \qquad (1.82)$$

Using the generally accepted form of writing the combustion time (1.75), τ_{Σ} is defined as

$$\tau_{\Sigma} = \frac{d_0^2}{k_г''}(1 + \chi), \qquad (1.83)$$

where k_g'' is the reduced combustion characteristic, the numerical values of which are given in Table 7; and χ is the relative combustion time of the coke residue.

The relative combustion time χ of the coke residue (Fig. 24) can also be represented in first approximation in the form of the approximating linear function

$$\chi = \chi_0 - \varepsilon d_0^2, \qquad (1.84)$$

where χ_0 is the initial value of χ at a drop diameter close to zero; ε is the proportionality factor.

The value of χ_0 for petroleum residue M80 varies within limits of 0.85-0.5 depending on the temperature and relative velocity of the stream. Considering the natural scatter of the experimental points, in first approximation one can use the average value of χ_0 = 0.75. For cracking residue, χ_0 will be somewhat higher, while the range of its variation is narrower. Considering this, we can take the mean value for cracking residue approximately as 0.9. The value of ε in turn is determined by the square of the drop diameter, the relative velocity of the stream and its temperature (see Fig. 24).

4. DROP COMBUSTION CHARACTERISTICS AS A FUNCTION OF EXTERNAL CONDITIONS

As follows from the above data, the numerical value of the combustion time for a fuel drop depends not only on the properties of the drop substance but also on the external combustion conditions. This indicates that the combustion characteristic k''_g is not constant for each liquid fuel grade, but varies with change in the ambient temperature, the airstream speed and other factors. It should be pointed out, however, that practically all investigations of the effect of various factors on the combustion characteristic were carried out either on pure individual hydrocarbons or light fuels of the kerosene type. Data on the variation of k''_g for heavy liquid fuels are virtually unavailable so that the influence of various factors on the value of k''_g for these fuels on the basis of the data given in the technical literature can be estimated only qualitatively.

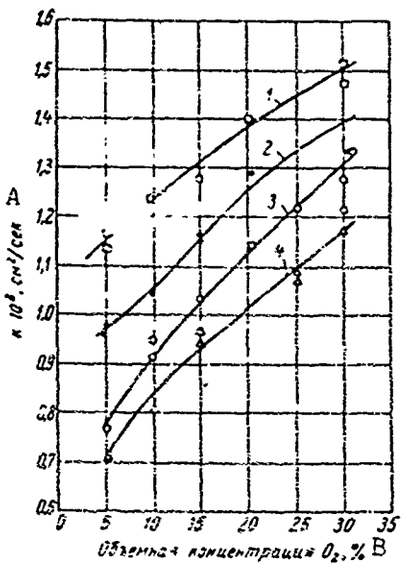

Fig. 25. Kerosene combustion characteristic as a function of the oxygen concentration in the ambient medium and the temperature: 1) t_{sr} = 840°C, $N_2 + O_2$; 2) t_{sr} = 790°C, $N_2 + O_2$; 3) t_{sr} = 710°C, $N_2 + O_2$; 4) t_{sr} = 700°C, $CO_2 + O_2$. A) $k\ 10^2$, cm^2/s; B) volume concentration of O_2, %.

Variation of the oxygen concentration in the ambient atmosphere [26] did not disrupt the established relation between the combustion time of single drops and the square of the drop diameter. With individual hydrocarbons, an increase in the weight content of oxygen in the ambient medium led to marked increases in the flame temperature and combustion rate and also caused the combustion zone to move nearer to the drop surface. For fuels such as

benzene and toluene, an increase in the oxygen concentration above 23% led to cessation of drop combustion owing to the formation of a deposit which burned independently at a much lower rate. Under real conditions, oxygen concentration is varied only in the direction of decrease. The combustion characteristics are markedly reduced at constant temperature of the medium and lower oxygen concentration (Fig. 25).

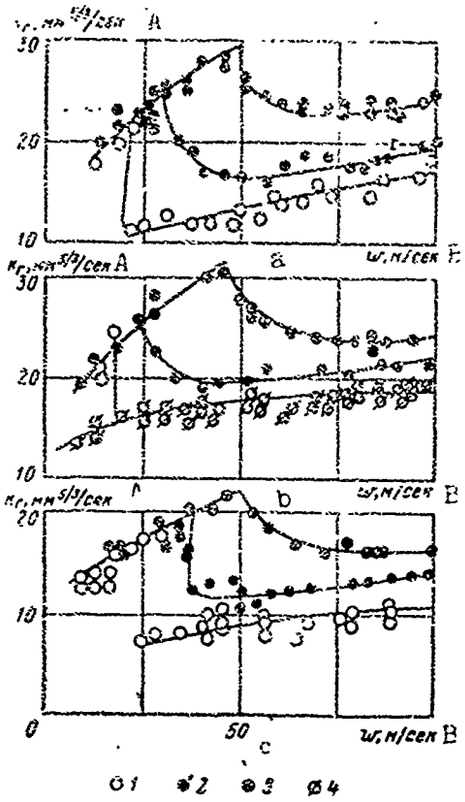

Fig. 26. Combustion characteristic as a function of the relative velocity of the drop: a) Kerosene; 1) 610°C; 2) 700°C; 3) 800°C; b) isooctane: 1) 600°C, combustion and vaporization in air; 2) 700°C; 3) 800°C; 4) 600°C, vaporization in nitrogen; c) ethyl alcohol: 1) 600°C; 2) 700°C; 3) 800°C. A) $мм^{5/3}/с$; B) м/с.

The relative velocity of the drop also exerts great influence on the magnitude of k''. Theoretical treatment of this problem [9] shows that the vaporization constant (combustion characteristic) is proportional to the cube root of the relative velocity within the range $5 < Re < 500$. The experimental data [9] for kerosene, isooctane and alcohol show that for these fuels the curves $k = f(w)$ have three fairly clearly recognizable sections (Fig. 26). In the first section where the entire drop is enveloped by the flame, the combustion characteristic increases in proportion to increasing stream velocity and is virtually independent of its temperature. When the airstream speed attains the critical value and flame breakaway occurs, the combustion characteristic also decreases suddenly, attaining its minimum when the flame focus is

located in the wake of the drop. A further increase in the velocity of the free stream leads to an increase in the characteristic, but not that of combust-on, but that of vaporization. The combustion focus which is still present in the wake of the drop is so far removed from its surface that the heat evolved by the combustion zone no longer exerts any great effect on the vaporization rate. Thus, at an airstream speed above critical the drop changes from a combustion regime to a regime of pure vaporization. Substitution of the airstream flowing around the drop with a stream of nitrogen having the same temperatures and velocities did not lead to any noticeable change of the vaporization characteristic which is direct confirmation of the degeneration of the combustion process into a pure vaporization process at large relative velocities. In this section, the mass vaporization rate depends on the velocity and temperature of the airstream. Investigations to determine the range of stable combustion for drops in a stream of hot air [27] also showed that the breakaway velocity of the airstream for drops of gasoline and kerosene is determined by the stream temperature (Fig. 27) and the oxygen concentration (Fig. 28). The breakaway velocity decreases greatly with decrease in temperature and oxygen concentration. With increasing drop size, the critical value of the relative velocity increases, and this indicates the more stable position of the flame front around such dorps.

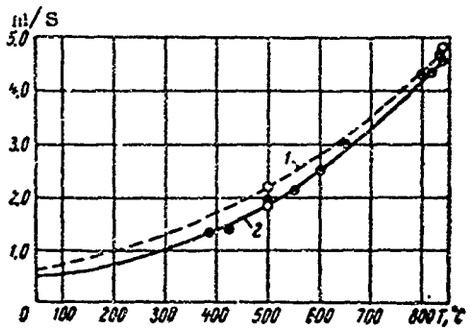

Fig. 27. Critical flow velocity around the drop as a function of stream temperature (d_k = 1.5-1.7 mm): 1) Gasoline; 2) kerosene.

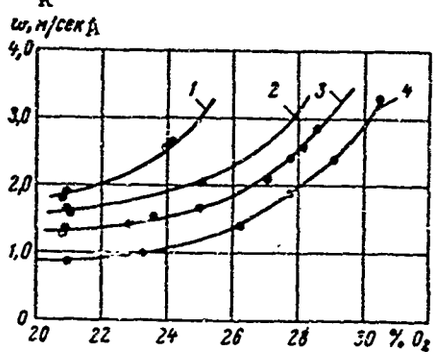

Fig. 28. Critical streamlining velocity for drops of different diameter as a function of the oxygen concentration in the ambient air: 1) d_k = 13.2 mm; 2) d_k = 9.52 mm; 3) d_k = 6.37 mm; 4) d_k = 3.15 mm. A) m/s.

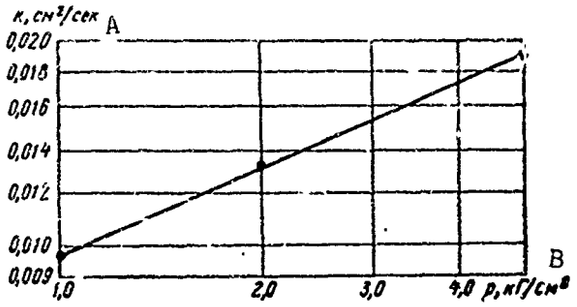

Fig. 29. Combustion characteristic of benzene in air as a function of pressure. A) cm^2/s; B) kgf/cm^2.

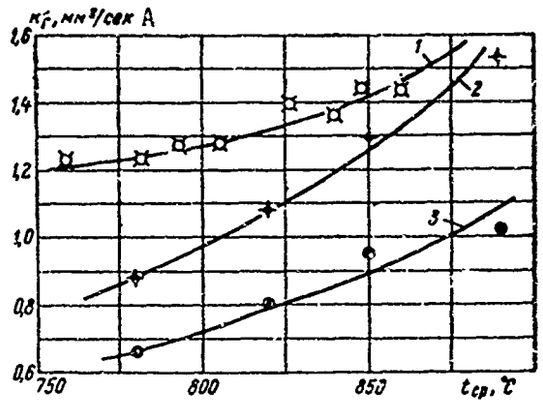

Fig. 30. Combustion characteristic of kerosene 1, diesel oil 2 and petroleum residue 3 as a function of temperature. A) mm^2/s.

The effect of the gas pressure on the combustion characteristic of single fuel drops was studied in [28]. It was found that for all investigated fuels (tetralin, decane, amylacetate, furfuryl alcohol, benzene) an increase in pressure causes a decrease in the distance between the combustion zone and the drop surface proportional to the logarithm of the pressure, the total combustion time decreasing analogously (Fig. 29). For real conditions it is very important to ascertain the effect of the air temperature on the combustion characteristics because the combustion process at constant pressure is most widespread whereas the temperature conditions vary continuously in any case of combustion in proportion to the combustion of the fuel in the flame.

Figure 30 gives some data on the variation of k''_g for several grades of liquid fuel as a function of the air temperature. For a drop of petroleum residue moving at a certain relative velocity, the rate of increase in k''_g is slightly slower than for diesel oil, which, at high temperatures, approximates the values of k''_g for

kerosene. On the basis of the very sparse data it may be concluded that the nature of the variation in k''_g for heavy fuels (of the petroleum residue type) as a function of external conditions remains approximately the same, although the numerical values are naturally correspondingly lower than for light fuels burned under the same conditions. If one compares the data given in the preceding section and in Fig. 26, it can be concluded that for heavy fuels the effect of the relative velocity will be more pronounced, i.e., flame breakaway from the drop surface will take place, other conditions being equal, at much lower relative velocities than with light fuels. Consequently, to preserve a high rate of combustion of heavy fuel drops moving relative to the gas stream, the gas temperature must be higher; otherwise flame breakaway from the surface of the drops will cause a considerable increase in the combustion time.

5. COMPLETENESS OF VAPOR COMBUSTION

Let us assume that the combustion of the drop takes place in a space bounded by heat-absorbing walls. The dimensions of this space are such as to ensure the combustion of a fuel drop with a virtually infinite excess of air. The temperature of the air near the wall as well as the temperature of the boundary wall are constant in time and the process of combustion of the drop is steady. In this case, the quantity of heat evolved from the unit surface of the combustion zone per unit time (assuming that the combustion process develops on the outer surface of the combustion zone) can be expressed as follows

$$q_1 = q_0 u \bar{\eta} \text{ kcal/m}^2\text{s} \qquad (1.85)$$

where q_0 is the specific weight calorific value of the fuel vapors (kcal/kg), assumed to be equal to the calorific value of the original fuel; u is the weight flow rate of the fuel vapors (quantity of fuel vapors in kg, passing through the unit surface of the combustion zone per unit time, kg/m^2·s); $\bar{\eta}$ is the weight fraction of the fuel vapors participating directly in the combustion reaction.

The weight flow rate of the fuel vapors is associated with the mass rate of combustion of the drop by a relation of the form

$$u = \frac{m}{4\pi r_r^2} \text{ kg/m}^2\text{s} \qquad (1.86)$$

where m is the mass rate of drop combustion in kg/s; r_g the radius of the combustion zone in m.

In turn, if the mass combustion rate is expressed by the combustion characteristic k''_g, Eq. (1.86) assumes the form

$$u = \frac{k_r \gamma_r r_0}{4 \cdot 10^4 \pi r_r^2}, \qquad (1.87)$$

where γ_t is the specific gravity of the fuel in kg/m^3; k_g is the combustion characteristic in cm^2/s; r_k is the drop radius in m.

Substituting (1.37) into (1.85), we obtain an expression for the specific surface density of the heat evolution on the surface of the combustion zone

$$q_1 = q_0 \frac{k_t \gamma_t r_k \bar{\eta}}{4 \cdot 10^4 \pi r_r^2}. \qquad (1.88)$$

The heat evolved at the surface of the combustion zone is spent on increasing the temperature of the combustion products from the ambient temperature (t_v) to the temperature of the zone (t_g), on increasing the temperature of the adjacent air layers (heat transfer by conduction) and on radiation. Strictly speaking, the heat evolved in the combustion zone is also spent on heating the drop, vaporization, superheating and decomposition of the vapor and also the dissociation of the combustion products. Taking into account, however, that a considerable fraction of the heat expended for vaporization in some form or other is returned to the combustion zone, and that the degree of dissociation of the combustion products is slight, they can be neglected.

The quantity of heat expended on heating the combustion products passing through the unit surface per unit time, taking into account that the combustion process takes place in stoichiometric ratio ($\alpha = 1$), is determined by the expression

$$q_2 = u c_{p.t} (1 + L_0)(T_r - T_v), \qquad (1.89)$$

where $c_{r.t}$ is the average weight heat capacity of the combustion products within the temperature range ($T_g - T_v$); L_0 is the theoretically required quantity of air for the combustion of the unit weight of fuel vapors.

To determine the specific heat flux per unit area, transmitted by the heat conduction of the ambient medium from the combustion zone, we use the general equation of the theory of heat conduction for a spherical heat source under steady conditions within a spherical space [4]:

$$Q_k = \frac{4\pi\lambda (T_r - T_v)}{\frac{1}{r_r} - \frac{1}{r_{st}}}, \qquad (1.90)$$

where λ is the thermal conductivity coefficient of the ambient medium, in kcal/m·h °C; r_{st} is the radius of the boundary wall in m.

By definition, $r_{st} \gg r_r$, so that $\frac{1}{r_{st}} \ll \frac{1}{r_r}$, which makes it possible to eliminate $1/r_{st}$ from further analysis. Relating Q_k to the unit surface of the combustion zone, we can write the expression for the specific heat flux transmitted to the ambient medium in

the form

$$q_n = \frac{\lambda}{r_r}(T_r - T_s). \qquad (1.91)$$

Analogously, by using the general form of the equation for radiative heat exchange between two bodies of which the smaller one (the burning drop) is located within the larger one (combustion zone), we obtain

$$Q_n = \varepsilon_n c_0 F_r \left[\left(\frac{T_r}{100}\right)^4 - \left(\frac{T_{cr}}{100}\right)^4\right],$$

$$\varepsilon_n = \frac{1}{\frac{1}{\varepsilon_1} + \frac{F_r}{F_{cr}}\left(\frac{1}{\varepsilon_2} - 1\right)}, \qquad (1.92)$$

where ε_p is the referred emissivity; ε_1 and ε_2 are the emissivities of the combustion zone and the heat-absorbing walls, respectively; F_g, and F_{st} are the surface of the combustion zone and the boundary walls, respectively; c_0 is the radiation coefficient of an absolute black body.

Since according to the condition $F_{st} >> F_g$, the specific radiative heat flux is defined as

$$q_n = \varepsilon_1 c_0 \left[\left(\frac{T_r}{100}\right)^4 - \left(\frac{T_{cr}}{100}\right)^4\right]. \qquad (1.93)$$

The equation for the heat balance of a surface element of the combustion zone can be written in first approximation in the form

$$q_1 = q_2 + \frac{q_k + q_n}{3600}. \qquad (1.94)$$

Substituting the corresponding values of the specific quantities in Eq. (1.94), taken from (1.88), (1.89) and (1.93), we find:

$$\bar{\eta} = \frac{(T_r - T_s)}{q_2}\left[c_{p.r}(1 + L_0) + \frac{34{,}89\sigma}{k_r \gamma_r}(\lambda + \sigma \varepsilon c_0 r_k \theta)\right], \qquad (1.95)$$

where

$$\theta = \frac{\left(\frac{T_r}{100}\right)^4 - \left(\frac{T_{cr}}{100}\right)^4}{T_r - T_{cr}},$$

$\sigma = r_g/r_k$ is the relative radius of the combustion zone.

Equation (1.95) makes it possible to estimate the qualitative effect of various factors on the quantity of fuel vapor which does not take part in the combustion process around the liquid drop.

Thus, if it is assumed in accordance with diffusion theory that the relative radius of the combustion zone is constant for a given fuel and the given combustion conditions, it follows directly from Eq. (1.95) that the fraction of vapor participating in the

the combustion reaction decreases with decreasing drop size. In other words, the smaller the drop, the greater the quantity of fuel vapor entrained beyond the combustion zone. The temperature of the combustion zone has the opposite effect: the higher the combustion zone temperature, the greater the quantity of vapor which will burn in the immediate vicinity of the drop surface. Based on this and using the data on the temperature variation in the combustion zone as a function of time, it can be assumed that removal of vapor will be minimum during the initial period of drop combustion; as the process develops it is intensified, and this in combination with other causes, results in a lowering of the temperature in the combustion zone. The combustion characteristic k_g also plays an important part. For light fuels with high vaporization characteristic values the entrainment of the vapor will be correspondingly greater than for heavy fuels burning under the same conditions. It is understandable that estimating the combined effect of all factors is at present impossible because only isolated data exist on this problem, pertaining only to light fuels of the gasoline type.

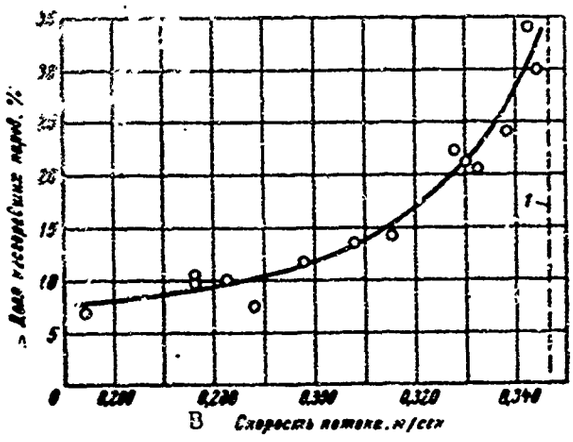

Fig. 31. Weight fraction of unburned fuel vapors as a function of the relative airstream velocity: 1) Flame breakaway. A) Fraction of unburnt vapors, %; B) air velocity, m/s.

Thus, as a result of an analysis of the effect of the finite chemical reaction rate on the characteristics of the combustion process for a fuel drop in [27, 29], the presence of considerable entrainment of the fuel vapors beyond the limits of the combustion zone is established. Experimental determination of the fraction of unburned vapors [27] was carried out by bubbling the combustion products of single drops of B-70 gasoline through a solution of sodium nitrate in concentrated sulfuric acid. On the basis of the color change in the reagent, which turned yellow when exposed to hydrocarbon vapor, the fact of the presence of such vapors in the combustion products was established. Quantitative determination of the fraction of unburned vapor for drops of B-70 gasoline, placed in a stream of air, showed that the fraction of unburned vapors

increased considerably with increase in the relative velocity of the air (Fig. 31). It is also pointed out that only part of the curve shown in Fig. 31 corresponds to combustion conditions under which the drop is completely enveloped by the flame. Even in this case, marked entrainment of the vapor can be observed.

Thus, analysis of the heat balance structure of the combustion zone around a single drop, burning in an infinite space, and also of the results of the experimental study of drop combustion, allow the conclusion that when fine drops of a volatile fuel burn under flame conditions, the combustion of single drops as well as that of the vapor in the space between the drops should be observed. The ratio of these two forms of combustion is determined, in particular, by the temperature conditions of the process and the atomization efficiency. The higher the temperature of the air which enters the combustion zone, the greater the fraction of fuel which burns in the vapor phase, if this is understood to mean the independent combustion of the vapor in the furnace. With heavier fuels and larger drops, the quantity of fuel vapor burning outside the combustion zone decreases and the flame itself acquires a more discrete structure.

We can expect that an increase in the air temperature and a marked improvement in the atomization efficiency during the combustion of heavy fuels will create favorable conditions for increasing the quantity of fuel vapor which leaves the individual combustion zones. In this case, not only the time required for the complete combustion of the drops will be shortened but also the transition to some extent of the regime of heterogeneous combustion to one closer to the combustion of gas mixtures, provided that suitable measures are taken to achieve this (for example, improving mixing within the flame). Otherwise, losses can occur because of chemically incomplete combustion.

Manuscript Page No.

Footnotes

24 The work was carried out under the guidance of Candidate of Physical and Mathematical Sciences, B.L. Zharkov.

Manuscript Page No.

Transliterated Symbols

5 ср = sr = sreda = medium

6 к = k = kaplya = drop

6 т = t = teploprovodnost' = thermal conductivity

7 ц = ts = tsentr = center

7 г = g = goryuchaye = fuel

7 к = k = konduktsiya = conduction

7 л = l = lucheispuskaniye = radiation

7 ф = f = fakel' - flame

13 в = v = ves = weight

16 п = p = poverkhnost' = surface

16 п.о = partsial'noye, okruzhayushchiy = partial, ambient

17 т = t = toplivo = fuel

18 р.о = r.o = raznost', okruzhayushthiy = difference, ambient

19 исп = isp = ispareniye = vaporization

19 т.к = t.k = toplivo kaplya = fuel drop

19 п = p = par = vapor

20 см = sm = smes' = mixture

20 в = v = vozdukh = air

21 в = v = vospiameneniye = ignition

22 р = r = [not identified]

23 инд = ind = induktsiya = induction

23 пр = pr = progrev = preheating

30 г = g = goreniye = combustion

35 ост = ost = ostatok = residue

35 кокс = koks = koks = coke

36 всп = vsp = vspyshka = flash

36 вн = vn = vneshniy = external

38 гор = gor = goreniye = combustion

54 р.т = r.t = raznost' temperatur = temperature difference

54 ст = st = stenka = wall

55 п = p = privedennyy = referred

Chapter 2

THE FLAME COMBUSTION PROCESS

6. FLAME STRUCTURE AND SEQUENCE OF THE ELEMENTARY PROCESSES

If one considers the drops present in a flame, the problem arises to what degree the sequence and the quantitative relationships of the partial processes in the combustion of the drop in a flame are preserved. The supply of the fuel to the furnace in a turbulent airstream and with various initial drop sizes at present makes extremely difficult the problem of ascertaining the features of the elementary processes in the flame. This complexity is determined mainly by the fact that in a given section of the flame at a certain instant of time, drops of various size are present, each of which is in a particular stage of the combustion process and the process of drop combustion itself develops under conditions of continuously varying temperatures, velocities and compositions of the medium.

The problem is simplified somewhat for the condition of a normal stationary flame burning in an airstream. In this case, with all external conditions being constant (velocities, temperatures, pressures and composition of the airstream and also the drop size), regions can be isolated in the flame whose parameters are time-independent and vary only from one section to another. Despite the extreme complexity and superposition of the individual stages, some basic general processes can be isolated which, for greater simplicity, are assumed to be mutually independent. These are usually considered to be the processes of formation of the mixture and the combustion of individual drops.

By mixture formation one usually understands the totality of the processes of fuel atomization in the airstream, the preheating and ignition of the drops. Very frequently, only the preignition processes are combined under the term "mixture formation," while the ignition of the drops is considered part of the combustion process. However, this does not introduce any important difference since the instant of ignition itself, i.e., the instant of the appearance of a visible flame, may be considered with equal justification as the initial instant of combustion or the end of the preparation process. The latter is more natural from our point of view. Following the ignition of the fuel, the totality of the physicochemical processes of vaporization in presence of a combustion zone around the drops, the thermal decomposition of the fuel vapor and of the substance of the drops, combustion and heat and mass transfer from the combustion zone into the ambient medium are usually included in the term "combustion."

The origin of these generalized concepts is found in the fact that in a burning stationary flame, as numerous direct observations have shown, at least three regions can be distirguished: a cold region or the section of the preflame processes, the core of the flame and the afterburning region. The flame front, i.e., the zone of sudden parameter variation in the fuel-air mixture, is usually taken as the boundary between the zone of the preflame processes and the flame core.

There is no clearly recognizable borderline between the flame core and the afterburning section and this borderline is usually established on the basis of indirect characteristics such as the beginning of smooth temperature decrease or decrease in the rate of the chemical reaction. The flame front also is not a strictly physical borderline between the zone of the preflame processes and the flame core since an intense increase in the temperature of the airstream is observed directly behind the flame front, attesting to the successive ignition and combustion of ever new portions of fuel. However, the choice of this borderline is convenient from a methodological point of view.

The process of mixture formation [30] can be schematically represented as follows: the stream of fuel drops from the spray nozzle moves relative to the ambient air. The initial velocity of the motion of fuel drops of various diameters is normally assumed to be the same and equal to the discharge velocity of the fuel or fuel-air mixture (in the case of airblast atomization from the spray nozzle. The trajectory and velocity of the subsequent motion of the drops will vary in dependence on the conditions of the fuel supply and the parameters of the medium. As a result of the preheating of the drops and their vaporization and also the diffusion of the fuel vapor into the ambient air, a fuel-air mixture is formed which is continuously enriched by vaporization of the fuel and which attains a concentration at which the rate of flame propagation becomes equal to the airstream velocity, thus determining the position of the flame front. If one takes into account that for hydrocarbon fuels of relatively light composition (gasolines, kerosene, diesel oil), the lower limit of stable combustion is determined by an excess air factor of ~3, the combustion concentration of fuel in the mixture is attained when approximately 30% of the injected fuel has vaporized. This indicates that only partial vaporization of the fuel can take place in the zone of the preflame processes, mainly at the expense of the small drops. A low content of small drops (coarse atomization) leads to later formation of the flame front and, with limited size of the furnace chamber, also to a reduction in the time available for completing the fuel combustion process.

A somewhat different point of view concerning the process of flame front formation (flame propagation process) is obtained if one considers the critical conditions for the ignition of a fuel drop, under the assumption that the ignition of adjacent, not yet burning drops and, consequently, also the flame propagation in a two-phase mixture, is possible when the induction period for the fuel vapor-air mixture forming around the not yet ignited drops is less than the lifetime of the drops already burning [31]. In other words, the ignition of the nonburning drop is achieved by the pro-

pagation of a spherical temperature wave from an adjacent burning drop. In this case, the space separating these drops may be filled with fuel vapor whose concentration is not sufficient for the formation of a combustible mixture. With this mechanism of flame propagation, the position of the flame front will be stabilized at a lower degree of fuel jet vaporization.

The study of the most general case of combustion, i.e., the combustion of a flame of atomized fuel, is still in the initial stage at present. It can merely be indicated that some authors [32, 33] are inclined to consider a burning flame as a continuous physical body whose characteristics vary continuously with time as a result of the processes of heat evolution and molecular interaction taking place within it. A model of the combustion process of atomized fuel is also proposed, analogous to the combustion process of a homogeneous gas-air mixture [32]. A group of fuel drops of equal size is introduced into an airstream (Fig. 32) whose motion takes place in the direction of the x-axis. In the interval between points A and B, these drops are distributed over the entire airstream and are ignited at point B. The process of mixture combustion taking place between points B and C, and the distributions of temperature and oxygen concentration correspond to the curves in Fig. 32.

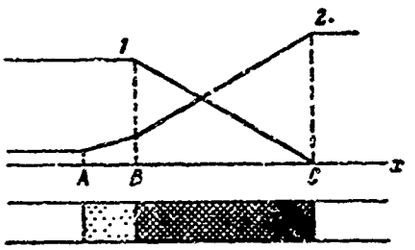

Fig. 32. Theoretical flame diagram after Kumagan: 1) Oxygen concentration; 2) temperature.

The combustion of liquid fuel is regarded as a process of the combustion of its vapor, the drops being considered merely as the vapor source. It is assumed that the rate or time of vaporization is determined by a constant corresponding to the vaporization conditions of single drops. On the other hand, the combustion of the fuel vapor, i.e., the chemical interaction between the fuel molecules and oxygen, takes place under condtiions of a quasi-homogeneous mixture at rates which depend on local concentratons, the reactants and temperature.

Another, basically opposite point of view on the development of the combustion process of atomized fuel is based on extending the laws of combustion of single drops to the combustion of the flame and taking a certain average drop size as the determining size [34, 35, 36]. By comparing these points of view it is easy to see that they proceed from two extreme cases: the process of combustion of a flame of atomized fuel is either reduced to the combustion of a homogeneous gas-air mixture and the combustion

of the individual fuel particles is neglected, or the flame is regarded as a simple accumulation of drops, none of which exerts any effect on the development of the combustion process of adjacent drops, and the possibility of the combustion of fuel vapor in the space between the drops is completely neglected. The problem as to which of these viewpoints is more applicable to the case of the flame combustion of heavy fuels can obviously be resolved by analysis of data on the structure of burning flames.

Investigations of flame structures in two-phase fuel-air mixtures have begun only very recently and the basic laws of the combustion process of atomized fuel have been insufficiently clarified to date. The basic problem in these investigations is to decide to what extent the laws discovered in the studies on the combustion of single drops can be applied under the conditions of their combustion in flames. The necessity for resolving this problem arises from the fact that the basic premises used in the analytical description of the process of the combustion of a single drop are correct either for very small or for large drops. Thus, for example, the assumption of spherical symmetry in the combustion zone is justified only for small drops where the convection currents arising around the burning drop do not play any significant part. On the other hand, the hypothesis of the stationary nature of the combustion process for the drop applies only to drops with larger diameter. Moreover, the ascertained dependence of the combustion constant on external conditions, such as the air temperature and the oxygen content indicates that the conditions of combustion of the drop in a flame must differ in some way from the conditions of its combustion in infinite space.

The investigation of the general structure of a flame of fuel atomized in turbulent air [37] showed first of all that such a flame is not homogeneous. Photography of a free flame revealed that with relatively long exposures (0.5 s), the entire combustion zone of atomized kerosene is uniformly luminous. As the exposure time is reduced, the general luminous background of the flame disappears and clearly distinguishable traces of burning drops in the form of bright bands appear against the continuous background of the flame.

Lowering the initial temperature of the mixture had the consequence that the general background of the flame was broken up into individual regions surrounding the bright tongues of flame. With further decrease in the temperature of the mixture and, consequently, also the initial concentration of the vapor phase, the background disappeared completely. Based on these data it is concluded that there is no continuous flame front at low initial temperatures of the mixture and at low fuel vapor concentration but that combustion of single drops as well as of their aggregates takes place [37]. When the temperature of the mixture and the initial concentration of the fuel vapor is increased, a continuous flame front can be formed. However, the individual foci of burning drops are preserved in this case as well.

Photographic exposures with great enlargement (19×) and using the principle of optical compensation made it possible to make individual fuel drops and the distances between them visible. It was found that the picture of the combustion zones is far more blurred

than the pictures of the drops. This indicates [38] that the combustion zones are more easily entrained by the turbulent pulsations of the airstream than the drops so that they can occupy the most diverse positions relative to the latter. Although individual combustion zones are formed around drops as well as around groups of drops, they do not all burn simultaneously. In Reference [39] it is pointed out that during the combustion of fuel under flame conditions, vaporization of the drops into the hot medium takes place in some cases with subsequent combustion of the fuel vapor at a certain distance from the drop. It should be remembered in any analysis of these data that they were obtained during studies on flames of comparatively light fuels (kerosene and gasoline) which have high vaporization characteristics.

The authors used the phenomenon of flame ionization for the study of flame structure in atomized diesel oil.

If two electrodes to which a certain voltage is applied are introduced into the burning flame, the conductivity of the interelectrode space is considerably increased by the ions formed in the flame. The ion concentration, in turn, will be determined by the properties of the fuel and the temperature and composition of the mixture [40, 41, 42, 43, 44].

As investigation results have shown, the ionization current, at the temperatures of the combustion products of kerosine, i.e., approximately 500°C, is an intermittent curve with individual pronounced peaks, the frequency and amplitude of which characterize the quantity and temperature of individual volumes of combustion products passing through the interelectrode space. The oscillographic trace of the ionization current (Fig. 33) attests to the existence of a certain constant component of the ionization current corresponding to the general ionization level of the combustion products and their temperature. The ionization current curve obtained for combustion products with a temperature of about 1000°C (see Fig. 33, A) does not have any separate and pronounced ionization current peaks such as were observed at lower temperatures. A study of the ionization current of a pulsating cold flame (~250°C) shows (see Fig. 33, C) that this flame consists of separate burning volumes of vapor, the number of which is not constant in time for any point of the flame. Oscillographic recording of the ionization current during ignition and combustion of atomized fuel in a turbulent airstream under various conditions generally gives the same pattern (see Fig. 33, D) with three clearly distinguishable regions typical for this process: a region of initial flame ignition, a region of flame propagation from the original combustion focus over the whole volume of the flame and a region of steady combustion. At the initial instant of time when the electric discharge takes place in the cold fuel-air mixture and ignites this mixture, the sensor records individual flashes of ionization current whose source is the electrical discharge itself (line 1 in Fig. 33). The ignition of the fuel can be judged from the lines of dynamic air pressure (line 3) which rises strongly at that instant. During the subsequent period, propagation of the flame from the initial focus over the flame volume takes place as indicated by the variation in the nature of the ionization current curve and the curve of the dynamic airstream pressure.

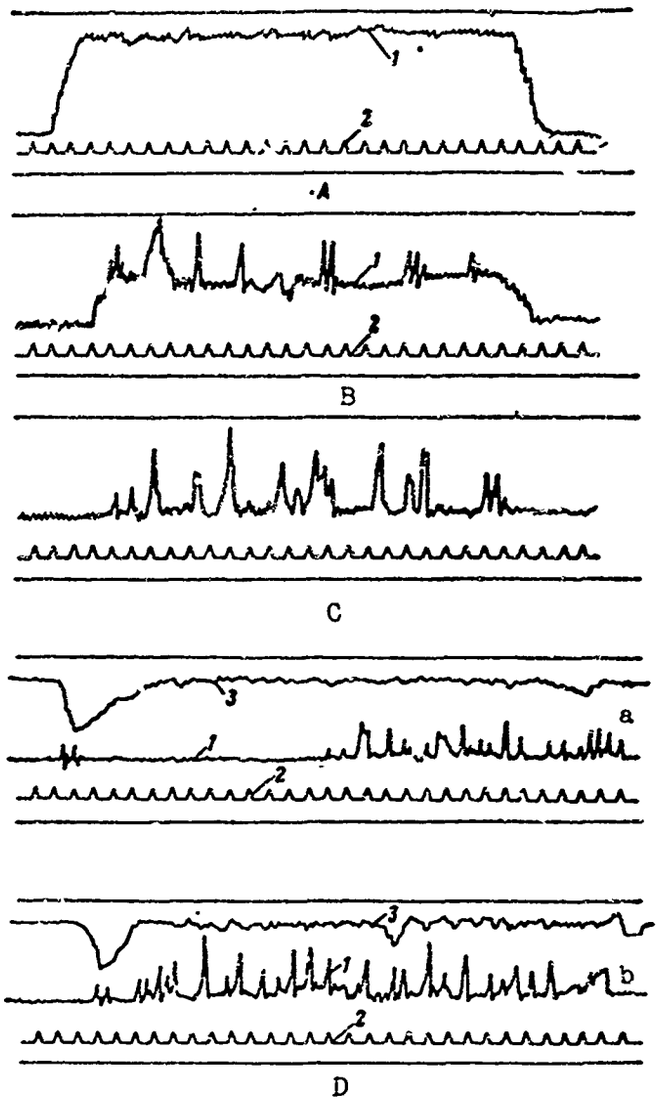

Fig. 33. Typical ionization current oscillograms: A) t = 1000°C; B) t = 500°C; C) t = 250°C; D) ionization current in a flame of atomized fuel. a) Lean mixture; b) rich mixture. 1) Ionization current; 2) time; 3) dynamic air pressure.

During this time, the sensor records individual, as yet weakly ionized volumes passing through it. In the region of the stationary process, the sensor records clearly separate ionizaton current peaks with considerably greater amplitude than in the retion of flame propagation. In this case, however, the lower limit of all flashes is the line of zero or initial ionization and the nature of the ionization current is analogous to that shown in Fig. 33, C. In the case of the ignition and combustion of a richer mixture (see Fig. 33, D) one observes a marked shortening of the period of flame propagation and also higher ionization currents.

The data obtained by the authors and other researchers in the study of ionization in atomized fuel flames, unfortunately, do not provide any means at present to determine the source of the pulsations in the ionization current: separate burning drops, group of these or separate large foci of burning vapor. These pulsations are ascribed to separate hot volumes of gas [44] because the size of the drops is much less than the dimensions of the sensing electrodes.

From our point of view the probability that individual burning drops can produce an ionization current is fairly great. It must be remembered here that what is important is not the diameter of the drops, estimated at 0.1-0.4 mm, and not even the radius of their combustion zone, which is 6-10 times greater than the drop size, but the region of high-temperature combustion products which extends around the drop to a distance of 20-40 drop diameters, which amounts to 2-4 mm, i.e., a distance comparable with the distance between the sensing electrodes.

Thus the results of the investigation into the structure of a burning flame of a two-phase fuel-air mixture (mainly of light fuels) permit the conclusion that the combustion of atomized fuel can take place in the form of combustion of separate drops or groups of drops as well as the combustion of a gas-air mixture. Direct data on the flame structure of heavy residual fuels of the petroleum and cracking residue type are not available. However, based on the data given in Chapter 1, it can be assumed with a sufficient degree of reliability that the process of combustion of a heavy fuel flame develops under conditions of a more discrete flame structure. This does not mean, naturally, that during the combustion of a heavy fuel the combustion of its vapor in the space between the drops is excluded. However, as follows from the data of Chapter 1, their quantity is determined not so much by the properties of the fuel as by the external combustion conditions, if by this is meant the temperature, velocity and composition of the air and also the size of the drops in the flame. Depending on these conditions, the quantity of fuel vapor which leaves the individual combustion zone of a drop of heavy fuel will vary in both directions, remaining, however, always much less than for drops of a light fuel under identical conditions. It follows from this directly that in the combustion of heavy fuels, the entire sequence of elementary stages, observed during the development of the process of combustion of single drops, is preserved in the main, although the duration of each of these stages will be affected by the presence of the other drops in the immediate vicinity.

7. PREHEATING AND IGNITION OF THE FUEL FLAME. MUTUAL EFFECT OF DROPS

As was shown in Chapter 1, one of the decisive factors which determine the preheating of the fuel drops in the initial region of the flame is the temperature of the gas medium. However, it is not yet possible to give an analytical expression for the laws of variation in airstream temperature in the zone of the preignition processes under real conditions. For the simplest conditions of flame preheating in a symmetrical stream with uniform drop distribution in front of the flame, the temperature variation in the stream can be approximately described by an equation

of the form

$$t_{cp} = t_0 + (t_\phi - t_0)\exp\left(-\frac{wx}{a}\right), \qquad (2.1)$$

where t_{sr} is the temperature of the airstream at a distance x from the flame front; t_0 is the initial temperature of the airstream; t_ϕ is the temperature in the flame front; w is the velocity of the airstream along the normal to the flame front; a is the thermal diffusivity of the medium.

Analysis of this equation shows that the temperature at each point of the preignition region of the flame is the higher, the higher the initial temperature of the airstream and the flame front. Increasing the velocity of the stream lowers this temperature. The combined effect of these factors has the result that the region within which an intense temperature rise is observed is relatively narrow and that the preheating of the drops is mainly determined by the initial temperature of the airstream. This is of very great significance for heavy fuels since much higher air temperatures are required to accelerate their preheating (see Chapter 1, §2). Accelerated preheating of the fuel flame is achieved primarily by increasing the initial temperature of the airstream and by intense turbulence. Both these problems are solved in practice by producing a rotary motion of the airstream by means of various types of turbulent flow devices, mainly vane impellers. For practical calculations it is normally assumed that the air temperature in the input part of the heating device remains constant and ranges for various designs of frontal structures and furnace chambers from 600 to 1000°C. Under these conditions, the preheating of the fuel jet can be approximately calculated in accordance with the laws of preheating and vaporization of single drops of liquid fuel, given in Chapter 1.

Highly interesting in the discussion of the preheating of the fuel jet is the role of radiative heat exchange in the total process of drop heating. The amount of direct data in the literature on the effect of the radiant heat flux from a burning flame in the process of heating of individual drops is extremely small. Thus, for example, it follows from the data presented in Chapter 1, §1 and in [45, 46] that the fraction of the heat radiation for each drop is negligibly small because the drop sizes are very small. However, in a real flame the quantity of such fine particles is fairly large and under certain conditions they can, as a whole, form a large heat-absorbing area.

Theoretical examination of this problem shows [47] that if a mixture consisting of a large number of small drops is subjected to the volume effect of radiative heat flux, each particle receives radiation from all sides because of the strong scattering of this flux by the other particles. Hence the particles of vaporizing liquid are rapidly heated and this intensifies vapor formation. Under the real conditions of preheating a fuel flame, the effect of the radiative component is clearly exerted only on the drops in the direct vicinity of the flame front, whereas the more remote drops are shielded by this layer to a considerable degree.

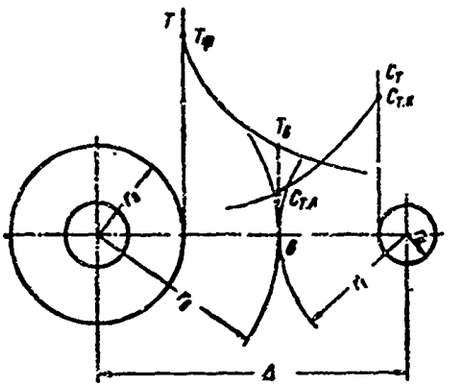

Fig. 34. Schematic representation of flame propagation in a two-phase mixture: Δ) distance between drops; r_g) radius of combustion zone, r_v) distance from the center of the burning drop to the ignition point; r_k) radius of unignited drop; $C_{t.k}$) fuel vapor concentration at the surface of an unignited drop; $C_{t.v}$) fuel vapor concentration at the ignition point; T_f) combustion zone temperature; T_v) ignition point temperature.

The ignition of the fuel flame is determined primarily by the conditions of flame propagation in the space between two adjacent drops. In accordance with [9] let us consider the idealized ignition conditions for a fuel drop located in the immediate vicinity of a burning drop. We assume that the distance between the centers of the drops is Δ, that this does not vary with time and that all processes take place in the absence of any convection (Fig. 34). The temperature field around the burning drop can be approximately described by an equation of the form

$$T = T_г\left(\frac{r_к}{r_г}\right)^{0.5}, \qquad (2.2)$$

where T is the temperature at a point in the space around the drop, determined by the instantaneous radius r_g; T_g is the temperature in the combustion zone, and r_g the radius of the combustion zone.

The distribution of vapor around the unignited drop can be characterized by the relation

$$C_г = C_{г.к}\frac{r_к}{r_1}, \qquad (2.3)$$

where $C_{t.k}$ is the vapor concentration at the surface of the unignited drop; r_k is the drop radius and r_1 is the current radius which characterizes the point in space under consideration.

The radius r_1 is correspondingly equal to

$$r_1 = \Delta - r. \tag{2.4}$$

The concentration of fuel vapor at the point in space with the temperature T can be calculated as

$$C_T = C_{T.K} \frac{r_K}{\Delta - r}. \tag{2.5}$$

At this point, the induction period of the fuel vapor is determined by the equation

$$\tau_{инд} = \frac{\Delta - r}{zC_{T.K} r_K} \exp\left(\frac{E\sqrt{\frac{r}{r_K}}}{RT_T}\right). \tag{2.6}$$

We seek the point in space where the induction period is at minimum. The coordinates of this point can be obtained by extremum analysis of Eq. (2.6). In this case, the radius r_V of the ignition point is expressed as

$$r_в = \frac{(z\Delta + \Omega) - \sqrt{4\Omega\Delta + \Omega^2}}{2}, \tag{2.7}$$

where

$$\Omega = \left(\frac{2\sqrt{r_T} RT_T}{E}\right)^2. \tag{2.7a}$$

The distance between the drops for the case of uniform distribution of the drops in space can be expressed by the excess air coefficient α

$$\Delta \simeq d_K \sqrt[3]{\alpha L_0 \frac{\gamma_T}{\gamma_в}}, \tag{2.8}$$

where γ_V and γ_t, respectively, are the specific gravity of the fuel and the air; Z_0 is the quantity of air theoretically required for combustion per unit weight of fuel.

The ratio of the combustion zone radius to the drop radius can be assumed to be constant, i.e.,

$$\sigma = \frac{r_T}{r_K} = \text{idem}. \tag{2.9}$$

Taking into account (2.9) and (2.8), we see that the coordinates of the ignition point are a function of the drop radius and the air excess. By introducing Expression (2.8) into the equation for the induction period, we obtain, after transformation, the following:

$$\tau_{инд}^{min} = \frac{1}{zC_{T.K}} \cdot f(\alpha), \tag{2.10}$$

where $f(\alpha)$ in turn is determined by the quantities

$$\theta = \frac{RT_r}{E} \text{ and } \eta = \sqrt[3]{L_0 \frac{\gamma_r}{\gamma_a}}. \qquad (2.10a)$$

Using the critical condition for the ignition of a fuel drop in a flame as an equation for the combustion time of the drop and the induction period of the fuel vapor, it can be shown that with increasing drop diameter the lower limit of flame propagation is shifted in the direction of large excesses of air. In other words, stable ignition of large drops, other conditions being equal, is achieved when the distance between them is large.

Of some interest is the problem of the initial ignition of the fuel flame. In the specialized technical literature which deals with the problems of the organization of combustion processes, the problem of the initial ignition is usually considered as secondary because the ignition of the fuel jet in any heating device, whether this is the furnace of a boiler or the combustion chamber of an engine, is effected from a secondary source (pilot flame, sparkplug, etc.).

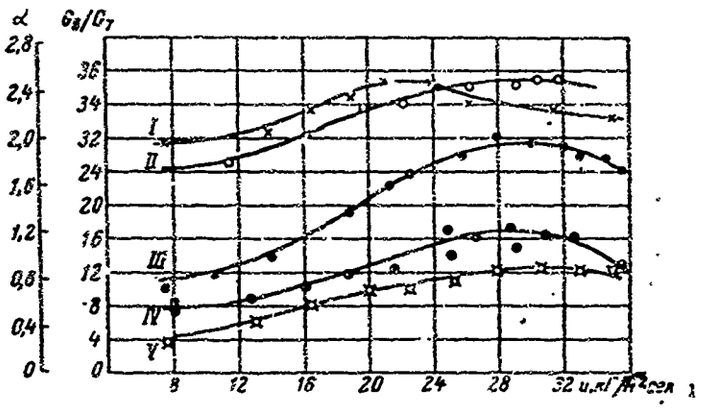

Fig. 35. Lower limit of flame propagation in a two-phase mixture as a function of the airstream velocity: I) Kerosene; II) diesel oil; III) mixture of 75% diesel oil (D) and 25% petroleum residue (M); IV mixture of 50% D and 50% M; V) mixture of 25% D and 75% M. 1) $kg/m^2 \cdot s$.

In heating devices designed for prolonged continuous burning of the flame in a space surrounded by incandescent walls, the initial ignition and its reliability are indeed of secondary importance. However, the role and importance of the initial ignition increases immeasurably for heating devices whose operating conditions require frequent stops and where the combustion process takes place in a completely shielded space, with walls whose temperature and capacity for heat accumudation are inadequate to make spontaneous ignition of the injected fuel possible. These heating devices include the combustion chambers of gas turbine engines,

particularly of the transport type, the furnaces of automated heating devices with relatively small capacity, industrial furnaces, etc. Small pilot flames, nozzles or special electrical igniters have been installed in recent times even in large furnaces to ignite the flames of the main burners in the case of flame interruption. Observations of the process of initial ignition for a flame of atomized liquid fuel, carried out by the authors on a model whose forward section was equipped with long high-voltage sparkplugs, have shown that stable ignition of the flame in each specific case occurred only at a certain fuel-air ratio.

Curves were obtained for various versions of air flow rate and fuel grades, which show the region of stable ignition of the investigated fuels under given conditions (Fig. 35). The experiments show that the range of stable ignition for various liquid fuels is narrowed with deterioration in fuel grade. With all the investigated fuels, the limit of stable ignition increases to a certain value with increase in the air flow rate and degree of turbulence of the airstream (Re = 20-100,000) and then decreases again. The widest range of stable ignition is obtained by the use of kerosene and diesel fuel and the narrowest by the use of fuels similar in composition to the light petroleum residues. From Fig. 35 follows also that the hydrodynamics of the airstream exerts significant influence on the process of primary ignition of the flame. With increase in the degree of turbulence of the airstream, characterized by the Re number, the conditions for the formation of the mixture and the ignition of the fuel at higher air excess values are improved. It can be assumed that at high airstream velocities and low fuel flow rates, the formation of local foci of inflammable fuel-air mixtures is possible in the discharge region whereas the entire volume of the heating device below the airstream is filled with a lean mixture outside of the ignition range.

The above-discussed mechanism of flame propagation in a two-phase mixture makes it possible to account for the phenomena observed during the period of primary ignition (in particular, the appearance of alternating flashes) by the fact that during the initial period the distances between individual groups of drops are above critical. In this case a flame focus arising in the discharge region cannot be propagated over the entire flame. Propagation of the flame becomes possible only when increased fuel consumption results in an increase in the spray density and, consequently, to a shortening of the distance between the drops to the required value. Since the formation of the cloud of fuel vapor around a drop of heavy fuel requires more time than for light fuels, the distance between the drops must be smaller, and this is possible only with higher fuel consumption (with richer mixtures). An increase in the turbulence of the airstream initially has a positive effect because the flame focus which has appeared and the unignited drops are given a relative motion toward each other, which shortens the distance between them. A further increase in the turbulence and translational velocity of the airstream improves mixing, but at the same time shortens the contact time between the burning and nonburning drops, which shifts the boundary of stable ignition in he direction of richer mixtures.

The boundary variations in the stable ignition region with

deterioration in fuel quality is also explained by the fact that the process of flame propagation from a local focus takes place by heat transfer to adjacent nonburning drops. For heavy fuels, successive ignition of the drops can be attained only when they are closer together or when the burning and nonburning drops are in loner contact, which is achieved by efficient atomization and large fuel consumption.

8. DROP COMBUSTION TIME IN A FLAME

As shown in the foregoing, the general sequence of elementary stages in the combustion process during the combustion of a single drop in the flame should be preserved, although the duration of these stages will be directly affected by adjacent drops, thus modifying the combustion conditions. This change in conditions is characterized, on the one hand, by a variation in the temperature conditions of the processes of preheating, vaporization and combustion for each drop and, on the other hand, by a variation in the combustion conditions for the fuel vapor owing to the decrease in the percentage oxygen concentration in the ambient medium. The presence of several simultaneously burning drops in the vicinity of a nonburning drop promotes its rapid preheating and intense vaporization. The fuel vapor thus formed can ignite and burn only when there is a sufficient quantity of oxygen around this drop. However, this may not be the case if the oxygen in the vicinity of the drop is consumed in maintaining the combustion of the adjacent drops. Thus, in this case, the processes of fuel preparation are intensified, whereas the process of fuel-vapor combustion is slowed down, if not completely stopped, and the drop is then subjected to vaporization only. The presence of turbulent pulsations with high intensity can also result in detachment of the combustion zone from the drop and thus modify the combustion conditions for each drop. The combined effect of all these factors obviously cannot be

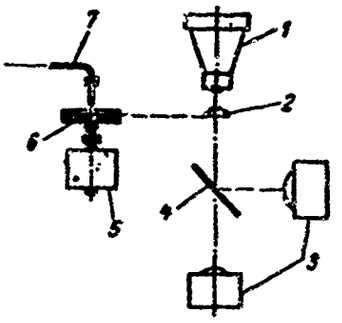

Fig. 36. Schematic representation of apparatus for the study of the combustion of a flat flame of atomized fuel: 1) Camera; 2) flame; 3) strobe lights; 4) semitransparent mirror; 5) air turbine; 6) disk atomizer; 7) fuel supply.

analytically expressed so that the study of the laws of combustion of a drop in a flame is carried out only experimentally. Investigations of the features of combustion in a fuel drop under conditions

of light fuel flames [48, 49, 50] showed that in this case the relationship between the square of the drop diameter and its combustion time is basically retained. However, the magnitude of the combustion characteristic differs from that for a single drop. An estimate of the combustion characteristic [49] for the case of combustion of a group of drops with approximately equal initial diameters shows that the value of k is about half that for the conditions of a single drop. These data were obtained by photographic recording of the drop size in an apparatus which is shown schematically in Fig. 36. Uniform atomization with regard to drop size was achieved by rotating (8000 r/min) a disk atomizer which yielded an average drop size in the flame of 90-100 μm. The fuel drops formed at the edge of the disk atomizer, during their motion in horizontal trajectory, passed through a small flame of a gas burner which ignited the drops, forming a flat flame. Part of this flame was photographed at certain time intervals in the transmitted light from two alternately actuated strobes. By means of these photographs, the mean velocity of the drops and the nature of the variation in their initial diameter could then be determined.

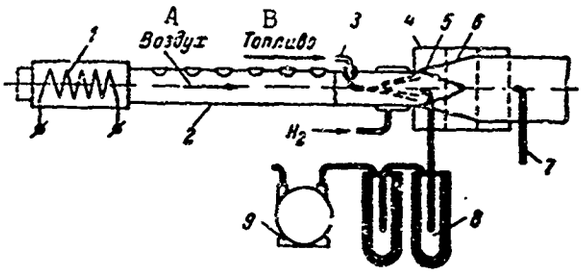

Fig. 37. Schematic view of apparatus for the study of the combustion process of atomized fuel in a turbulent airstream: 1) Electric motor; 2) tube; 3) nozzle; 4) pilot flame; 5) turbulent mixing device; 6) combustion chamber; 7) sampler; 8) liquid nitrogen traps; 9) gas meter. A) Air; B) fuel.

An analysis of the data presented in [49] reveals the existence of a linear relation between the square of the drop diameter and its combustion time. The slope of the corresponding curves indicates the invariability of the combustion constant for a given fuel type. Comparison of the combustion constants obtained in [49] with the corresponding values for single drops shows that the value of k for drops buring in a flame is approximately half that of a single drop buring in an infinite medium.

A slightly different method of investigating the special features of drop combustion under flame conditions was used in [50]. Simultaneous use of gas analysis and photography of the drops made it possible to trace the time variation of the completeness of combustion of atomized fuel. The apparatus is schematically shown in Fig. 37.

Analysis of the number and sizes of fuel-drop images along the streamline [50] gave us an idea of the nature of time varia-

tion in the mean drop diameter. The variation of this diameter characterized the quantity of fuel vaporizing in the various sections of the flame, while the sizes and numbers of drop images at each point of the flame make it possible to judge the quantity of unburned fuel.

An analysis of the gaseous combustion products at these points of the flame makes it possible to determine the portion of the fuel that has been burned on the basis of the quantity of CO_2 and CO. Comparison of these data made it possible to trace the nature of the combustion process along the streamline and, consequently, the variation in time. Despite some scatter of the points, there is no great difference between the completeness of combustion of the fuel as determined by the two independent methods. The quantity of vaporized but unburned fuel is practically nil or negligibly small.

The mean value of the combustion characteristic for the investigated operating conditions is smaller by a factor of approximately 1.5 than in the tests on single drops. However, they are in fairly good agreement with the experimental data on the combustion characteristic of a fuel drop which forms part of a group of drops [50].

An analysis of the images also shows that the lifetime of fairly small drops (20-60 μm) in a turbulent flame can be several times longer than their combustion time under conditions of an infinite medium. The difference between the lifetime of the drop in the flame and its combustion time is considerably reduced with increase in the initial diameter. This is explained by the absence of simultaneity in the ignition and combustion of all fuel drops which enter the burning flame and it is proposed to take this into account by introducing into the original equation of drop combustion the probability function

$$d_0^2 - d_\tau^2 = k\tau f(p), \qquad (2.11)$$

where $f(p)$ is some probability function.

The largest values for $f(p)$ are found for large drops which, owing to their great inertia, virtually do not react to the turbulence pulsations, in consequence of which the combustion zone around them is the most stable. For small drops, the combustion probability also increases with time and is virtually equal to unity in certain flame sections.

Thus, the results of the investigations into the features of drop combustion under flame conditions provide a basis for the assumption that during the combustion of atomized fuels the combustion time of the largest fuel drops corresponds approximately to that for single drop combustion whereas the combustion time of the small drops may considerably exceed the combustion time of the single drop. Drops of medium size obviously burn with a combustion constant smaller by a factor of 1.5-2.0 than under the conditions of a single fuel drop. It must be emphasized here that all these results were obtained in studies of the combustion process of fuels such as benzene, gasoline or kerosene. However, data on the combustion time or rate of a drop of heavy fuel under flame

conditions are not yet available.

9. FORMATION OF SMOKE AND CARBON DEPOSITS DURING THE COMBUSTION OF HEAVY FUELS

One of the features of the combustion process of atomized heavy fuels in furnaces for the most diverse applications is the considerable smoke content of the combustion products and the copious formation of carbon deposits on relatively cold surfaces of the furnace or gas conduits.

A large number of theoretical and experimental works [51-60] is devoted to research into the physical properties of smoke and carbon deposits as well as the causes of their formation. Despite this, accurate concepts of smoke, deposits, soot and other solid residues of the incomplete combustion of liquid fuel have not yet been developed.

Smoke is a term conventionally applied to solid particles of carbon which are ejected into the atmosphere together with the gaseous combustion products, and carbon deposits are the part of the unburned fuel which is deposited on the cold surfaces of the furnace chamber or gas conduit together with ash.

Despite its artificiality, this division of concepts in principle gives an indication concerning the two independent sources or causes of the formation of smoke and carbon deposits.

The fuel vapor formed at the drop surface is subjected during its motion toward the combustion zone to further heating by the surface temperature of the drop to the temperature of the combustion zone. The temperature of the drop surface during combustion does not exceed 400-500°K; whereas the average temperature of the combustion zone amounts to 1800-1900°C. Thus, the conditions of existence of the fuel vapors up to the instant of their combustion correspond to the conditions of intense cracking and high-temperature pyrolysis.

The basic cracking reaction of low paraffin hydrocarbons is decomposition of the carbon skeleton with formation of free radicals which react with undecomposed molecules, causing their dehydrogenation and the formation of unsaturated hydrocarbons of the olefin type. The multiatomic (higher) homologs of methane are split into molecules of saturated and unsaturated hydrocarbons of lower molecular weight. This process is also accompanied by the splitting off of a certain number of hydrogen atoms. The decomposition of the unsaturated hydrocarbons proceeds more readily and in turn is accompanied by evolution of hydrogen in consequence of the reaction between the free radicals and the molecules. The dehydrogenation of the olefins and the synthesis of aromatic hydrocarbons begins at 700°C.

Ethylene at 1400°C is almost completely dehydrogenated to acetylene, the simplest of the aromatic hydrocarbons. As a result of the chemical transformation processes, a fairly strong dehydrogenation takes place, i.e., copious evolution of hydrogen. At higher temperatures, the hydrocarbons decompose further as they

approach the combustion zone. The possibility of the complete decomposition of molecules with the formation of free carbon and hydrogen cannot be excluded. Based on these ideas, it can be assumed that the combustion process of the fuel vapor develops in the following way. As a molecule of hydrocarbon with fairly complex composition moves into the combustion zone and is heated, it is decomposed with loss of a certain number of hydrogen atoms. The freed valency bonds of the carbon combine, forming unsaturated compounds. Further heating leads to further dehydrogenation of the molecule and the formation of free carbon.

In the reaction zone, the hydrogen combines with atmospheric oxygen. The energy liberated during this is partly consumed in the breaking of bonds between the carbon atoms which can then combine with oxygen. In consequence of a possible local oxygen deficiency the unreacted carbon atoms should move further away from the combustion zone into the ambient medium which is richer in oxygen. During this motion, the temperature of the medium drops; the rate of the temperature decrease is entirely determined by the external conditions.

The carbon bonds may then again join, forming stable carbon compounds which cannot combine with oxygen under these conditions. Thus it can be assumed that smoke is always formed in the combustion of any industrial fuel, be it gasoline or fuel oil burned in atomized form. Differences in the grade of the fuel and its structure mainly determine its greater or lesser tendency to smoke formation.

As the smoke forms in the outer part of the combustion zone it would be natural to assume that by creating suitable conditions for the complete combustion of the smoke (oxygen and high temperature) smoking can be considerably reduced or completely eliminated. As investigations showed, a jet of smoke formed in a diffusion flame was readily burned in a secondary Bunsen flame [60, 61]. It was also found that maximum smoking of furnaces is observed during the kindling period when the walls enclosing the flame are cold and the heat radiated by the flame is completely absorbed by them. As the furnace heats up, smoke formation diminishes and may disappear altogether under certain conditions.

When examining the conditions for the formation of carbon deposits, a distinction must be made between the deposits which form on cold surfaces and the unburned fuel which is entrained with the combustion products. The carbon deposits observed on the walls of furnace chambers and gas conduits is of very diverse composition, forming either a soft downy deposit or hard, brittle coatings.

A microscopic study of carbon deposits [53] showed that soft deposits consist of almost spherical particles embedded in an amorphous binder substance, while the hard deposits are a vitreous substance. It is assumed that solid carbon deposits consist of petroleum coke, formed as a result of liquid-phase cracking, subsequent pyrolysis and, finally, coking of the fuel which has come into contact with the wall. The wall temperature plays an important part in this [62, 63, 64]: if it exceeds 450-500°C, deposits of carbon are not observed even during the combustion of heavy fuels. In real flames the process of complete drop combustion, by virtue of some

or other circumstances (inadequate atomization, low temperature level of the process, etc.) may not terminate within the furnace volume and in this case the partly or completely coked drop will be entrained into the atmosphere together with the gaseous combustion products or precipitated on the furnace of gas conduit surfaces of the boiler.

This brief discussion of the conditions of formation of smoke and carbonaceous deposits thus allows the conclusion that during the combustion of heavy hydrocarbon fuels in general and, particularly, of fuels rich in aromatic substances, smoke is always formed and its subsequent elimination is determined by the external conditions, i.e., the presence of oxygen and high temperature. The formation of scaling is determined by the properties of the fuel, mainly its content of tar-asphaltene substances as well as by the combustion conditions which in turn are determined by the quality of atomization, the temperature and hydrodynamics of the flame. These factors exert a direct influence on the time required for the complete combustion of the liquid phase and the coke residue within the furnace volume.

On the basis of these assumptions one has to be very careful with regard to various "radical" methods of combating the formation of smoke and carbon deposits during the combustion of liquid fuel, publicized fairly frequently in the recent literature (continuous electrical discharge [65], steam sirens, etc.).

These methods to combat the formation of smoke and carbon deposits during the combustion of heavy fuels were based on the desire to improve and accelerate the combustion process of each drop by acting on it from without, for example, by a high-voltage discharge or high-frequency sound vibrations. In the first case it was thought that the electric discharge with its enormous energy instantly breaks up all molecules of heavy hydrocarbons with formation of a large number of active particles and the evolution of a large quantity of heat. These particles and the high-temperature wave propagating from the discharge zone should serve as some kind of activator. However, as special tests carried out by the authors have shown, such an effect is not observed within a very wide range of variation in furnace loads and combustion conditions.

By using high-frequency vibrations (produced by steam sirens, etc.) for the intensification of the combustion process of atomized fuel, it was hoped to achieve an effect of combustion acceleration through an improvement in the supply of oxygen from the ambient air and by accelerated removal of the combustion products from the combustion zone with vibrational motion of the air around the burning source. This proposal is correct in principle since it corresponds entirely to the experimental data obtained in the study of the combustion of moving drops. For the flame as a whole, however, it is less convincing. The fact is that a sound wave is subject to considerable modification when it passes through a medium of different density, such as a burning flame. The combustion zone around the individual drop is a very effective shield for the sound waves. A large number of drops located around the source of the sound waves represents a shielding zone which prevents the vibrations from penetrating into the depth of the flame. An experimental check

of this hypothesis, carried out by the authors in a booster chamber, completely confirmed this assumption.

From our point of view, the most effective means of combating smoking and formation of carbon deposits is the correct management of the combustion process, based on accurate knowledge of the laws of combustion of liquid fuel and all its stages. Practical means of combating smoke and deposit formation are a high process temperature level, efficient atomization and thorough mixing.

10. COMBUSTION OF LIQUID FUELS WITH MODERATE AND HIGH SULFUR CONTENT

The use of liquid fuels with moderate and high sulfur content, the percentage of which in the nation's fuel balance is increasing steadily, has revealed great technical difficulties at large power stations in connection with the intense wear of the heating surfaces and their corrosion. The ash formed on combustion of fuels with moderate and high sulfur content is deposited on the convective heating surfaces and reduces their performance efficiency which results in a lowering of the general economic indicators of the entire installation. Moreover, ash deposits and corrosion greatly reduce the reliability and service life of the outlet surfaces in contact with the waste gases and thus of the entire unit [66-69].

The most comprehensive and systematic data on the performance of boilers operating on high-sulfur fuels are given in [69]. In the PK-10 steam boiler furnaces (230 tons/h, 100 kgf/cm^2, 510°C) and in the BKZ-210-140F (210 tons/h, 140 kgf/cm^2, 570°C), stabilized high-sulfur crude oil from the Arlan deposit with a sulfur content of ≈3% and sulfur-rich petroleum residues of the M20-M40 grades from the Ufa NPZ [petroleum production plant] were burned. The furnaces of these boilers were equipped with burners and frontal switchchambers (540 mm diameter for the PK-10 boiler and 530 mm diameter for the BKZ boiler) and with centrifugal spray nozzles with a fuel capacity of 1100-2500 kg/h.

Observation of the combustion process showed that the visible flame virtually filled the entire furnace space and terminated 1-2 m from the hingle plate.

The temperature in the core of the flame was virtually independent of the type of fuel and varied within the range of 1600°C (crude) and 1660°C (petroleum residue). However, the temperature field was greatly modified on transition from crude oil to petroleum residue. During the combustion of Arlan crude oil the flame became shorter and the temperature gradient along the flame was steeper than in the petroleum residue flame. With decreasing α, the length of the flame increased slightly. At the same time it was found that the location of the burners greatly affects the temperature distribution within the flame.

By variation of the air flow rate with simultaneous sampling of the combustion products and the determination of their gas components, the authors of [69] were able to establish that under certain conditions of combustion of petroleum residue (insufficient

turbulence of the air and other factors), heat loss due to chemically incomplete combustion can occur even in presence of considerable air excess. Thus, chromatography revealed the presence of H_2, CO and CH_4 in the combustion products; a curve of the losses as a function of the chemical incompleteness of combustion in the presence of excess air was plotted on the basis of the data thus obtained (Fig. 38). The heat losses due to mechanical incompleteness of combustion during the combustion of petroleum residue amounted to 0.05-0.1% and with Arlan crude oil amounted to 0.01% and less.

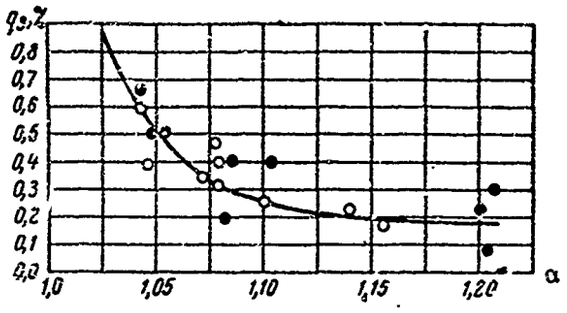

Fig. 38. Heat loss as a function of chemical combustion incompleteness in presence of excess air. Q = 110-130·10^3 kcal/m^3·h. Various nozzles. Petroleum residue and Arlan crude oil.

As in other works, the intense wear of the convective heating surfaces is pointed out in [69]. Thus, when sulfur-containing petroleum residue of the M20-M40 grades – atomized by means of a centrifugal nozzle – is burned, a considerable increase in the flow resistance of the gas conduit (25 mm per 1000 h of work) is observed despite protectie measures which had been taken (sand-blasting and introduction of magnesite into the convection part of the boiler). When Arlan crude oil was burned without sandblasting and magnesite, ash deposition was intensified and the flow resistance of the boiler gas conduits increased to 30 mm per 1000 h of operation.

The foregoing and other examples of the combustion of fuels with average and high sulfur content above all indicate the fact that the process of their combustion does not differ in principle from that of low-sulfur fuels. However, even at a relatively low ash content in the sulfur-containing fuels, the ash deposits formed on the convective heating surfaces with the conventional methods of combustion of these fuels lead to considerable trouble in the operation of the heating device and the entire installation and to lowering of the operational economic indicators.

An analysis of the ash deposits shows that with higher original fuel sulfur content, ash acidity is increased, which, moreover, also increases as the flue gases move through the gas conduits of the boiler [70, 71].

The basic difference between the deposits formed in the com-

bustion of sulfur-containing fuels and the deposits formed in the combustion of low-sulfur petroleum residues is the high content of vanadium in the form of the pentoxide V_2O_5 in the former [72, 73]. Because an increased sulfur content in the ash of the original fuel is accompanied by an increased vanadium content, the following forms of corrosion caused by the ash deposits are possible and actually observed with the usual methods of combustion of sulfur-containing fuels: high-temperature (vanadium) corrosion and low-temperature (sulfur) corrosion

High-temperature (vanadium) corrosion arises through interaction of vanadium-containing ash particles with surfaces at a temperature above 600-650°C. The exact mechanism of the corrosive effect of the fuel ash containing vanadium has not yet been determined. However, the presence of vanadium pentoxide V_2O_5 in the ash, which usually also contains sodium oxide makes it probable that the corrosive effect of the V_2O_5 on the metal results from the melting of the protective oxide film. In this case the V_2O_5 plays the part of a catalyst.

Vanadium corrosion of boiler surfaces is relatively rarely encountered nowadays because the wall temperatures of steam superheater tubes hardly ever attains the critical value of ~600-650°C corresponding to softening of the V_2O_5.

As regards low-temperature (sulfur) corrosion, as indicated in the foregoing, this is virtually always observed in the conventional combustion of fuels with average and high sulfur content. This form of corrosion is due to the presence of sulfuric anhydride SO_3 in the combustion products leads to a considerable increase in the dew point so that the flue gases containing SO_3 during their passage through the relatively cold parts of the convective surfaces permit the combination of the SO_3 with water vapor, forming sulfuric acid. Under these conditions, part of the surface with a temperature below the dew point sweats (water economizer and entrance section of the air preheater). In consequence, the fly ash sticks to these surfaces and sulfuric acid corrosion occurs under this ash layer. Beginning at isolated points, the sweating and ash deposition zone extends to adjacent regions leading to complete clogging of the entire first preheater stage.

Several methods are currently used to combat ash deposits and corrosion of the heating surfaces when liquid fuels with average and high sulfur content are burned.

The first method, borrowed from the practice of the combustion of low-sulfur liquid fuels, consists in trying to eliminate the deposits by periodic steam-cleaning of the heating surfaces, by washing them with water or by mechanical vibration of the surfaces of the coils. However, this method has been abandoned almost everywhere because of its very low efficiency. Cleaning by sandblasting is used at present [74, 75]. Practical experience with sandblasting equipment has shown that it is efficient in removing the deposits when they are not sticky. Although it prevents the formation of deposits, sandblasting is nonetheless not a very effective method of combating the sulfuric acid corrosion of low-temperature heating surfaces.

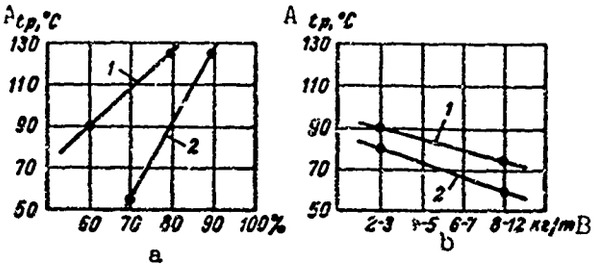

Fig. 39. Dependence of the dew point: a) On particle size; b) on magnesite dose. 1) MgO = 68%; 2) MgO = 76%. A) Dew point; B) kg/ /ton.

Another widely used method of fighting corrosion at the present time is the use of various kinds of additives. To prevent vanadium corrosion, small doses of VNII-NP-702 and other additives are added to the fuel, and these enter into chemical reaction with vanadium contained in the fuel ash and bind it. As a result, the softening temperature of the ash is considerably increased and the ash becomes friable, nonaggressive and can be readily removed from the surface. To prevent sulfuric acid corrosion in the gas conduits, additives are introduced to combine with the SO_3 formed during the combustion of sulfur-bearing fuels. Compositions with a fairly high content of calcium or magnesium oxide are normally used as such additives (slaked lime, 50-60% CaO; dolomite: a mixture of 30-34% CaO, 21-22% MgO and 38-48% CaO_2 [sic]; magnesite, 92% MgO and others).

Addition of 2-3% of the fuel weight of magnesite with an MgO content of 70% and ground to a dispersity of 18% and a mesh size of 88 μm lowers the dew point by 10-15°C [76]. The total effect of continuous use of magnesite additive in combination with periodic sandblasting is quite considerable: the corrosion rate of the metal is considerably reduced and the duration of boiler operation is increased two to three times. An increase in the fineness of the magnesite to 65 μm at the same dose lowers the dew points to 100-90°C. Increasing the MgO content to 76% at a fineness of 75 μm reduces the dew point to 70-80°C. An increase in the dose to 8-12% of the fuel weight gives a further reduction in the dew point of the fuel wight gives a further reduction in the dew point to 70-65°C (Fig. 39). However, the positive effect of the additive is explained not so much by the lowering of the dew point as shown in Fig. 39 as by the fact that the magnesite on the surface of the tubes combines chemically with the sulfuric acid, binding it and thus crying the surface. Hence, the ash particles do not stick to surface and can be readily removed. As concerns the measurement of the dew point, it was shown in [77] that the drying effect of the magnesite on the measuring head of the device led to a fictive lowering of the dew point. The very low magnesite content of the flue gases cannot greatly reduce the SO_3 content by binding and absorbing it on the magnesite particles since there is a volume of 20-40 cm^3 of flue gas for each average particle [77].

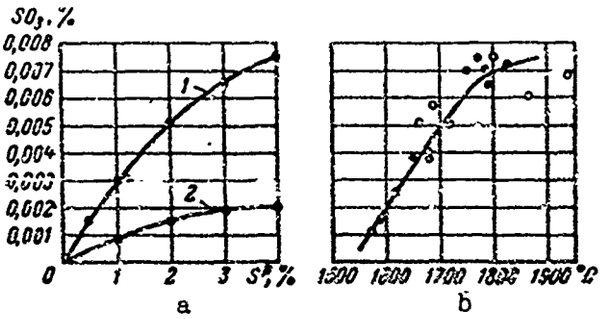

Fig. 40. Volume concentration of SO_3 in the flue gases as a function of: a) The sulfur content of the fuel; b) flame temperature. 1) t = 1200°C; 2) t = 1600°C.

Attempts were made in some cases to lower the dew point markedly by combined combustion of sulfur-bearing petroleum residue and gas. An attempt was made in the furnace of a TP-41 boiler to lower the SO_3 concentration in the flue gases during combustion of petroleum residue of the M40-M100 grades with a sulfur content of 2.5-3.4% by adding various quantities of natural gas [78]. However, a positive effect was not achieved although the proportion of gas was varied within wide limits (from 0 to 62%).

The above data point to the fact that both these trends in the fight against sulfuric acid corrosion, although fairly good when used in combination, are not promising because they are essentially passive methods which do not affect the mechanism producing the aggressive components of the combustion products and the ash. Moreover, the use of a whole complex of corrosion protection measures involves a considerable complexity in the general technological scheme and, consequently, an increase in the prime and labor costs.

A novel method of combating ash deposition and corrosion in the combustion of high-sulfur liquid fuels which differs in principle from the previous methods has found application in recent times. The principle of this method consists in conducting the combustion process of the liquid fuel with an absolute minimum of excess air (α = 1). This (at stoichiometric ratios) prevents the formation of sulfuric anhydride SO_3 and of vanadium pentoxide V_2O_5 in the combustion products. This assumption is based on the following facts. As numerous experiments have shown, the combustion products of sulfur-containing fuels contain, in addition to SO_2, the SO_3 formed in a quantity which depends on the sulfur content of the original fuel and the operating parameters air excess, temperature, etc.) which is illustrated by the curves of Fig. 40.

During combustion of sulfur-containing fuels, up to 5% of the total sulfur is transformed into SO_3 and the SO_3 concentration of the flue gas can attain 0.005% [79, 80]. The exact mechanism of

SO_3 formation during the combustion of the sulfur has not yet been completely established.

In sulfuric acid production, as we know, the SO_2 is oxidized to SO_3 only under certain conditions, i.e., presence of a suitable catalyst and relatively low temperatures since SO_3 is unstable at higher temperatures and decomposes at temperatures as low as $t \approx 1370°C$

$$2SO_3 \rightarrow 2SO_2 + O_2.$$

The data of [79] presented in Fig. 40, however, do not agree with this scheme. As the flame temperature increases, the SO_3 concentration in the combustion products increases [79] and at $t \simeq 1750°C$ approaches a certain constant value. The hypothesis has been advanced in several works [81, 82] that the SO_3 formation during the combustion of sulfur-containing fuels is determined by the catalytic effect of the sulfates, and the iron and vanadium oxide in the fuel ash and also in the top layer of the heating surfaces.

It is believed that the SO_3 is almost exclusively formed during the combustion process of the liquid fuel [83]. The SO_3 yield increases with increase in excess air and decrease of temperature. The gasification of the liquid fuel vapors moving into the combustion zone of each individual drop and the combustion of the coke residue as a function of the intensity of the air supply and the temperature level are accompanied by the evolution of CO, H_2, C_2H_2, CH_4 and other heavier hydrocarbons and by copious soot formation. Under these conditions, the formation of SO_3 is accompanied by reducing reactions of the $SO_3 + CO \rightarrow CO_2 + SO_2$.

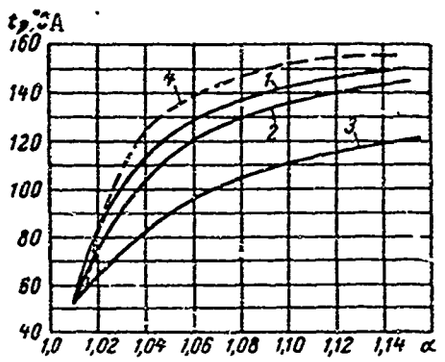

Fig. 41. Dew point as a function of the air excess: Data of [84]: 1) 3.2% S; 2) 2.42% S; 3) 1.33% S; 4) data of [69]. A) Dew point.

This mechanism of SO_3 formation, in our opinion, is not highly probable. It was found from numerous observations that the dew point of flue gases formed during the combustion of high-sulfur fuels, determined by the SO_3 concentration in them, is a strong function of the air excess [84, 85]. As follows from Fig. 41, the dew point of the flue gases decreases sharply with decrease in the air excess and at $\alpha \approx 1.0$ it becomes virtually equal to the dew

point of pure steam, regardless of the sulfur content in the fuel. This provided a basis for assuming that when fuel-air mixtures are burned at close to stoichiometric ratios, the sulfur content of the fuel is of no importance [84, 85]. Special investigations were carried out on the process of combustion of sulfur-containing fuels in steam boilers with extremely small amounts of excess air. The results of these investigations fully confirmed this hypothesis. Whereas earlier, with conventional combustion methods for liquid fuels with high sulfur content, despite measures to protect the surfaces exposed to the gases against wear and corrosion, it was not possible to prevent these altogether, all heating surfaces situated in the flue section of the boiler retained their metallic luster without the slightest sign of corrosion and the service life of the furnace was increased to 26,000 h when the combustion process was carried out at values of $\alpha = 1.01-1.02$. All additional equipment, installed in the boiler to combat wear and corrosion, was removed.

Thus, practical experience in the combustion of high-sulfur fuels with small air excess contradicts data in Fig. 40 and confirms the general mechanism of SO_2 and SO_3 formation in free oxygen at moderate temperatures. There are also grounds for assuming reduction of air excess has a positive effect on the high-temperature (vanadium) corrosion since the formation of V_2O_5 takes place in stages by successive oxidation of the lower oxides of vanadium. Since the lower oxides of vanadium have higher softening points than V_2O_5, the elimination of the possibility of its formation allows considerable increase in the temperature of the heat-absorbing walls between which the gases pass.

Despite its basic simplicity, the method of burning high-sulfur fuels necessitates the resolution of technological difficulties because of a need to maintain combustion efficiency. Indeed, in the fuel combustion with a minimum air excess there is the danger of great losses due to chemical and mechanical combustion incompleteness because of formation of local zones with evident deficiency of air. This is of particular importance in large-volume furnaces with a large number of burner devices. As the experiments of the VTI [Dzerzhinskiy All-Union Heat Engineering Institute] and of Bashkirenergo [69] showed, even with conventional methods of liquid fuel combustion, losses due to chemically incomplete combustion increase with greater nonuniformity in the fuel and air supply to individual burners (Fig. 42). Reducing the air excess increases these losses so greatly that the problem of uniform loading of the burners becomes dominant.

Moreover, the problem of mixing fuel and air in the furnace space assumes great significance when air excess is reduced. According to data in [69] great effect is achieved by increasing the air velocity at the nozzles to 80 m/s. In this case, the depth of air jet penetration becomes sufficient for satisfactory mixing in various parts of the flame. Improved mixing of the atomized fuel with air in the combustion space at low air excess can be achieved by providing stagewise supply of air to the flame, i.e., by controlling the combustion process in accordance with a scheme similar to that of gas turbine [GT] (ГТУ) chambers. Separation into primary and secondary air makes it possible to shorten consider-

ably the duration of the elementary stages of the process, to reduce the total flame length and to reduce the probability of the flame extending into the flue of the boiler.

Furthermore, in the combustion of atomized fuel with small air excess, it is necessary to maintain the prescribed combustion conditions during all variations of the load on the unit. These difficulties can be overcome only when a highly sensitive control system with low lag is available.

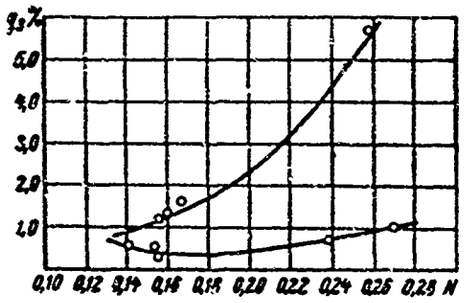

Fig. 42. Heat losses due to chemically incomplete combustion as a function of fuel and air distribution nonuniformity among the burners (BKZ-210-140F boilers, fuel, petroleum residue).

The positive effect of this control of the combustion process also includes a considerable saving in materials, primarily due to the fact that the large decrease in the dew point of the flue gas allows it to be cooled to a lower temperature. This gives a certain increase in the efficiency of the unit and corresponding fuel economy. The reduction in the air consumption of the furnace reduces the electric power required to drive the fans, which also has a positive effect on the total efficiency of the thermal power unit. According to the data of [86], the total saving achieved by changing the boilers to operation with low air excess is estimated to amount approximately to 20,000 to 60,000 dollars annually. The lower figure applies to the saving in the combustion of gas and petroleum residue and the larger figure, to the combustion of petroleum residue alone.

Manuscript Page No.

Transliterated Symbols

66 ср = sr = sreda = medium

66 Ф = f = front = front

67 г = g = goreniye = combustion

67 в = v = vosplameneniya = ignition

67 К = k = kaplya = drop

67 Т.К = t.k = toplivnaya kaplya = fuel drop

67 Т.В = t.v = toplivo, vosplameneniye = fuel, ignition

68 ИНД = ind = induktsiya = induction

68 В = v = vozdukn = air

68 Т = t = toplivo = fuel

69 Д = D = Dizel' = diesel oil

69 М = M = Mazut = mazout [petroleum residue]

Chapter 3

ATOMIZATION OF LIQUID FUELS

11. ATOMIZATION PROCESS RELATIONSHIPS

The first theoretical studies of the atomization process were based on the assumption that the basic and sole cause of the disintegration of a jet is the existence of unstable oscillations [87]. Owing to unevenness of the cylindrical walls of the nozzle, vibration of the spray nozzle, turbulent pulsations, movement of the air around the jet, etc., the surface of the jet is subjected to initial perturbations. As a result, the jet begins to pulsate and loses stability, disintegrating into drops at a certain wavelength or oscillation period.

The disintegration of a low-viscosity fluid begins with oscillations at a wavelength exceeding the circumference of the unperturbed jet [87]. On investigation of the discharge of viscous jets at high velocities it was found [88] that the jet pulsations are modified with appearance of two kinds of oscillations: axisymmetric and wavelike. The frequency and wavelength of these oscillations depends on the flow conditions of the liquid, the shape of the nozzle aperture [89] and the velocity and physical properties of the liquid and the medium in which the atomization takes place. A large number of recent works [90-96] analyzes the different forms of oscillation (axisymmetric, wavelike) and the conditions under which a jet disintegrates on emerging from orifices with circular, elliptical, triangular, annular and other shapes. Increasing the pressure of the liquid or the velocity of the ambient air reduces the length of the unbroken liquid jet emerging from the nozzle virtually to zero because the fuel is atomized directly at the nozzle outlet. The dependence of the disintegration of a liquid due to vibrational motions is extended not only to continuous jets but also to drops [95].

It has not yet been possible to derive equations to calculate the drop size on the basis of an analysis of the vibration processes in the fuel jet. Hence, the theoretical relations between the length of the critical (unstable) waves, the flow parameters of the liquid and the ambient air are used to select the criteria which characterize the atomization process.

References [97-101] present equations derived for the calculation of atomization fineness on assumption that drops are stable as long as surface tension is greater than the drop aerodynamic forces.

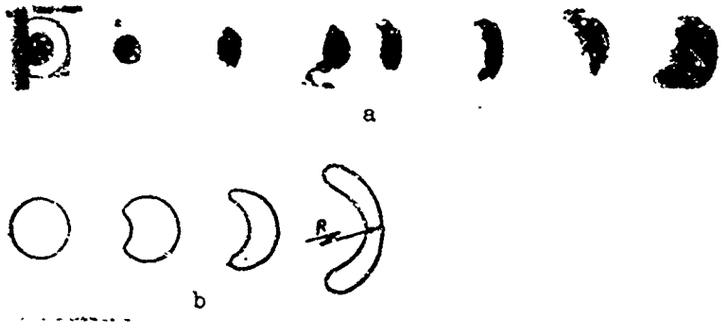

Fig. 43. Disintegration of drops in an airstream: a) Photomicrograph of the process; b) schematic representation of variation in drop shape.

The mechanism of liquid particle disintegration can be divided into several stages. The airflow compresses the liquid drop which assumes a parachute-like shape. This concave film is then ruptured and smaller drops are formed (Fig. 43). The process of liquid particle disintegration is clearly evident from the photomicrographs of various stages of drop deformation (see Fig. 43a) investigated in [102].

Direct determination of drop breakdown as a function of the relative air velocity showed that there exists for each drop size a critical velocity above which the drop disintegrates. The experiments were staged in the following manner. Single drops were released into the airstream and photographed. It was found that drop disintegration in various liquids (mercury, water, gasoline, kerosene, alcohol, etc.) with a diameter of more than 2 mm begins at $D_{kr} = 14$ [103].

$$D_{kp} = \frac{2w^2\rho r_k}{\sigma}. \qquad (3.1)$$

In a study of free falling drops the value of D_{kr} varied from 15.4 to 30.0 and attained 47.0 in some cases [104].

Investigatons of the disintegration of small drops ($2r_k < 2$ mm) showed that the criterion D_{kr} is not constant and increases with decrease in the drop diameter [105]. In the same reference it is claimed that for every liquid there exists a maximum drop diameter which is stable in an airstream of any velocity. The velocity of the drops under the influence of the airstream was not measured in these studies so that considerable differences in the value of the criterion D_{kr} for large and small drops were obtained. The forces which cause the deformation and then also the disintegration of the drops are determined by the relative velocity [106] which is greater for large drops at the same absolute velocity of the free airstream. The conclusion of the existence of maximum drop sizes stable at any absolute airspeed becomes comprehensible when we take this into account. The smaller the drop, the greater the relative velocity at

which its deformation begins. However, with small drops within the time required for the deformation it is impossible to produce considerable relative velocities because these drops are easily entrained by the airflow and for a short time assume a velocity which is virtually the same as that of the airstream.

Considering the equilibrium of the forces acting on the drop at the instant of its maximum deformation (see Fig. 43b), let us determine the pressure on the inside where the airstream impinges on the drop

$$p_1 = p + \frac{\varrho_в (v-w)^2}{2}, \tag{3.2}$$

where p is the static pressure; v is the velocity of the air; w is the speed of the drop; $\varrho_в$ is the air density.

On the lee side, the pressure is

$$p_2 = p - \frac{\varrho_г (v-w)^2}{6}. \tag{3.3}$$

The force due to the difference of these pressures at the critical instant corresponding to the disintegration of the drop should be equal to the force of the surface tension

$$\pi r_к^2 (p_1 - p_2) = 4\pi r_к \sigma, \tag{3.4}$$

where $r_к$ is the curvature radius of the deformed drop at the thinnest part;

$$p_1 - p_2 = \frac{2\varrho_в (v-w)^2}{3}. \tag{3.5}$$

Solving Eqs. (3.4) and (3.5) jointly, we obtain

$$\frac{2}{3}\pi r_к^2 \varrho_в (v-w)^2 = 4\pi r_к \sigma, \tag{3.6}$$

whence D_{kr} = 12 (when w is replaced by the difference $(w - v)$ in Eq. (3.1).

Based on experimental data, it was found that the ratio of curvature radius for the deformed drop to drop radius is ~3.3. In the criterion D_{kr} by replacing the quantity $r_к$ by the drop radius, we obtain D_{kr} = 3.63. Processing experimental data of [103, 105] yielded values for the criterion D_{kr} within 2.2 to 3.6 for a wide range of drop sizes. Analytical calculations carried out on the assumption of drop disintegration as a result of unstable oscillations (pulsations) gave a value of D_{kr} = 5 [96].

The deviation of the dropshape from the spherical and the appearance of a hollow result in instability because at the point of the hollow the surface tension does not counteract the aerodynamic pressure but promotes an increase in deformation which causes drop disintegration. Hence, it can be assumed that if the drop does

not disintegrate, it has a spherical shape, i.e., after atomization, the flame should contain only spherical droplets. Photomicrographs of drops in flight confirmed this assumption because circular silhouettes are obtained in photography of the flying drops [107].

The maximum drop size which can exist in the jet is determined from the condition of equality between surface tension and aerodynamic pressure:

$$2\pi r_к \sigma = \varphi \frac{\pi r_к^2 \rho w^2}{2}, \qquad (3.7)$$

where $r_к$ is the drop radius; σ is the surface tension coefficient for the liquid; w is the drop velocity; ρ is the specific gravity of the liquid and is the resistance to drop motion.

Solving Eq. (3.7), we obtain

$$r_к = \frac{4\sigma}{\varphi \rho w^2}. \qquad (3.8)$$

Comparing Expressions (3.1) and (3.8) for D_{kr}, we can write the following relation:

$$\varphi = \frac{8}{D_{кр}}. \qquad (3.9)$$

Despite the significant differences in the values of φ, obtained by various authors [108-110] experimentally as well as theoretically, the resistance coefficient, calculated from D_{kr} in (3.9), exceeds the experimental values for a sphere tenfold. This indicates the sharp deceleration of the deformed drops, which takes place only at the initial instant of jet discharge from the nozzle.

Jet disintegration into drops by turbulent pulsation can be described in the simplest schematic form as follows. On fuel discharge from the nozzle, particle-detachment from the basic jet is prevented by surface tension which creates a film as a kind of extension of the nozzle. This film is ruptured under the influence of the turbulent pulsations and the jet disintegrates into single drops. In [111] the process of drop formation in a fuel jet is divided into two periods: the first during which the jet is broken up into particles by turbulent pulsations and the second one in which the drops coagulate so that their mean diameter increases. In this theory of fuel disintegration, nowever, the effect of air resistance is neglected, the laws of the kinetic theory of gases are applied to a liquid jet and a theoretical scheme of drop size increase by coagulation is used without sufficient proof.

For such coagulation of drops they would have to collide at some relative velocity [112]. Since the drops in the jet have various sizes and speeds, it could hardly be assumed that a considerable proportion of collisions would lead to coagulation of drops. Furthermore, the drops are fairly widely spaced. This distance increases with increasing distance from the spray nozzle. For example, at a distance of 50 mm from the spray nozzle with a fuel flowrate of 100 kg/h, a

jet angle of 60°, a drop velocity of 80 m/s and a mean drop diameter of 0.2 mm, the distance between drops is 2.6 mm, i.e., 13 drop diameters. In this case, the probability of a single drop striking a drop in the subject layer is only 0.47%.

Some experiments whose results are treated as indication of intense drop coagulation leading to considerable modification of jet dispersion characteristics are based on serious methodological errors. For example, in [113], compressor oil through two or four channels was fed into the airstream through a Venturi nozzle. Approximately the same quantity of liquid passed through each channel. When four channels were used, larger drops were obtained than with two channels. This was explained by coagulation of the drops. However, the atomization conditions were not the same since with two channels in operation, the air flowrate was 3.88 kg per 1 kg of oil, whereas with four-channel operation it was 1.79 kg/kg, i.e., only half as much. Consequently, the expenditure of atomization energy was not the same, which accounts for the increased mean drop size when the oil was passed through four channels.

Thus, although the possibility of drop coagulation exists in the jet, the coagulation process cannot greatly modify the jet composition with respect to drop size. Hence, the hypothesis of the two-stage process of jet disintegration lacks sufficient foundation.

The scheme for the primary breakup of the jet into drops because of turbulence effects can be used as a simplified model of the liquid atomization process. The theoretical premises and analytical relations for drop sizes require further elaboration.

Another scheme of jet disintegration is based on the assumption that the cause of the breakdown of a single liquid flow into drops is to be sought in cavitation processes [114]. At a high fuel flow velocity in the nozzle, static pressure decreases and when it attains values corresponding to the vapor pressure of the liquid, cavitation zones are formed in the flow in the form of individual bubbles. These bubbles disappear when they leave the nozzle where the pressure is restored to atmospheric, thus destroying the integrity of the jet. The formation of the cavitation voids takes place with rigorous periodicity at a frequency depending on the flow velocity [115]. In a study of liquid flow [116], the following relation was found between the number of collapsing cavitation voids and the velocity:

Flow velocity, m/s	4,3	5,0	8,2	8,9	11,2
Number of collapsing cavitation voids per 1 s	106	219	247	249	322

With increasing flow velocity, the cavitation bubbles are formed not only on the surface but also in the interior of the jet and a vapor-gas emulsion emerges from the nozzle. The bubble envelope consisting of a liquid to be atomized, coagulates into drops under the action of the surface tension at which point the bubbles disappear. The cavitation phenomena start at the surface of the jet; thus the thinner the jet, the greater the relative depth to which the cavitation bubbles can penetrate at equal discharge velocities. Vortex motion (in centrifugal-spray nozzles) promotes

the formation of cavitation bubbles over the entire jet cross section.

As follows from the brief description of the basic physical mechanisms of jet disintegration, the process is fairly complex and it is difficult to indicate preference for any of the above-discussed theories at the present time. It can be concluded from the numerous experimental investigations that the disintegration of the jet is due to the action of numerous factors. Various forms of oscillation, turbulent pulsations, aerodynamic shocks and cavitation phenomena all contribute to the complex process of jet disintegration.

Depending on the atomization conditions, the effect of the various factors is not equal and some of them can be neglected. For example, the effect of the force of gravity is normally neglected in all these mechanisms. However, of the flow velocity is very low, this force is the one mainly affecting the disintegration since the breakup of the jet takes place as a result of the difference between the flow velocity and the velocity of free fall. An increase in flow velocity is accompanied by the formation of axisymmetric [91] and then wavelike [90, 92] oscillations of the entire jet which lead to its disintegration. Further increase in velocity is accompanied by formation of a wavy surface and the detachment of isolated strands or films from this surface. Detachment of layers and drops from the wavy surface is observed when liquid flow encounters an airstream in a tube [117, 118]. An increase in the velocity difference at the interface between two phases is accompanied by the appearance of waves and detachment of annular liquid films. The detachment of individual strands and drops from a liquid surface can be observed in jets of large diameter flowing from a nozzle at high velocities (hydraulic excavators, firepumps, etc. [119]). Cavitation phenomena not only promote the formation of waves but are obviously one of the causes of disintegration and the detachment of drops from a thin filament of liquid [120].

A jet of atomized liquid has a relatively small diameter and thus it is difficult to observe the detachment of fuel films from the surface because the waves and the zone of the cavitation phenomena penetrate deeply into the center of the jet in consequence of which atomization takes place directly at the nozzle. The aerodynamic effect of the ambient air influences formation of waves, detachment of parts of the liquid and further atomization. The parts which separate from the continuous jet are filaments with several bulges [121]. A high-speed microkinematography study of atomization [122] shows that a liquid which flows from a nozzle at a certain pressure forms a kind of spatial lattice over the entire jet cross section. The presence of voids in the center of the jet is evidently due to a cavitation phenomena. Under the influence of aerodynamic resistance, external pressure and the pulsations of individual liquid particles, this network, composed of liquid particles with irregular shape, then disintegrates into drops. The maximum drop size is determined by the magnitude of the aerodynamic forces.

Photographs (Fig. 44) indicate diffusion of the jet by the mass of ambient air, and this can be explained by turbulent mixing. Owing to the association between the motion of the drops and the air, an energy exchange takes place between the fuel particles and

the airstream. This process is very intense in the section directly behind the nozzle and the drops quickly lose their singularity. It may therefore be stated that the drops formed at the nozzle do not subsequently change in size if one neglects the size decrease owing to vaporization.

During atomization, the liquid drops acquire an electrical charge and their further interaction is also due to electrical forces. The presence of a charge on the drop surface gives rise to forces which are opposed to the surface tension which promotes disintegration of the drops [123]. It is not possible by means of mathematical equations, to take into account all the currently known forces and phenomena accompanying or causing the disintegration of a continuous liquid jet into drops. However, as in any other change of state, the transformation of a continuous liquid jet into a system of small drops requires the expenditure of a certain amount of energy. If we neglect the detailed intermediate stages of the jet energy transformation into the energy of the drops, the equality

$$E_0 = E_\phi + E_p, \qquad (3.10)$$

must be satisfied. here E_0 is the energy expended on atomization, E_f is the energy of the atomized jet; E_p is the irreversible loss due to friction, sudden expansion of the jet, impact, heating of the drops, pulsations, etc.

Fig. 44. Variation in jet structure as a function of fuel pressure.

Atomization is accomplished by the very energy of the fuel jet produced from the operation of the fuel pump (in the mechanical atomizer spray nozzles), by the energy of the atomizing medium (the air or steam in pneumatic or steam spray nozzles) or by the energy of the fuel jet and of the steam (in combined vapor-mechanical spray nozzles). This energy can be defined as

$$E_0 = \frac{2gH_T m_T}{2} + \frac{2gH_B m_B}{2}, \qquad (3.11)$$

where H_t and H_v are the total pressure in the fuel and air systems; m_t and m_v are the mass of the fuel and air in kg·s^2/m.

In the mechanical atomizers, H_v and m_v are zero and the second term of Eq. (3.11) is absent, while in the pneumatic atomizers the fuel pressure H_t is negligibly small, so that the first term in Eq. (3.11) can be neglected. In the study of flow processes it is more convenient rather than the total energy of the fuel or atomizer medium to consider the specific energy per unit weight of fuel:

$$e_0 = H_т + \frac{m_в}{m_т} H_в. \tag{3.12}$$

The potential ram energy is expended on overcoming friction as the liquid moves through the spray nozzle, on excitation of the turbulent pulsations, on the disintegration of the jet and on imparting a certain velocity to the drops formed. The energy loss due to friction depend on the viscosity of the fuel and the spray nozzle design. In pneumatic spray nozzles, the loss amounts to a fraction of one per cent of the total energy, whereas in mechanical spray nozzles it attains several per cent.

The energy expended in the creation of turbulence is equal to

$$E_{тр} = \pi\varrho \int_0^R (\bar{w}^3 + \bar{v}^3 + \bar{u}^3) r\, dr, \tag{3.13}$$

where $\bar{w}$, $\bar{v}$, $\bar{u}$ are the components of the pulsation velocity of the liquid particle along the three coordinate axes.

The averaged values of these three components can be considered to be equal; thus

$$E_{тр} = 3\pi\varrho \int_0^R \bar{w}^3 r\, dr. \tag{3.14}$$

The experimental relation obtained in [124], according to which the energy E_{tr} (3.13) of the turbulent pulsations for the airstream does not exceed 3% of the kinetic energy of the jet can be used to estimate the energy of the turbulent pulsations. For a fuel jet which has a much higher viscosity than air, the turbulent pulsation energy amounts to less than 1% of the total jet energy. The main part of the potential ram energy is transformed into kinetic energy. Taking into account the negligible energy of the turbulent pulsations and losses, it can be assumed for practical computations that the entire ram pressure is transformed into a velocity head and the kinetic energy of the jet is then:

for mechanical spray nozzles

$$e_0 = \frac{w_т^2}{2g}, \tag{3.15}$$

for pneumatic spray nozzles

$$e_0 = \frac{m_a}{m_T}\frac{w_a^2}{2g}. \qquad (3.16)$$

The energy of the atomized jet consists of the potential energy of the surface layer and the kinetic energy of the moving drops. The potential energy of the surface layer can be determined from the equation

$$E_\sigma = F_k\sigma = \pi\sigma\sum_{i=1}^{i=n} d_{k_i}^2 N_i, \qquad (3.17)$$

where F_k is the total surface of the fuel drops; σ is the surface tension; d_{k_i} is the diameter of the drops in the fuel jet; N_i is the number of drops with diameter d_{k_i}.

The atomized fuel jet has an indeterminate number of drops; hence, it is preferable to relate the energy equation to the unit fuel flowrate.

$$e_\sigma = \frac{F_k\sigma}{G} = \frac{6\sigma}{\gamma_T \bar{d}_k}, \qquad (3.18)$$

$$\bar{d}_k = \left(\sum_{i=1}^{i=n} d_{k_i}^3 N_i\right)\left(\sum_{i=1}^{i=n} d_{k_i}^2 N_i\right)^{-1}, \qquad (3.19)$$

where $\bar{d}_k$ is the average drop diameter; γ_t is the specific gravity of the fuel.

The kinetic energy of the drops can be represented as the sum of the energies of their translational motion and their rotation about an axis passing through the center of gravity of the drop:

$$E_k = \sum\left(\frac{m_k w_k^2}{2} + \frac{J_k\omega_k^2}{2}\right), \qquad (3.20)$$

where ω_k is the speed of rotation; J_k is the inertial moment;for a spherical drop this will be

$$J_k = \frac{\pi\rho d_k^5}{60}. \qquad (3.21)$$

The drops may not have any rotational velocity component if the resultant of the external forces is directed along the bridge connecting the drop with the jet at the instant of detachment. When the resultant of the external forces is perpendicular to this line (Fig. 45) in drops which break away from the crest, the angular momentum will be maximum.

The speed of drop rotation was not measured experimentally,

but for solid particles whose rotation is due to impact or oscillation of particles irregular in shape along a flow [125] the rotation energy is only ~0.1% of the kinetic energy of the moving particle.

The potential energy of the surface layer in % of the total expended energy can be determined from the relation

$$\frac{e_0}{e_e}\,100 = \frac{6\sigma}{\gamma_n \bar{d}_k \left(H_т + \frac{m_в}{m_т} H_в\right)}. \qquad (3.22)$$

On the basis of experimental data for diesel spray nozzles [126, 127] this ratio is 0.03 to 0.058%, for centrifugal spray nozzles [128-131] from 0.02 to 0.22% and for the pneumatic type [132-134], from 0.005 to 0.03%.

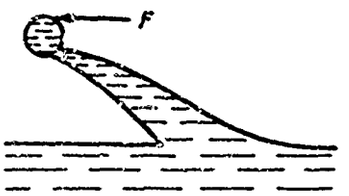

Fig. 45. Schematic representation of forces at the instant of drop detachment from a liquid jet.

The lowest ratio of drop surface layer energy to the total expended energy was found for pneumatic spray nozzles because here the entire energy is not transferred to the fuel, but only 20 to 60%, depending on spray nozzle design.

According to the theory of liquid disintegration [120], the site where the integrity of the jet is disrupted is a gas or vapor bubble whose appearance may be due to thermal fluctuations. This bubble grows if the vapor pressure p_p of the liquid is greater than the ambient pressure (the hydrostatic pressure p and the surface tension):

$$p_n > p + \frac{\sigma}{d_k}, \qquad (3.23)$$

where p_p is the vapor pressure of the liquid.

The work on the formation of the bubble consists of the work of forming the void in the liquid, the work of filling this volume with liquid vapor and the potential energy of the surface layer of the inner sphere of the bubble. By summing these parts of the work and replacing the dimension d_k by the critical value from Relation (3.23), we obtain

$$E_p = \frac{16\pi\sigma^3}{3(p_n - p)^2}. \qquad (3.24)$$

The energy expended on the formation of the bubble, according to data presented in [135], depends on the negative pressure applied to the liquid and can be determined from the relation

$$E_p = \frac{8 \cdot 10^{-6}}{p}, \qquad (3.25)$$

where E_p is the work of bubble formation, in ergs; p is the pressure in kgf/cm^2.

As calculations show, the dimensions of the critical bubble come close to those of a molecule and the energy expended in its formation approaches the thermal energy of molecules (~$4 \cdot 10^{-14}$ ergs) when the negative pressure is close to the molecular tensile strength of the liquid. Consequently, the work expended on disintegration need not be considered in the over-all energy balance of the fuel drops.

Analysis of energy relations obtaining in liquid atomization shows that potential ram energy is mainly transformed into kinetic drop energy.

The energy directly expended on liquid disintegration depends on the discharge velocity and, according to experimental data, is proportional to $E^{-0.15}$-$E^{-0.38}$ for jet spray nozzles, to $E^{-0.35}$ for centrifugal spray nozzles and $E^{-0.45}$ for pneumatic spray nozzles. The proportionality factor is on the order of 0.08-0.03 and depends on the method of transforming the potential energy of pressure into the atomization energy. Any deviation of the jet and particularly of its surface from regular smooth shape provides optimum conditions for aerodynamic action and the detachment of particles from the surface of the jet. The shape of the jet and the energy directly expended in drop formation also depend on the design and dimensions of the spray nozzle.

12. DROP SIZE DISTRIBUTION IN THE ATOMIZATION PROCESS

In the very first studies of spray nozzles, it was found that the jet of atomized fuel consists of drops of various sizes. The cause of jet composition nonuniformity is usually explained by various random phenomena, and for mathematical description of size distribution one uses the laws of probability theory and the equations of statistical curves. According to the definitions of probability theory, a jet of atomized liquid is a statistical set for which the diameter is the argument and its separate values form a set series. Although a distribution curve corresponds to each set, the number of such curves is limited.

The measurement results for the entire spectrum of drop sizes are characterized by the frequency curve

$$\frac{N_i}{\sum N_i} = f(d_{ni}), \qquad (3.26)$$

or the total weight curve

$$R = f(d_n). \qquad (3.27)$$

where N_i is the number of drops with diameter d_{k_i}; R is the total weight of the drops with a diameter greater than d_{k_i} in %.

In the processing of experimental results in the form of Relation (3.26), various equations have been proposed to characterize this curve [136], but with direct measurements, the curves obtained by various researchers are not of the same nature: some curves [137] do not have a maximum and rise sharply on approach to the ordinate (including the curves obtained in the processing of our experiments), others [138] have a maximum and then decrease to zero (Fig. 46). In some cases [139] the distribution curves are extrapolated to zero without any justification.

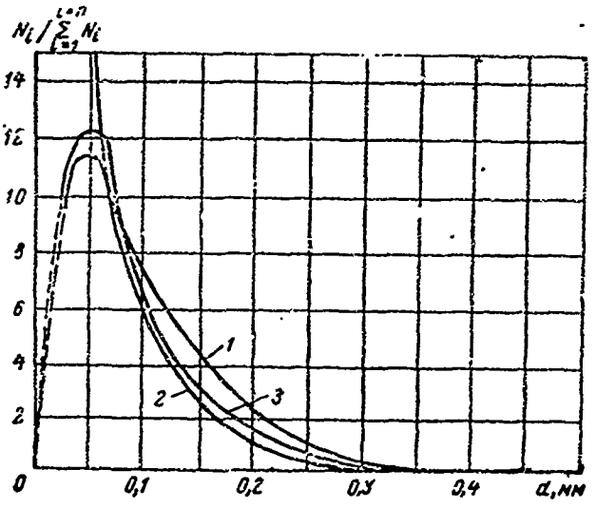

Fig. 46. Frequency curve: 1) According to the Li experiments; 2, 3) according to the I.V. Astakhov experiments.

The discrepancies between the frequency curves obtained by various investigators is explained by the fact that the drop measurements are usually carried out with plates coated with soot and a thin layer of magnesia. It is very difficult to measure and count small drops with this method.

The number of drops not included in the measurements (particularly those which have vaporized) can be enormous although by weight they may represent only a negligible fraction of the fuel trapped on the plate. Moreover, the frequency curves do not give a clear idea concerning the atomization quality because a slight variation in the number of large drops has virtually no effect on the characteristic of the curve, but the mass of these drops may exceed the mass of all the small drops. (This is understandable from the simple relation: the mass of a drop with a diameter of 300 μm corresponds to the mass of 27,000 drops with a diameter of 10 μm. And, conversely, an apparent significant variation in the distribution of drop sizes in the range of small sizes will be slight relative to mass

distribution and will have virtually no effect on the process of flame combustion.

The Rosin-Rammler equation [140] has been most widely used to characterize the weight distribution of the drops

$$R = \exp\left[-\left(\frac{d_k}{\bar{d}}\right)^m\right]. \tag{3.28}$$

The coefficient m for pneumatic and mechanical spray nozzles ranges from 2 to 4 and for rotational spray nozzles it increases to 8. The mean drop diameter $\bar{d}$ corresponds to a value of R = 36.6%. The curve of Eq. (3.28), like many other curves characterizing a statistical set, has a range of variation for the variable d_{k_i} from 0 to ∞. The range of variation for d_{k_i} is limited for practical calculations. The extreme drop sizes obtained directly in the measurements or the values corresponding to a definite value of d_{k_i} which satisfy the stated problem can be taken as the boundary values. In the processing of experimental data in statistics, the limit dimension of the variable corresponds to the probability 0.27%. Now, if these conditions are used for the distribution curve of (3.28), the maximum and minimum diameters of the drops will correspond to the points on the curve of (3.28) whose ordinate R is 0.27 and 99.73%. Accordingly, the maximum drop diameter is calculated by means of the formula

$$d_{k.\max} = \bar{d}\sqrt[m]{5{,}924}, \tag{3.29}$$

and the minimum diameter

$$d_{k.\min} = \bar{d}\sqrt[m]{0{,}002761}. \tag{3.30}$$

The range of drop diameter variation in the flame according to Eqs. (3.29) and (3.30) is

$$\frac{d_{k.\max}}{d_{k.\min}} = \sqrt[m]{2142}, \tag{3.31}$$

which for the practical limits of m (2 and 4) will be 46.28 and 6.9.

In addition to the Rosin-Rammler equation, expressions proposed by Nukiyama-Tanasawa [141] are used for the weight distribution of the drops:

$$\frac{dR}{dd_k} = \frac{a^{\frac{6}{n}}}{\Gamma\left(\frac{6}{n}\right)} d_{k_i}^5 \exp\left(-a d_{k_i}^n\right), \tag{3.32}$$

where a and n are coefficients characterizing atomization; Γ is the sign of the gamma function.

The equation of the normal logarithmic distribution has also been used

$$\frac{dR}{dy} = \frac{\delta}{\sqrt{\pi}} \exp(-\delta^2 y^2), \tag{3.33}$$

$$y = \ln \frac{d_{кл}}{d} \tag{3.34}$$

and the "upper limit" equation [142] which differs from the preceding only in the expression for y:

$$y = \ln \frac{ad_{кл}}{d_{max} - d_{min}}, \tag{3.35}$$

where a and δ are atomization parameters, determined from the measurerent results.

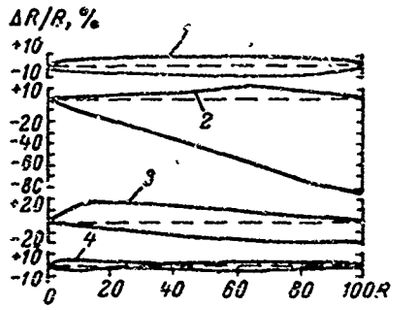

Fig. 47. Comparison of atomization characteristic curve accuracy: 1) Rosin-Rammler curve; 2) Nukiyama-Tanasawa curve; 3) normal logarithmic distribution curve; 4) "upper limit" curve.

Investigation of deviation in the experimental data from several proposed relations showed [143] that the lowest errors are given by the "upper limit" equation and the Rosin-Rammler equation (Fig. 47) obtained by processing experimental data. There are extremely few references to date on the physical pattern of formation of drops of various sizes. Based on the theory of jet disintegration under the influence of wave oscillations, a hypothesis was advanced [144] according to which several unstable waves of various lengths are formed in the jet, and these determine the wide range of drop sizes. This concept has not been developed further. Experimental investigations were usually limited to finding the distribution curve and its mathematical interpretation. The dependence of range in drop-size variation on external conditions, atomization energy, etc., wre not investigated; at most, the distribution characteristic was defined as a function of spray nozzle design [134].

It was found during experimental research on the disintegration of drops in an airstream [102] that the nature of drop disintegration changes with increase in the relative velocity of the air: at moderate velocities, the drop is deformed and flies apart into several parts, whereas in the case of supercritical velocity, the atomization of the drop takes place by detachment of a liquid layer from the surface, with the main part of the drop being preserved.

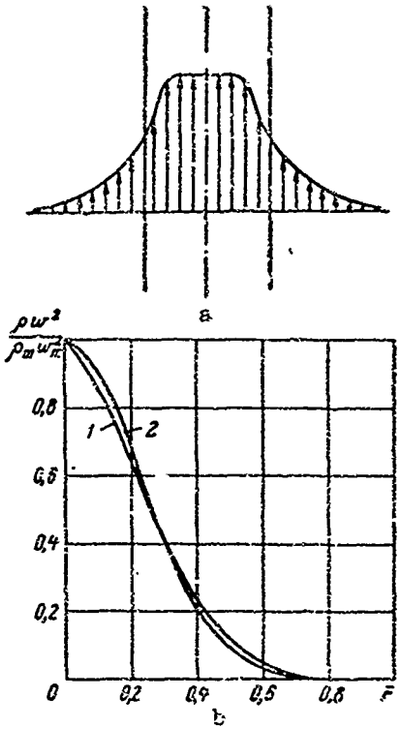

Fig. 48. Diagram of velocities (a) and energies (b) in the transition section of a two-phase stream: 1) After Eq. (3.39); 2) after Eq. (3.40).

If one analyzes the drop size distribution over the section of the jet, the following quantitative relationship is observed: the largest drops are formed in the center of the fuel jet (for centrifugal spray nozzles, the middle of the fuel film) and the smallest at the flame boundary (the outside boundary as well as the inside boundary).

This distribution can be explained by examining the atomization of a large-diameter jet. At the boundary with the ambient medium (air), because of great relative velocity, the formed waves cause part of the liquid to break away from the surface in the form of filaments and drops. The subsequent atomization process takes place in the same manner, with the difference that the jet is now surrounded by a mixture of drops and air which has a lower relative velocity with respect to the jet. The next layer stripped from the jet will have an even lower relative velocity, etc. The variation in relative velocity during detachment from the surface of the liquid jet causes a change in the size of the drops formed from each separated layer. Hence, the nearer to the center of the jet, the larger the drops.

If the theory of turbulent jets is applied to the study of interaction between fuel and airflow, the diagram of the relative velocities in the initial part of the jet (before the disintegration

of the central part of the fuel flow) will have the form of Fig. 48a. Two-phase flow in tubes exhibits analogous velocity distribution [145, 146]. In the opinion of some authors [147, 148], the specific flow energy ρw^2 is of decisive importance for turbulent mixing.

For a free submerged jet flow, depending on the dimensionless ratio of the axial flow velocity w at any point to the axial velocity w_m in the center of the jet is defined by the formula (149)

$$\frac{w}{w_m} = (1 - \bar{r}^{1.5})^2, \tag{3.36}$$

$$\bar{r} = \frac{y}{r}, \tag{3.37}$$

where y is the distance from the flow axis; r is the jet radius in the subject cross section.

We assume in first approximation that the density variation is proportional to the concentration variation

$$\frac{\rho}{\rho_m} \approx \frac{C}{C_m}, \tag{3.38}$$

where C is the admixture concentration equal to the ratio of the admixture weight to the weight of the ambient medium at the subject point of the jet; C_m is the admixture concentration in the center of the jet.

For a jet with heavy admixtures, the dimensionless admixture concentration in the gas jet is equal to the square root of the dimensionless velocity. Hence the energy distribution over the jet cross section can be expressed by the relation

$$\frac{\rho w^2}{\rho_m w_m^2} = (1 - \bar{r}^{1.5})^5. \tag{3.39}$$

According to the experimental data of [147], the value of ρw^2 in any section of the jet is defined by the equation

$$\frac{\rho w^2}{\rho_m w_m^2} = \exp\left[-1{,}42\left(\frac{y}{ax}\right)^2\right], \tag{3.40}$$

where ρ is the density of the flow at the point under discussion; ρ_m is the density in the center of the jet; w is the axial velocity at the subject point; y is the distance of the point from the flow axis; x is the distance from the pole of the jet along the flow axis (may be assumed equal to the distance from the end of the spray nozzle); a is an experimental coefficient depending on the initial turbulence of the flow.

At $r = 2.61ax$, the two curves $\rho w^2/\rho_m w_m^2 = f(y)$ are very similar (see Fig. 48b) and for further analysis of the quantitative relationships of distribution in drop sizes we use Eq. (3.39).

As shown by results from processing numerous experimental data, drop sizes can be defined as an exponential function of jet energy [18]

$$d = kE^{n}. \tag{3.41}$$

Since formation of the wave surface and drop detachment from the continuous jet occur because of the velocity difference between the liquid flow and the ambient medium, the velocity difference and, consequently, the energy spent on drop size reduction, will decrease nearer the jet center. Considering this, we can write drop size as a function of energy in the form

$$\frac{d_{max}}{d_{k_i}} = \left(\frac{E}{E_{max}}\right)^{n} = \left(\frac{\varrho w^2}{\varrho_m w_m^2}\right)^{n}, \tag{3.42}$$

or

$$\frac{d_{max}}{d_{k_i}} = (1 - f^{1,5})^{\frac{1}{2n}}. \tag{3.43}$$

The number of drops of each size depends on the mass of the jet which has acquired a given kinetic energy. With a uniform velocity profile in the fuel jet at the initial instant, the distribution of its mass over the cross section is proportional to the square of the radius.

$$\frac{G}{G_0} = \frac{\pi r^2 \varrho w_0}{\pi r_0^2 \varrho w_0} = \frac{r^2}{r_0^2} = R. \tag{3.44}$$

where r_0 is the radius of the spray nozzle.

The simultaneous solution of Eqs. (3.43) and (3.44) yields an expression for the law of drop distribution by size

$$R = \left[1 - \left(\frac{d_{max}}{d_{k_i}}\right)^{\frac{1}{2n}}\right]^{3/2}, \tag{3.45}$$

or, replacing $1/5b$ by n, this relation can be written in a simpler form:

$$R^{3/2} = 1 - \left(\frac{d}{d_{max}}\right)^{n}. \tag{3.46}$$

These equations were derived on examination of a highly simplified scheme of jet disintegration into drops and can serve as a mathematical illustration of the process of forming drops of various diameters. Since during disintegration of each layer of the fuel jet, finer drops are formed in addition to the drops whose size is typical of this layer thickness, the curve of Eq. (3.46) gives the upper limits for the number of large drops in the flame.

For comparison of Relation (3.46) with the distribution according to the Rosin-Rammler equation, the characteristic (average) dimension $\bar{d}$ (3.28) must be replaced by the maximum. Using Relation (3.29), we find

$$R = \exp\left[-5{,}924\left(\frac{d}{d_{max}}\right)^{m}\right]. \tag{3.47}$$

Comparison of the distribution equations (3.46) and (3.47) with the measurement results for drops obtained by various research-

ers [129-134] shows that in the atomization of fuels with pneumatic (Fig. 49a) and diesel (Fig. 49b) spray nozzles, the experimental points occupy a zone which is bounded by Eqs. (3.46) and (3.47). The value of m in Eq. (3.47) is 3 and that of n in (3.46) is 2.5.

For a centrifugal spray nozzle, one can carry out the same calculation by treating the conical film as a flat jet or by dividing the film into several separate segments and then summing the results. The rigorous mathematical solution of this problem involves great difficulties although the physical pattern of the disintegration of the jet and the conical film is of the same nature. Experimental data obtained by the authors of [150] during the measurement of the fineness of atomization by trapping methods, modeling with paraffin and by sediment measurement methods (concerning these methods, see Chapter 6) showed that the drop weight distribution for centrifugal atomizers can be described by the same functional relation as for jet and pneumatic atomizers.

The measurement of the fuel drops was carried out for different types of atomizers (single-stage, two-nozzle and two-circuit centrifugal atomizers); the following fuels were used: diesel oil, petroleum residue ФС-50, М20, М40, М80, and paraffin. The results of all the experimental data, represented in the form of the dimensionless relation $R = f(d/d_{max})$ in the diagram fit into a zone limited by the distribution curves (3.46) and (3.47) with the characteristics $n = 3.22$ and $m = 2.5$ (Fig. 50).

The values n and m determine the range of variation of the drop diameters, i.e., the uniformity of atomization. The larger n (or m), the smaller is the difference between the minimum and maximum drop size which follows from Eq. (3.29). The index n, as follows from the experimental data, depends on the shape and thickness of the jet, the properties of the atomized fuel and the flow velocity.

During the disintegration of the jet into drops, the separation of the fuel from the surface takes place in the form of rings or filaments. Since at the boundary of two phases a rapid deceleration of the flow occurs, the boundary layer will have a velocity distribution which differs somewhat from that of the main flow. According to researches on turbulent flow [151], the thickness of the boundary layer is determined by means of the relation

$$\delta = kx\,\mathrm{Re}^{-p}. \qquad (3.48)$$

For laminar flow conditions in the boundary layer, $p = 0.5$; for turbulent conditions, $p = 0.14$. It follows from Eq. (3.48) that the thickness of the layer increases with decreasing velocity (and, consequently, also of Re). The next layer should separate from the jet at the same velocity gradient. In view of the lower velocity at the boundary of the jet, the layer will be thicker. With increase in the diameter of the jet, the number of layers and the thickness of the last central layer increase and, at the same time, the maximum drop size should increase. The increase in the absolute size of the large drops modifies the nature of the distribution curve $(dR/dd_x = f(d_x)$ which comprises a large range of drop sizes and, correspondingly, the index m in Expressions (3.28) and (3.46) will de-

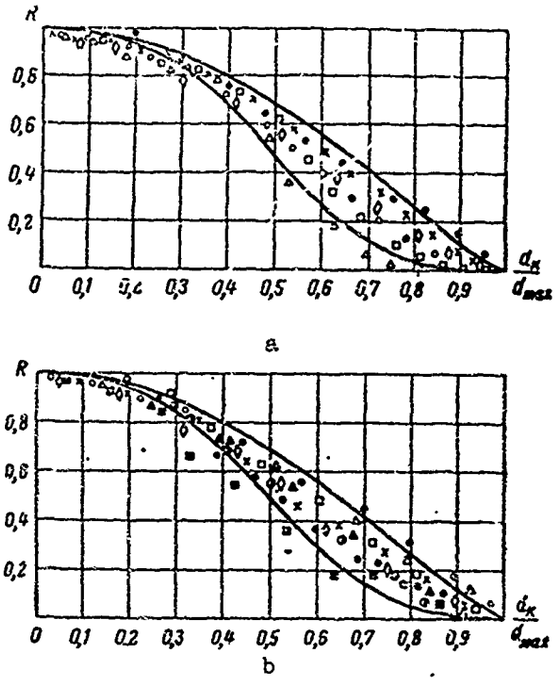

Fig. 49. Weight distribution of the fuel drops produced by: a) Diesel spray nozzles; b) pneumatic spray nozzles.

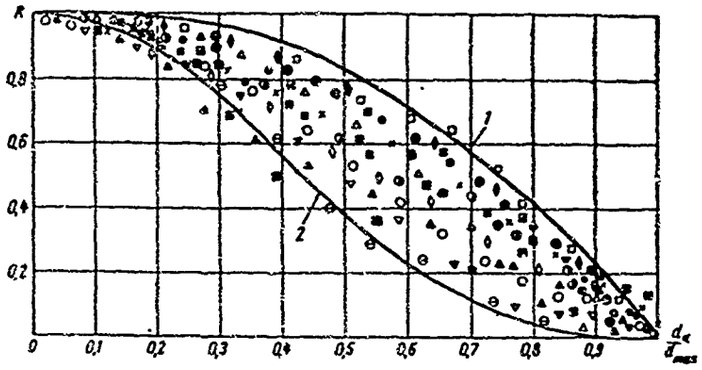

Fig. 50. Weight distribution of the fuel drops during atomization with centrifugal sprayers. Curves plotted on the basis of Eqs. (3.46) and (3.47): 1) at m = 3.0; 2) at n = 2.5.

crease. This assumption was confirmed by experiment [121]. When fuel was atomized by sprayers at approximately the same pressure and a constant ratio of nozzle length to diameter, the maximum and minimum drop diameters were obtained as a function of the nozzle size (Table 8).

TABLE 8

Results of the Measurement of Drop Size

Диаметр сопла, мм 1	Давление топлива, кГ/см² 2	Диаметр капли, мк 3	
		минимальный 4	максимальный 5
0,25	700	100	145
0,35	685	130	160
0,45	720	130	182

1) Nozzle diameter, mm; 2) fuel pressure, kgf/cm²; 3) drop diameter, μ; 4) minimum; 5) maximum.

As follows from the data of Table 8, the minimum drop size is practically unaffected by an increase in nozzle diameter and the differences in them are within the limits of experimental error. The maximum drop size, however, increases markedly. The same conclusion can be derived from the experimental data of the other investigators [127, 137].

For atomizers with film flow it is also possible to prove the effect of fuel film thickness on the drop size distribution if the results of the atomization of fuel with centrifugal and rotational spray nozzles are compared. The latter have a film thickness 5-10 times less than the centrifugal types and, accordingly, the characteristic m in the distribution equation (3.28) for rotational spray nozzles increases and amounts to 4-9, which corresponds to a very narrow scatter of drop sizes (the ratio of maximum to minimum size is only 6.9-1.21).

The variation of the velocity gradient and the energy transfer between the layers depend on the viscosity of the fuel. The higher the viscosity, the smaller are the waves and perturbations on the surface of the jet and, consequently, the conditions for energy exchange between the jet and the ambient airstream are less favorable. The energy and velocity distribution within the fuel-air jet takes place more uniformly. According to Eq. (3.48), the thickness of the boundary layer is proportional to the viscosity, the exponent being 0.5-0.14. The power exponent for the viscosity in many other relations characterizing the fineness of atomization is of the same order [126, 127, 130, 152]. With increase in the viscosity of the fuel, the thickness of the boundary layer increases and the total number of layers in the jet decreases. Consequently,

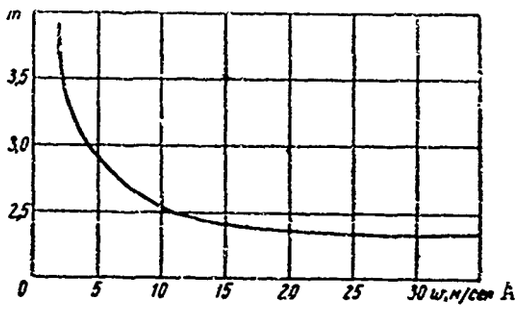

Fig. 51. Effect of the fuel velocity on the drop distribution (on the characteristic m in Eq. (3.28)). A) m/s.

the range of variation of drop sizes is restricted, i.e., the atomization will be more uniform. The increase in the thickness of the initial layers and the size of the small drops results in an increase in the mean size. Experiments carried out by the authors on the atomization of petroleum residues of grade M12, M40 and M80, confirmed this assumption. An increase in the temperature of these petroleum residues (consequently, a decrease of the viscosity of the fuel) caused a variation not only of the mean size but also of the coefficient m (3.28). For example, with increase in the temperature of the petroleum residue M12 from 75 to 120°C, the coefficient m changed from 3.1 to 1.8, which corresponds to a variation of the ratio of maximum to minimum drop size from 11.0 to 71.3 (3.31).

The effect of the viscosity of the fuel on the atomization has been investigated in several works in which, as a rule, attention was given only to the variation of the average drop size. The works [126, 138] give the variation of several types of averages as a function of the viscosity, each of which depends in a different manner on the size of the drops constituting the flame. Based on a study of the effect of viscosity on these averages it can be inferred that when the viscosity of the fuel is increased, the range of drop sizes is narrowed with simultaneous increase of the same.

The flow velocity of the fuel also affects the distribution of the drops: the greater the velocity, the greater is the turbulence, the easier the energy transfer and the smaller the difference in the effect on the fuel over the entire cross section of the jet. Consequently, the atomization will be more uniform with increase in the flow velocity of the fuel (or air in pneumatic atomizers). Figure 51 shows the index m (3.28) of the uniformity of the drop size distribution as a function of the velocity.

13. ATOMIZATION CHARACTERISTICS AND THEIR DEPENDENCE ON THE PHYSICAL PROPERTIES OF THE FUEL

To estimate the atomization quality it is more convenient in many cases to use a single average characteristic instead of the whole drop size distribution curve. The choice of this characteristic should be dictated by the problem to be solved or the measurement method which gives directly the average. If the aim of the investigations is to compare the performance of various spray nozzles, it is expedient to use one of the averages used in statistics. In the choice and calculation of the average it is also necessary to take into account the effect of the measurement accuracy on the atomization characteristic.

Most authors use one of the following quantities for characterizing the degree of atomization obtained in their experiments:

the arithmetic average

$$\bar{d}_a = \frac{\sum_{i=1}^{i=n} d_{k_i} N_i}{\sum_{i=1}^{i=n} N_i}, \tag{3.49}$$

the average surface

$$\bar{d}_n = \left(\frac{\sum_{i=1}^{i=n} d_{k_i}^2 N_i}{\sum_{i=1}^{i=n} N_i} \right)^{1/2}, \tag{3.50}$$

the average volume

$$\bar{d}_0 = \left(\frac{\sum_{i=1}^{i=n} d_{k_i}^3 N_i}{\sum_{i=1}^{i=n} N_i} \right)^{1/3}, \tag{3.51}$$

the average weight

$$\bar{d}_s = \frac{\sum_{i=1}^{i=n} q_i d_{k_i}}{\sum_{i=1}^{i=n} q_i}, \tag{3.52}$$

where q_i is the total weight of the drops with diameter d_{k_i}.

In the study of the processes of breakdown of the jet, vaporization and combustion, the experimental data must be processed on the basis of the assumed physical pattern of the process in such a way that the averages characterize the process under study.

For example, assuming that the drops are formed under the influence of the resistance to their motion and the surface tension, the average which characterizes the fineness of atomization, is defined as

$$\bar{d}_p = \frac{\sum_{i=1}^{i=n} d_i^2 N_i}{\sum_{i=1}^{i=n} d_i N_i}. \qquad (3.53)$$

This expression reflects the relation of the forces acting during atomization: the force of aerodynamic resistance which is proportional to the drop surface, and the force of the surface tension which is proportional to the sum of the drop diameters. When we compare the flame of an atomized fuel with regard to the vaporization rate, we must use the mean diameter at which the ratio of vaporization rate to volume is equal to the ratio of the vaporization rate of the entire flame to the volume of all drops in the flame. This diameter, according to the calculation of Probert [35], can be computed by means of the formula

$$\bar{d}_n = \bar{d} \sqrt{\frac{\Gamma(1+2/m)}{2}}, \qquad (3.54)$$

where $\bar{d}$ and m are the characteristics of the atomization curve (3.28).

The average drop sizes obtained by indirect measurements, depend on the property of the drops used for the measurement: optical, electrical, mechanical, thermodynamic, etc. (see Chapter 6). For example, with the photometric method, the average drop size is

$$\bar{d}_\phi = \frac{\sum_{i=1}^{i=n} d_{\kappa_i}^3 N_i}{\sum_{i=1}^{i=n} d_{\kappa_i}^2 N_i}. \qquad (3.55)$$

When the electrical method is used, the average drop size is determined as

$$\bar{d}_3 = \sqrt{\frac{\sum_{i=1}^{i=n} d_{\kappa_i}^3 N_i}{\sum_{i=1}^{i=n} d_{\kappa_i} N_i}}. \qquad (3.56)$$

In view of the fact that a large number of different averages is used at present to characterize the atomization of a fuel, the possibility of using experimental data on atomization is greatly limited.

The problem of finding a relationship between different averages can be solved only if the size distribution law of the drops can be expressed analytically.

In a general case, any average can be found by means of the weight distribution equation from the following relation:

$$\bar{d}_{qp} = \left(\int_{d_{min}}^{d_{max}} d^{q-3} \frac{d\varphi(R)}{dd_k} dd_k \right)^{\frac{1}{q-p}} \left(\int_{d_{min}}^{d_{max}} d^{p-3} \frac{d\varphi(R)}{dd_k} dd_k \right)^{\frac{1}{p-q}}, \qquad (3.57)$$

where d_{qp} is the average drop size, defined as the ratio of the sums of the drop diameters raised to the qth power to the sum of the drop diameters raised to the pth power. (R) is the function of the weight variation of the drops as a function of their diameter.

In characterizing the weight distribution of the drops by means of the Rosin-Rammler equation, the mean drop size for the cases where $3 - q < m$ and $3 - p < m$ can be calculated by means of the gamma-function

$$\bar{d}_{qp} = \bar{d} \left[\Gamma\left(\frac{q-3}{m} + 1 \right) \right]^{\frac{1}{q-p}} \left[\Gamma\left(\frac{p-3}{m} + 1 \right) \right]^{\frac{1}{p-q}}. \qquad (3.58)$$

For example, for computing the average weight of the drops, this equation assumes the form

$$\bar{d}_{43} = \bar{d} \Gamma\left(\frac{1}{m} + 1 \right). \qquad (3.59)$$

An expression for any kind of average, given above, can be found analogously.

In addition to the above averages, the median diameter has been widely used for estimating atomization efficiency. The median of any population is the argument corresponding to a value of the integral distribution function of 0.5. The median of the distribution function described by Eq. (3.28), is

$$\bar{d}_{med} = \bar{d} (\ln 2)^{1/m} = \bar{d} \sqrt[m]{0{,}5931}. \qquad (3.60)$$

A second, also widely used distribution curve characteristic is the mode, i.e., the abscissa of the maximum of the differential distribution curve $dR/dd_k = f(d_k)$. For the curve described by Eq. (3.28), the mode is connected with the maximum diameter by the relation

$$\bar{d}_{mod} = \bar{d} \sqrt[m]{\frac{m-1}{m}}. \qquad (3.61)$$

If conditions connected with the investigation of some physical process are not made in the determination of the atomization characteristic, the choice of the average should be carried out on the basis of an estimate of the accuracy of its determination. To calculate the error involved in various characteristics, special measurements of atomization efficiency were carried out under identical conditions at the All Union Central Scientific Research Institute – Ministry of Railroads [AUCSRI – MR](ЦНИИ МПС). Averages of

TABLE 9

Results of the Measurement of Atomization Efficiency

Характеристика распыливания [1]	$\bar{d}_v$ [2] $q=1$, $p=0$	$\bar{d}_0$ $q=3$, $p=0$	$\bar{d}_r$ [3] $q=4$, $p=3$	$\bar{d}_r$ [3] $q=2$, $p=1$	$\bar{d}_i$ [4]	$\bar{d}_f$ [5] $q=3$, $p=2$	$\bar{d}_e$ [6] $q=3$; $p=1$	$\bar{d}$	m	$\bar{d}_{med}$	$\bar{d}_{mod}$
Полученные методом улавливания [7]											
$\bar{d}_{ср}$, мк [8]	46	96	222	122	177	186	156	264	3,1	235	229
σ, мк [9]	16	16,4	24,4	26,6	17,3	21,3	16,4	24,2	0,42	19,1	16,6
ε, %	104	53,1	30,1	55,0	24,8	28,5	40,4	23,9	33,3	23,4	24,4
ν, %	100	51,3	33,0	65,5	29,4	34,4	36,2	27,5	40,7	24,4	21,8
Полученные методом моделирования [10]											
$\bar{d}_{ср}$, мк [8]	44	62	156	59	139	93	75	202	2,3	171	154
σ, мк [9]	3,6	6,6	12,1	8,7	8,8	15,2	11,1	12,3	0,15	10,01	9,2
ε, %	26,5	27,1	18,4	43,5	14,9	40,3	41,4	15,4	17,4	15,9	18,5
ν, %	24,7	31,9	23,3	43,7	19,0	48,7	44,5	18,3	19,6	17,5	17,9
Полученные седиментометрическим методом [11]											
$\bar{d}_{ср}$, мк [8]	25	74	226	94	173	182	129	259	3,2	231	229
σ, мк [9]	7,8	14,3	11,2	24,3	9,4	8,8	18,3	13,9	2,5	12,4	12,4
ε, %	85,8	56,0	14,8	73,0	15,7	14,9	41,0	15,1	25,0	14,9	16,3
ν, %	92,0	57,5	14,8	77,0	16,3	14,5	42,0	16,2	23,4	16,1	16,3

$$\bar{d}_{ср}=\frac{\sum \bar{d}N}{\sum N};\quad \sigma=\sqrt{\frac{\sum(\bar{d}-d_{ср})^2}{\sum N-1}};\quad \varepsilon=\frac{\bar{d}_{max}-\bar{d}_{min}}{d_{ср}}\cdot 100;\quad \nu=\frac{3\sigma}{\bar{d}_{ср}}\cdot 100.$$

$\bar{d}$ — характеристика распыливания; N — число опытов.

[12] [13]

1) Atomization characteristic; 2) d_v; 3) d_r; 4) d_i; 5) d_f; 6) d_e; 7) obtained by the method of drop catching; 8) d_{sr}, μ; 9) μ; 10) obtained by the model method; 11) obtained by sedimentometric method; 12) atomization characteristic; 13) number of tests.

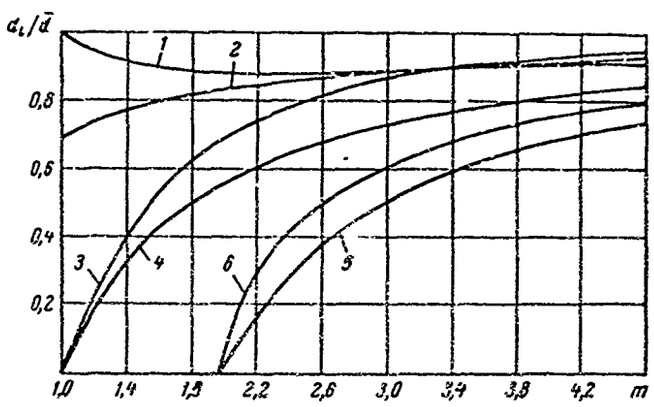

Fig. 52. Relations between different atomization characteristics.

$1-\frac{d_{32}}{\bar{d}}=f(m)$; $2-\frac{\sigma_{med}}{\bar{d}}=f_2(m)$; $3-\frac{d_{med}}{\bar{d}}=f_3(m)$; $4-\frac{d_{43}}{\bar{d}}=f_4(m)$;

$5-\frac{d_{2,1}}{\bar{d}}=f_5(m)$; $6-\frac{d_{3,2}}{\bar{d}}=f_6(m)$

the type $\bar{d}_{qp}$ were calculated on the basis of the results of measurements of the entire drop spectrum and the statistical characteristics were determined on the basis of distribution curves of Type (3.28): the median (3.60) and the mode (3.61) and also the quantities $\bar{d}$ and m.

It was found on the basis of an analysis of the results obtained by processing experimental data (Table 9) that the absolute values of the average drop size increase with increase in the exponent at $\bar{d}_{qp}$ (q and p). With increase in the exponent, the dependence of these averages on the size of the large drops increases whereas the small drops do not exert any important influence. The accuracy of the characteristics $\bar{d}_{qp}$ at q = 1-3 and p = 0, i.e., the mean arithmetic, the average surface and average volume drop diameter, is determined mainly by the accuracy of the measurement and calculation of the number of small drops. The measurement accuracy of these quantities is considerably less than for thelarge drops, hence the greatest errors (~100%) were obtained for the averages $\bar{d}_{10}$.

The least errors occur with the average weight and median characteristics which are preferably used for determining the atomization efficiency if the problem does not call for the choice of a special average.

Comparison of the theoretical and experimental dependencies of different kinds of averages on $\bar{d}$ (3.28) shows (Table 10) that the differences in the results are within the limits of experimental error and that Eq. (3.58) can be used for converting one form of average drop diameter into another.

As follows from Eq. (3.58), the difference between all averages decreases with increase in the index m whcih is evident from the relation of Fig. 52. Even at m = 3, the average weight, median and mode are virtually equal.

Depending on the adopted characteristic (average drop size) the same results can differ considerably. For example, according to the experimental data [138] given in Fig. 53, an increase in the viscosity from 3 to 10°VU increases the drop size by approximately 40% if the atomization is estimated by the mean arithmetic diameter (d_{10}). If the atomization efficiency is gauged by means of the Sauter average diameter (d_{32}), the same data allow the conclusion that the atomization efficiency has been more than halved. The use of the average weight diameter ($\bar{d}_{43}$) for the characteristic would give an even greater difference. Analogous results were obtained in the work [126]. This difference is explained by the effect of the viscosity of the fuel on the drop distribution.

TABLE 10

Results of Determination of the Atomization Characteristic as a Function of $\bar{d}$ (3.28)

Отношение характеристик 1	Значения отношений 2	Результаты по сериям опытов 3					
		1	2	3	4	5	6
$\bar{d}_{32} : \bar{d}$	Теоретическое 4	0,90	0,90	0,91	0,88	0,68	0,90
	Опытное . . . 5. . .	0,81	0,84	0,83	0,77	0,74	0,87
$\bar{d}_{31} : \bar{d}$	Теоретическое . 4. . .	0,74	0,74	0,78	0,65	0,62	0,75
	Опытное . . . 5. . .	0,71	0,70	0,72	0,46	0,45	0,71
$\bar{d}_{30} : \bar{d}$	Теоретическое . 4. . .	0,63	0,63	0,70	0,36	0,30	0,65
	Опытное . . . 5. . .	0,52	0,58	0,63	0,37	0,38	0,50
$\bar{d}_{21} : \bar{d}$	Теоретическое . 4. . .	0,53	0,53	0,61	0,23	0,20	0,53
	Опытное . . . 5. . .	0,46	0,48	0,57	0,30	0,33	0,37

1) Ratio of characteristics; 2) values of the ratios; 3) results based on test series; 4) theoretical; 5) experimental.

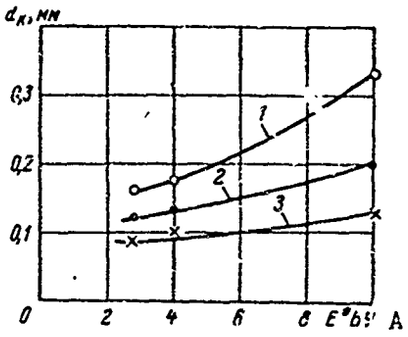

Fig. 53. Effect of the viscosity of the fuel on the magnitude of the aver ge drop size: 1) Mean arithmetic (d_{10}); 2) mean volume (d_{30}); 3) average according to Sauter (d_{32}); A) VU.

The average size like the entire drop spectrum, composing the flame, is determined by the energy consumed in the atomization. The utilization of this energy directly for the atomization of the jet depends on various factors, the main one of which, as was shown in the foregoing, is the velocity difference at the surface of the jet and the ambient atmosphere. The thicker the fuel jet, the smaller is the velocity difference in the central part. Most of the experimental data show a proportionality between the average drop size and the nozzle diameter. The interaction between the flows and the energy transfer (ρw^2) from one layer of fuel to another depend essentially on the viscosity. With increase in the viscosity, the internal friction offers a greater resistance to the detachment of layers which causes a decrease in atomization efficiency. The surface tension also hinders the breakup of the jet. The larger the

surface tension coefficient, the larger are the drops formed during atomization.

The specific gravity of the fuel has the least effect on the atomization process and on the average drop size; it determines the inertial forces on which only the throwing power of the flame depends. A study of the conditions of the disintegration of drops due to aerodynamic forces showed that a variation in the density of the liquid by a factor of 13.6 (from water to mercury) does not affect the drop size and the atomization criterion [103]. Since the specific gravity of the heavy fuels varies within the range of 860-950 kg/$/m^3$, a detailed study of the effect of liquid density on the atomization is not of practical interest.

The surface tension coefficient is a more important characteristic in the study of atomization because on the magnitude of this force depend the oscillations, the profile of the jet surface and the resistance to the effect of the aerodynamic forces and turbulent pulsations. The existence of the surface tension force is responsible for the spherical shape of the drops of atomized fuel. In many analytical equations [80-82], the effect of the surface tension on the drop size is expressed by a direct proportionality. The criterion relations obtained by processing of experimental data show a much less important influence of the surface tension coefficient on the drop size than would follow from the theoretical relations.

The differences in surface tension between petroleum residues of different grades [155] do not exceed 7-8%. Heating reduces the surface tension only slightly. For example, when cracking residue of the grade M80 is heated from 50 to 100°C, the surface tension decreases by 8.7%.

The greatest differences between fuel grades are in their viscosity. If we analyze the analytical expressions for the determination of the average drop diameters [100, 121], the viscosity is not taken into account at all in some cases. In other works, the effect of the viscosity on the average drop diameter is estimated to be proportional to the viscosity coefficient with an exponent of 0.2-0.5. This discrepancy between the experimental data and then also the criterion relations, is explained by the fact that the viscosity force not only affects the process of size reduction itself, but determines also the velocity profile and energy loss of the jet and, in centrifugal spray nozzles, also the thickness of the jet of outflowing fuel. Since the energy losses depend on the design of the particular spray nozzle, it is impossible to establish a generally valid relationship.

As the experimental data obtained by us (Fig. 54a) show, the viscosity of the fuel, from values of ν = 6-7 mm^3/s downwards, has practically no effect on the average drop diameter. With increase in viscosity, the average diameter increases steeply. The viscosity effect is particularly evident in the operation of atomizers with low fuel pressure (for mechanical) or with small specific air flowrate (for pneumatic spray nozzles). In the centrifugal spray nozzle, the greater the viscosity of the fuel, the greater is the pressure at which the atomization takes place directly at the nozzle (in the absence of a compact fuel film) (see Fig. 54b).

In connection with the very complex processes taking place during atomization, numerous experiments have been staged, the results of which have now been generalized by criterion relations. The choice of dimensionless criteria is based on dimension theory or on the theoretical assumptions which explain the disintegration of the jet. In either case, the final equation includes the following variables: d_k, average drop diameter; d_s, the nozzle diameter, or δ, the thickness of the fuel film; w, the relative velocity of the liquid; σ, the surface tension coefficient; ν_t, ν_v, the viscosity of the liquid and the ambient atmosphere (air); ρ_t, ρ_v, the density of the liquid and the ambient atmosphere.

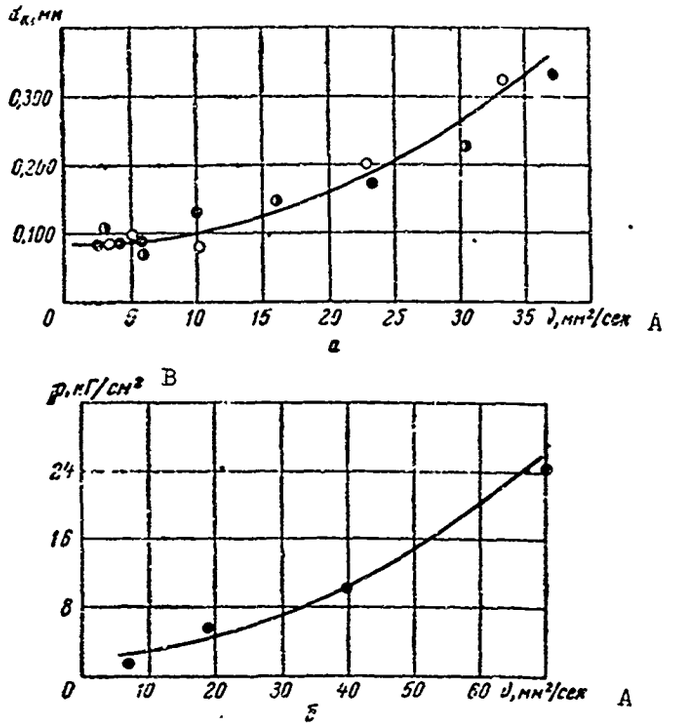

Fig. 54. Effect of the viscosity of the fuel on atomization: a) On the average (median) drop diameter; b) on atomization without visible stable film. A) mm²/s; B) kgf/cm².

Another quantity q_v, the specific air consumption of the spray nozzle, is included for the pneumatic spray nozzles.

The estimate of the atomization efficiency is usually carried out by a combination of the following criteria and simplexes:

$\mathrm{Re} = \frac{d_c w}{\nu_t}$ — the Reynolds criterion, which characterizes the conditions of fuel flow;

$\mathrm{We} = \frac{w^2 d_c \rho_t}{\sigma}$ — the Weber criterion which gives the ratio of the inertial force and the surface

tension force;

$Lp = \frac{d_e \sigma}{\nu_ж^2 \rho_ж}$ — the Laplace criterion which is the ratio of the surface tension and viscosity;

$M = \frac{\rho_г}{\rho_ж}$ and $N = \frac{\nu_г}{\nu_ж}$ — the simplexes which express the ratio of the inertial forces and the viscosity of the ambient atmosphere in the atomized liquid.

Many researchers have shown that the viscosity of the ambient atmosphere has little effect on the atomization efficiency, so that this parameter N is usually left out of the equations.

The most widely used criterion relations have equations of the form

$$\frac{d_к}{d_e} = F(We;\ Re;\ M) \tag{3.62}$$

or

$$\frac{d_к}{\delta} = f(We;\ Lp;\ M). \tag{3.63}$$

On the basis of processing of experimental data for jet spray nozzles, the equations [107, 108] are recommended

$$\frac{d_к}{d_e} = 3{,}31 \frac{1}{M^{0.266} Re^{0.1466} We^{0.1927}}, \tag{3.64}$$

or for pin-type spray nozzles

$$\frac{d_к}{d_э} = \frac{12}{Re^{0.3}}, \text{ for } Re = 60 - 710, \tag{3.65}$$

$$\frac{d_к}{d_э} = \frac{407 \cdot 10^4}{Re^{1.7} We^{0.36}}, \text{ for } Re = 710 - 1585, \tag{3.65a}$$

$$\frac{d_к}{d_э} = \frac{275{,}5}{Re^{0.4} We^{0.36}}, \text{ for } Re = 1585, \tag{3.65b}$$

where d_e is the equivalent diameter, equal to the ratio of the annular passage cross section of the atomizer and the "wetted perimeter"

$$d_э = 4R_г = 2\delta, \tag{3.66}$$

where R_g is the hydraulic radius; δ the minimum radial clearance between the pin and the spray nozzle housing.

The following criterion relations have been proposed for centrifugal spray nozzles [129, 130, 152]:

$$\frac{d_к}{d_e} = \frac{47{,}8 Lp^{0.1}}{A^{0.6} Re^{0.7}}, \tag{3.67}$$

where A is a complex which combines the geometrical dimensions of the spray nozzle

$$\lg \frac{d_к}{\delta} = B Lp^{-1.3} - 0{,}35 \lg We. \tag{3.68}$$

According to the experimental data, the coefficient for the case of atomization of water or aqueous solutions of glycerol is $B = 4.47$, for kerosene and molten paraffin, $B = 2.29$.

$$\frac{d_к}{\cdot} = \frac{190{,}5N^{0.2}}{\mathrm{Re}^{0.6}}. \qquad (3.69)$$

An empirical formula, proposed in the work of Nukiyama and Tanasawa [141] for pneumatic spray nozzles is widely used:

$$d_к = \frac{585\sqrt{\sigma}}{\omega\sqrt{\rho_т}} + 597\left(\frac{v_т\sqrt{\rho_т}}{\sqrt{\sigma}}\right)^{0.45}\cdot\left(\frac{1000q_в}{q_в\rho_т}\right)^{1.5}. \qquad (3.70)$$

This equation was obtained within the following range of variation: σ = 19-73 dyne/cm; $\rho_т$ = 0.7-1.2 g/cm^3; ω = 100-300 m/s; $\rho_в q_в \rho_т^{-1}$ = 600—1000. The diameter of the drops $d_к$, taking the above-indicated dimensions entering into Formula (3.70) into account, is obtained in microns.

In the work [18], a criterion relation is proposed in the form:

$$\frac{d_к}{d_c} = B\mathrm{We}^{-0.45}. \qquad (3.71)$$

The coefficient B is determined experimentally and varies from 1.2 to 0.61, depending on the spray nozzle design.

From our point of view, the equations for calculating the atomization efficiency, should include a complex which characterizes the energy expended in atomization. Whereas for mechanical spray nozzles the Weber criterion (We) can serve as such a complex, this is inadequate for pneumatic (or steam) spray nozzles because the expended energy depends also on the specific flowrate of atomizing medium (air or steam). If the air flowrate is included in the equation for the determination of the average drop size (3.71), better agreement with the experimental data is obtained. However, separation of the velocity and specific air flowrate into two components does not correspond to the physical pattern of atomization because both these parameters are combined in the common concept of energy. When calculating the energy flowrate in pneumatic spray nozzles, it is necessary to determine the useful (transferred to the fuel) part of the spray nozzle energy.

Manuscript Page No.

Transliterated Symbols

87 кр = kr = kriticheskiy = critical

87 к = k = kaplya = drop

88 в = v = vozdukh = air

88 д = d = deformirovannyy = distorted

92 Ф = f = fakel = flame

92 т = t = toplivo = fuel

93 тр = tr = turbulentnyy = turbulent

95 п = p = poterya = lon

95 п = p = par = vapor

102 в = v = ves = weight

108 ф = f = fotometricheskiy = photometric

109 э = e = elektricheskiy = electric

109 ЦНИИ МПС = TsNII MPS = Tsentralnyy nauchno-issledovatel'skiy institut ministerstva putey soobshcheniya = Central Scientific Research Institute of the Ministry of Railways

112 ВУ = VU = vyazkost' uslovnaya = conventional viscosity

114 с = s = soplo = nozzle

115 э = e = ekvivalentnyy = equivalent

115 г = g = gidravlicheskiy = hydraulic

Chapter 4

PRINCIPLES OF ORGANIZATION OF THE FLAME PROCESS

14. PRINCIPAL DIAGRAMS OF HEATING UNITS

According to the terminology of Professor G.F. Knorre [156], the whole diversity of heating devices used in different fields of stationary and transport power engineering can be divided into two basic classes: furnaces of the heating type and furnaces in power installations. To the heating type belong the furnaces of stationary and movable boiler installations, industrial furnaces and devices in which the heat, evolved during the process of combustion of a fuel, is transferred to another body, but where the combustion products do not perform useful work (excepting the work of displacement of the gases). Typical for furnaces of this type is the simultaneous evolution and absorption of heat. The tendency to maximum utilization of the radiative heat of the flame results in the need for the utmost development of radiation-absorbing surfaces, the accommodation of which compels the use only of simple, mainly rectangular configurations of heating devices with large dimensions.

In furnaces of the power type, the main purpose of which is the production of a working gas fluid with certain parameters, the aim followed is a maximum intensification of the process of heat evolution. The processes of heat removal from the flame and the combustion products within the limits of the furnaces are secondary and, generally speaking, undesirable. As a rule, the furnaces of the power type are not only technologically but also with regard to the design combined with the other units of the device.

The different purpose of heating devices limits to some degree the possibility of selecting a single principal diagram. Thus, for furnaces of the heating type, the conditions of the arrangement of te shielding surfaces is of primary importance whereas for power furnaces the decisive factor is the weight and size limitation.

However, independently of their purpose and operating conditions, the following common technical requirements apply to both types of furnaces.

1. The design of the heating device should ensure a maximum degree of combustion of the fuel and stable combustion under all operating conditions of the power installation at high heat stresses and a minimum of hydraulic losses.

2. The process of combustion of the fuel under all operating conditions of the heating device must take place without formation of deposits and smoke.

3. The products of the combustion of the fuel should not have a corrosive and erosive effect on the metal parts located in the path of their flow and should also not cause asn and coke deposits.

4. The design of the heating device should ensure safe operation and the possibility of inspection, maintenance or the replacement of individual parts or the furnace itself.

5. The service life of the heating device should be adequate.

The requirement to attain high rates of heat transfer in the furnace volume is equivalent to the requirement to shorten considerably all stages of the combustion process of each separate drop in the flame. The requirement for completeness of the combustion can be reduced to the requirement of a complete combustion of all fuel drops (This implies not only the complete disappearance of the mass of the liquid drop during its combustion, but also the complete combustion of its vapor even outside the individual combustion zone). It is technically impossible to fulfill these requirements simply by reducing the size of the drops arriving in the furnace. As has been shown in Chapter 1, a marked acceleration of the combustion process requires an increase in the temperature level of the process and the supply of oxidant to each drop. These conditions can be achieved by thcrough mixing of the atomized fuel with the air which is either strongly preheated or added in slight excess. The intense agitation of the airstream in which the combustion takes place involves additional energy expenditure which is responsible for the higher hydraulic losses.

Finally, the requirement of stability of the combustion process under all operating conditions of the heating device means to achieve reliable ignition of the fuel jet upon variation of the furnace load within given limits. This requirement can be met by a large increase in the agitation of the fuel jet or by providing for a recirculation of part of the high-temperature combustion products to the root of the flame which also increases the hydraulic losses.

Thus, the requirement of boosted operation and low hydraulic loss is to some degree contradictory.

As follows from the preceding chapters, the development of the process of combustion of a fuel drop during a certain stage can also take place without supply of air, simply in the gas medium with high temperature. Such a stage is the preheating of the drop, the duration of which increases considerably for heavier fuels, increase in drop size and lowering of the ambient temperature. Under the usual conditions of combustion of heavy fuels this amounts to 30% of the total combustion time of the drop. Extending this assumption to the entire flame which contains drops of different sizes, it can be concluded that the supply of the air required for the combustion of the flame to the nozzle orifice is not such a necessary

measure as thought previously. Most likely, the supply of the entire air to the root of the fuel flame is not inexpedient because this lowers the temperature and the process of preparation of the drop for combustion (preheating) is correspondingly extended in time. The slower development of the preparatory processes involves a change in the combustion conditions in connection with the slower temperature rise and the shift of the flame center in the direction of the airstream. Simultaneously with this, reliable ignition of the jet by return of part of the combustion products requires the provision of a larger zone of return flow which naturally increases the hydraulic losses. Rapid attenuation of the initial turbulent flow in the burning flame, provided to achieve mixing in the depth of the flame, requires an increase in the flow velocity of the air which also increases teh hydraulic losses.

The best solution for shortening the duration of all stages of the combustion process and for lowering the level of the hydraulic losses is to distribute the air supply along the length of the flame, supplying only that part of it to the root of the flame which is indispensable for the ignition and combustion of the smallest drops. The remainder of the air is distributed along the flame to provide for the ignition and combustion of the larger drops.

This arrangement of the process, first carried out in 1886 by the engineer Pashinin for ship's boilers [157], enabled the total efficiency of combustion of the fuel to be greatly increased with considerable increase in the steam output of the boiler.

Practically all power furnaces (combustion chambers of gas turbine engines [GTE](ГТУ) now operate on this combustion principle. However, for boiler furnaces, the use of separate air supply involves considerable engineering difficulties due to the specific design of these furnaces.

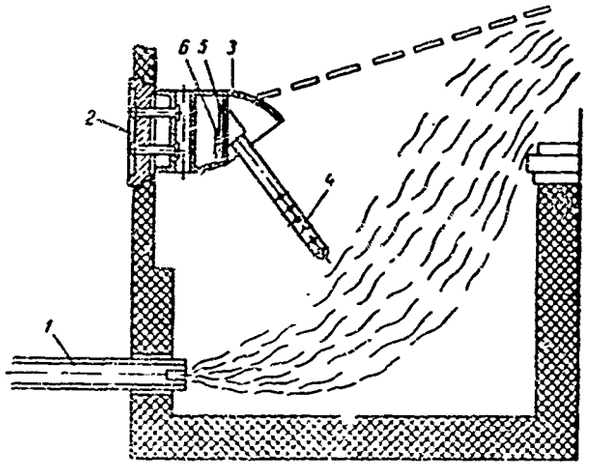

Fig. 55. Facility for injecting secondary air into the zone of combustion of petroleum residue: 1) Working spray nozzle; 2) input orifices; 3) air preheater; 4) outlet nozzles; 5) control valve; 6) gate.

The provision of nonlocal air supply depends primarily on the possibility of achieving the required range of the air jet. For power furnaces, the necessary depth of penetration of the lateral (with regard to the flame) air jet is achieved at relatively low initial flow velocities and small orifices which makes it possible to match the quantity of air necessary for supply to a certain flame zone and its velocity. For normal boiler furnaces, the transverse dimensions of which are very large and are determined by the arrangement of the shielding surfaces, this matching is obviously impossible without the use of special high-pressure air supply devices although some proposals in this direction have already been made. One of the devices which improve the combustion process of heavy fuels, is represented in Fig. 55. According to [158], the secondary air is supplied via orifices in the air preheater which is located in the furnace chamber. From the preheater, the air passes through nozzles into the combsution zone. The quantity of secondary air supplied to the flame is controlled by means of a gate and special valves.

The heating device shown in Fig. 56 may also be a certain interest. This heating device is a combustion chamber to which the air for combustion is supplied in stages, in proportion to the combustion of the fuel flame. The first stage, usually termed the gasification chamber, is a closed volume to which a small proportion of the air (~30%) required for the combustion of the fuel is supplied via the atomizer. This air reaches the furnace volume through numerous orifices in the walls. The combustion products together with partly vaporized and gasified fuel arrive in the second stage (afterburning chamber), where the remainder of the air is directed.

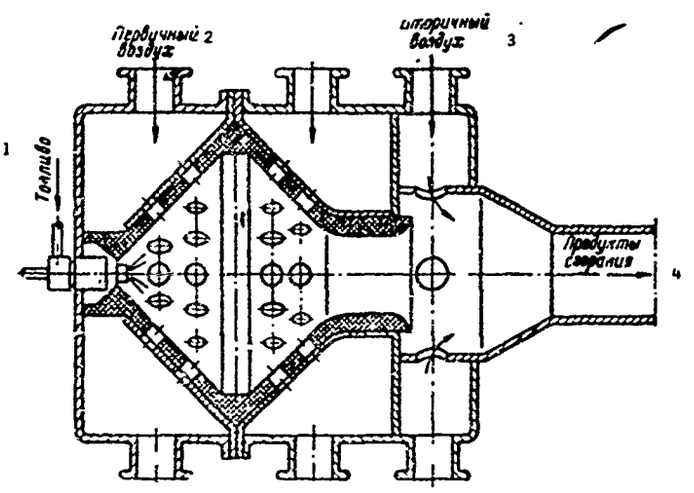

Fig. 56. Schematic view of a firebox for the combustion of sulfur-containing fuels. 1) Fuel; 2) primary air; 3) secondary air; 4) combustion products.

However, neither of these sclutions is radical enough, and suitable for general application since one of them can be used only for furnaces with small volume and the other requires a special

furnace design.

Thus, the design of a heating device which completely satisfies all requirements is very difficult at present. These difficulties are further aggravated by the fact that the currently used standard method for the calculation of furnaces [159] is not suitable for selecting the most rational methods of handling the combustion process but is merely a method of determining the final parameters of the combustion products for given operating conditions of the furnace.

These factors had the consequence that the design of all furnaces of the power as well as the heating type is carried out mainly experimentally on the basis of data on the performance of analogous designs at the disposal of the designers. This, in turn, led to the appearance of a very large number of types and designs of furnaces for the most diverse purposes. It should be pointed out, however, that for furnaces of the heating type it would be more correct to speak of the creation of a large number of types of burner devices and not of furnaces, since the design of the latter is determined mainly by the arrangement of the shielding surfaces as mentioned in the foregoing.

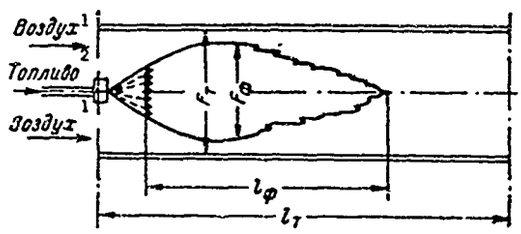

Fig. 57. Scheme of the simplest single-pass furnace chamber: F_t, F_f) Cross sections of furnace and flame; l_t, l_f) length of furnace and flame; 1) Air; 2) fuel.

It should also be pointed out that the design features of boiler furnaces, mainly those with large capacity, compel the use of a large number of burners in order to achieve adequate filling of the furnace volume with the flame.

Despite the great diversity of the burner device designs, they can be divided in principle on the basis of the handling of the relative motion of the fuel and air into single-pass and tangential burners and, with respect to the method of air supply, into straight-jet and vortex (turbulent) burners. An additional attribute for classification is the method of supply the air to the flame.

Most burners in operation at present are of the type in which the entire air required for combustion is supplied to the root of the flame. However, burners in which a separation into primary and secondary air is used, are beginning to find wider application.

Figure 57 shows the simplest scheme of a single-pass burner which has been widely used in the past in stationary power and heating installations. The inherent deficiencies of this design are the very limited range of stable combustion and the practical impossibility of achieving high volume and cross-section boosting of the furnace. This is due, firstly, to the fact that as the flow moves away from the nozzle, the combustion products impede the flow more and more, thus hindering the access of oxidant to the unburned drops. Secondly, as the flow progresses in the furnace, a considerable decrease of the relative drop velocity occurs which causes a marked decrease in the mixing intensity and, consequently, prolongs the afterburning of the flame. And, finally and thirdly, the peripheral layers of the introduced air practically do not participate in the combustion. Hence, the process of combustion of atomized fuel takes place with a much smaller average excess of air than would be assumed on the basis of the fuel-air ratio.

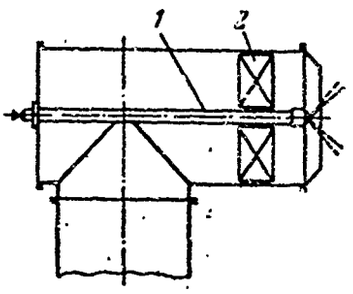

Fig. 58. Scheme of turbulent burner with vane damper: 1) Spray nozzle; 2) damper.

A zone of reverse currents develops in the annular rotating airstream produced in the burners of the turbulent type. The dimensions of this zone are determined by the tangential velocity component of the vortex flow. Above all, this made it possible to improve greatly the conditions of continuous ignition of the introduced fuel by conveying part of the hot combustion products to the root of the fuel flame. Furthermore, the high initial turbulence of the flow caused more intense delivery of oxygen to the burning drops at the end of the flame. Thus, the twisting of the airflow made it possible to solve two main problems successfully: to shorten considerably the duration of the preparatory stages of the combustion process (preheating and ignition of the fuel) and to actively influence the final stage of the process, the afterburning of the coke particles. The twisting of the flow proved to be so effective that this principle is now perhaps the basic one in the practice of designing and construction of the most diverse burner devices for heavy fuels.

Burners in which the turbulent flow and vortex formation are achieved by incorporating a vane damper have found widespread application.

A mechanical spray nozzle, usually of the centrifugal type, is located in the center of this damper (Fig. 58).

The vortex effect in the airflow can also be obtained by tangential supply of the air to the burner as in the simplest form of burner, shown in Fig. 59([OEN](OЗН) burner). A distinguishing feature of this burner is that the energy of the airflow is also used for the atomization of the fuel. More complex in design and operating principle is the burner depicted in Fig. 60. The air required for combustion, the quantity of which can be controlled by peripheral contoured vanes, enters the burner duct under an angle to the burner axis, thus acquiring a tangential component. A specialIly shaped damper located in the burner axis, divides the airstream into two parts, one of which is delivered via tangential channels with rectangular section in the body of the damper to the root of the fuel jet, formed by a mechanical (centrifugal) spray nozzle, while the other by-passes the damper and enters the furnace chamber.

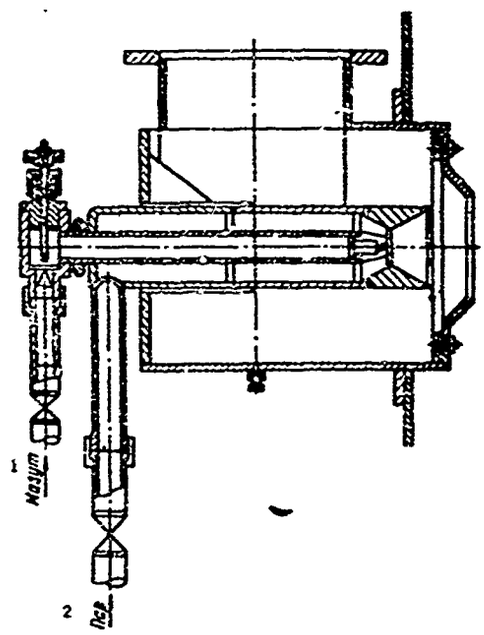

Fig. 59. Schematic view of turbulent burner with tangential air supply. 1) Petroleum residue; 2) steam.

The burner shown in Fig. 61 is very similar in principle to the preceding one.

In this design, the division of the airstream into a primary one deflected towards the root of the fuel flame and a secondary one, is more obvious. It is achieved by means of a vane damper situated in the center of the burner, through which the primary air enters, and a system of orifices at the periphery, through which the second-

ary air is supplied to the burning flame.

It can be inferred from an examination of the basic operating principles and designs of burner devices that the most significant aspect in the development of burners for heavy liquid fuels is the use of a vortex flow with division of the air into primary and secondary; this was verified experimentally in power-type furnaces and presented itself in the best light.

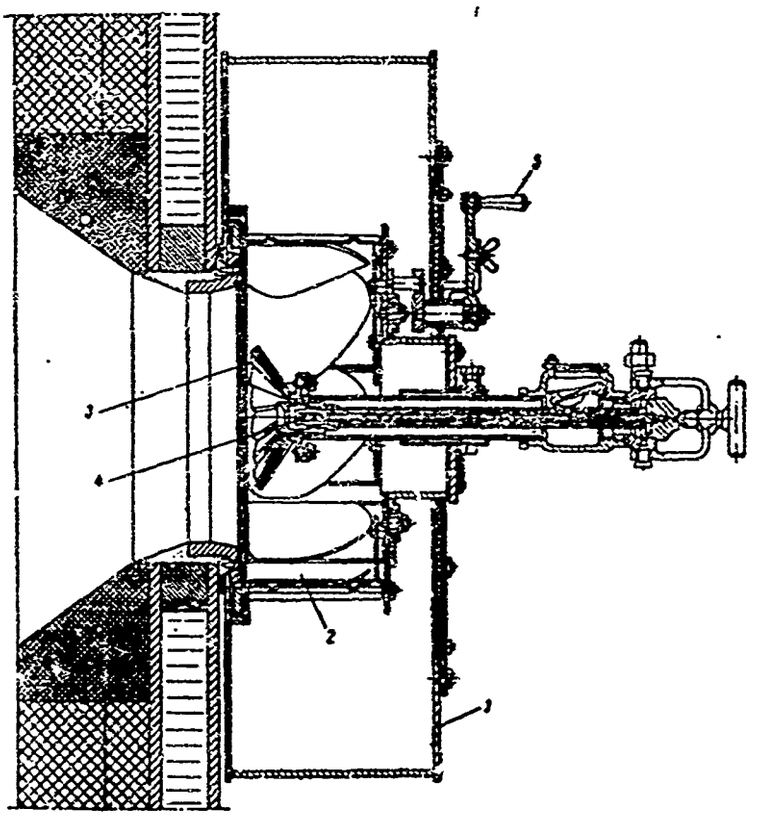

Fig. 60. Turbulent burner with separate air supply: 1) Air duct; 2) control vanes; 3) conical blade damper; 4) spray nozzle; 5) crank handle for rotating the blades.

One of the factors which determine the rate of combustion of the flame and, consequently, the specific thermal load in the furnace volume, is the process of afterburning of the coke residue as well as the gaseous products of the incomplete combustion of the fuel vapor. The speed of this process is determined by the hydrodynamic conditions and the transverse dimensions of the airflow. The smaller these dimensions are, the better will be the mixing and the more rapid the afterburning, other conditions being equal. In the multiburner furnaces, the transverse dimensions of the flame are considerable, which, naturally, makes it more difficult to achieve through mixing. This circumstance is aggravated by the mutual influ-

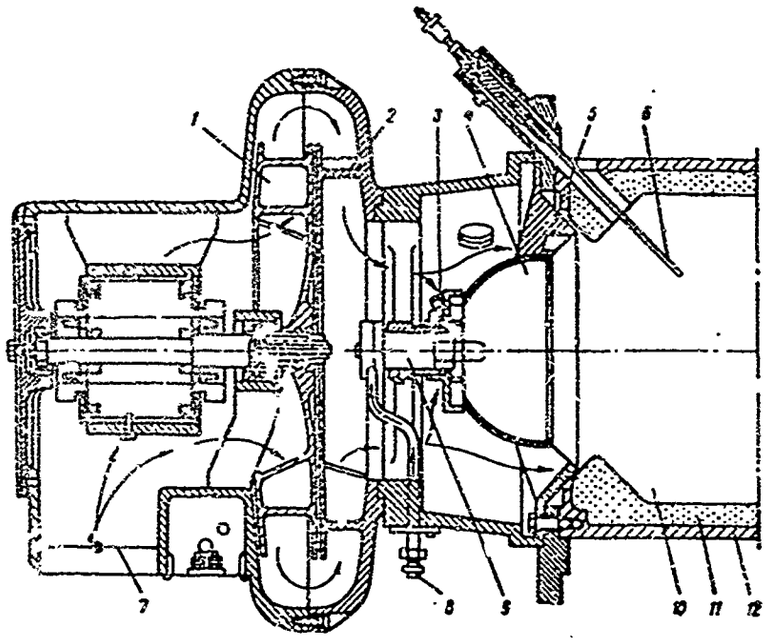

Fig. 61. Turbulent burner with separate air supply: 1) Fan; 2) guiding vanes; 3) primary air vortex former; 4) ignition zone; 5) nozzles for the supply of secondary air; 6) flame indicator (ionization sensor); 7) air control gate; 8) fuel supply; 9) centrifugal spray nozzle; 10) combustion zone; 11) refractory coat; 12) steel body of burner.

ence of adjacent flames.

Based on these concepts, it is recommended in the work [160] to divide large furnaces into separate sections by installing duplex shields of the type of honeycomb furnace of the single-pass boiler No. 1 of TETs-9 of Mosenergo or by installing parallel series of tubes (glove-type boilers). Each such cell is equipped with its own burner. The realization of this hypothesis should give a very efficient operation due to the increased radiating surface as well as the possibility of a considerable increase in the specific heat transfer rates in the furnace volume, as attested to by the practical operation of the small-size power furnaces of the type of GTU combustion chamber in which heat transfer-rates were achieved which were ten times higher than in large-volume boiler furnaces.

15. DISTRIBUTION OF THE FUEL OVER THE FURNACE VOLUME

Two theories are currently used for calculating the local fuel concentration at every point of the furnace volume. According to one of these [161-163], the motion of the flame is regarded as the motion of a physical body with variable density, and, consequently, with a variable resistance coefficient. Here belongs also the theory of turbulent flows which examines the motion of a gas flow with solid

impurities [149]. The assumption is made in this case that a constant quantity of fuel passes through any cross section of the flow. In reality, the quantity of fuel decreases with increasing distance from the burner nozzle since the flight distance of the drops, other conditions being equal, is determined by the drop size. The greater the diameter of the drop, the further it flies.

According to the second theory [108-110], the calculation is carried out for each drop separately, making use of the equation of motion of the mass center of a solid sphere but it does not take into account the flow of the ambient air entrained by the stream of drops.

As a study of the flight of solid particles in an airstream [125] shows, their velocity does not vary during their motion in the same way as that of the air. The airflow is decelerated considerably more efficiently than the solid particles.

In the initial part of the fuel flame, where the distance between drops is small, the particles exert a mutual influence and on the surrounding air, entraining it and imparting to it a velocity close to that of the drops. In proportion to the increasing distance of the drops from the nozzle, the distance between them increases, the interaction decreases and the motion of each drop becomes independent. Thus, the jet can be regarded in its first section as an integral body which does not give off individual drops and, in the second, one can study the motion of individual drops in the airstream entrained in the initial section. The length of the initial section depends on the angle of the jet, the flow velocity and fuel consumption and also on the quality of atomization. The larger the angle of the jet, the shorter is the initial section and the interaction between drops ceases nearer to the nozzle. The velocity and fuel consumption have the opposite effect.

With coarse atomization, the independent motion of the drops begins sooner because the larger the drops, the smaller is their number in the stream and the greater the distance between them. Consequently, not only the average drop size but also the size distribution of the drops affects the nature of the aerodynamic interaction between the fuel and air stream.

In the case of mechanical atomization, the large drops with their large wake, entrain a greater mass of air than the small drops and exert a considerable influence on the motion of the small drops. In the pneumatic spray nozzles, more time is required for equalizing the velocities of the large drops and the dispersing medium in the initial section, where the velocity of the air is greater than that of the drops, as well as during the deceleration when the velocity of the drops is greater. The small drops will have a velocity close to that of the airstream for a considerable proportion of their path in the furnace. The sudden velocity drop of the air in pneumatic atomization takes place after the initial section, which, according to the theory of turbulent flow [149] amounts to

$$x_0 = \frac{0{,}56R_0}{a}, \qquad (4.1)$$

where x_0 is the length of the initial section; R_0 the initial radius

of the jet; a, the degree of initial turbulence of the airstream, amounts to 0.06-0.075 according to the experimental data.

On the basis of an analysis of this physical pattern of the motion of the jet it can be inferred that while the drops have the same velocity at the moment of their formation, the velocity of the drops from the moment of their independent motion (when their mutual distance is large and they no longer exert a mutual aerodynamic effect) will depend on their size.

In real spray nozzles, the initial section of the flame is short compared with the total flight path of the drops and it can be assumed for practical calculations in first approximation that the drops begin their independent motion directly after their emergence from the atomizer nozzle.

Using the equation of the drop motion (1.21) and (1.29), we find that the total acceleration is

$$j = \frac{dw}{d\tau} = -\varphi_x \frac{w^{1.5}}{d_k^{1.5}}. \qquad (4.2)$$

The solution of Eq. (4.2) at the initial values of $\tau = 0$, $x = 0$, $w = kw_0$ will have the form

$$x = \frac{2d_k^{1.5} k w_0 \tau}{2d_k^{1.5} + \varphi_x k^{0.5} w_0^{0.5} \tau}, \qquad (4.3)$$

where k is a coefficient which takes into account the deviation of the velocity of the drops during their independent motion from the average flow velocity of the fuel; according to the experimental data, k depends on the drop radius and can be approximately calculated by means of the empirical formula

$$k = 0{,}16 + 0{,}84 \exp(-8d_k), \qquad (4.4)$$

where d is expressed in mm.

As follows from Eq. (4.3), the flight distance of the drops depends essentially on the drop radius. If we assume that the motion of the jet terminates at $\tau = \infty$, then we can calculate for each drop its maximum distance from the spray nozzle (Fig. 62).

The velocity variation along the length of the flame can be determined if we replace the variables in Eq. (4.2); since

$$j = \frac{dw}{d\tau} = \frac{dw}{dx}\frac{dx}{d\tau} = w\frac{dw}{dx}, \qquad (4.5)$$

we obtain

$$w\frac{dw}{dx} = -\varphi_x \frac{w^{1.5}}{d_k^{1.5}}. \qquad (4.6)$$

As a result of the solution of (4.6), taking into account that at $x = 0$, $w = w_0$, we find the velocity of the drops at any distance from the spray nozzle

$$w = \left(k^{0.5} w_0^{0.5} - \frac{\varphi_x x}{2d_k^{1.5}}\right)^2. \qquad (4.7)$$

At $w = 0$, the solution of this equation gives the maximum flight distance of the drops and coincides with Eq. (4.3) at $\tau = \infty$.

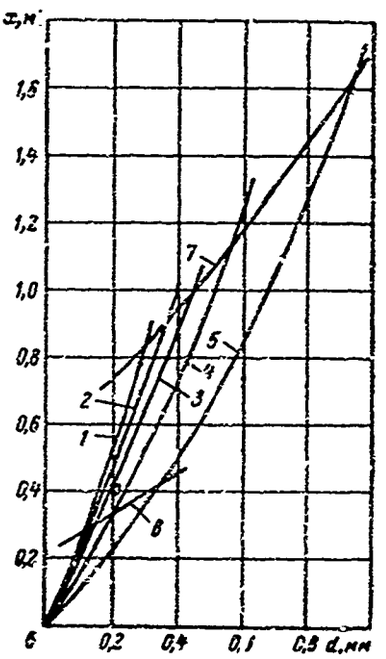

Fig. 62. Flight distance of drops of petroleum residue as a function of their diameter and initial velocity (w): 1) w = 100 m/s; 2) w = 80 m/s; 3) w = 60 m/s; 4) w = 40 m/s; 5) w = 20 m/s; 6) maximum drop sizes of petroleum residue at B = 154 (Eq. (3.28) and 7) at B = 4.36.

Owing to the turbulent impulse exchange with the ambient air during the motion of the fuel, a deviation of the drop trajectory from the axis takes place which imparts a conical shape to the jet. On the basis of theoretical studies, using the laws of turbulent diffusion [164], an equation was obtained which characterizes the relative density of the stream over the cross section for jet-type spray nozzles

$$\frac{q}{q_\tau} = \exp\left[-0{,}693\left(\frac{r}{r_0}\right)^2\right], \qquad (4.8)$$

where q is the mass of fuel in the considered section at a certain radius; q_t the mass of fuel in the center of the flame; r, the instantaneous radius;

$$r_0 = 2 \ln 2 k_r a_t x^2, \qquad (4.9)$$

where a_t is a constant characterizing the turbulence of the jet; k_r a constant which characterizes the quality of atomization.

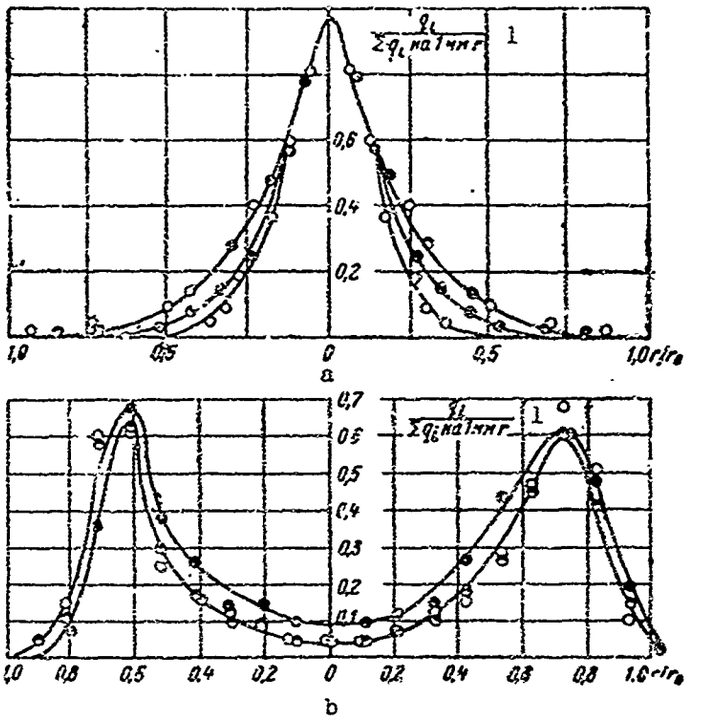

Fig. 63. Distribution of the fuel along the radius: a) For jet-type spray nozzles; b) for centrifugal spray nozzles. 1) per 1 mm of r.

Experimental verification of Eq. (4.8) gave good agreement with the theoretical values. As follows from (4.8), the distribution of the fuel along the radius of the jet becomes more uniform with increasing distance from the spray nozzle (Fig. 63a).

When we consider the distribution of the fuel in the flame of centrifugal spray nozzles we must take into account the presence of a rotational moment in the vortex chamber and nozzle of the spray nozzle which imparts a peculiar shape (hollow cone) to the fuel jet. Since the centrifugal spray nozzles have a large jet angle, consideration of the motion of the drops along the axis only does not by any means give a complete picture. For these spray nozzles, the variation of the trajectory is considered with respect to two mutually perpendicular directions: along the axis and the radius of the flame. In this case, the components of the acceleration, resistance, and initial velocity along the x axis will be:

$$j_x = \frac{dw_x}{d\tau}, \tag{4.10}$$

$$R_x = \varphi_x \frac{w^{1.5}}{d_k^{1.5}} \cos\frac{\alpha}{2}, \tag{4.11}$$

$$w_{x.0} = w_0 \cos \alpha/2; \tag{4.12}$$

and for the y axis

$$j_y = \frac{dw_y}{d\tau}, \tag{4.13}$$

$$R_y = \varphi_x \frac{w^{1.5}}{d_k^{1.5}} \sin\frac{\alpha}{2}, \tag{4.14}$$

$$w_{y.0} = w_0 \sin\frac{\alpha}{2}, \tag{4.15}$$

where $\alpha/2$ is the slope angle of the drop trajectory at the moment of the emergence of the drop from the nozzle.

The total velocity of the drop can be expressed as $w = \frac{w_x}{\cos \alpha/2}$ or $w = -\frac{w_y}{\sin \alpha/2}$ and the initial differential equations assume the form

$$\frac{dw_x}{d\tau} = -\varphi_x \frac{w^{1.5}}{\left(\cos\frac{\alpha}{2}\right)^{0.5} d_k^{1.5}}, \tag{4.16}$$

$$\frac{dw_y}{d\tau} = -\varphi_x \frac{w^{1.5}}{\left(\sin\frac{\alpha}{2}\right)^{0.5} d_k^{1.5}}. \tag{4.17}$$

Following solution of (4.16) and (4.17), taking into account the initial conditions, we find the drop coordinates during its motion

$$x = \frac{2d_k^{1.5} k w_0 \cos\frac{\alpha}{2}\tau}{2d_k^{1.5} + \varphi_x k^{0.5} w_0^{0.5} \tau}, \tag{4.18}$$

$$y = \frac{2d_k^{1.5} k w_0 \sin\frac{\alpha}{2}\tau}{2d_k^{1.5} + \varphi_x k^{0.5} w_0^{0.5} \tau}. \tag{4.19}$$

The data of this equation differ from those of the equation for the jet-type spray nozzle (4.3) merely by one factor which depends on the flame angle. The flight distance as a function of the drop size for jet and centrifugal spray nozzles can be described by the same diagram (see Fig. 62). As follows from Fig. 62, the flight distance of the drops increases in proportion to their size and initial velocity. However, these parameters (drop size and velocity) are also interrelated; for a given spray nozzle design and fuel, the maximum drop size will be determined by the initial velocity of the jet. Consequently, each of the curves (see Fig. 62) should have complete-

ly defined boundaries. If we use Eq. (3.68), we find the following relation for the mean drop size of petroleum residue at a thickness of the conical film of 0.25 mm:

$$d_k = \frac{B}{w^{0.7}}, \qquad (4.20)$$

and for the maximum size, assuming $m = 3$, in accordance with Eq. (4.20), we obtain

$$d_{max} = \frac{1.88}{w^{0.7}}, \qquad (4.21)$$

where B for the chosen conditions [$\delta = 0.25$ mm, $\rho_t = 91.7$ (kgf·s^2/m^4, $\nu = 5.8$ mm^2/s (~1.5°VU)] is 1.54, with d_{max} expressed in mm and w in m/s.

Having determined the maximum drop diameters by means of the diagrams of Fig. 62, we have then the flight distance of the largest drops (or the length of the flame). This dependence can be expressed analytically for the chosen conditions:

$$x_{max} = \frac{2B^{1.5}}{\varphi_k w^{0.55}}. \qquad (4.22)$$

As follows from Eq. (4.22), the flame length decreases with increase in the initial velocity of the fuel. This is explained by the fact that an increase in the initial velocity has an important effect on the drop size. The resultant decrease in the maximum drop size causes a shortening of the flame length.

A combined analysis of Eqs. (3.68) and (4.18) makes possible the assertion that with increase in the thickness of the conical film the flame length will increase since the flame will contain larger drops. With increase in surface tension, viscosity and specific gravity of the fuel, the flame length also increases. For example, if the viscosity increases to 3°VU (~20 mm^2/s) $B = 4.36$ (4.20), and the line limiting the maximum range will accordingly be shifted higher (see Fig. 62.7).

The mass of the flame varies with increasing distance from the nozzle. For example, at $x_0 = 0.6$ m ($w_0 = 60$ m/s), all drops with a diameter less than 275 μ lose their axial velocity and settle under the action of gravity (see Fig. 62), consequently, the mass of fuel passing through a furnace cross section at the distance x_i will be less than near the spray nozzle. The weight of the drops for each diameter can be determined from the distribution equation (3.28) or (3.42). Excluding the weight of the drops which have lost their axial velocity, we find the variation of the mass of the fuel along the length of the flame (Fig. 64a) for the case of $B = 4.36$ (Eq. 4.20).

Not only the total mass of fuel but also the average drop size varies along the length of the flame. To determine the average weight diameter we can use the equation

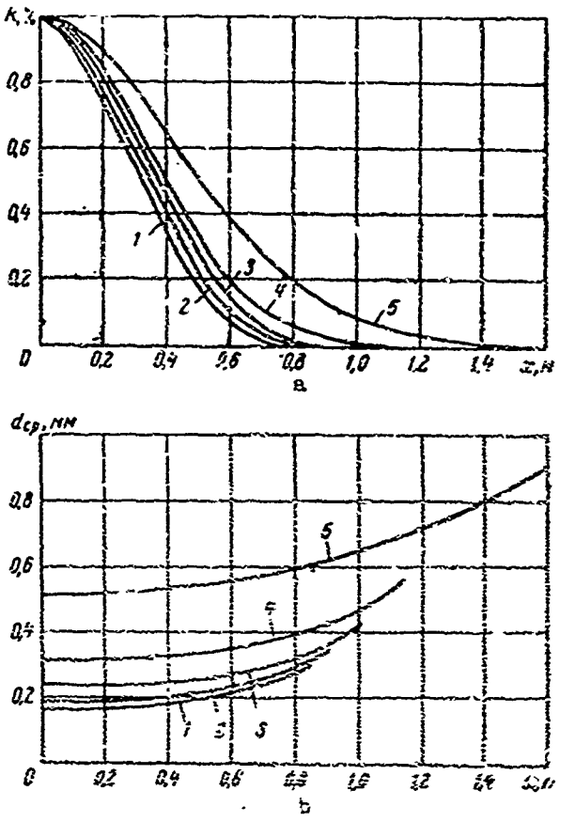

Fig. 64. Variation of the mass of fuel (a) and the average drop size (b) along the length of the flame: 1) w = 100 m/s; 2) w = 80 m/s; 3) w = 60 m/s; 4) w = 40 m/s; 5) w = 20 m/s.

$$d_{k,3} = \left(\sum_{i=1}^{i=n} q_i d_{k_i} - \sum_{i=1}^{i=k} q_i d_{k_i}\right)\left(\sum_{i=1}^{i=n} q_i - \sum_{i=1}^{i=k} q_i\right)^{-1}, \qquad (4.25)$$

where d_{k_i} are the discrete drop diameters; q_i the weight of drops with the diameter d_{k_i}; n is the total number of drop size groups; k is the drop size the flight distance of which is limited by the cross section of the flame under consideration.

The variation of the mass and size composition of the flame also takes place in radial direction. It follows from the equations for the drop trajectories (4.18) and (4.19) that the large drops are located in the flame periphery and the small drops closer to the center. Figure 65a shows schematically one of the typical drop distributions over the flame cross section, obtained by the authors in a study on several centrifugal spray nozzles. Each line gives

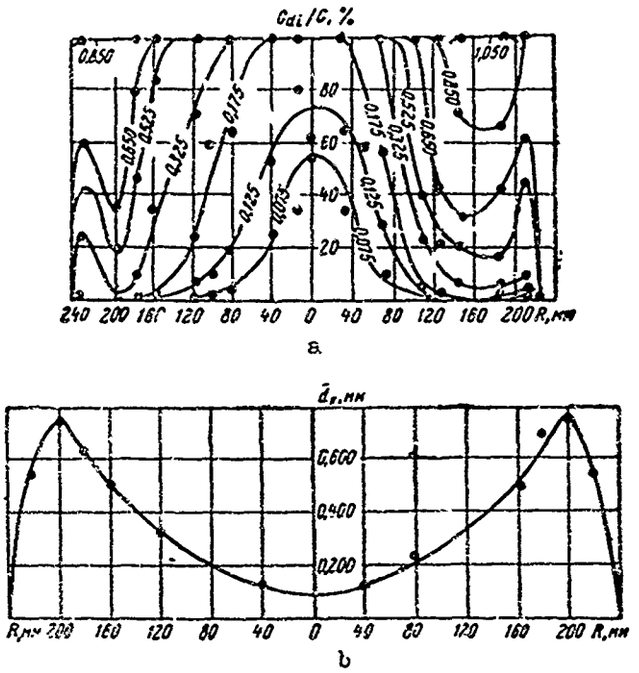

Fig. 65. Distribution of fuel drops with respect to size in radial direction: a) Dispersion composition in %; b) average sizes.

the weight of drops of a certain size relative to the weight of fuel at this point. As follows from the above-given relations, the periphery contains a small quantity of small drops which is in contradiction with Eq. (4.19). The deviation of the small drops from the theoretical trajectory takes place because during the flight of the drops, as a result of the turbulent exchange with the ambient air, the latter will move along the axis. By interacting with the fuel drops, the entrained air changes the trajectory of the drops away from the nozzle axis. The air has the greatest effect on the small drops so that a certain redistribution takes place and a small quantity of small drops reaches the periphery. With regard to their weight percentage, these drops amount to a negligibly small quantity.

The deviation of the large drops, containing the main mass of the fuel, from the axis also determines the distribution of the fuel over the cross section with two maxima, typical for the centrifugal spray nozzles (see Fig. 63b). Knowing the distribution of the drop weight on the basis of the sizes (3.28) or (3.42), it is possible to obtain, by using Eq. (4.22), the flame density as a function of the radius (see Fig. 63b) and, conversely, by means of the flame density one can calculate the distribution curve of the drop weights by means of the sizes.

The motion and development of the fuel jet in furnaces takes place in an airstream. If the airstream with the velocity v is in the direction of the flame axis, the force of resistance R to the

motion of the drops is determined by the relative velocity. The differential equations of motion can then be written thus

$$\frac{dw_x}{d\tau} = -\varphi_\kappa \frac{(w_x - v_s)^{1.5}}{d_\kappa^{1.5}} (1 + c^2)^{0.25}, \tag{4.24}$$

$$\frac{dw_y}{d\tau} = -\varphi_\kappa \frac{w_y^{1.5}}{d_\kappa^{1.5}} \left(1 + \frac{1}{c^2}\right)^{0.25}, \tag{4.25}$$

where

$$c = \frac{w \sin \frac{\alpha}{2}}{w \cos \frac{\alpha}{2} - v_s}. \tag{4.26}$$

The solution of these equations under the initial conditions $\tau = 0, w_x = kw_0 \cos \frac{\alpha}{2} - v_s$, $x = 0$, $w_y = kw_0 \sin \frac{\alpha}{2}$, $y = 0$ gives the following expressions for the determination of the drop coordinates relative to the spray nozzle

$$x = \frac{kw_0 \cos \alpha/2 - v_s}{\frac{\varphi_\kappa (1 + c^2)^{0.25} \sqrt{kw_0 \cos \alpha/2 - v_s}}{2d_\kappa^{1.5}} + \frac{1}{\tau}} + v_s \tau, \tag{4.27}$$

$$y = \frac{kw_0 \sin \alpha/2}{\frac{\varphi_\kappa (1 + c^2)^{0.25} \sqrt{kw_0 \sin \alpha/2}}{2d_\kappa^{1.5} c^{0.5}} + \frac{1}{\tau}}. \tag{4.28}$$

These equations have a limited range of application because with increasing velocity of the air, the relative velocity of the drops and correspondingly the parameter Re decrease. Furthermore, the air velocity in real furnaces does not remain constant over the entire path of motion of the drops.

If most of the path of the drop is traversed under conditions of Re being considerably smaller than 50, it is expedient to use the Stokes equation for calculating the resistance coefficient

$$\varphi_\kappa = \frac{24}{Re}. \tag{4.29}$$

The final expression for calculating the flight distance of the drops will then have the form

$$x = \frac{d_\kappa^2}{\varphi_\kappa} \left[1 - \exp\left(-\frac{\varphi_\kappa}{d_\kappa^2} \tau\right)\right] w_0 \cos \frac{\alpha}{2}, \tag{4.30}$$

$$y = \frac{d_\kappa^2}{\varphi_\kappa} \left[1 - \exp\left(-\frac{\varphi_\kappa}{d_\kappa^2} \tau\right)\right] w_0 \sin \frac{\alpha}{2}, \tag{4.31}$$

$$\varphi_\kappa = 18 \frac{\nu \varrho_0}{\varrho_\tau} k_\varphi. \tag{4.32}$$

Since the Stokes formula is correct only for low values of Re

(under 0.1) we must introduce a correction [165] intc Eq. (4.32)

$$k_\varphi = \frac{\psi}{\psi_c}. \qquad (4.33)$$

The values of the coefficient k_φ as a function of Re and the errors at the limiting values of Re are given in Table 11.

TABLE 11

Corrections to Eq. (4.32)

1 Величина поправки	1,0	1,17	1,31	1,50	1,73	1,98	2,54	2,88
2 Пределы значений Re	0,1—1	1-2	2—4	4—7	7—11	11—16	16—23	31—42
3 Ошибка, %:								
4 в начале участка	+5	+7	+7	+7	+7	+7	+7	+7
5 в конце участка	—5	—7	—7	—7	—7	—7	—7	—7

1) Correction; 2) limits of the value of Re; 3) error, %; 4) in the initial part of the section; 5) at the end of the section.

Tc simplify the calculations, a correction of 0.4 of the maximum for all trajectories of drop motion can be applied.

The calculation of the fuel distribution in the furnace will be more complex in the case of atomization with pneumatic or steam spray nozzles with a high degree of atomization and uniform size distribution of the drops, one can use the equation of motion for a jet with heavy impurities [149]. However, in the practice of fuel atomization with pneumatic spray nozzles, particularly those operating with low pressure, relatively large drops are obtained (~0.3-0.4 mm) with a large range of size variation. Hence, it is necessary to consider the motion of the individual drops for an analysis of the drop distribution in the flame. During the initial moment of the action of the spray nozzle on the fuel, an energy exchange takes place, as a result of which the average velocities of the fuel drops and the atomizing medium becomes equal to

$$w = \frac{w_{0.т} + \beta q v_{0.в}}{1+q}, \qquad (4.34)$$

where $v_{0.v}$ is the initial velocity of the atomizing medium; $w_{0.t}$ the initial velocity of the fuel; q the specific flowrate of the spray nozzle in kg/kg; β the efficiency factor of the kinetic energy of the spray nozzle which characterizes the degree of energy transfer from the air to the fuel.

The flight of the drops in atomization with pneumatic spray nozzles is characterized by sudden variations of the resistance and the parameter Re. Thus, the velocity of the drops in the initial section is considerably lower than the velocity of tne air and Re

has higher values. Then the velocities are equalized and Re = 0. Re then increases again but only slightly because the velocities of the drops and the air decrease. Considering the motion of the drops from the moment of equality of the velocities (which is the case [166, 167] over a short distance) the Stokes formula (4.29) can be used to determine the resistance coefficient. The differential equations of motion then assume the form

$$m\frac{dw}{d\tau} = -\frac{24\pi d_к^2 \varrho_в (w-v)^2}{8\mathrm{Re}}, \tag{4.35}$$

or

$$\frac{dw}{d\tau} = -\frac{\varphi_к}{d_к^2}(w-v), \tag{4.36}$$

$$\varphi_к = 18\frac{\nu\varrho_в}{\varrho_т}. \tag{4.37}$$

As a result of the transverse velocity components and the energy exchange with the ambient gas (air) in turbulent jets, an increase in the cross section of the jet takes place. The drops deviate from the axial direction and their trajectories recede from each other already in the main section to a distance at which they no longer interact. However, the atomizing air (steam) retains a considerable velocity for some time. According to the laws of submerged jets, the axial velocity of the air jet will decrease in inverse ratio to the distance

$$v = v_0\frac{0{,}96R_0}{ax}, \tag{4.38}$$

where x is the distance from the spray nozzle; v_0 the initial velocity of the stream.

The solution of Eq. (4.38) gives the following relations:

$$\frac{dx}{d\tau} = v_0\frac{0{,}96R_0}{ax}, \tag{4.39}$$

$$x^2 = v_0\frac{2\cdot 0{,}96R_0}{a}\tau + c. \tag{4.40}$$

According to the above scheme of motion, x at $\tau = 0$ should be equal to the length of the initial section, when

$$v = \sqrt{\frac{bv_0}{\tau + b/v_0}}, \tag{4.41}$$

where

$$b = \frac{0{,}96R_0}{2a}. \tag{4.42}$$

Substituting the expression for v (4.41) into (4.35), we obtain the differential equation of the drop motion with variable resistance

$$\frac{dw}{d\tau} = -\frac{\varphi_к}{d_к^2}\left(w - \sqrt{\frac{bv_0}{\tau + b/v_0}}\right). \qquad (4.43)$$

The solution of this equation has the form

$$w = \exp\left(-\frac{\varphi_к}{d_к^2}\tau\right)\left[\frac{\varphi_к}{d_к^2}\sqrt{bv_{0.5}}\int^{\tau}\frac{\exp\left(\frac{\varphi_к}{d_к^2}\tau\right)}{\sqrt{\tau + b/v_0}}d\tau + c\right]. \qquad (4.44)$$

The integral contained in this equation does not have a general solution and cannot be expressed by any elementary function. For concrete quantities entering into the equation, one can use the expansion of $\left(\frac{\varphi_к}{d_к^2}\tau\right)$ in a series and integration of this series. The number of terms in the series depends on the concrete conditions.

At equal initial velocities, the flight distance of drops produced with a pneumatic spray nozzle, is greater than those produced with a mechanical spray nozzle.

The distribution of the fuel over the flame cross section for the case of atomization with pneumatic spray nozzles can be described by the theory of turbulent jets for a two-phase flow by a relation of the type

$$\frac{q}{q_\tau} = \left[1 - \left(\frac{r}{r_0}\right)^{1.5}\right]^3, \qquad (4.45)$$

where q is the spraying density of the fuel at a given point; q_t the spraying density in the center of the jet; r the distance of the point under consideration from the jet axis; r_0 the radius of the jet in the investigated section.

According to the experimental data [18], the density of the fuel jet in atomization with a pneumatic spray nozzle varies in accordance with the following relation:

$$\frac{q}{q_\tau} = \exp\left[-0{,}7\left(\frac{r}{r_{0.5}}\right)^{1.6}\right], \qquad (4.46)$$

where $r_{0.5}$ is the distance from the jet axis to the point of the section where

$$\frac{q}{q_\tau} = \frac{1}{2}. \qquad (4.47)$$

There is good agreement between the theoretical and empirical relations, obtained by generalization of the experimental data. The variation of the local fuel concentration in the flame sections corresponds to a qualitative difference characterized by the composition of the dispersion. The average drop size along the burner axis can be determined on the basis of the flight distance of the drops as a function of their sizes and the distribution law of the drop sizes (3.42). As follows from the experimental data, obtained by the authors, the variation of the average drop size in the trans-

verse section of the flame is characterized by similar profiles (Fig. 66a) at any distance from the spray nozzle. Owing to this distribution law, the dependence of the average drop sizes on the flame radius can be generalized by a single curve (Fig. 66b) plotted in the coordinates

$$\frac{d_{cp}}{\bar{d}_{cp}} = f\left(\frac{r}{r_0}\right), \qquad (4.48)$$

where d_{sr} is the average drop diameter in the considered section; $\bar{d}_{sr}$ the average drop diameter, determined over the given cross section; r the distance of the section under consideration from the flame axis; r_0 the maximum flame radius in this section.

The variation of the average drop size along the axis, with pneumatic atomization, is characterized by the relation represented in Fig. 66c.

As follows from a consideration of the laws of motion of the fuel drops in the furnace volume, only the density has a direct effect on the flight distance of the drops. The viscosity and the surface tension affect the general distribution of the fuel only indirectly via their effect on the drop size.

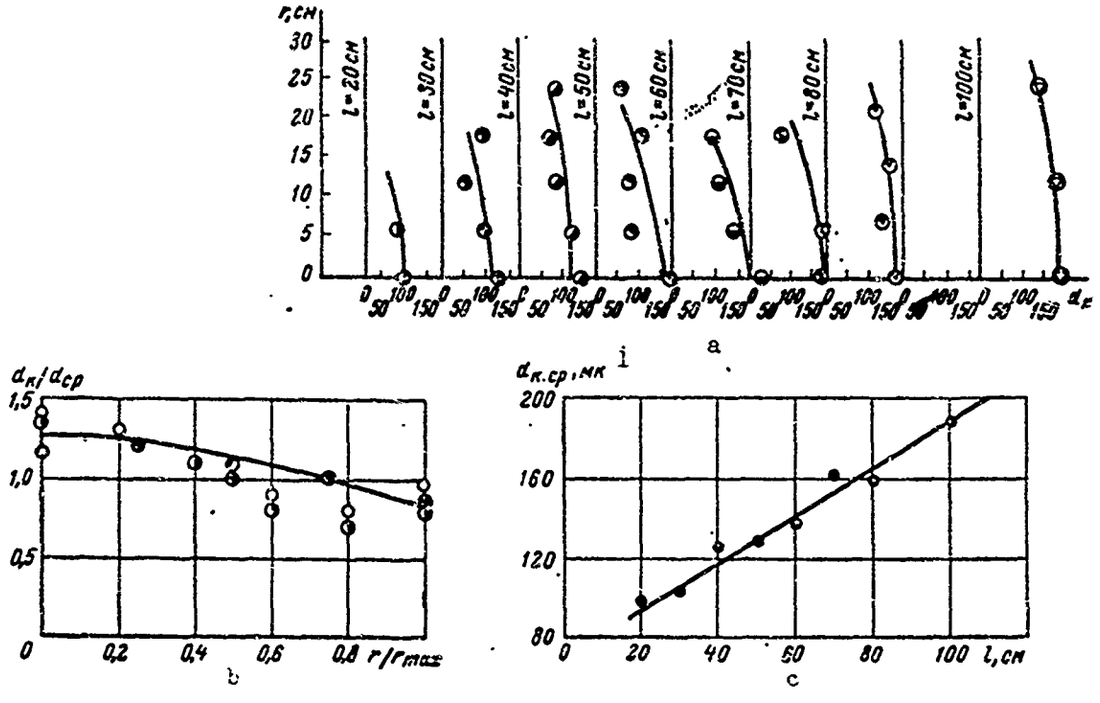

Fig. 66. Distribution of the drop size during pneumatic spraying of a fuel: a) General diagram of drop size variation over the sections; b) drop size variation over the radius; c) variation of the average (radius) drop size along the flame axis. l) μ.

The nature of the fuel distribution and the laws of motion change during the burning of the flame. These changes are due to the decrease in the mass and size of the drops during their flight, the decrease in the resistance coefficient of a burning drop compared with a nonburning drop of the same size and the variation of the viscosity, density and velocity of the ambient gas in consequence of the temperature increase. With increase in the kinematic viscosity of gases during a temperature rise from 200 to 1000°C, the resistance coefficient increases nearly 5 times. On the other hand, the resistance coefficient of a burning drop decreases slightly owing to improved flow [168]. The increase in the gas velocity reduces the relative length of the jet. To take all these factors into account analytically is very difficult but the general relation for the motion of a burning flame will be characterized by a decrease in the flight distance of the drops and a more rapid velocity decrease. The parameter Re also varies greatly for burning drops since the drop diameter and velocity decrease, while the viscosity of the air increases. In this case, the Stokes law can be used to determine the resistance coefficient and the differential equation of motion can be written in the form

$$m\frac{dw}{d\tau} = -\frac{24\pi d_к^2 w^2 \rho_в}{8\mathrm{Re}}. \qquad (4.49)$$

On the basis of the material presented in Chapter 1, it can be assumed that for single-component fuels the drop sizes vary during combustion as a function of time in accordance with the equation

$$d_к^2 = d_0^2 - k_т\tau. \qquad (4.50)$$

Relations (1.72) and (1.81) can be used for the combustion of heavy fuels; assuming for approximate calculation that the decrease in the drop surface takes place in proportion to the time, we obtain:

$$d_к^2 = d_0^2 - \lambda\tau, \qquad (4.51)$$

where

$$\lambda = \frac{k_т^*}{1+\chi}. \qquad (4.52)$$

Using Relations (4.49) and (4.51), we find for the conditions of a burning drop the equation for the equilibrium of forces during its motion

$$-\frac{1}{6}\pi\rho_т (d_0^2 - \lambda\tau)^{1.5}\frac{dw}{d\tau} = 3\pi\nu\rho_в w (d_0^2 - \lambda\tau)^{0.5}. \qquad (4.53)$$

The solution of this equation under the initial conditions $\tau = 0$, $w = w_0$, has the form

$$w = w_0\left(1 - \frac{\lambda\tau}{d_0^2}\right)^{\frac{\varphi_к}{\lambda}}, \qquad (4.54)$$

where

$$\varphi_к = \frac{18\nu\varrho_в}{\varrho_т}. \qquad (4.55)$$

The dependence of the path traversed by the drop on the time can be found by integrating Eq. (4.54) under the boundary conditions $\tau = 0$, $x = 0$

$$x = \frac{w_0 d_0^2}{\varphi_к + \lambda}\left[1 - \left(1 - \frac{\lambda\tau}{d_0^2}\right)^{\frac{\varphi_к}{\lambda}+1}\right]. \qquad (4.56)$$

The flight distance of the drops, determined by the time of its complete combustion $\tau = \frac{d_0^2}{\lambda}$ is equal to

$$x_{max} = \frac{w_0 d_0^2}{\varphi_к + \lambda}. \qquad (4.57)$$

The flight distance up to the moment when the acceleration along the axis and the gravitational acceleration are equal can be calculated by solving Eq. (4.56) at

$$\tau = \frac{1}{\lambda}\left[d_0^2 - \left(\frac{g d_в}{\varphi_к w_в}\right)^{\frac{2\varphi_к}{\lambda}}\right]^{\frac{\lambda}{\varphi_к - \chi}}. \qquad (4.58)$$

The difference between the time thus obtained and the time of complete combustion of the drop amounts to less than 0.001%, thus the flight distance of the drop can be calculated for both cases by means of Eq. (4.57).

In order to find the variation of the fuel mass along the flame in the case of motion of burning drops one has to allow for the fact that the decrease in the total mass of unburned fuel takes place not only on account of completely burned but also partially burned drops.

Knowing the variation of the diameter of any drop as a function of the combustion time, the weight of unburned fuel up to the time τ can be determined:

$$q = \frac{\pi}{6} g\varrho_т \sum_{i=1}^{i=n} N_i (d_0^2 - \lambda\tau)^{1,5}, \qquad (4.59)$$

where N_i is the number of drops with size $d_к$ determined by means of the equation for the weight distribution of the drops (3.28).

According to the Rosin-Rammler distribution, the number of drops of each diameter per unit weight of fuel, is

$$\frac{N_i}{Q} = \frac{6m}{\pi g \varrho_т \bar{d}^m} d^{m-4} \exp\left[-\left(\frac{d}{\bar{d}}\right)^m\right]. \qquad (4.60)$$

By combined solution of Eqs. (4.59) and (4.60) and replacement of the sum by the integral, we obtain

$$q = \frac{m}{\bar{d}^m} \int d^{m-4} (d_к^2 - d_0^2)^{1,5} \exp\left[-\left(\frac{d_к}{\bar{d}}\right)^m\right] dd_к. \qquad (4.61)$$

The integration limits in these equations should be the maximum drop diameter and the diameter of a drop which has completely burned up to the moment τ, equal to $d = \sqrt{\lambda\tau}$. The results of the graphic integration of Eq. (4.61) are shown in Fig. 67. Using this relation and Eq. (4.56), it is possible to obtain the mass variation of the burning fuel along the length of the flame by excluding the time τ.

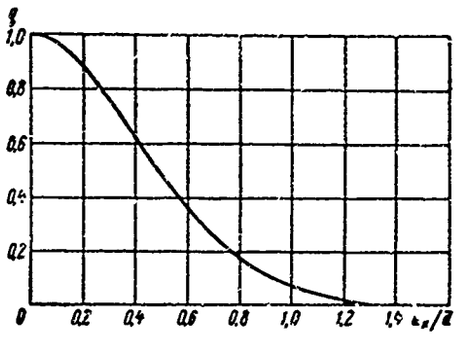

Fig. 67. Weight of the unburned fuel as a function of the ratio $d_к/\bar{d}$ on the drop size distribution according to Eq. (3.28).

The above-presented variants of equations make it possible, depending on the initial conditions of the movement of the fuel in the furnace, to estimate very approximately the distribution of the fuel and to calculate its motion along the flame. Since considerable variations of the conditions of motion take place during the flight of the drops in an operating furnace, it is difficult to find a common equation suitable for calculating the motion along the entire length of the flame. The most marked change in conditions of motion for the heavy fuel drops takes place at the moment of ignition, thus the flight trajectory of the drops must be divided into two parts for a first correction of the mathematical relations: from the moment when the drop leaves the nozzle to the moment of ignition, and from the ignition to its complete combustion.

For the drops which leave the spray nozzle in the direction of the airstream, the velocity and distance from the spray nozzle can be determined by means of the equation

$$w = \frac{4d^3 (w_0 - v)}{\left[\varphi_к (w_0 - v)^{0,5} \tau + 2d^{1,5}\right]^2} + v, \qquad (4.62)$$

$$x = \frac{2d^{1,5} (w_0 - v)\tau}{\varphi_к (w_0 - v)^{0,5} \tau + 2d^{1,5}} + v\tau. \qquad (4.63)$$

The flight time of the drop up to the moment of ignition can be assumed to be equal to the combustion time (see Chapter 1), ne-

glecting the induction time:

$$\tau_{пр} = \frac{d_0^2}{k_э}. \qquad (4.64)$$

The subsequent motion of the drop must be calculated by means of equations which take into account the variation of the drop mass (4.54), (4.56).

For motion of the air at the constant velocity v, the equation for calculating the displacement of the drops assumes the form

$$w = (w_0^* - v)\left(1 - \frac{\lambda\tau}{d_0^2}\right)^{\frac{\varphi_к}{\lambda}} + v \qquad (4.65)$$

and

$$x = \frac{(w_0^* - v)\, d_0^2}{\varphi_к + \lambda}\left[1 - \left(1 - \frac{\lambda\tau}{d_0^2}\right)^{\frac{\varphi_к + \lambda}{\lambda}}\right] + v\tau. \qquad (4.66)$$

The value of the velocity w_0^* in the above expressions is determined from Eqs. (4.62) and (4.64)

$$(w_0^* - v) = \frac{4k_э^2 (w_0 - v)}{(\varphi_к)\sqrt{d(w_0 - v)} + 2k_э)^2}. \qquad (4.67)$$

For large drops of petroleum residue ($d_к \geq 0.3$ mm) the second term of the denominator of (4.67) is ten times smaller than the first; neglecting this term, we obtain

$$w_0^* - v < \frac{4k_э^2}{\varphi_к^2 d_0}. \qquad (4.68)$$

The solution of Inequality (4.68) for the motion of a drop of petroleum residue in a gas stream with a mean temperature of $t \simeq 600°C$ gives the following relation:

$$w_0^* - v < \frac{1.8}{100d},$$

where d is given in mm.

It follows from this relation that for a burning drop with large diameter, the velocity practically coincides with the velocity of the air. For small drops, the two terms in the denominator of Eq. (4.67) become comparable; consequently, the difference in velocities $w_0^* - v$ will be even less than according to (4.66). In Eqs. (4.65) and (4.66) the velocity difference $w_0^* - v$ enters as a multiplicand, the cofactor of which is smaller than 1. Thus, the motion of burning drops can be considered as being identical with that of the air, i.e., it can be assumed that $w_0^* \simeq v$, $x \simeq v\tau$

Induced fortex formation and stagewise air supply and also the reverse currents which arise modify the nature of the distribution somewhat in the sense of a shortening of the flame. Hence it can be assumed that the above-proposed relations give limit values, which must be corrected experimentally.

16. REQUIRED ATOMIZATION QUALITY

Cases are not rare in the practical operation of heating devices in whichthe use of burners which have given excellent service in a certain unit, did not give the expected effect in other furnaces. The choice of the nozzle, which fully corresponds to all requirements of a certain installation, is effected purely by experimental methods which delays greatly the starting up of the furnace or causes a large fuel consumption. This situation is due to the circumstance that the current technical literature contains extremely few data on the basis of which the technical requirements for burners with regard to atomization quality can be formulated, taking the special features of each heating device, its operating conditions and the grade of liquid fuel into account.

The opinions of the researchers on the effect of atomization quality on the combustion process in the flame diverge greatly. Some authors believe [169, 174] that the limiting process is the formation of the mixture (vaporization) determined by a large number of physical and hydrodynamic factors. In this case, the intensity and completeness of the combustion of the fuel flame depends directly on the drop size, and the appearance of losses due to mechanical incomplete combustion is explained by the difference between the combustion time of the fuel particle and its residence time in the furnace chamber. Extremely fine atomization can lead to inefficient mixing [171] because the fuel particles lose their velocity quickly and are entrained by the airstream. The fuel is distributed near the nozzle producing an extremely rich mixture in which the diffusion processes cannot achieve the required composition within the given time interval. On the basis of this reasoning it is claimed that to every design of combustion chamber (furnace) and to each grade of fuel corresponds a most advantageous particle size spectrum, determined by the conditions and nature of distribution of the air along the flame and its turbulence.

Other authors [175, 176, 177], assuming that the combustion of atomized fuel takes place in the gas phase, consider the chemical reaction between the fuel vapor and the oxidant as the limiting process and regard the degree of dispersion of the fuel in the flame as a secondary factor.

The scheme in which the combustion reaction is regarded as the limiting process, can account only for the losses due to cessation of the chemical reaction or its low rate. Hence, the losses can be in the form of products of incomplete combustion or fuel vapor.

It follows from the data given in Chapters 1 and 2, that for fuels with fairly high evaporation characteristic and optimum conditions for the preparation of the combustible mixture (fine atom-

ization, high ambient temperature), the chemical reaction of the combination of the fuel vapor with the oxidant may indeed be the limiting process under certain conditions. When heavy residual fuels of the type of petroleum residues are used, the process of preparation of the combustible mixture and the evaporation determine the total time required for their combustion.

An analysis of the experimental data from this point of view cannot be carried out at present, however, because in the practice of investigation of furnace devices, the atomization quality given by the burner is not measured, as a rule. However, as a result of calculating the specific atomization energy, carried out on the basis of data obtained in studies of different types of burners established in different types of furnaces, a graphic dependence of the total losses of the furnace process on the specific energy $(e_p)^1$ was obtained, which is shown in Fig. 68. As follows from Fig. 68, all the experimental points fit well into a very narrow region determined by natural scatter due to the large errors in the determination of e_p.

The general dependence of the total loss on the specific atomization energy or, which is the same, the quality of atomization, is clearly evident here. Furthermore, at sufficiently large values of e_p, i.e., with sufficiently fine atomization, the differences in atomizer and furnace design cease to be significant and the scattering region of the experimental points is constricted practically to a curve which tends asymptotically towards zero loss. This attests to the fact that with sufficiently fine atomization, the quality of mixing of the atomized fuel with the air begins to assume decisive significance.

The authors carried out special studies [178] in order to obtain direct data on the total effect of the quality of atomization of the liquid fuel on the basic economic indices of the operation of furnaces. In these works, the measurement of the atomization quality was achieved by variation of the spray nozzle design

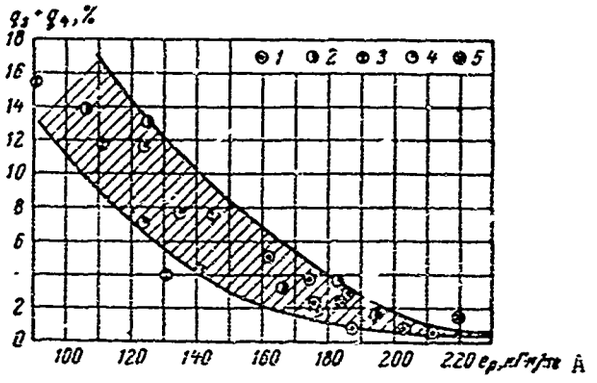

Fig. 68. Furnace losses as a function of the specific atomization energy: 1) Spray nozzle ОЭН-350; 2) spray nozzle НГМ-500; 3) P'yankov's steam spray nozzle; 4) slotted steam spray nozzle; 5) spray nozzle НГМ-500 installed under the boiler ДКВ-10. A) kgf·m/kg.

and its operating parameters and also by variation of the operating conditions of the furnace, using different grades of liquid fuel. Since every deviation of the combustion conditions in the flame from optimum is most clearly manifested under conditions of boosted operation, a cylindrical, fully shielded combustion chamber was chosen as test object. A centrifugal and pneumatic spray nozzle was used.

As a result of processing of the experimental data, graphs were plotted showing the completeness of combustion as a function of the operating conditions and the average drop size in the fuel jet (Fig. 69). As follows from Fig. 69, the quantity η_z for diesel oil tends to decrease with increasing drop size. Thus, for a jet with an average drop size of 200 μ, η_z is about 90%. An increase in the drop diameter to ~300 μ led to a decrease in the completeness of combustion to η_z = 83%.

This relation is more marked and clearer for distillate oil and petroleum residue. In this case, the increase in the drop size within the same limits led to a decrease in the completeness of combustion of 0.85 and 0.75, respectively. These data attest to the fact that the limiting process in the combustion of real heavy fuels in booster furnaces is the process of mixture formation (atomization and vaporization of the drops). Owing to the lowering of the general temperature level of the combustion process with decrease in the boosting, the effect of the atomization quality becomes specially noticeable. Let us examine in first approximation the conditions which should be observed for the realization of given heat transfer rates in the volume of a fully shielded furnace. It is assumed as a working hypothesis that when heavy fuels of the type of petroleum residue are used, the flame has a more discrete structure than in the combustion of light fuels. In this case, the combustion of the large drops and the drops located at the periphery of the fuel jet will differ relatively little from the combustion conditions in an unlimited medium, i.e., from the combustion conditions of a single drop.

A basic condition for the complete combustion of fuel in the furnace volume is the equality of the combustion time of a fuel drop (τ_Σ) and its residence time in the furnace volume (z). The residence time of the fuel drop in the furnace volume cannot be determined without ambiguity because the fuel drops move along different trajectories. The quantity z can be determined most simply for the drops the trajectory of which coincides with the furnace axis and, consequently, with the general direction of motion of the combustion products. In this case

$$z_c = \frac{l_t}{w_t}, \tag{4.69}$$

where l_t is the length of the furnace; w_g is the average velocity of the combustion products.

$$w_t = \frac{V_t}{F_t}. \tag{4.70}$$

Here V_g is the volume throughput of the combustion products; F_t the furnace cross section.

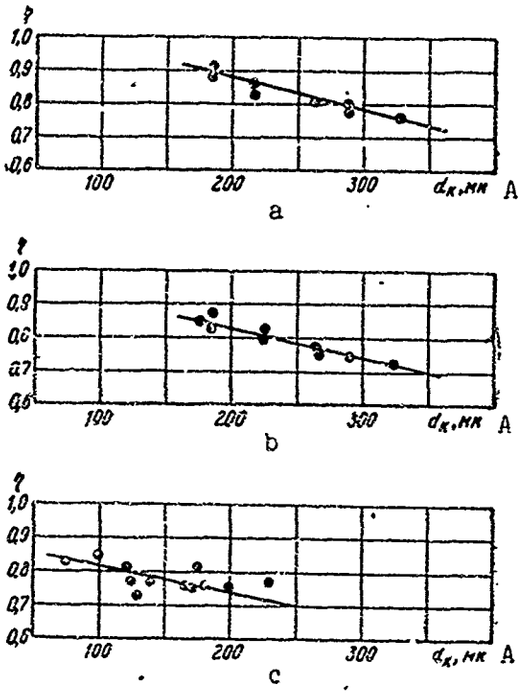

Fig. 69. Variation of the completeness of combustion of the fuel in a furnace chamber as a function of the average drop size in the fuel jet (with constant operating conditions of the furnace); a) Diesel oil; b) distillate oil; c) petroleum residue ◆-12. A) μ.

Substituting (4.70) into (4.69), we obtain

$$z_c = \frac{l_T F_T}{V_T} = \frac{V_T}{V_T}. \qquad (4.71)$$

In reality, however, the length of the furnace and its cross section are not fully utilized, hence the real residence time will be shorter than the available time. If we designate the utilization factor of the furnace volume (coefficient of filling of the furnace volume by the flame) by ψ_t, we have

$$z = \psi_T \frac{V_T}{V_T}. \qquad (4.72)$$

The volume V_g of combustion products per second (volume throughput per second) depends on the operating conditions of the furnace and is determined by

$$V_T = \frac{G_{ces}}{\gamma} = \frac{B_T RT(1+\alpha L_0)}{3600p}, \qquad (4.73)$$

where G_{sek} is the weight throughput of combustion products per second; γ the specific gravity of the combustion products; B_t the hourly fuel consumption; α the excess air coefficient; L_0 the quantity of air theoretically required for the combustion of unit weight of a given fuel; p the pressurein the reaction zone; R the gas constant of the combustion products; T the average temperature of the combustion products in the reaction zone of the furnace.

Equating (1.83) and (4.72) and solving this equation relative to the initial drop diameter, we obtain

$$d_0 = \sqrt{\frac{\psi_r V_r k_r^2}{V_r (1+\chi)}}. \tag{4.74}$$

By replacing the quantity V_g by its expression via the weight throughput and the parameters of the combustion products (4.73), we obtain

$$d_0 = \sqrt{\frac{\psi_r V_r \cdot 10^4 p \cdot 3600}{B_r (1+\alpha L_0)(1+\chi) RT}}. \tag{4.75}$$

It is more difficult to determine the sizes of the drops which leave the nozzle at an angle to its axis and the furnace axis. In this case, the condition which limits the drop size, is the absence of coke formation on the cold heat-absorbing surfaces located in the furnace. According to this, the fuel drops which leave the nozzle under an angle to the furnace axis, should burn completely before striking these surfaces.

The time of flight of the fuel drop from the center of the nozzle to the point on the furnace surface under consideration (z_τ) can be estimated from the condition of motion of the drop along a trajectory, at each point of which all necessary parameters of the medium are known (temperature, flow velocity, pressure, and other properties of the medium). The general solution for this case cannot yet be obtained because the laws of variation of the parameters of the medium as they apply to a flame of atomized fuel as a function of the coordinates of the furnace are unknown. For the simplest case in which all parameters of the medium in which the drop moves are constant, z_τ can be determined from the equation of the trauectory of the drop

$$y = \frac{w_0 \sin\alpha}{\frac{1}{z_\tau} + k\sqrt{w_0 \sin\alpha}}; \quad x = py + w_0 z_\tau, \tag{4.76}$$

where

$$k = \frac{5{,}25\sqrt{\rho_0 \mu_0}}{\rho_r d_\alpha^{1.5}} \cdot \sqrt[4]{1+p^2}, \tag{4.76a}$$

$$p = \frac{w_0 \cos\alpha - w_0}{w_0 \sin\alpha}; \tag{4.76b}$$

z_τ is the time; ρ_v, μ_v, respectively, are the density and dynamic viscosity of the medium; ρ_t the specific gravity of the fuel.

These equations are valid only for the initial section of the trajectory, i.e., where the motion of the drop coincides in time with the development of the preparatory processes (preheating, preliminary vaporization and ignition). Following the ignition of the drop, when it retains its relative velocity, its trajectory will be determined by a different relation between the resistance coefficient and the velocity because the appearance of the flame around the drop creates an additional resistance to its motion. However, the following must be remembered: for drops located on the outer fringes of the fuel jet, i.e., drops which leave the nozzle at the maximum angle to its axis, the conditions for preheating and ignition will be much less favorable because the drops are compelled to move all the time in a medium the temperature of which increases very slowly in connection with the general heating of the incoming air. This also has the consequence that the loss of relative velocity of the drop will obviously occur within a time comparable (if not less than) with the time required for the ignition of the drop. The increase in the resistance of the drop after the appearance of the flame increases the rate of the loss of relative velocity even more, and the trajectory of of the burning drop practically coincides with the direction of motion of the combustion products, i.e., it will be practically parallel to the furnace axis. These factors permit the assumption that the following relations give a first approximation:

$$\tau_в = z_\tau, \tag{4.77}$$

$$y_{max} = h, \tag{4.78}$$

where τ_v is the ignition time of the fuel drop; y_{max} is the maximum deviation of the drop trajectory from the furnace axis (of the atomizer); h is the distance from the furnace axis to the boundary wall.

Substituting (4.77) and (4.78) into (4.76), we obtain

$$h = \frac{w_0 \sin\alpha}{\frac{1}{\tau_в} + k\sqrt{w_0 \sin\alpha}}. \tag{4.79}$$

The ignition time, as shown in Chapter 1, is determined by the square of the initial drop diameter, the chemical induction time and the ignition characteristic (k_v) of the given fuel grade.

Equation (4.79), taking into account the expression for τ_v, assumes the form

$$h = \frac{w_0 \sin\alpha}{\frac{k_в}{d_0^2 + k_в\tau_{инд}} + k\sqrt{w_0 \sin\alpha}}. \tag{4.79a}$$

If we designate by b the quantity

$$b = \frac{1.25\sqrt{\rho_в\mu_в}\cdot\sqrt{1-\rho^2}}{\rho_т}\cdot\sqrt{w_0 \sin\alpha} \tag{4.79b}$$

we find

$$h = \frac{w_0 \sin\alpha}{\frac{b}{d_к^{1.5}} + \frac{k_э}{d_к^2 + k_э \tau_{инд}}}. \qquad (4.80)$$

Having carried out the simplest transformations, we obtain the following equation for the determination of the critical drop diameter:

$$d^{3.5} - d^2 b^1 + d^{1.5} k_э \left(\tau_{инд} - \frac{h}{w_0 \sin\alpha}\right) - b^1 k_э \tau_{инд} = 0, \qquad (4.81)$$

where

$$b^1 = \frac{5{,}25h \sqrt{\rho_э \mu_э} \cdot \sqrt[4]{1+p^2}}{\rho_т \sqrt{w_0 \sin\alpha}}. \qquad (4.81a)$$

If it is assumed that the fuel drop is fairly large and its preheating time considerably longer than the chemical induction time, Eq. (4.81) assumes the form

$$d^2 - d^{0.5} b' - \frac{k_э h}{w_0 \sin\alpha} = 0; \; d^2 - d^{0.5} b' - a = 0. \qquad (4.82)$$

An estimate of the numerical values of the quantities forming part of the parameters b' and a, taking into account the real atomization and preheating conditions of the fuel drops, shows that their range of variation can be limited by the following values:

$$0 < b^1 < 0{,}04 \; мм^{1.5},$$
$$0 < a < 0{,}3 \cdot мм^2.$$

Accordingly, the range of variation of the drop sizes will be limited by the maximum 600 μ. Figure 70 shows a nomogram for the determination of the drop size as a function of the total set of the values of the parameters b' and a from which it is evident that the parameter a has the decisive effect on the maximum fuel drop size which is limited by the condition of its ignition prior to impinging on the cold wall. The variation of b' over its entire range has an extremely insignificant effect on the initial drop size. Hence we can neglect the term $d^{0.5} b'$ in Eq. (4.82) without causing a large error. Then the drop size is determined as

$$d = \sqrt{\frac{k_э h}{w_0 \sin\alpha}}. \qquad (4.83)$$

By way of an example, let us consider the problem, what maximum drop size we can permit for a furnace with a volume of 3.98 m^3, a width of 1.2 m and a length of 2.7 m in which a volume heat transfer rate of the order of $1.3 \cdot 10^6$ kcal/m^3h is to be achieved. The fuel is atomized by means of a mechanical sprayhead under a pressure of ~25 kgf/cm^2 and forms a fuel jet with an angle at the apex of $2\alpha = 120°$. The fuel is petroleum residue ($\gamma = 960$) with the ignition characteristic $k_э = 0.003$ cm^2/s. For comparison purposes, we determine also the diameter of diesel oil drops ($\gamma =$

= 860) for which k_v = 0.0058 cm²/s. Having first determined the flow velocity of the fuel from the spray nozzle and assuming that the two fuels have the same pressure and velocity coefficients, we obtain the following drop diameters:

for petroleum residue $d_к = \frac{0{,}003 \cdot 0{,}6}{45{,}3} = 0{,}0063$ см = 62 мк;

for diesel oil $d_к = \frac{0{,}0058 \cdot 0{,}3}{48} = 0{,}0084$ см = 84 мк.

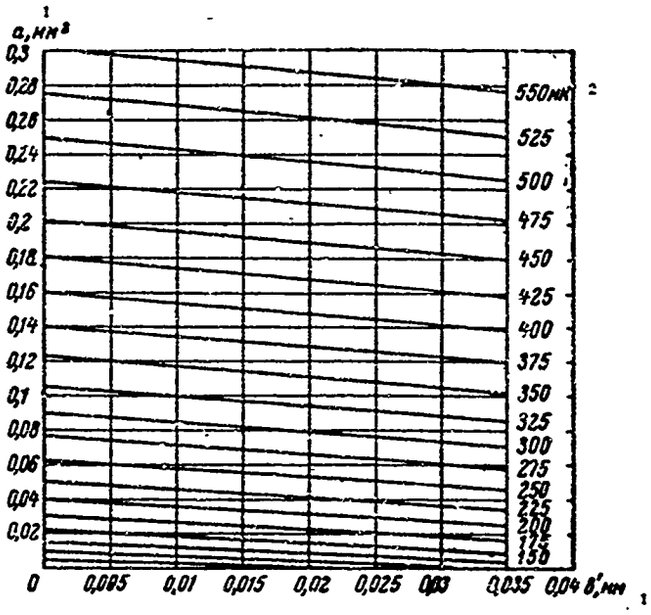

Fig. 70. Diagram for determination of drop size as a function of the parameters b' and a. 1) mm; 2) μ.

For a fuel drop moving along the furnace axis, we find after substitution of the numerical values:

for petroleum residue $d_к = 0{,}294 \sqrt[3]{\frac{k_т''}{1+x}} = 0{,}0129$ см (129 мк);

for diesel oil $d_к = 0{,}294 \sqrt[3]{0{,}0078} = 0{,}0260$ см

Thus, to achieve heat transfer rates of the order of $1.30 \cdot 10^6$ kcal/m³h (furnace chamber of steam locomotive boiler) which corresponds to a fuel consumption of ~550 kg/h, the atomization quality should be very good for diesel oil and particularly for petroleum residue. The greatest danger in this case are the lateral drops because they should be approximately half the size of those in the center of the flame. Despite the relatively low calculation accuracy, the absolute drop sizes determined by this method, are very close to the drop sizes observed in reality in highly effective combustion of atomized fuel.

It should be remembered, however, that the drop sizes determined by computation, although they are limits, determined on the basis of the ignition and complete combustion conditions, they cannot be the limit sizes with respect to the atomization characteristic, i.e., the drops for which $R = 0$. Strictly speaking, the number of such drops should be determined on the basis of the given law of heat evolution along the furnace. However, as a first approximation, it can be assumed to be within the limits of 10-15% and then the average drop diameter in the flame by means of which the quality of atomization is normally gaged, can be readily ascertained by means of Eq. (3.28).

It must also be remembered that in a large number of cases (at low flow velocity and small aperture angle of the fuel flame) the drop sizes determined by means of Eq. (4.83) will be much larger than in the above example. In this case, an additional verification of the completeness of combustion of this drop over the remaining furnace length is required on the assumption that the subsequent motion will be over a linear trajectory with zero relative velocity. The control relation in this case will have the form

$$x_{пред} > x_{max}, \qquad (4.84)$$

where x_{pred} is the maximum permissible distance of the fuel drop from the spray nozzle in the furnace axis; x_{max} is the real distance of the fuel drop, determined by means of Eq. (4.76) at $z_\tau = \tau_v$.

The quantity x_{pred}, in turn, is determined from the equation

$$x_{пред} = l_т - \frac{d_0^2}{k_г}(1 + \chi) w_г, \qquad (4.85)$$

where l_t is the furnace length; k_g the combustion characteristic of the fuel grade concerned (without taking into account the ignition time); x is the ratio of the combustion time of the coke residue to the combustion time of the liquid phase; w_g is the average velocity of the gases and combustion products formed in the furnace.

If the Condition (4.84) is not fulfilled, this means that the chosen parameters of burner operation do not allow complete combustion of the fuel drop under the given conditions.

Manuscript Page No.

Footnotes

144 [1]The processing of the experimental data was carried out by the Candidate of Technical Sciences, E.M. Yudayeva who kindly communicated the results to the authors.

Manuscript Page No.	Transliterated Symbols
120	ГТУ = GTU = gazoturbinnaya ustanovka = gas-turbine powerplant
122	т = t= topka = fire box
122	ф = f = famel = flame jet
128	к = k = kaplya = drop
129	т = t = toplivo = fuel
129	т = turbilentnost' = turbulence
130	р = r = raspyliveniye = atomization
132	ВУ = VU = vyazkost' uslovnaya = conventional viscosity
135	в = v = vozdukh = air
139	ср = sr = sredniy = average
140	г = g = goreniye = combustion
146	сек = sek = sekunde = second
149	инд = ind = induktsiya = induction
151	пред = pred = predel = limit

Chapter 5

ENGINEERING METHOD OF ORGANIZATION OF THE FLAME PROCESSES

17. CENTRIFUGAL ATOMIZER DESIGNS

The idea to use the centrifugal forces in a vortex flow for the atomization of fuel was realized in the first mechanical atomizer built by engineers of the Tentelevka plant [157]. This atomizer was equipped with helical channels (Fig. 71) like, later on, the Kerting atomizer which was widely used in the fuel preparation system of the steam boilers of the firm Babcock-Wilcox. The flame angle in the burners with helical inset was determined by controlling the pitch of the helix. Instead of the helical inset, a multiple-thread endless worm can be used.

The best fuel atomization effect is achieved in centrifugal atomizers with channels which extend tangentially from the periphery to the vortex chamber. One of these designs which was widely used at the time, is the atomizer of P. I. Grigor'ev [180], known under the name "Atom" (Fig. 72). In this atomizer, the fuel passes through tangential grooves cut in the conical insert into the vortex chamber and then through a nozzle into the furnace volume.

In most current designs, the vortex flow is achieved by tangential feed of the fuel into a cylindrical chamber located in front of the nozzle orifice. This atomizer is shown schematically in Fig. 73. Via several channels (with round or rectangular cross-section), arranged tangentially to the cylindrical surface of the vortex chamber, the fuel enters the vortex chamber and then, via the nozzle, the combustion zone. Owing to the tangential feed of the fuel through the nozzle, a vortex flow is established. The fuel particles in the vortex chamber move along a flat spiral and in the nozzle, along a helix. Because of the flow and rotational motion during the outflow of the fuel, an air cavity is formed which extends through the entire fuel flow including that within the burner (Fig. 74). Thus, the fuel flows out through an annular cross section, the dimensions of which depend on the diameters of the nozzle and the air vortex, which later is determined by the magnitude of the tangential velocity component.

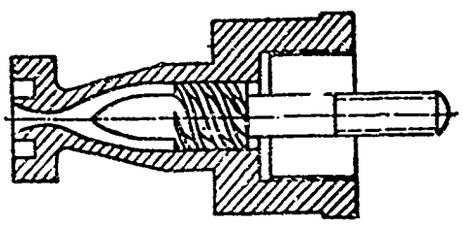

Fig. 71. Burner designed by the engineers of the Tentelevka Plant with helical atomizer.

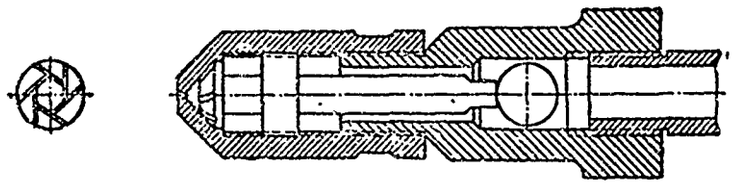

Fig. 72. The burner "Atom," designed by P. I. Grigor'ev.

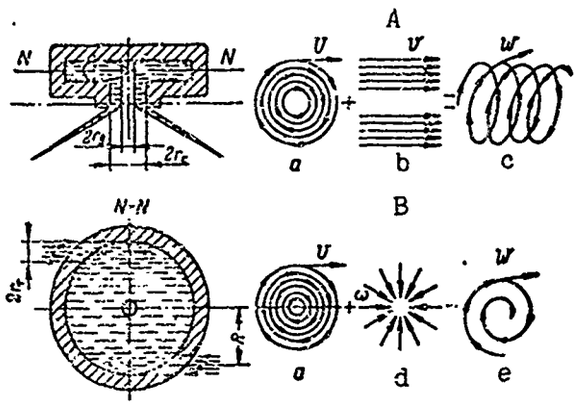

Fig. 73. Principle of centrifugal atomizer with vortex chamber. Motion of the liquid particles: A) in the nozzle; B) in the vortex chamber; a) tangential; b) axial; c) total (helical path); d) radial; e) total (flat spiral).

Graphic Not Reproducible

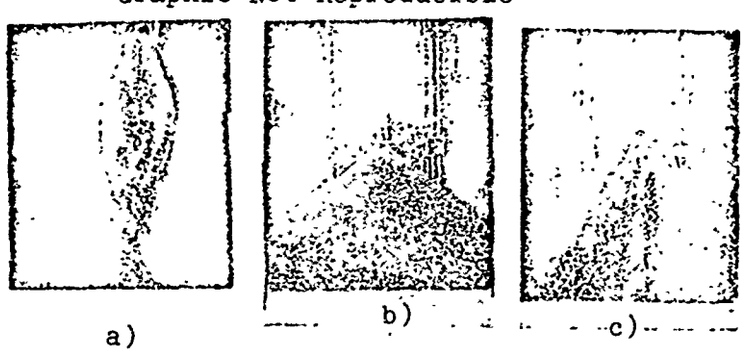

Fig. 74. Flame shapes with atomization in a centrifugal burner: a) at low pressure; b) at high pressure; c) with relative shift of the nozzle and vortex chamber axis.

Following their discharge from the nozzle, the fuel particles fly in the direction of the composite velocity and form a thin film in the shape of a revolution hyperboloid of one sheet. At low pressure, under the action of the surface tension, the aerodynamic resistance and the weight of the fuel, this film is gradually constricted and then disintegrates into individual drops (see Fig. 74,a). This form of jet has been termed "tulip." With increase in the pressure, the velocity of the fuel increases and the constriction of the film is not observed (see Fig. 74,b). The maximum pressure at which the fuel

disintegrates into drops without formation of a film, depends on the physical characteristics of the fuel (viscosity, surface tension) and the geometrical dimensions of the atomizer.

Of great importance in the centrifugal atomizers is the coincidence of the axes of the vortex chamber and nozzle since any deviation from this coaxial arrangement results in curving of the air vortex (see Fig. 74,c) and if the shift is larger, the vortex disappears altogether. Prior to the disappearance of the air vortex, the fuel consumption in the part of the flame close to the axis of the vortex chamber increases; large drops appear here, thus interfering with the atomization quality.

To produce a symmetrical flame it is essential that the atomizer has several tangential feeds. However, when the number of orifices is increased, their diameters must be decreased in order to retain the optimum ratios of the passage cross sections and this lowers the reliability of operation of the fuel system and increases the risk of clogging. The number of tangential orifices in the centrifugal atomizers is usually 2-6.

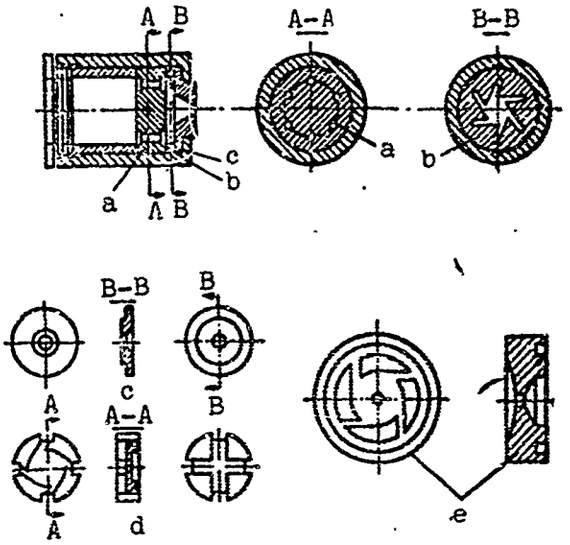

Fig. 75. Centrifugal atomizer with three discs: a) distribution disc; b) disc with vortex chamber; c) disc with nozzle orifice; d) combined detail of the distribution disc and the vortex chamber; e) combined detail of vortex chamber and nozzle (burner of the Baltiyskiy plant).

In several centrifugal atomizer designs, the film formation is attained by means of a disc with tangential slots placed in front of the nozzle orifice (Fig. 75). The burners for steam boilers made at the "Ilmarine" Plant [181] are built on the same principle. The burner design with these discs is more complex than that discussed in the foregoing. Furthermore, the presence of several parts centered by means of the burner housing in order to prevent a displacement of the vortex chamber and nozzle axes requires very accurate manufacture.

A more efficient design which gives a better centering of the axes of the nozzle and vortex chamber, was proposed by the Baltiyskiy Plant [182] for burners with by-pass (see Fig. 75,e).

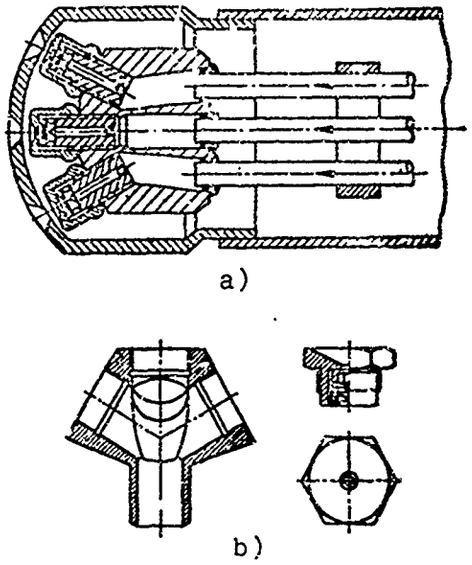

a)

b)

Fig. 76. Centrifugal burner with several atomizers: a) with separate fuel ducts; b) with common fuel duct.

During the operation of furnaces with variable operating conditions, when the fuel supply varies by a factor of two or more, the simple centrifugal design does not give good atomization at low loads. The range of control of the fuel consumption can be enlarged in a burner with several atomizers or with controllable cross section of the tangential channels. The burner of the Nevskiy factory design (Fig. 76,a) contains five atomizers. The fuel consumption in this burner can be reduced by successive switching off of atomizers and lowering of the fuel pressure. When the load is reduced. the fuel pressure in one of the five petroleum residue channels is reduced. This channel is then disconnected and only four atomizer nozzles are in operation. When the load decreases, the pressure is successively reduced and the second, third, and fourth nozzle is disconnected. The fifth nozzle is for idling and is disconnected only when the unit is stopped. Thus, a smooth as well as a sudden variation of the consumption takes place.

The assembly of a system of burners is due not only to the need for enlarging the control range but is also necessary to achieve large fuel consumptions because with a single burner the atomization quality decreases with increased fuel throughput at the same pressure. Large fuel consumptions with good atomization (up to 3 tons/h) can be achieved with multinozzle burners [183] in which the fuel is supplied via a common channel to several (4-5) atomizers (see Fig. 76,b) of the centrifugal type. The multinozzle burners are compact, give a wide flame and good filling of the combustion zone with fuel. However, the conditions for the air supply are less favorable.

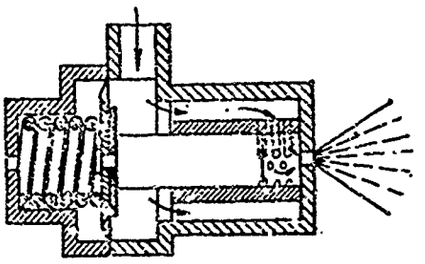

Fig. 77. Principle of burner with controllable cross section of the tangential orifices.

In burners with variable tangential cross sections, the throughput can be controlled by variation of the fuel pressure or the total area of the tangential orifices. Such burners usually have a mobile gate in the form of a piston or cylinder which closes the tangential orifices during its displacement along the burner axis (Fig. 77). The cross section can be controlled by reducing the tangential orifices in one cross section for which purpose it is necessary to rotate a ring with orifices which is mounted on the atomizer body [184]. Some burner designs make use of a combined control method with simultaneous variation of the pressure and the cross section of the tangential channel. In the simplest case, this is achieved by installing a piston with a spring. The piston is displaced under the fuel pressure, increasing the tangential passage, and when the pressure is reduced the piston, actuated by the spring, closes the tangential cross section.

Two-stage centrifugal burners are widely used in gas turbine power plants. The control of the fuel throughput in these burners is achieved by variation of the pressure in one of the stages. The pressure in the other stage is adjusted automatically by means of special valves. The burners of this type give a mixing of the two fuel flows thus achieving good atomization at a large range of variation of the consumption.

The fuel flow from the two stages can be mixed in the atomizer (with a single nozzle) and in the furnace volume (two-nozzle burner). The two-stage burners with single nozzle are of two types, single-chamber and double-chamber. The first burner (Fig. 78,a) has two groups of tangential channels which discharge into a common vortex chamber. One stage, usually the first one, has a smaller cross section of the tangential orifices and is calculated for low output. When a certain pressure is reached in the first stage (14-17 kgf/cm^2), the second stage is switched in. The fuel of the second stage, which has a low velocity, is mixed with the fuel of the first stage and is supplied to the combustion zone at a certain average velocity.

The nonuniformity of the fuel throughput by single burners operated from a single fuel system is due not only to the difference in the geometry and local resistance of the fuel duct but also to the large fluctuations of the counter pressures. The counter pressure is produced by the fuel of one stage in the direction of the other stage. Under operating conitions in which the pressure in the first stage is high and the second stage is only beginning to work, the error in

the counter pressure is comparable with the feed pressure of the second stage. Taking into account that the fuel throughput in the second stage is considerably higher than in the first, the nonuniformity of the counter pressure during the operation of the burner system from a single fuel pump may lead to differences in the throughput of individual burners of up to 200% under certain operating conditions.

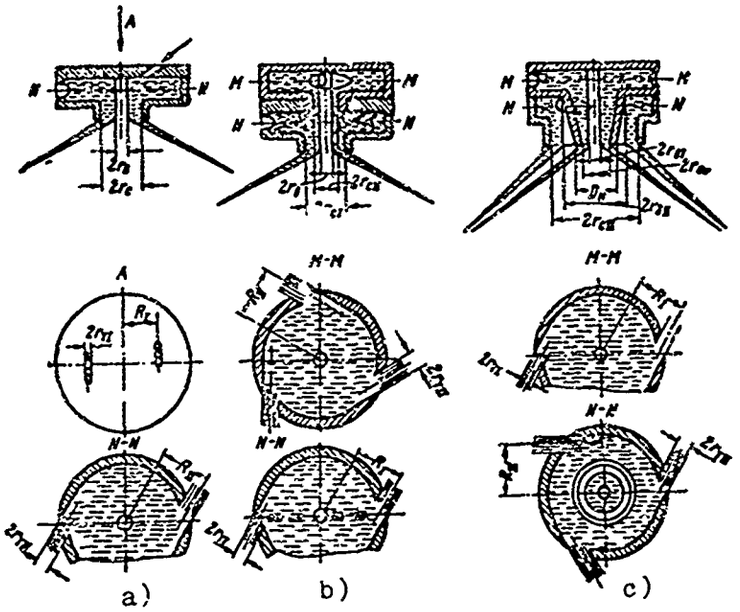

Fig. 78. Principle of the two-stage burner: a) with single vortex chamber; b) with single nozzle; c) with two nozzles.

Less effect on the counter pressure have errors in the manufacture of double-circuit burners since the fuel of the second stage of this burner enters the center of the vortex chamber of the first stage where the counter pressure is low on account of the air vortex. This burner (see Fig. 78,b) is made in the form of two independent centrifugal burners one of which is pressed into the other (the second one into the first). The fuel from the first stage is atomized directly into the furnace volume. The fuel from the second stage in the form of an annular film with a considerable tangential velocity component arrives in the vortex chamber of the first stage and then in the combustion zone. Under intermediate operating conditions, the first stage operates under high pressure and the second one under low pressure. Due to the mixing of the fuel within the nozzle, a certain average velocity is established with which the fuel arrives in the combustion zone. The direction of the vortex formation in the two stages should coincide, otherwise, in spite of the good mixing of the fuel, the atomization quality is reduced owing to the large energy losses.

In the two-nozzle burner, the fuel from both stages interacts outside the burner and the quality of atomization is determined by size population of the drops from both stages. The two-nozzle burner

(see Fig. 78,c) has two circuits with independent tangential fuel supply, vortex chambers and nozzle orifices; the nozzle orifice of the second stage has an annular shape.

Both stages of the two-circuit burners (see Fig. 78,b) with single nozzle are made, as a rule, in accordance with the classical design with a vortex chamber and tangential orifices. Sometimes, the tangential orifices in the first stage are not arranged at a right angle to the generatrix of the cylindrical surface of the vortex chamber. This scheme is typical for two-stage burners with a single vortex chamber.

In order to enlarge the range of variation of the fuel throughput [185], three-stage burners have been proposed which are a combination of a two-nozzle and single-nozzle double-circuit burners. Owing to their complexity of design and control, the three-stage burners have not been used in practice.

Much used in present-day boilers are burners [182, 186] with consumption control by means of fuel overflow (Fig. 79). At maximum load, the by-pass line in these burners is completely closed and all the fuel enters the combustion zone. When the load is to be reduced, the same quantity of fuel is supplied to the burner but part of it is bled off from the vortex chamber into the fuel supply line. This reduces the quality of atomization somewhat although it remains considerably better than at the same throughput reduction in the case of a simple burner. With decreasing throughput the flame angle increases.

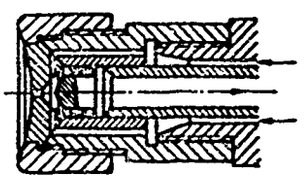

Fig. 79. Principle of burner with fuel by-pass.

A great disadvantage of the by-pass burner is the fact that under all operating conditions (including the rated capacity) the pump must be operated at maximum load. The fuel can be bled off in the by-pass burners from the central part or the periphery of the vortex chamber (in the Peabody system) or from the nozzle (in the Todd system). Burners with analogous designs have also been proposed for the combustion chambers of gas turbine power plants [187].

Synchronously operating slide valves are installed in the burner with simultaneous control of the fuel in the output and by-pass lines [188] (Fig. 80,a). With open by-pass channel and low fuel pressure, the rod 1 is actuated by the spring and closes the nozzle; the fuel, after passing all the internal channels of the atomizer, enters the by-pass system. When the pressure in the by-pass line increases, the rod is lifted and opens the nozzle orifice and simultaneously closes the

by-pass line with its shoulder 2. The system of valves and rods with springs in the burner is adjusted in such a way that the fuel passes through the nozzle at high pressure which ensures a good quality of atomization at different fuel throughputs.

A more complex variant of the combined by-pass burner which gives a wide range of variation of fuel throughput was proposed by A. M. Prakhov [189]. This burner (see Fig. 80,b) at small loads supplies fuel only to one (the central) stage; any fuel arriving through the channel 1 in the second circuit is completely by-passed into the reservoir via the conduit 2. With increasing supply of fuel to the central stage, its amount in the outer circuit increases, not all the fuel being by-passed out of the burner but part of it passing through the annular nozzle of the second stage into the combustion zone. When a certain pressure has been attained in the first stage, a further increase in throughput is achieved by covering the channel of the bypass 2. At maximum loads, fuel enters the by-pass line and the burner operates in accordance with a scheme similar to that of a two-nozzle burner.

The burner of the "Velox" boilers [18] is also a combination design. The burner (Fig. 81) operates under constant pressure. At the initial moment, the control is achieved by lifting of the rod 1, which opens the nozzle and the tangential orifices of the inner stage. An increase in throughput after complete opening of the tangential orifices is attained by lifting of the inner atomizer 2, which opens the nozzle and the tangential orifices of the second stage. Thus, at the first moment, the burner operates with control of the cross sections of the tangential orifices in accordance with the scheme of Fig. 77 and then as a two-stage burner according to Fig. 78,c.

The rotating atomizers with rotating nozzle, proposed in 1930 by Professor V. V. Uvarov [190] can be counted among the centrifugal type because of the nature of flow of the fuel (in the form of a conical film due to the tangential velocity component). In atomizers of this type (Fig. 82), the vortex formation in the fuel is attained by rotation of a conical atomizer. The greater the speed of rotation, the thinner is the fuel film, the larger the flame angle and the higher the degree of dispersion. The fuel pressure is determined by the resistance of the fuel ducts, the diameter of which is practically unlimited and makes possible a reliable supply of fuel at any throughput. In consequence of the variation of the speed of rotation, the rotational atomizers give fine atomization within a large range of throughput variation.

An original atomizer design which gives film atomization due to the jet-propulsion forces arising during the escape of the fuel, was proposed by the Kolomna Locomotive Plant [191]. In this atomizer (Fig. 83), the fuel enters the central atomizer with tangentially arranged nozzles through a system of orifices. At a fuel pressure above 2 kgf/cm^2, the atomizer begins to rotate, producing a fuel film; further increase in the pressure causes an increase in the number of revolutions of the atomizer. At a pressure above 7 kgf/cm^2, the fuel film disappears and the disintegration of the fuel into drops takes place directly at the nozzle. The number of revolutions of the atomizer attains several thousand per minute.

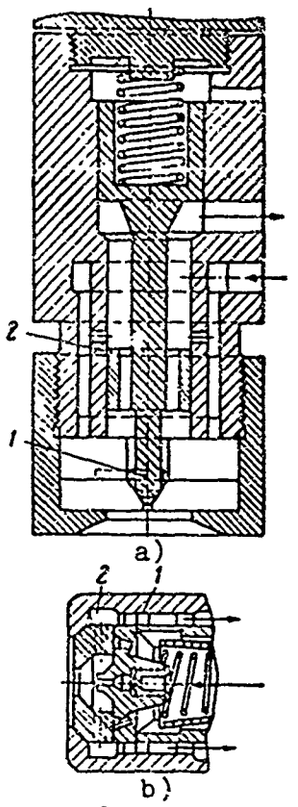

Fig. 80.

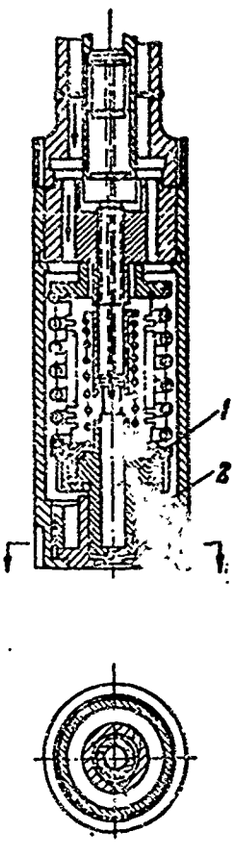

Fig. 81.

Fig. 80. By-pass burners of combined design: a) burner with simultaneous control in the throughput and by-pass lines; b) burner of A. M. Prakhov.

Fig. 81. Burner of the boiler "Velox."

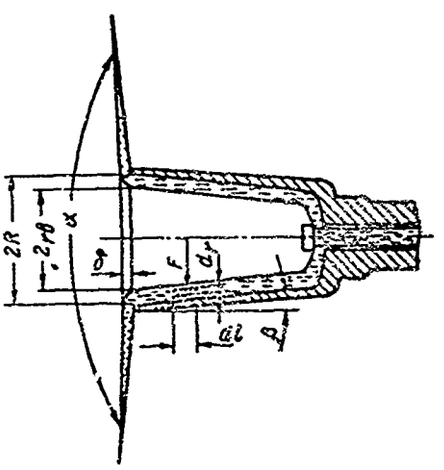

Fig. 82. Rotational atomizer.

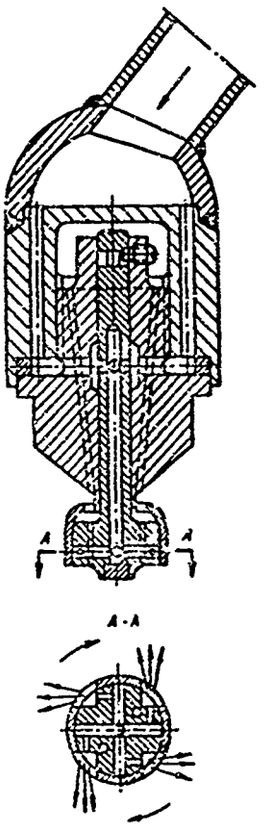

Fig. 83. Turbojet atomizer.

The above-discussed designs of centrifugal atomizers are merely different principles of construction and do not by any means exhaust the large number of designs used in numerous variants of furnace devices.

18. THEORY OF THE CALCULATION OF SINGLE-STAGE CENTRIFUGAL ATOMIZERS

In a discussion of the design principles of centrifugal atomizers it is evident that they are all based on the same principle of film flow of the fuel. Hence the calculation of any centrifugal atomizer is based on the laws of operation of the simple single-nozzle centrifugal atomizer. The calculation of the atomizer boils down to determining its basic geometrical dimensions which ensure the quality of atomization required for the given combustion conditions at a given consumption characteristic and flame angle.

Two basic methods of establishing the mathematical relations for centrifugal atomizers are known: one on the basis of the principle of maximum throughput [192-197] and another on the basis of the use of equations of the momentum [198-201]. The most widespread theory is that of Professor G. N. Abramovich [192] based on the assumption that the air vortex within the atomizer has a size which gives a maximum fuel throughput. This condition corresponds to the critical flow

velocity of the fuel, equal to the velocity of propagation of long waves on the free surface of a fluid in a field of centrifugal forces. In cases of flow with slight vortex formation and in atomizers with sudden transition from the diameter of the vortex chamber to that of the nozzle when the radial velocity component must be taken into account, the theory of calculation using the momentum equations [201] gives the best agreement with the experimental data.

The fuel consumption in centrifugal atomizers, like that in flow from any orifice, is equal to the product of the cross section of the orifice and the velocity. The rotary moment in the centrifugal atomizers causes a considerable decrease in the active section compared with the nozzle cross section. The decrease in cross section and the deviation of the fuel velocity from the axial direction is taken into account by the consumption coefficient μ. In order to determine this throughput coefficient, let us consider the motion of the fuel in the atomizer. A peculiarity of the centrifugal atomizer is the presence of a momentum M relative to the axis the variation of which along the radius can be described by a differential equation, proposed by L. A. Klyachko, of the form

$$\frac{dM}{M^2} = \frac{\pi f r_\tau}{2\varrho_\tau Q} dr, \tag{5.1}$$

where f is the friction coefficient in the vortex chamber; r_t the radius of the tangential orifices; ρ_t the specific gravity of the fuel; and Q the fuel throughput.

This equation was obtained under the following conditions: the variation of the momentum is equal to the frictional moment at the end face of the vortex chamber; the radial velocity is negligible compared with the tangential velocity.

By integrating Eq. (5.1) within the limits of variation of r from R to r_s and, correspondingly, of M from M_0 to M_s

$$M_0 = \varrho_\tau w_\tau R = \frac{\varrho_\tau Q R}{\pi l \mu_\tau r_\tau^2}, \tag{5.2}$$

we obtain

$$M_c = \frac{\varrho_\tau Q}{\pi r_c} A_3, \tag{5.3}$$

$$A_3 = \frac{R r_c}{\mu_\tau l r_\tau^2 + 0{,}5 f R (R - r_c)}; \tag{5.4}$$

at f = 0

$$A_3 = A = \frac{R r_c}{\mu_\tau l r_c^2}, \tag{5.5}$$

where A_e is the equivalent geometrical characteristic; A the geometrical characteristic; w_t the velocity of the fuel upon emergence from the tangential orifices; R the vortex radius, equal to the distance from the nozzle axis to the axis of the tangential orifice; μ_t the fuel throughput coefficient in the tangential orifices.

The loss of friction moment in the vortex chamber is allowed for by variation of A_e compared with A.

The vector of the fuel velocity in the nozzle can be divided into two components: an axial and a tangential. The axial velocity at the nozzle entry is constant over the whole cross section and equal to

$$v = \frac{G}{\pi(r_c^2 - r_s^2)} = \frac{Q}{\pi\varphi r_c^2}, \tag{5.6}$$

where ϕ is the coefficient of the active cross section,

$$\varphi = 1 - \frac{r_s^2}{r_c^2}. \tag{5.7}$$

At the boundary with the air vortex, the excess pressure is zero and the radial velocity is very small so that it can be assumed that

$$v^2 + u^2 = 2gH, \tag{5.8}$$

where H is the total excess pressure of the fuel in front of the nozzle, equal to the difference between the total pressure H_0 in front of the atomizer and the friction loss, expressed by the pressure ΔH,

$$H = H_0 - \Delta H.$$

The axial velocity at the boundary with the air vortex is determined by Eq. (5.6) and the tangential velocity can be found by means of Eq. (5.3) at $r = r_v$ and is expressed by the relation

$$u = \frac{M_c}{\varrho r_v} = \frac{Q A_s}{\pi r_c^2 \sqrt{1-\varphi}}. \tag{5.9}$$

Substituting the value of v (5.6) and u (5.9) into (5.8) and solving this for Q, we find

$$Q = \pi\mu r_c^2 \sqrt{2gH}, \tag{5.10}$$

whence

$$\mu = \frac{1}{\sqrt{\frac{A_s^2}{1-\varphi} + \frac{1}{\varphi^2}}}. \tag{5.11}$$

A relation which is insufficient for determining the throughput is found on the basis of the assumption that stable flow of the fuel will occur at a size of the vortex (or ϕ) which gives a maximum throughput, i.e., at

$$\frac{d\mu}{d\varphi} = 0. \tag{5.12}$$

Then,

$$A_s = \frac{1-\varphi}{\sqrt{\frac{\varphi^3}{2}}}, \tag{5.13}$$

$$\mu = \sqrt{\frac{\varphi^3}{2-\varphi}}. \tag{5.14}$$

Thus, the equations (5.4), (5.10), (5.13), and (5.14) express the relationship between the geometrical dimensions and the operating conditions (pressure) of the centrifugal atomizers and the fuel throughput.

For an accurate calculation of the real pressure it is necessary to allow for the energy losses in the atomizer. In the vortex chamber of a centrifugal atomizer these can be regarded as the work of the friction force over the pathway of the fuel. For unit volume of fuel, this work (or tne energy loss) is equal to

$$dE = -\frac{f}{8r_r}\varrho_r w^2 ds, \tag{5.15}$$

$$ds = \cos(r; s)\, dr = \frac{w}{\omega} dr, \tag{5.16}$$

where w is the total velocity of the fuel particle; s the path traversed by the particle; ω the radial velocity component; r the distance of the element under consideration from the axis of the vortex chamber.

Since

$$w = \sqrt{\omega^2 + u^2} \approx u, \tag{5.17}$$

where u is the tangential velocity component which is considerably larger than ω.

The radial component ω can be determined as

$$\omega = \frac{Q}{2\pi b r}, \tag{5.18}$$

where b is the height of the vortex chamber; normally, $b = 2r_t$.

Following replacement of w and u and substitution of the value obtained from Eq. (5.14) for ω, the energy loss can be represented in the form of the following relation:

$$dE = -\frac{\pi f}{2Q} \varrho_r u^3 r\, dr. \tag{5.19}$$

The tangential velocity is expressed via the momentum which is determined by integration of Eq. (5.1) for the limits of r from R to r_s:

$$u = \frac{2Q}{\pi f \left(\frac{2r_c}{fA} + R - r\right) r}. \tag{5.20}$$

Substituting the expression for u (5.20) into (5.19) and integrating this within the limits of variation of r from R to r_s, we find the energy lost by the fuel as a result of the friction at the end face of the vortex chamber

$$E_n = E_0 - E = \frac{\varrho Q^2}{2\pi^2 r_c^4} \Delta; \tag{5.21}$$

$$\Delta = \frac{f}{\xi^2}\left\{\frac{1}{\xi}\left(1 - \frac{1}{c^*}\right) + f\left[\left(\frac{A}{2} - \frac{1}{2\xi - f}\right)\left(\frac{2}{\xi} + \right.\right.\right.$$

$$\left.\left.\left. + \frac{A}{2} + \frac{1}{2\xi - f}\right) + \frac{3}{2\xi^2} \ln \frac{(2\xi - f) Ac^*}{2}\right]\right\}, \tag{5.22}$$

where

$$\xi = \frac{1}{A} + \frac{f}{2} c^*; \; c^* = \frac{R}{r_c}.$$

This energy, lost by the fuel in the vortex chamber, must be deducted from the pressure H. In this case, the throughput equation is written thus:

$$Q = \pi \mu r_c^2 \sqrt{2gH - \frac{Q^2}{\pi^2 r_c^4} \Delta}. \tag{5.23}$$

If we replace μ by μ*, the throughput equation can be retained in the form (5.10), as under

$$\mu^* = \frac{\mu}{\sqrt{1 + \Delta\mu^2}} = \frac{1}{\sqrt{\frac{A_0^2}{1 - \varphi} + \frac{1}{\varphi^2} + \Delta}}. \tag{5.24}$$

The above-derived equations do not make allowance for the energy loss in consequence of the friction at the lateral surfaces of the vortex chamber.

The method of calculating centrifugal atomizers, taking into account the height of the vortex chamber, have been worked out by Professor V. I. Kirsanov and the Engineer M. P. Korobkov. They proposed the following equation for calculating the throughput coefficient:

$$\mu = \sqrt{\frac{1}{\frac{A_T^2}{1-\varphi} + \frac{1}{\varphi^2} + B}}, \qquad (5.25)$$

where A_t is the geometrical characteristic taking into account the friction loss along the length of the vortex chamber; the connection between this characteristic with μ and φ is the same as for A_e and is given by Eqs. (5.13) and (5.14).

After some simplifications, carried out by the authors, we have:

$$A_T = \frac{Rr_c}{\mu_T r_T^2 + \frac{l}{2} \cdot \frac{L}{2} R}. \qquad (5.26)$$

This equation is analogous in its form to the expression for the equivalent geometrical characteristic (5.15) the only difference being that the difference $R - r_s$ in it is replaced by the quantity $L/2$ since in its derivation account was taken of the fact that the momentum was reduced due to friction at the face end of the vortex chamber over the path $R - r_s$, while Eq. (5.26) reflects the decrease in the momentum along the length of the vortex chamber.

The part of the quantity Δ which takes into account the energy loss due to friction at the end face of the vortex chamber is played in Eq. (5.25) by the quantity B which allows for the energy loss during the motion of the fuel along the height of the fuel chamber. B can be determined approximately thus

$$B = \left(1 - \frac{\mu_T^2 A_T^2}{A^2}\right)\left(\frac{1}{\varphi_c^2} + \frac{r_c^2 A^2}{\mu_T R^2}\right). \qquad (5.27)$$

An experimentally determined friction coefficient enters into the equation for calculating burners with allowance being made for the losses along the height and the radius of the vortex chamber. According to the experiments carried out by L. A. Klyachko, this coefficient is a function of the Reynolds number

$$\lg(100f) = \frac{25{,}8}{(\lg \mathrm{Re})^{2.5}}. \qquad (5.28)$$

The Reynolds number is calculated on the basis of the entry conditions for the flow of the fuel in the tangential channels.

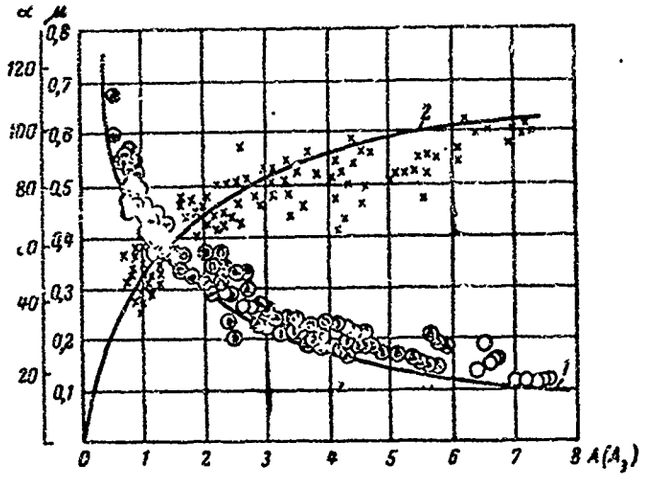

Fig. 84. Throughput coefficient 1 and flame angle 2 as a function of the variation of the equivalent geometrical characteristic.

Authors of the TsNII MPS determined the throughput coefficients for atomization of fuel in simple single-stage burners with a vortex chamber made integrally with the nozzle. The fuel throughput was found to vary from 120 to 410 kg/h at a fuel supply pressure of 5 to 55 kgf/cm^2. Figure 84 gives the experimental values of the throughput coefficients as a function of the equivalent geometrical characteristic A_e and the theoretical relation calculated by means of Eqs. (5.13) and (5.14). The coefficient μ was determined by means of Eq. (5.10). An experimental investigation of centrifugal burners with rectangular tangential channels arranged under an angle β to the burner axis also showed good agreement with theoretical data.

The equivalent geometrical characteristic of these burners is determined by means of the equation

$$A_э = \frac{Rr_c \cos\beta}{\varepsilon i r_э^2 + 0.5 i R (R - r_c) \cos\beta}, \qquad (5.29)$$

where r_e is the radius of a circle, the area of which is equal to that of the tangential orifice:

$$r_э = \sqrt{\frac{bs}{\pi}}, \qquad (5.30)$$

where b and s are the sides of the orifice; ε is the coefficient of the resistance to the motion of the fuel in the tangential orifices:

$$\varepsilon = \frac{r_1}{r_э}, \qquad (5.31)$$

where r_g is the hydraulic radius of the tangential orifices:

$$r_r = \frac{bs}{2(b+s)}. \qquad (5.32)$$

The frictional energy losses and the loss of momentum due to the friction at the cylindrical wall of the vortex chamber were not taken into account in these experiments. At the dimensional ratios of the burners used in the experiments, the loss of momentum was compensated by the energy loss.

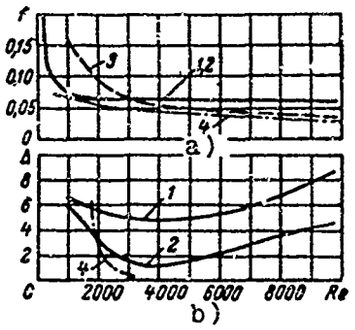

Fig. 85. Dependence of: a) the friction coefficient f and, b the loss coefficient Δ as a function of the Reynolds number: 1) for atomizers with straight tangential channels; 2) for atomizers with circular input channels, located at an angle to the nozzle axis (according to the experiments of Z. I. Geller and M. Ya. Moroshkin); 3) for burners with helical vortex chambers (according to the experiments of V. I. Kirsanov); 4) for burners with channels with circular cross section (according to the experiments of L. A. Klyachko).

The experimental data obtained in atomization of the petroleum residues FS5 and M20, heated to temperatures at which their viscosity is 5-6 mm^2/s, agreed completely with the data obtained under the same conditions with diesel oil.

Comprehensive investigations of centrifugal atomizers and heavy residual fuels were carried out at the Groznyy Petroleum Institute [129].

The results of these investigations were processed, using the theoretical relations obtained by means of the theory of maximum throughput. The variation of the momentum in the vortex chamber was taken into account by means of Eq. (5.4) and the pressure loss, by means of (5.24). The loss coefficient Δ was determined by means of an experimental curve which generalizes the experimental data (Fig. 85). For the friction coefficient f, the dependence on the Reynolds number, proposed in the work [129] differs slightly (particularly in the range of low values) from the corresponding relations, given by L. A. Klyachko and V. I. Kirsanov (see Fig. 85).

In some cases, attempts are made in the processing of the experimental data [202] to derive a general relation for the throughput coefficient as a function of the dimension and operating parameters which would combine the loss of momentum and pressure. The calculation of the burner is carried out in this case for an ideal liquid and the throughput coefficient is then corrected by means of the equation

$$\mu = \mu_0 \cdot 1{,}29 \left(\frac{R}{r_c}\right)^{0.5} \mathrm{Re}^{-0.33}, \qquad (5.33)$$

where μ_0 is the throughput coefficient, calculated for the flow of an ideal liquid by means of A (at f = 0); μ is the real throughput coefficient.

This combination had the consequence that the measurement result is affected by the special design features not only of the atomizing (centrifugal) unit but also the system for delivering the fuel to this unit. Difference in the design and dimensions of fuel delivery system have a considerable effect on the experimental results. Investigations of the burner of the type TsKKB (see Fig. 75) have shown that the pressure drop of the fuel before it arrives in the vortex chamber (in the burner body and particularly in the distribution disc) can attain 50% of the available pressure [203] under some operating conditions (Q = 1600 kg/h, p = 20 kgf/cm^2). These losses are not unavoidable for centrifugal burners but are typical for a particular burner and are due to the local resistances at the entry and exit of the distribution disc (see Fig. 75,a), the deflection of the jet at the entry to the vortex former and the resistances at the entry to the vortex chamber. Hence, to obtain more accurate results, the losses are preferably calculated for the different elements: for the motion in the supply channels, the constriction and expansion, in front of the tangential channels, in the tangential channels, and the losses inherent in the centrifugal atomizer (in the vortex chamber). As a result of taking these losses into account, the theoretical throughput coefficient is always smaller than for an ideal liquid. When only the loss of momentum is taken into account the throughput coefficient will be larger. The real (experimental throughput coefficient can be larger than for an ideal liquid which is typical for burners with low throughputs and high values of the geometrical characteristic A or less, which is the case for burners with large throughputs [204] and small value of A. Evidently, the loss of momentum in the first case exerts a more important effect on the throughput than the hydraulic pressure loss, whereas the reverse is the case in the second.

For the calculation of the second parameter of burner operation, the flame angle, we shall make the following simplifying assumptions: we neglect the radial velocity component in the nozzle and take as the flame angle the angle of the asymptotical cone of the hyperboloid of rotation, formed by the flight trajectories of the fuel particles. In this case the tangents of the departure angle of any fuel particle is equal to the ratio of the velocities

$$\mathrm{tg}\,\frac{\alpha_f}{2} = \frac{u_f}{w_f} = \frac{\mu A r_c}{\sqrt{r^2 - \mu^2 A^2 r_c^2}}. \qquad (5.34)$$

The departure angle of the liquid particles from the burner depends on their distance from the burner axis (r):

at the burner wall ($r = r_s$) the angle is equal to

$$\alpha_c = 2\operatorname{arctg}\frac{\mu A_s}{\sqrt{1-\mu^2 A_s^2}} = 2\arcsin\mu A_s, \tag{5.35}$$

at the boundary with the air vortex

$$\alpha_s = 2\operatorname{arctg}\frac{\mu A_s}{\sqrt{s^2-\mu^2 A_s^2}} = 2\arcsin\frac{\mu A_s}{s}, \tag{5.36}$$

where $s = \frac{r_v}{r_s}$ is the relative size of the air vortex, which is determined from the equation

$$\mu = \sqrt{1-\mu^2 A_s^2} - s\sqrt{s^2-\mu^2 A_s^2} - \mu^2 A_s^2 \ln\frac{1+\sqrt{1-\mu^2 A_s^2}}{s+\sqrt{s^2-\mu^2 A_s^2}}. \tag{5.37}$$

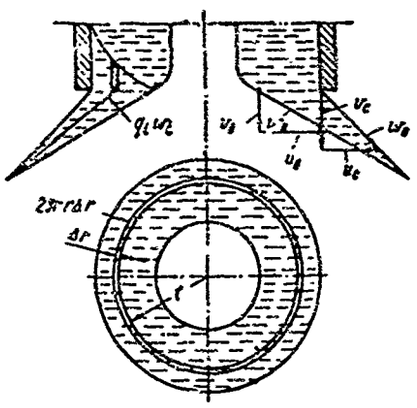

Fig. 86. Schematic representation of the flow of fuel from the nozzle and the formation of the flame angle.

The flame angle is largely determined by the angle under which the liquid flows from the outer ring. This is explained by the fact that the outer ring has a large area and the axial velocity of the fuel particles at the nozzle wall is higher than at the boundary with the air vortex, consequently, more liquid passes at the nozzle wall in unit time than through equal area elements at the boundary with the air vortex [205]. To determine the flame angle, we divide the nozzle cross section into elementary rings and consider the outflow of the liquid from these rings (Fig. 86).

The momentum for each elementary ring (q_i) is determined by the equation

$$q_i = 2\pi\rho v_i r \Delta r. \tag{5.38}$$

Substituting into this expression the value of q_1, we have

$$q_i = 2\pi \sqrt{2\rho p} \cdot \sqrt{r^2 - \mu^2 A_y^2 r_c^2}\,\Delta r. \tag{5.39}$$

The sum of the vectors of the momenta of all elementary rings is equal to

$$Qw_c = \sum_{i=1}^{i=n} q_i w_i, \tag{5.40}$$

where w_0 is the resulting velocity.

Projecting all vectors (5.40) on the burner axis and the total momentum vector, we find

$$Qw_0 \cos\frac{\alpha_\phi}{2} = \sum_{i=1}^{i=n} q_i w_i \cos\frac{\alpha_i}{2}, \tag{5.41}$$

$$Qv_0 = \sum_{i=1}^{i=n} q_i w_i \cos\frac{\alpha_\phi - \alpha_i}{2}, \tag{5.42}$$

where α_ϕ is the flame angle; α_i the departure angle of the liquid particles of each elementary ring.

According to Eq. (5.8), $w_i = \sqrt{u_i^2 + v_i^2}$ and is independent of the ring radius, hence

$$Qw_0 \cos\frac{\alpha_\phi}{2} = w \sum_{i=1}^{i=n} q_i \cos\frac{\alpha_i}{2}. \tag{5.43}$$

$$Qw_0 = w \sum_{i=1}^{i=n} q_i \cos\frac{\alpha_\phi - \alpha_i}{2}. \tag{5.44}$$

As a result of the combined solution of Eqs. (5.43) and (5.44) we obtain

$$\operatorname{tg}\frac{\alpha}{2} = \left(\sum_{i=1}^{i=n} q_i \sin\frac{\alpha_i}{2}\right)\left(\sum_{i=1}^{i=n} q_i \cos\frac{\alpha_i}{2}\right)^{-1}, \tag{5.45}$$

$$\sin\frac{\alpha_i}{2} = \frac{u_i}{w_i} = \frac{\mu A_y r_c}{r}, \tag{5.46}$$

$$\cos\frac{\alpha_i}{2} = \frac{v_i}{w_i} = \sqrt{1 - \frac{\mu^2 A_y^2 r_c^2}{r^2}}. \tag{5.47}$$

Replacing q_1, $\sin\frac{\alpha}{2}$ and $\cos\frac{\alpha}{2}$ by their values from (5.39, 46, 47) and determining the limits of the sums of the numerator and denominator of Eq. (5.45), we obtain the equation for determining the flame angle

$$\operatorname{tg}\frac{\alpha_\phi}{2}=\frac{2\mu A_s\left[\sqrt{1-\mu^2A_s^2}-\sqrt{s^2-\mu^2A_s^2}-\right.}{1-s^2+2\mu^2A_s^2\ln s}\frac{\left.-\mu A_s\left(\arccos\mu A_s-\arccos\frac{\mu A_s}{s}\right)\right]}{1-s^2+2\mu^2A_s^2\ln s}. \qquad (5.48)$$

Like the departure angles of the extreme fuel particles (α_s and α_v), the total flame angle according to (5.48), (5.37), (5.13) and (5.14), is a function of a single parameter, the equivalent geometrical characteristic A_e. Investigations, taking into account the frictional pressure loss in atomizers with high output operating with petroleum residue, gave good agreement between the experimental and theoretical values. For diesel oil, as our investigations have shown, if the friction losses are neglected, a deviation of the experimental points from the theoretical curve was found (see Fig. 84). These deviations are explained by the loss of tangential component as a result of the friction at the side walls of the chamber and nozzle. In the studies on the throughput coefficient, these losses were compensated by the pressure loss and since the flame angle is independent of the pressure, the experimental points are mainly located below the theoretical curve.

In accordance with the theory of the disintegration of the jet under the action of the initial vibration or, of turbulent pulsation, the thickness of the dispersion of proportional to the diameter of the nozzle or of another geometrical parameter.

In the central sprayers, we use for a parameter of this type, the thickness of the conical film. The geometric forms (see Fig. 73) are derived from the thickness of the conical fuel film in the central sprayers, and are equal to

$$\delta=(r_c-r_s)\cos\frac{\alpha_s}{2}=r_c(1-s)\cos\frac{\alpha_s}{2}. \qquad (5.49)$$

With replacing $\cos\frac{\alpha_v}{2}$ by its expression from (5.36), we obtain an equation for calculating the thickness of the conical fuel film

$$\delta=r_c\frac{1-s}{s}\sqrt{s^2-\mu^2A_s^2}, \qquad (5.50)$$

and thus the relative thickness of the conical film is

$$\frac{\delta}{r_n}=\frac{1-s}{s}\sqrt{s^2-\mu^2A_s^2}. \qquad (5.51)$$

The equation for determining the thickness of the conical film can be obtained from the continuity condition as proposed by N. N. Strulevich. If we consider a film with a cone angle of α_ϕ, the fuel throughput through the active section at the nozzle is written as

$$Q = Fw = \pi\delta\left(2r_c - \delta\cos\frac{\alpha_\phi}{2}\right)w. \tag{5.52}$$

If we disregard the losses in the burner nozzle and assume

$$w = \sqrt{\frac{2p}{\varrho}}, \tag{5.53}$$

then, solving in combination (5.52) and the equation for the fuel throughput (5.10), we obtain

$$\frac{\delta}{r_c} = \frac{1 - \sqrt{1 - \mu\cos\frac{\alpha_\phi}{2}}}{\cos\frac{\alpha_\phi}{2}}. \tag{5.54}$$

The relative thickness of the conical film is a function of the geometrical characteristic A_e (Fig. 87), with the curves plotted according to the equations (5.51) and (5.54), differing only slightly over the entire range of values of practical interest.

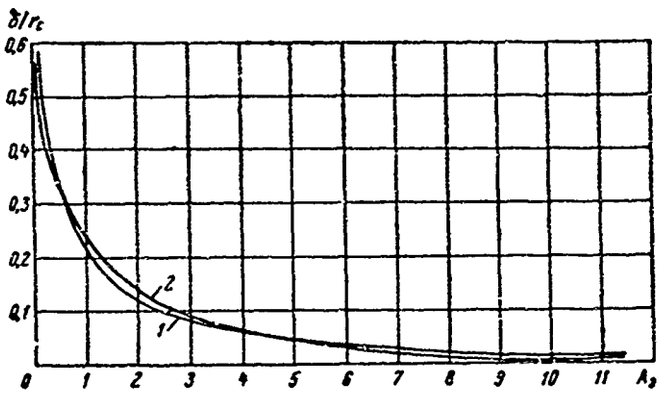

Fig. 87. Relative thickness of the conical film as a function of the equivalent geometrical characteristic: 1) according to Eq. (5.51); 2) according to Eq. (5.54).

Experimental investigations [206] showed that the mean drop diameter is proportional to the thickness of the conical film (Fig. 88). In the work [207], a linear relation was found between the drop diameter and the parameter $r_s/\sin\alpha_\phi/2$ which can serve as a characteristic of the geometrical form of the jet which is connected with the thickness of the conical film by a linear relation. Of the physical properties of the fuel, the viscosity is of the greatest importance for the performance of the atomizers since it not only

affects directly the quality of atomization as a force which opposes the disintegration of the jet but also causes an energy loss due to the friction losses and increases the thickness of the conical film. Figure 89 shows the relative thickness of the conical film as a function of the viscosity of the fuel for the case of a centrifugal atomizer. The variation of the mean drop diameter during the operation of this atomizer as a function of the viscosity of the petroleum residue and paraffin at different preheating temperatures is shown in Fig. 54,a.

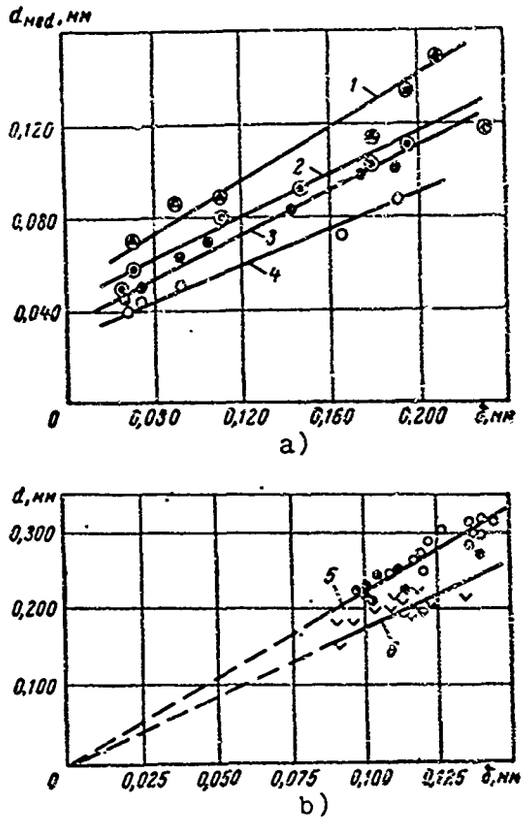

Fig. 88. Average (median) drop diameter as a function of the thickness of the conical film: a) experiments of N. N. Strulevich; b) experiments of the authors. Fuel pressure: 1) 8 kgf/cm^2; 2) 10 kgf/cm^2; 3) 20 kgf/cm^2; 4) 40 kgf/cm^2; 5) 4 kgf/cm^2; 6) 13 kgf/cm^2.

The desired quality of atomization can be achieved by using designs with minimum thickness of the conical film. This involves an increase in the geometrical characteristic which causes a variation in the throughput and flame angle, the dimensions of the atomizer which enter into the geometrical characteristic having a different effect on its performance.

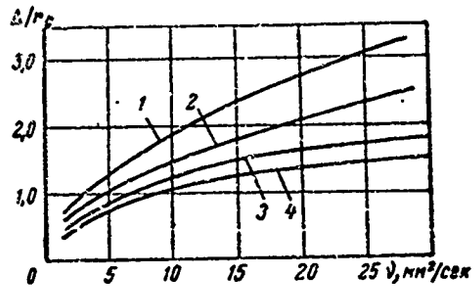

Fig. 89. Relative thickness of the conical film as a function of the viscosity of the fuel for an atomizer with a nozzle diameter of 2 mm, a diameter of the vortex chamber of 7 mm and four tangential orifices with a diameter of 0.75 mm: 1) p = 1 kgf/cm^2; 2) p = 2.5 kgf/cm^2; 3) p = 4 kgf/cm^2; 4) p = 10 kgf/cm^2.

With decrease in the nozzle diameter, the fuel throughput usually decreases but when the friction coefficient is large, the reverse can be observed: the fuel throughput increases with decrease in the nozzle diameter. At the same time, the equivalent geometrical characteristic decreases markedly while the fuel throughput coefficient approaches unity which is the cause of the increased throughput. An extremum analysis of the function $Q = \psi(2r_s)$ (variation of the fuel throughput with only the nozzle diameter as variable) shows that the function has a minimum at the value

$$r_c = \frac{1}{2-\varphi}\left(\frac{2l\mu_f r_z^2}{fR} + R\right).$$

This is explained by the fact that with decreasing nozzle diameter, the tangential velocity component diminishes owing to the friction and the flow from the atomizer becomes similar to that from the jet-type with sudden increase in the throughput coefficient.

With decrease in the friction coefficient f (at low viscosity of the fuel and large flow velocity), the value of r_s, corresponding to the extremum of the function $Q = \psi(2r_s)$, increases and tends to infinity. However, since $2r_s$ cannot be larger than the diameter of the vortex chamber, the throughput practically depends unequivocally on the nozzle diameter at small friction coefficients.

With increase in the nozzle diameter, the equivalent geometrical characteristic of the atomizer increases sharply and the flame angle increases.

As follows from Eq. (5.51), the thickness of the conical film is directly proportional to the nozzle radius and increases with increase in the nozzle orifice. Simultaneously, the equivalent geometrical characteristic increases and, consequently, the thickness of the conical film decreases (see Fig. 89). The radius of the atomizer nozzle corresponding to the maximum of the function $\delta = \psi(2r_s)$ for practical purposes can be determined by means of the equation

$$r_c = \frac{(1-z)(2\mu_z r_z^2 + fR^2)}{fR}, \qquad (5.55)$$

where z is determined graphically as a function of the equivalent geometrical characteristic or by means of an empirical expression which corresponds to the diagram with sufficient accuracy [206]:

$$z = \lg 3{,}5A_e^{0.43}. \qquad (5.56)$$

The extremum of the nozzle radius is connected with the friction coefficient f. The latter is a function of the Reynolds number, consequently, the viscosity and the velocity of the fuel affect the extremum of $\delta = \psi(2r_s)$.

With decrease in the friction coefficient f, the maximum of the function $\delta = \psi(2r_s)$ moves away from the ordinate axis. For an ideal fluid this function does not have the maximum ($2r_s \to \infty$) and with increasing nozzle radius the quality of atomization also decreases. For real liquids, the extremum value of the nozzle radius decreases with increasing viscosity and decreasing flow velocity. When the nozzle radius is decreased or increased compared with the extremum, the quality of atomization increases.

The radius of the vortex chamber does not directly enter into the equations which determine the performance parameters but is contained in the expression for the equivalent geometrical characteristic.

The function A = F(R) has a maximum at

$$R = r_z \sqrt{\frac{2\mu_z}{f}}. \qquad (5.57)$$

Consequently, at this value of the vortex radius the throughput coefficient and the thickness of the conical film will be a minimum and the flame angle a maximum (all other atomizer dimensions remaining constant). The extremum of the vortex radius depends on the viscosity and flow velocity of the fuel. When the viscosity of the fuel decreases and the velocity increases (i.e., when the friction coefficient f is decreased), the maximum of the function $A_e = F(R)$ deviates from the ordinate axis, while for an ideal fluid (f = 0) this function does not have a maximum ($R_{ekstr} \to \infty$). Hence, during the atomization of a low-viscosity liquid, the fuel throughput decreases, the flame angle and the quality of atomization increase with increase in the vortex radius.

In addition to the basic dimensions of the atomizer (nozzle diameter, diameter of the tangential orifices and the vortex-forming shoulder) the parameters of its performance are affected by the height of the nozzle and the vortex chamber, the length of the tangential

orifices, the entry and exit angle of the nozzle aperture and the tangential orifices and also the relative position of the axes of the nozzle aperatures and the vortex chamber. With increase in the length of the vortex chamber, the loss of momentum relative to the axis and the loss of total pressure increases which causes a change in the fuel throughput, a decrease of the flame angle and a deterioration in the quality of atomization.

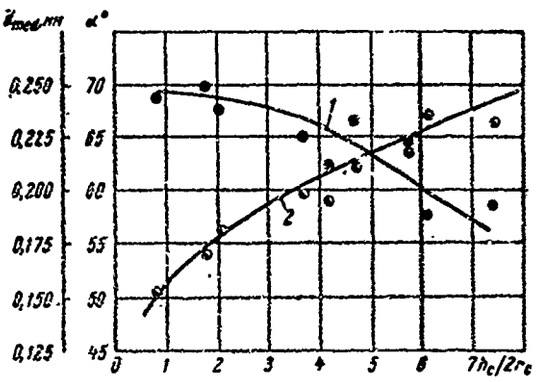

Fig. 90. Flame angle 1 and mean drop diameter 2 as a function of the relative height of the nozzle.

An experimental study of the performance of centrifugal atomizers showed [208] that with increasing nozzle height, as a result of the friction between the fuel and its walls, the tangential as well as the axial velocity components decrease. With decrease of the tangential component, the active cross section of the nozzle increases, thus the throughput remains practically constant, whereas the flame angle and the atomization quality decrease (Fig. 90). The increase in the drop size takes place as a result of the thickening of the conical film and the reduction in the total velocity. These regularities hold as long as the flow from the nozzle is in the form of a film, i.e., as long as the atomizer performs as a centrifugal atomizer.

The vortex formation in the fuel and the centrifugal effect of the atomizer depend to a large degree on the length of the tangential channels. If the length of the channels is short, the fuel flow cannot be given the required direction and deviates towards the chamber axis which results in a decrease of the initial momentum, an increase in the throughput coefficient, a decrease of the flame angle and less efficient atomization. Extreme lengthening of the tangential channels (more than 6-8 r_t) leads to a reduction in the velocity of the fuel during its passage through these channels which naturally affects the performance parameters of the atomizer. A variation of the length of the tangential orifices within the range of 1.5-4 diameters does not affect the performance parameters of atomizers.

The performance parameters of atomizers are affected not only by the dimensions of the tangential orifices, the vortex chamber and nozzle but also by their mutual position and the form of transition.

Depending on the slope angle of the tangential orifices, the vortex momentum varies. When the angle of the tangential orifices deviates from the direction of the tangent on the cylindrical part of the combustion chamber (nontangential orifices), the vortex shoulder is made smaller and the geometrical characteristic and the performance parameters of the atomizers are correspondingly reduced.

The angle of the transition from the vortex chamber to the nozzle has a noticeable effect on the performance parameters of the atomizer only at low values of the geometrical characteristic. In this case, the fuel throughput decreases, the flame angle increases and the atomization efficiency increases with increase in the transition angle. With very small angles of transition, the path of the fuel to the nozzle is lengthened, the length of the vortex chamber is practically increased and the performance parameters of the atomizers are accordingly modified.

For the calculation, designing and manufacture of atomizers it is essential to indicate the optimum class of precision of its dimensions [209]. The equations (5.4) (5.10), (5.13), (5.14), (5.37), (5.48) and (5.51) can be used to determine the deviations of the performance parameters of centrifugal atomizers from their nominal values as a function of the tolerances of the basic dimensions. By way of an example, Table 12 presents the results of the determination of the relative deviations of the fuel throughput, the flame angle and the mean drop diameter as a function of the class of precision of the achievement of the atomizer dimensions (nozzle diameter 1.85 mm, vortex chamber diameter 4 mm, number of tangential orifices 4, their diameter 0.95 mm).

The computations shown in Table 12 were obtained for an ideal fluid which can be used for atomizers working with low-viscosity fuels at high feed pressures. When working with high-viscosity fuels, the calculations of the tolerances [208] show the possibility of producing the basic dimensions in lower class of precision. An analysis of the calculation shows that the smaller the fuel throughput, the more accurate must be the fabrication of the dosing elements of the atomizer. For atomizers with large fuel throughput, the relative deviations of the geometrical forms and dimensions will be slight, accordingly the deviations of the performance parameters of the atomizers will also decrease with increase in the dimensions of the cross sections of the fuel passages. It was found as a result of measurements of the geometrical dimensions of a lot of factory-made atomizers [204] that the higher the fuel throughput, the smaller is the scatter of the throughput characteristics of the atomizers.

Thus, in the calculation of a centrifugal atomizer one can find the geometrical characteristic (see Fig. 84) on the basis of the given flame angle. The throughput coefficient μ is determined by means of Eqs. (5.13) and (5.14). Knowing the throughput and the fuel pressure, the nozzle radius is readily determined (5.10).

TABLE 12

Deviation of the Performance Parameters of Atomizers as a Function of the Class of Precision of the Basic Dimensions

1 Класс точности изготовления основных размеров форсунки	2 Отклонение параметров в % к номинальному значению		
	3 по расходу топлива	4 по углу факела	5 по размеру капель
1	1,17	0,5	1,09
2	2,36	0,85	1,58
2а	3,24	1,20	2,60
3	4,78	1,75	3,84

1) Class of precision of the basic dimensions of the atomizers; 2) Derivation of the parameters in % of the nominal value; 3) with respect to fuel throughput; 4) with respect to flame angle; 5) with respect to drop size.

For the determination of the diameter of the vortex shoulder one can use the relation $\frac{R}{ir_t^2} = \frac{A}{r_s}$, the number of tangential orifices is preferably made greater than 3 in order to prevent skewing of the flame, and the diameter of the tangential orifices should not be less than ~0.7 mm. The maximum diameter of the vortex shoulder should not exceed $R < r_t\sqrt{\frac{2i}{f}}$ (5.55), and the coefficient f can be determined on the basis of the throughput and r_t.

Following the selection of approximate values for the basic dimensions, an estimate must be made on the basis of the available experimental data and theoretical relations of the expected pressure loss Δp and the pressure $p - \Delta p$ calculated, with allowance being made for the friction coefficient f. The atomizer dimensions are chosen by the method of successive approximations. The final verification must be made, taking the atomization efficiency of the fuel in the flame into account. To determine the atomization efficiency, one has to find by means of Eq. (5.50) the thickness of the conical film and, by means of the expression (3.68), the drop size which must be checked (by means of the equations given in § 17) to see whether it corresponds to the furnace device; the distribution of the fuel in the furnace volume is estimated by means of the data in § 16.

19. PECULIARITIES OF THE CALCULATION OF COMPLEX CENTRIFUGAL ATOMIZERS

The above-presented basic theoretical relations for the simple centrifugal atomizer can be used for calculating more complex atomizer designs. Thus, the performance of a two-state single-circuit atomizer (see Fig. 78,a) may be regarded as the performance of a single-stage atomizer with fuel supply via two systems of tangential orifices. As in the case of the simple single-stage atomizer, we obtain Eq. (5.1) by equating the variation of the momentum and the friction moment. For the case that both stages are operating, the solution of this equation must be divided into two stages. First one calculates the momentum of the fuel in the section, defined by the distance between the tangential orifices of the first and second stage and then in the second section, from the tangential orifices to the output nozzle, for the entire mass of fuel arriving through the two stages. For practical calculations it can be assumed that the two flows (of the first and second stage) move independently in the vortex chamber and that the momentum of the fuel in the nozzle is equal to the sum of the momenta of the fuel in the two stages. Then, solving Eq. (5.1) for the two flows, we find

$$M_{c.\,I} = \frac{\varrho_f Q_I A_{s.\,I}}{\pi r_c}, \tag{5.58,a}$$

$$M_{c.\,II} = \frac{\varrho_f Q_{II}}{\pi r_c} A_{s.\,II}, \tag{5.58,b}$$

$$M_c = M_{c.\,I} + M_{c.\,II} = \frac{\varrho_f}{\pi r_c}(Q_I A_{s.\,I} + Q_{II} A_{s.\,II}) =$$

$$= \frac{\varrho_f Q}{\pi r_c} A_c, \tag{5.58}$$

$$A_{s.\,I} = \frac{R_I r_c}{\mu_f f_I r_{r.\,I}^2 + 0{,}5 f R_I (R_I - r_c)}, \tag{5.59,a}$$

$$A_{s.\,II} = \frac{R_{II} r_c}{\mu_f f_{II} r_{r.\,II}^2 + 0{,}5 f R_{II} (R_{II} - r_c)}, \tag{5.59,b}$$

$$A_c = \frac{Q_I A_{s.\,I} + Q_{II} A_{s.\,II}}{Q_I + Q_{II}}, \tag{5.59}$$

where A_s is the total geometrical characteristic, the other symbols being the same as for the simple single-stage atomizer; the indices I and II refer to the first and second stage, respectively.

For the calculation of the throughput coefficient, the flame angle and the thickness of the conical film, the corresponding equations for the simple centrifugal atomizers can be used, except that the total geometrical characteristic must be used instead of the equivalent geometrical characteristic. For the calculation of the fuel throughput and the atomization efficiency, the flow rate of the fuel can be approximately assumed as being equal to

$$w_c = \sqrt{\frac{w_I^2 Q_I + w_{II}^2 Q_{II}}{Q_I + Q_{II}}}. \tag{5.60}$$

The operation of an atomizer on the second stage along does not differ in any way from the operation of the simple centrifugal atomizer and all the theoretical and experimental data which were obtained on the simple atomizer, can be applied. When the fuel is supplied only to the first stage, the equations for the simple single-circuit atomizer can also be used but the large losses of momentum and pressure due to the zone filled with fuel must be taken into account (from the entry of the first stage along the cylindrical surface of the vortex chamber which has a braking effect). Hence the atomization efficiency during the operation of the first stage alone will be considerably less than when both stages are working (under the same pressure).

The double-circuit atomizers with single output nozzle have the best characteristics (see Fig. 78,b). When the fuel is supplied only through the first stage, its basic parameters (throughput, flame angle, atomization efficiency) can be determined by means of the equations given in § 18.

Using the basic equations for the calculation of the simple centrifugal atomizers, we determine the fuel throughput when it is supplied only through the second stage of the double-circuit atomizer with single output nozzle. If we regard the first stage of the atomizer as a simple single-stage atomizer, in which the fuel is supplied via the annular gap in the face of the vortex chamber, the equation of the variation of the momentum for this atomizer is analogous to Eq. (5.1).

Integrating this equation within the limits of variation of r from $r = r_{s.II}$ ($r_{s.II}$ is the nozzle radius of the second stage) to $r = r_{s.I}$ ($r_{s.I}$ is the radius of the nozzle of the first stage), we find after several transformations

$$M_{c.I} = \frac{2\varrho_T Q_{II} M_{c.II}}{\pi f_I M_{c.II}(r_{c.II} - r_{c.I}) + 2\varrho_T Q_{II}}, \tag{5.61}$$

where $M_{s.I}$ and $M_{s.II}$ are the momenta at the point of emergence of the fuel from the nozzle of the first and second stage, respectively.

According to Eq. (5.59,b):

$$M_{c.II} = \frac{A_{s.II}\varrho_T Q_{II}}{\pi r_{c.II}}. \tag{5.62}$$

Eq. (5.61) can be written in the form

$$M_{c.I} = \frac{A_{cI}\varrho_T Q_{II}}{\pi r_{c.I}}, \tag{5.63}$$

where

$$A_{c.I} = \frac{A_{s.II}}{\frac{r_{c.II}}{r_{c.I}}\left(\frac{f_I A_{s.II}}{2} + 1\right) - \frac{f_I \cdot A_{s.II}}{2}}. \tag{5.64}$$

The further calculation is carried out by means of the equations of § 18 by replacing A_e by the reduced geometrical characteristic A_p.

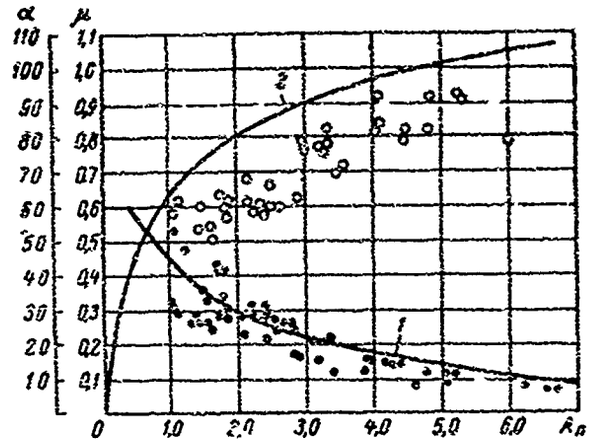

Fig. 91. Coefficient of fuel throughput 1 and flame angle 2 as a function of the parameter A_p during the operation of the second stage only of a double-circuit atomizer with single output nozzle.

Figure 91 shows the dependence of the theoretical and experimental values of the fuel throughput coefficient 1 and the flame angle 2 on A_p. The basic theoretical dimensions of the tested atomizers and the test results are given in Table 13.

The discrepancies between the experimental and theoretical results are explained by the fact that the equations for the calculation of the flame angle do not take into account the losses of the tangential velocity component in consequence of the friction between the fuel and the cylindrical part of the vortex chamber and in the nozzle.

The radius of the nozzle of the first stage ($r_{s.I}$) does not affect the atomization efficiency of the fuel because the dependence of A_p on $R_{s.I}$ and δ on A_p are of a reciprocal nature and compensate each other. Experimental studies have shown (see Table 13) that at the same fuel supply pressure, the differences in the atomization efficiency of the fuel are within the limits of the experimental error. However, the mean drop sizes exceed those for single-stage atomizers with the same geometrical characteristics.

TABLE 13

Operating Parameters of Double-Stage Atomizer with Single Output Nozzle when the Fuel is Supplied Only Through the Second-Stage (Variable Dimensions of the First Stage)

1 Номер форсунки и ее размеры	3 p, кгс/см²	4 Q, кг/ч	$A_{э.II}$	A_n	μ	α	b, мм	$\bar{d}$, мм
2 Форсунка 1 $2r_{c.1} = 1{,}03$ мм $R_1 = 4$ мм	5	45,11	2,067	1,055	0,523	58	0,113	0,275
	10	58,80	2,438	1,255	0,480	61	0,095	0,240
	30	90,00	3,008	1,568	0,426	56	0,077	0,200
	50	112,50	3,273	1,717	0,413	55	0,070	0,160
2 Форсунка 2 $2r_{c.1} = 1{,}3$ мм $R_1 = 4$ мм	5	48,00	2,182	1,454	0,349	56	0,104	0,247
	10	65,21	2,571	1,723	0,335	65	0,082	0,220
	30	104,04	3,180	2,155	0,309	70	0,073	0,202
	50	133,23	3,465	2,355	0,307	60	0,065	0,171
2 Форсунка 3 $2r_{c.1} = 1{,}36$ мм $R_1 = 4$ мм	5	48,00	2,175	1,527	0,323	51	0,103	0,300
	10	63,82	2,543	1,794	0,300	59	0,088	0,232
	30	104,65	3,184	2,266	0,284	60	0,071	0,207
2 Форсунка 4 $2r_{c.1} = 1{,}44$ мм $R_1 = 4$ мм	5	49,86	2,237	1,679	0,295	63	0,101	0,300
	10	67,28	2,599	1,959	0,282	64	0,089	0,262
	30	110,43	3,286	2,499	0,268	64	0,069	0,168
	50	137,40	3,482	2,652	0,258	66	0,066	0,147
2 Форсунка 5 $2r_{c.1} = 1{,}5$ мм $R_1 = 4$ мм	5	58,06	0,471	1,026	0,317	57	0,162	0,345
	10	76,27	0,991	1,153	0,295	46	0,146	0,327
	30	124,14	1,233	1,425	0,277	55	0,121	0,190
	50	156,52	1,346	1,554	0,270	56	0,112	0,142
2 Форсунка 6 $2r_{c.1} = 1{,}7$ мм $R_1 = 4$ мм	5	51,72	2,273	2,079	0,220	62	0,098	0,315
	10	69,50	2,628	2,407	0,209	55	0,084	0,274
	30	118,00	3,366	3,092	0,205	74	0,068	0,187
	50	147,50	3,534	3,248	0,198	70	0,065	0,142
2 Форсунка 7 $2r_{c.1} = 2{,}1$ мм $R_1 = 4$ мм	5	56,12	2,396	2,781	0,163	63	0,092	0,304
	10	75,63	2,151	3,185	0,154	74	0,081	0,266
	30	124,13	3,398	3,915	0,146	73	0,064	0,208
2 Форсунка 8 $2r_{c.1} = 2{,}1$ мм $R_1 = 3$ мм	5	55,50	2,388	2,831	0,155	74	0,090	0,321
	30	122,44	3,366	3,957	0,139	83	0,066	0,220
	50	156,52	3,625	4,252	0,138	79	0,060	0,196
2 Форсунка 9 $2r_{c.1} = 2{,}1$ мм $R_1 = 2$ мм	5	55,64	2,388	2,831	0,155	78	0,090	0,273
	10	74,07	2,688	3,171	0,146	82	0,084	0,260
	30	122,44	3,366	3,957	0,139	92	0,066	0,183
	50	153,19	3,625	4,252	0,135	83	0,060	0,140
2 Форсунка 10 $2r_{c.1} = 2{,}43$ мм $R_1 = 4$ мм	5	55,04	2,388	3,414	0,114	74	0,089	0,306
	10	75 31	2,740	3,890	0,111	73	0,076	0,250
	30	125,00	3,398	4,761	0,106	88	0,061	0,209
	50	157,69	3,625	5,056	0,104	84	0,058	0,186
2 Форсунка 11 $2r_{c.1} = 3$ мм $R_1 = 4$ мм	5	57,11	2,401	4,574	0,078	83	0,0	0,306
	10	76,10	2,730	5,046	0,074	87	0,0	0,301
	30	128,57	3,488	6,283	0,072	92	0,0	0,250
	50	157,89	3,625	6,559	0,068	90	0,050	0,190

1) Number of atomizer and dimensions; 2) Atomizer; 3) kgf/cm^2; 4) kg/h.

During simultaneous operation of both stages of a double-circuit atomizer, a mixing of the two fuel flows takes place in the vortex chamber of the first stage. The counter pressure thus produced normally amounts to only a small proportion of the pressure under which the fuel is supplied. However, under transitional operating conditions when the fuel pressure in the first stage is much higher than the fuel pressure in the second stage, the latter is comparable with the counter pressure in the first stage. The fuel of the first stage, according to Eq. (5.6), has an axial velocity constant over the entire cross section at the boundary between the vortex chamber and the nozzle. Hence, the counter pressure produced by the fuel of the first stage on the second will be equal to

$$p_{пр.1} = \frac{\rho_1 w^2}{2} = \frac{\rho_1 Q_1^2}{2\pi^2 \varphi_1^2 r_c^4}. \qquad (5.65)$$

By replacing Q by its expression from (5.10), we obtain

$$p_{пр.1} = \left(\frac{\mu_1}{\varphi_1}\right)^2 p_1 = k_1 p_1, \qquad (5.66)$$

where

$$k_1 = \left(\frac{\mu_1}{\varphi_1}\right)^2.$$

Figure 92 shows the ratio of the theoretical counter pressure to the experimental pressure as a function of the ratio of the nozzle diameter of the second stage to the diameter of the air vortex of the first stage. Investigations showed [198] that Eq. (5.66) for the calculation of the counter pressure is correct only at values of $r_{s.I}/r_{v.II} > 1$.

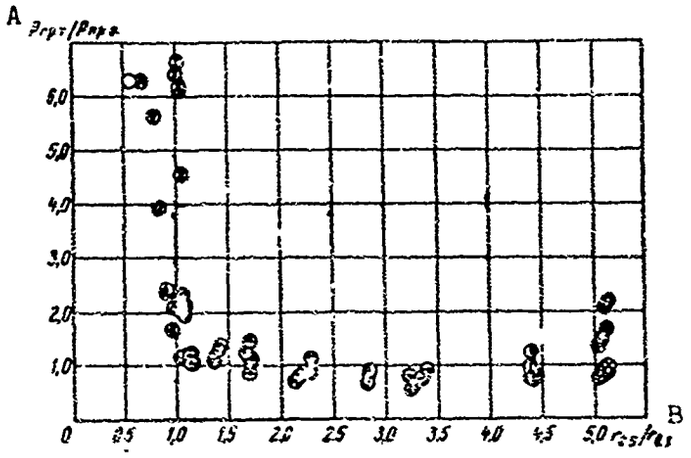

Fig. 92. Ratio of theoretical to experimental counter pressure as a function of the ratio of the nozzle diameter of the second stage to the diameter of the air vortex of the first stage. A) $p_{pr.t}/p_{pr.o}$; B) $r_{s.II}/r_{v.I}$.

It was found as the result of the study of a series of atomizers that the fuel throughput during operation of both stages is equal to the sum of throughputs of each stage. The fuel throughput of each stage corresponded to a point on the throughput curve (recorded during independent operation of the stages) with a pressure equal to the difference between the pressure and counter pressure in the stage.

According to the experimental data, the counter pressure in double-circuit atomizers with single output nozzle amounts to 5 to 20% of the fuel pressure in the first stage (p_1) which is 0.75 to 3.0 kgf/cm^2 at p_1 = 15 kgf/cm^2. These values are comparable with the fuel feed pressure in the second stage. The fuel throughput through the second stage, corresponding to these pressures, is usually larger than the fuel throughput through the first stage. In designing double-circuit atomizers, the diameter of the nozzle of the second stage must not be made equal to the diameter of the air vortex of the first stage or have similar values since in this case the slightest deviation in nozzle diameter (even within the limits of tolerance of the first class) can lead to large changes in the counter pressure and throughput of the fuel.

It is best to make the diameter of the nozzle of the second stage smaller than the diameter of the air vortex of the first stage. In this case the counter pressure will be only a negligible proportion of the pressure and will not exert any significant effect on the throughput.

The counter pressure of the fuel in the second stage in the direction of the first under all operating conditions of the atomizer represents a negligible proportion of the feed pressure of the fuel in the second stage and practically has no effect on the operating parameters of the atomizer.

The measurements carried out by the authors showed that the curves of total fuel throughput during the operation of both stages under equal pressure, obtained by direct measurement of the throughput characteristics of each stage with allowance made for the counter pressure, practically coincide.

In furnaces, the two stages operate at the same fuel feed pressure only at 100% load. Under intermediate operating conditions, the pressure in the first stage is considerably greater than in the second but for this case also, the theoretical and experimental total consumptions are in good agreement as follows from Table 14.

The flame angle and the thickness of the conical film of a double-circuit atomizer can be determined by means of the equations presented in § 18, using the total geometrical characteristic A_s (5.59).

TABLE 14
Results of the Determination of the Total Fuel Throughput by Calculation and Experiment

1 Показатели	2 p_1 — давление топлива перед первой ступенью, кГ/см²							
	15	15	20	20	25	25	30	40
	3 p_2 — давление топлива перед второй ступенью, кГ/см²							
	3	4	4	5	5	7	7	10
4 p_1^* — действительное давление топлива в первой ступени, кГ/см²	14,8	14,6	19,7	19,5	24,6	24,2	29,3	39
5 Расход топлива через первую ступень, кг/ч	66,5	66	74,6	74,4	84	81,5	90	101
6 p_2^* — действительное давление топлива во второй ступени, кГ/см²	1,15	2,18	1,53	2,55	1,95	3,96	3,32	5,12
7 Расход топлива через вторую ступень, кг/ч	14	26	21	28	24,5	44	38	50,5
8 Расчетное значение суммарного расхода, кг/ч	80,5	92	95,5	102,4	106,5	125,5	128	151,5
9 Экспериментальное значение суммарного расхода, кг/ч	81,2	92,7	95,9	101,2	104,3	124,9	127,6	152,3

1) Indices; 2) fuel pressure in front of the first stage, kgf/cm^2; 3) fuel pressure in front of the second stage, kgf/cm^2; 4) real fuel pressure in the first stage, kgf/cm^2; 5) fuel throughput through the first stage, kg/h; 6) real fuel pressure in the second stage, kgf/cm^2; 7) Fuel throughput in the second stage, kg/h; 8) Calculated total throughput, kg/h; 9) Experimentally determined total throughput, kg/h.

Figure 93 gives the average (median) drop diameter as a function of the fuel pressure during operation of each stage separately and in combination. When the fuel is supplied to the second stage, the atomization efficiency is much less than during operation of the first stage. This is explained by the large fuel throughput at the same pressures and, consequently, the great thickness of the fuel film and also the energy loss during the passage of the fuel through two stages. The energy losses are particularly large when the atomizer works on the second stage only. When the fuel is supplied through both stages, the fuel arriving through the first stage, does not fill the whole volume of the vortex chamber but leaves an air channel in the center (air vortex). The fuel of the second stage arrives along the "walls" of this air channel, narrowing the air vortex somewhat and partially forcing back the fuel passing through the first stage. When both stages are operating, a sudden expansion of the fuel flow in the second stage does not take place as when the first stage is shut off, in which case the atomization takes place twice, once from the second stage into the vortex chamber of the first stage and then through the first stage nozzle into the combustion zone. As a result of this motion of the fuel, the tangential velocity component is greatly

reduced. Furthermore, the energy losses of the fuel jet result in a decrease of the total velocity (including the axial component) and to an increase in the active cross section of the jet. All these factors (the energy loss, the decrease of the flame angle, the increase in the active section) exert a one-sided effect on the atomization efficiency, as a result of which a rapid increase in drop size is observed when the second stage is alone operating (see Fig. 93).

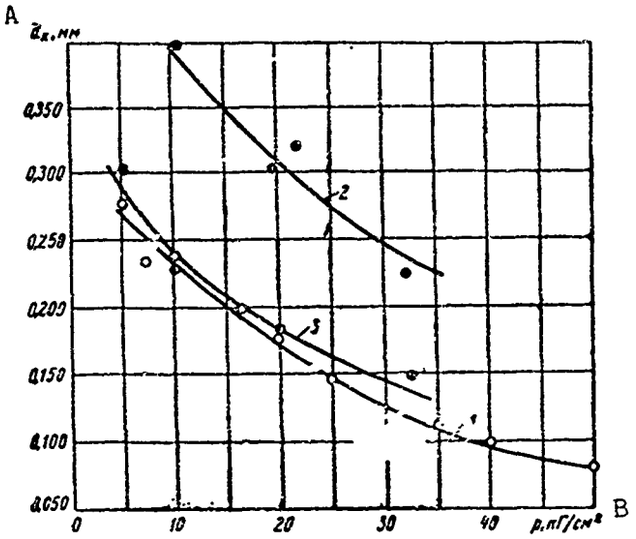

Fig. 93. Average (median) drop diameter as a function of pressure during the atomization of fuel in a double-circuit atomizer with single output nozzle: 1) during operation of the first stage only; 2) during operation of the second stage only; 3) during combined operation of both stages. A) d_k, mm; B) p, kgf/cm^2.

The measurements of the atomization efficiency of the fuel for double-circuit atomizers with single output nozzle at different ratios of the pressure and fuel throughput in the two stages are given in Table 15.

The data represented in Fig. 93 (Curves 1 and 3) and in Table 15, can be described by a general relation (Fig. 94) of the form

$$\frac{d_к}{\delta} = \frac{33{,}11}{e^{0{,}4}}, \qquad (5.67)$$

where d_k is the average drop diameter; δ the thickness of the conical film, determined by means of (5.51); and e the specific energy of the fuel

$$e = \frac{Q_I \varphi_I^2 + Q_{II} \varphi_{II}^2}{2g\,(Q_I + Q_{II})}, \qquad (5.68)$$

where Q_I, Q_{II} are the mass of fuel arriving via the first and second stage; w_1, w_2 the velocities of the fuel in the first and second stage.

TABLE 15
Results of the Measurement of the Atomization Efficiency of the Fuel

1 Суммарный расход топлива, кг/ч	2 Давление топлива, кГ/см²		5 Удельный расход энергии на распыливание топлива, кГ·м/кг	6 Медианный диаметр капель $d_к$, мк	7 Угол факела, градусы	8 Толщина конусной пленки δ, мк	9 Относительный диаметр капель $d_к/\delta$
	3 в первой ступени	4 во второй ступени					
60	9	0	102,5	236	69	41,2	5,78
59	5	3	55,6	300	77	51,4	5,83
58	2	8	80,4	325	50	48,5	6,70
110	36	0	417,8	112	79	34,1	3,30
96	28	6	311,8	175	70	36,9	4,74
105	8	13	128,5	235	52	52,7	4,46
96,5	7	8	89,4	260	60	57,3	4,54
130	13	17	180,3	200	58	52,4	3,82
129	41	12	409,0	164	66	44,0	3,73
126	20	20	228,0	170	54	59,9	2,84
212	50	45,5	567,0	140	42	38,5	2,37

1) Total fuel throughput, kg/h; 2) Fuel pressure, kgf/cm^2; 3) in the first stage; 4) in the second stage; 5) Specific energy consumption in fuel atomization, kgf-m/kg; 6) Median drop diameter d_k, μ; 7) Flame angle, degrees; 8) Thickness δ of the conical film, μ; 9) Relative drop diameter, d_k/δ.

The exponent in Eq. (5.67) is close to the value obtained by other researchers for single-stage atomizers. Consequently, the parameter which includes the energy of the jet, is a more universal similarity criterion.

Two-nozzle atomizers have also found widespread application, (see Fig. 78,c). In the two-nozzle centrifugal atomizers each stage performs like an ordinary single-stage atomizer. If the outer diameter $D_{n.I}$ of the nozzle of the first stage is larger than the air vortex of the second stage, the coefficient of the active cross section will not be determined by the size of the air vortex but by the outer diameter of the nozzle

$$\varphi^* = 1 - \left(\frac{D_{n.I}}{2r_{c.II}}\right)^2, \tag{5.69}$$

where $D_{n.I}$ is the outer diameter of the nozzle of the first stage; $2r_{s.II}$ is the diameter of the nozzle of the second stage.

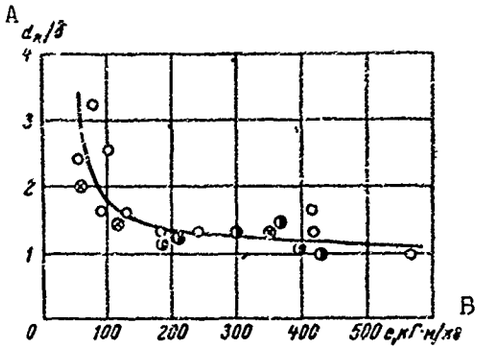

Fig. 94. Relative drop size d_k/δ as a function of the specific fuel energy. A) d_k/δ; B) e, kgf-m/kg.

In contrast to the coefficient ϕ of the active cross section for normal centrifugal atomizers, we shall designate the design coefficient of the active cross section by ϕ^*. If $\phi^* > \phi$, the operating parameters of the second stage of a centrifugal atomizer can be calculated by means of the above derived equations for a simple single-stage atomizer [211].

It follows from (5.13) that the larger the geomertical characteristic, the smaller is ϕ and the larger is the diameter of the air vortex. In the atomizers used in practice, the geomertical characteristic of the second stage is usually larger than 2.5-3.0 according to Eqs. (5.7) and (5.13), for these values $2r_{v.II} = (0.75\text{-}0.77)\, 2r_{s.II}$. Consequently, the first stage will not affect the operation of the second if $D_{n.I} < (0.75\text{-}0.77)\, 2r_{s.II}$. It is not difficult to meet these conditions in practice but is very important to obtain a reliable operation of the second atomizer stage.

n consequence of the fact that each stage has its independent circuit, the fuel consumption during the simultaneous operation of both stages of a two-stage atomizer is determined as the arithmetic sum of the throughputs of the first and second stage at any pressure in each stage [195]. The flame angle of a two-nozzle atomizer is equal to the flame angle of the outer (second) stage when this is larger than the flame angle of the first stage. If the flame angle of the first stage is larger than the flame angle of the second stage, the trajectories of motion of the fuel emerging from the two stages will interesect and the flame angle will have a certain average value determined by the equation

$$\cos\frac{\alpha}{2} = \frac{w_I Q_I \cos\frac{\alpha_I}{2} + w_{II} Q_{II} \cos\frac{\alpha_{II}}{2}}{w_I Q_I + w_{II} Q_{II}}, \qquad (5.70)$$

where w_I, w_{II}, Q_I, Q_{II}, α_I and α_{II} are the fuel velocity, the fuel throughput, and the flame angle of the first and second stage, respectively.

Table 16 gives the results of the flame angle measurement for one atomizer during the simultaneous operation of both stages of a two-nozzle atomizer. The flame angles computed by means of (5.70), are given in the same table for comparison.

It follows from the data of Table 16, that the theoretical and experimental flame angles are very similar.

TABLE 16
Flame Angles of a Two-Nozzle Atomizer

1 Показатели	2 Давление топлива в первой ступени, кГ/см²							
	20	25	30	30	35	35	40	60
	3 Давление топлива во второй ступени, кГ/см²							
	4	5	6	10	5	15	40	60
4 Угол факела первой ступени, градусы	81	79	77	77	75	75	74,5	73
5 Угол факела второй ступени, градусы	38,5	58	58	74	58	75	73	73
6 Экспериментальное значение общего угла факела, градусы	69	70	68	72	68	76,5	74	75
7 Теоретическое значение общего угла факела по уравнению (5. 70), градусы	67	71	70	75	69,5	75	73.2	73

1) Indices; 2) Fuel pressure in the first stage, kgf/cm^2; 3) Fuel pressure in the second stage, kgf/cm^2; 4) Flame angle of the first stage, degrees; 5) Flame angle of the second stage, degrees; 6) Experimental total flame angle, degrees; 7) Theoretical total flame angle according to Eq. (5.70), degrees.

The atomization efficiency for each stage of the atomizer separately can be determined for each stage by means of the equations for the single-circuit atomizers. When the two stages operate simultaneously, the conditions for the disintegration of the jet of each stage are less favorable. When they operate separately, the external air acts on the fuel cone from outside as well as inside. When the fuel is supplied through both stages, the fuel cone of the second stage is in contact on its inner side with the fuel cone of the first stage. In this case, the effect of the air on the atomization of the fuel from each stage decreases and the degree of dispersion of the fuel flame is accordingly less.

When both stages are operating it can be assumed that the fuel flow takes place with a greater thickness of the conical film than in the separate stages.

It can be assumed approximately that in the range of values of μ from 0.1 to 0.7, the relative thickness of the conical film (δ/r_s) is proportional to the throughput coefficient. Taking this into account and assuming equal flow speeds of the fuel in both stages, we can write

$$\frac{\delta r_{c.II}}{\delta r_{c.I}} = \frac{\mu_I}{\mu_{II}} = \frac{Q_I r_{c.II}^2}{Q_{II} r_{c.I}^2}, \tag{5.71}$$

whence

$$\frac{\delta_I}{\delta_{II}} = \frac{Q_I r_{c.II}}{Q_{II} r_{c.I}}. \tag{5.72}$$

Under the assumption that during the operation of both stages all the fuel comes from the large nozzle (the nozzle of the second stage) we obtain in analogy to the expression (5.72) an equation for the determination of the thickness of the nominal conical film

$$\delta_c = \delta_I \frac{r_{c.I}(Q_I + Q_{II})}{r_{c.II} \cdot Q_I} \tag{5.73}$$

or

$$\delta_c = \delta_{II} \frac{r_{c.II}(Q_I + Q_{II})}{r_{c.I} \cdot Q_{II}}. \tag{5.74}$$

A direct proportionality exists between the average median drop diameter and the thickness of the conical film (see Fig. 88). Taking this into account, we can derive an equation for determining the mean drop diameter for the joint operation of both stages

$$d_{cp} = d_I \frac{(Q_I + Q_{II}) r_{c.I}}{r_{c.II} Q_I} \tag{5.75}$$

or

$$d_{cp} = d_{II} \frac{r_{c.II}(Q_I + Q_{II})}{r_{c.I} Q_{II}}, \tag{5.76}$$

where d_I and d_{II} are the average drop diameters during the operation of the first [illegible] second stage, respectively.

The curve of the average drop diameters during joint operation of both stages, calculated by means of Eq. (5.76), is very similar to the experimental curve (Fig. 95,5). Curve 4, calculated by mea[illegible] of Eq. (5.75) lies above the experimental curve which is explained by the pressure loss in the first stage.

When the fuel feed pressure in the two stages is different, the average drop diameter is determined by means of the equation

$$d'_{cp} = d_{cp} \frac{Q_A}{Q_{cp}}, \tag{5.77}$$

where d_{sr} is the average drop diameter, corresponding to a pressure of p_{sr} in the two stages; Q_{sr} is the fuel throughput through the two stages at a fuel pressure p_{sr} in the two stages; Q_d is the real fuel throughput at a fuel supply pressure in the first stage of p_I and in the second stage of p_{II}.

In accordance with Eq. (5.60), the average pressure p_{sr} is equal to

$$p_{cp} = \left(\frac{Q_I \sqrt{p_I} + Q_{II} \sqrt{p_{II}}}{Q_I + Q_{II}}\right)^2, \qquad (5.78)$$

where p_I and p_{II} are the fuel pressure in the first and second stage, respectively.

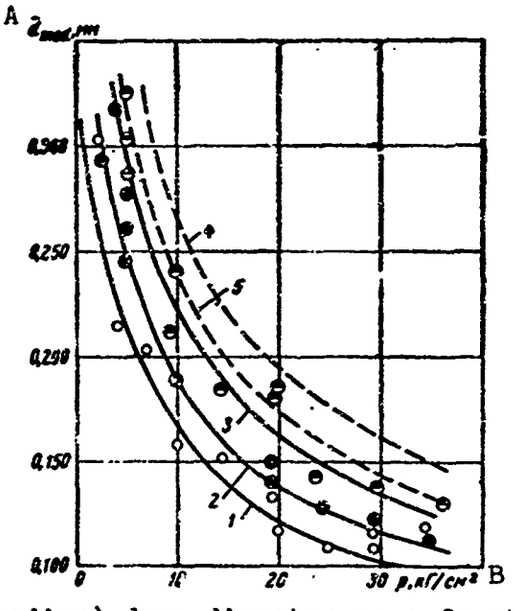

Fig. 95. Average (median) drop diameter as a function of the pressure during atomization of fuel in a two-nozzle atomizer: 1) when only the first stage is working; 2) when only the second stage is working; 3) when both stages are working; 4) and 5) curves corresponding to Eqs. (5.75) and (5.76). A) d_{med}, mm; B) p, kg/cm^2.

Table 17 presents the results of measurements of the atomization efficiency during supply of fuel to the two stages of a two-nozzle atomizer at different pressures. The feed pressure of the fuel in each stage corresponds approximately to the pressure during operation of the atomizer at small loads.

TABLE 17
Average Drop Diameter

1 Показатели	2 Давление топлива в первой ступени, кГ/см²					
	20	25	30	30	35	35
	3 Давление топлива во второй ступени, кГ/см²					
	4	6	5	10	8	15
4 Экспериментальное значение среднего диаметра капель, мм	0,205	0,190	0,180	0,177	0,132	0,155
5 Теоретическое значение среднего диаметра капель, мм	0,193	0,167	0,166	0,168	0,129	0,154

1) Indices; 2) Fuel pressure in the first stage, kgf/cm^2; 3) Fuel pressure in the second stage, kgf/cm^2; 4) Experimental values of the average drop diameter, mm; 5) Theoretical value of the average drop diameter, mm.

It follows from the data of Table 17 that the experimental and theoretical average drop diameters are very similar. Using Eq. (5.77) and (5.78), the optimum pressure ratios in the first and second stage at which the atomization efficiency is an optimum for all operating conditions of the atomizer can be easily determined.

Let us consider the performance of the rotating atomizers which have much in common with the centrifugal type but belong to the rotational atomizers because of the method of producing the torque. In these atomizers, the fuel, arriving on the rotating cup, participates in two motions, a rotational one together with the nozzle and a translational one along the generatrix of the atomizer.

To simplify the calculation of the rotational atomizers let us assume that the speed of rotation of the fuel is equal to the speed of the atomizer, i.e., that no slip takes place, and let us neglect the force of gravity. At speeds of revolution corresponding to the operating conditions of the atomizers, these assumptions practically do not affect the accuracy of the relations thus obtained.

A centrifugal force F, perpendicular to the atomizer axis, acts on a liquid element (see Fig. 82) in a cross section of the atomizer with radius r. This force can be divided into two components which are perpendicular and parallel to the atomizer; the motion of the fuel takes place under the influence of the latter. The motion of the fuel is impeded by the tangential forces T_1 and T_2 due to the internal friction of the liquid (viscosity). In accordance with the d'Alembert principle, these forces are opposed and should add up to zero.

$$F \sin\beta - T_1 + T_2 = 0; \tag{5.79}$$

$$F = \omega^2 r dm = 2\pi\rho r^3 \omega^2 dl dr; \tag{5.80}$$

$$T_1 = 2\pi r\tau dl \text{ и } T_2 = 2\pi(\tau + \Delta\tau) r dl; \tag{5.81}$$

$$\tau = \mu \frac{dV}{dr}, \tag{5.82}$$

where τ is the tangential stress; μ the coefficient of the kinematic viscosity; and ω the angular velocity of the atomizer.

After substitution of the values of F, T_1, and T_2 into Eq. (5.79), its solution at the initial conditions $r = r_v$, $\tau = 0$ has the form

$$\tau = -\frac{\rho\omega^2}{2}\sin\beta\left(r^2 - r_v^2\right), \tag{5.83}$$

where r_v is the radius of the air cavity in the rotating nozzle.

After replacing τ by its value from (5.82) and cond integration, we obtain an expression for the translational velocity

$$v = \frac{\omega^2}{6\nu}\sin\beta\left(R^3 - 3r_v^2R + 3r_v^2r - r^3\right), \tag{5.84}$$

where $\nu = \mu/\rho$ is the coefficient of the kinematic viscosity.

The integration constant of Eq. (5.84) is determined from the condition that the velocity at the nozzle wall (r = R) is zero.

The unknown diameter of the air cavity in the atomizer can be found from the throughput equation

$$Q = \int_{r_v}^{R} 2\pi v\cos\beta r\,dr = \frac{\pi\omega^2}{60\nu}\sin 2\beta\left(3R^5 - 10R^3r_v^2 + 15Rr_v^4 - 8r_v^5\right). \tag{5.85}$$

On the basis of Eq. (5.85) the average velocity over the cross section is

$$v_{cp} = \frac{\omega^2\sin\beta\left(3R^5 - 10R^3r_v^2 + 15Rr_v^4 - 8r_v^5\right)}{30\nu\left(R^2 - r_v^2\right)} \tag{5.86}$$

When the fuel emerges from the rotating nozzle (as in the centrifugal atomizers), the particle trajectories describe a hyperboloid of rotation. The angle of the asymptotic cone of this hyperboloid can be determined from the velocity relations. The radial and tangential components of the total velocity of the fuel particles lie in a plane, perpendicular to the atomizer axis, hence the flame angle is calculated by means of the equation

$$\operatorname{tg}\frac{\alpha}{2} = \frac{\sqrt{0{,}25\omega^2\left(R + r_v\right)^2 + v_{cp}^2\sin^2\beta}}{v_{cp}\cos\beta}. \tag{5.87}$$

After substitution of $v_{sr}\cos\beta$ (5.86) and transformation we obtain

$$\operatorname{tg}\frac{\alpha}{2} = \sqrt{\frac{225\left(R + r_v\right)^2\left(R - r_v\right)^2\nu^2}{\cos^2\beta\sin^2\beta\left(3R^5 - 10R^3r_v^2 + 15Rr_v^4 - 8r_v^5\right)^2\omega^2} + \operatorname{tg}^2\beta}. \tag{5.88}$$

In consequence of the sudden change in the direction of the moving fuel film upon leaving the atomizer and the transformation of the speed of rotation into translational (tangential) velocity, the thickness of the fuel film changes in accordance with the equation

$$\delta = \frac{v_{cp}(R^2 - r_s^2)}{2v_{cym}R} = \frac{Q}{2v_{cym}R\pi\cos\beta}, \quad (5.89)$$

$$v_{cym} = \sqrt{0{,}25\omega^2(R + r_s)^2 + v_{cp}^2}. \quad (5.90)$$

An atomizer radius of 50 mm, an atomizer angle of 5° and a viscosity of the fuel of $6 \cdot 10^{-6}$ m^2/s are assumed in the calculations.

As follows from the calculation (Table 18), the tangential and total velocity exceed the axial velocity many times and the fuel, upon leaving the nozzle, is atomized practically in the plane of the nozzle (the deviation does not amount to more than 6°). Our observations of the atomization of a rotational atomizer and also the published data [212] show that, depending on the operating conditions, (primarily, the throughput), three forms of disintegration of the liquid can result: direct drop formation, filamentary disintegration and film disintegration. These forms are due to the effect of the force of surface tension on the fuel film. When the fuel throughput decreases, the thickness of the fuel film approaches the critical value until the potential energy of the surface layer exceeds a certain level, as a result of which the film is transformed into several filaments with a thickness which is greater than that of the film. Further decrease in the throughput leads to a decrease in the diameter of the filaments, when the potential energy again exceeds a certain level, and the number of these filaments decreases with decrease in the throughput. The decrease of the filament diameter has a limit beginning with which the fuel flies off the edges of the nozzle in the form of individual drops. As a result of the very small thinness of the film, the drops size distribution is fairly uniform. This uniformity is characterized by the quantity m = 8, consequently, the ratio of maximum to minimum drop size is 2.63, and, in the centrifugal atomizers, 7-46.3. An increase in throughput increases the nonuniformity of the atomization of the fuel slightly.

The rotational atomizers have much larger control ranges than the other forms of centrifugal atomizers. The atomization efficiency increases when the fuel throughput decreases. The throughput and drop size can be controlled independently, if necessary, by lowering the number of revolutions of the atomizer.

With rare exceptions (gas turbine atomizers), the rotational atomizers in industry are used in combination with pneumatic atomization. However, the role of the airstream consists not merely in an improvement of the atomization efficiency as in a variation of the direction of motion of the drops.

TABLE 18
Results of the Calculation of the Basic Performance Parameters of Rotational Atomizers

1 Показатели	2 При 2800 об/мин			3 При 5760 об/мин		
4 Расход топлива, кг/ч	250	500	750	250	500	750
5 Радиус воздушной полости, мм	49,75	49,71	49,68	49,9	49,85	49,80
6 Средняя скорость вдоль оси, м/сек	1,1	1,7	2,3	2,4	2,9	3,7
7 Суммарная скорость, м/сек	15,08	15,12	15,20	30,22	30,2	30,32
8 Угол факела	86°	85°	84°	87°	5°	86°
9 Толщина топливной пленки, мк	16,3	32,5	48,5	8,13	6,25	24,3

1) Indices; 2) At 2800 r/min; 3) At 5760 r/min; 4) Fuel throughput, kg/h; 5) Radius of the air cavity, mm; 6) Average velocity along the axis, m/s; 7) Total velocity, m/s; 8) Flame angle; 9) Thickness of the fuel film, μ.

20. BASIC DESIGNS OF PNEUMATIC ATOMIZERS

All pneumatic and steam atomizers are conventionally divided in the technical literature into two groups, depending on the pressure of the atomizing agent: into low-pressure atomizers using air from a blower with a pressure of 300-700 mm water column and high-pressure atomizers with a pressure of 1-6 kg/cm^2. With regard to the design these atomizers differ in the ratio of the diameters of the passage cross sections but with regard to the design principles they can be discussed together. The atomizers are divided with respect to the relative motions of the fuel and air (steam) flow into straight-jet atomizers with parallel flow, counter flow and vortex flow. Depending on the atomization method, one distinguishes single-stage, two-stage and multistage atomizers. To the single-stage atomizers with parallel flow belongs the shukhov atomizer which was widely used in its time (Fig. 96,a). To the same group belongs the low-pressure Rockwell atomizer (see Fig. 96,b) in which the dimensions of the air passages are greatly enlarged in order to achieve a much greater air throughput. In the atomizers of Danilin and Lapinykh [213] and in some others the air (or stream) is supplied through the inner channel and the fuel through the outer (annular) channel (Fig. 97). The variants of the atomizers of this type differ in the shape of the fuel channel and the system of air supply, i.e., a compact jet or via separate orifices, as in the atomizer of Lapinykh (see Fig. 97,b).

The atomizers with parallel flow can have mixing chambers where the collision between the atomizing agent and fuel takes place and the mixture thus formed reaches the furnace through a common nozzle. To increase the velocity of the mixture, the output nozzle is made in the form of a Laval nozzle and if the flame angle must be increased, the output nozzle has several orifices with different angles. In some atomizers, the site of interaction between the two flows is located at a considerable distance from the output nozzle and the process of fuel supply is divided into two stages: the formation of an emulsion and the transport of this emulsion to the combustion zone. A pneumatic Shukhov atomizer is used to form the emulsion by atomization of the fuel in a closed volume in the form of a cylinder.

The combustion process is intensified by supplying a ready fuel-air mixture and is completed earlier than in the case of atomization of the fuel in a straight-jet pneumatic atomizer [214] The emulsion burners have larger conduit cross sections and are not clogged by coke formation. If the emulsion is supplied in a single jet, the furnace volume is not completely filled, hence multinozzle burners have been proposed in which the emulsion is supplied through an annular nozzle (Fig. 98). As tests of such burners have shown, the steam or air consumption is much higher than in the conventional steam or mechanical atomizers and amounts per 1 kg of fuel to 0.76 to 1.3 kg of steam or 0.63-1.63 kg or air.

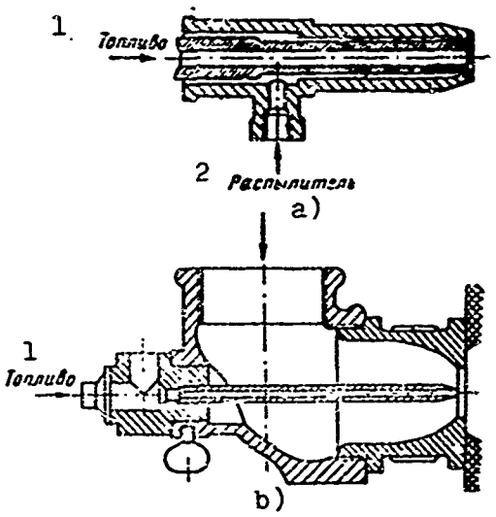

Fig. 96. Atomizer with parallel flow in which the fuel is supplied through a central duct: a) high-pressure (Shukhov); b) low-pressure (Rockwell). 1) Fuel; 2) Atomizer.

Double-stage atomizers have been proposed in order to improve the process of disintegration of the fuel jet, in which the air is supplied twice during the motion of the fuel (Fig. 99). The air first breaks down the compact fuel jet and the primary mixture arrives in an intermediate nozzle and when it emerges from this, another airstream acts on it, producing an additional disintegration of the fuel, an increase in the total velocity of the mixture and improved mixing. In some cases, the primary and secondary air have different parameters. The primary atomization is usually achieved with high-pressure air and the secondary atomization, with air under low pressure. Steam is used instead of primary air in the steam-pneumatic atomizers. Atomizers with multistage air supply have also been developed (three-stage and more). However, with this system of air supply, a marked improvement in atomization may not be attained because as a result of the increased path of the mixture part of the energy is lost in the intermediate nozzles. Furthermore, the probability of collision and coalescence of fuel drops during the motion of the fuel particles through relatively small nozzle cross sections is increased. With respect to the energy required for atomization, the multistage atomizers are less economical than the single-stage design.

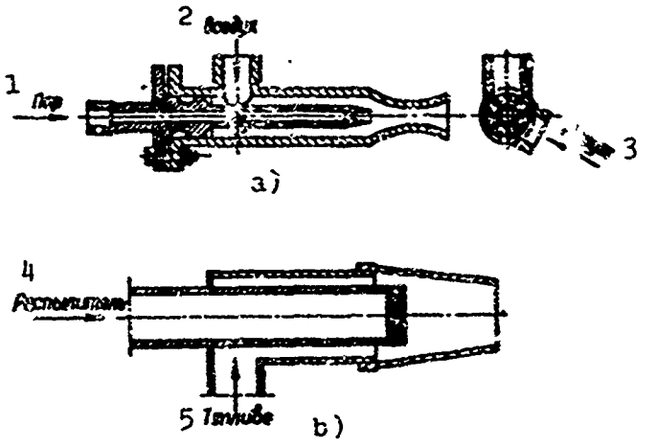

Fig. 97. Atomizers with parallel flow and air supply through a central duct: a) atomizer of Danilin; b) atomizer of Lapinykh. 1) Steam; 2) Air; 3) Petroleum residue; 4) Atomizing agent; 5) Fuel.

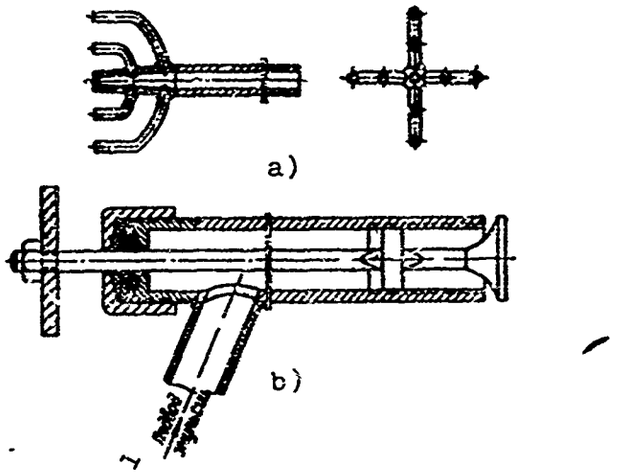

Fig. 98. Emulsion burners: a) single-nozzle; b) with annular nozzle. 1) Supply of emulsion.

In order to improve the conditions of interaction between the fuel and airflow, some designs of pneumatic atomizers provide a mutually perpendicular or even opposed flow. In the simplest case, the fuel is supplied through bores along the periphery of an inner tube with a blind end (Fig. 100). High pressure and low pressure atomizers are built in accordance with this design principle [215]. In the FDM, FDB [216], and some others atomizers, the variation of the impact angle of the air and fuel is achieved by letting the air impinge on the fuel which flows in a central channel along the burner axis from the opposite direction or at right angles.

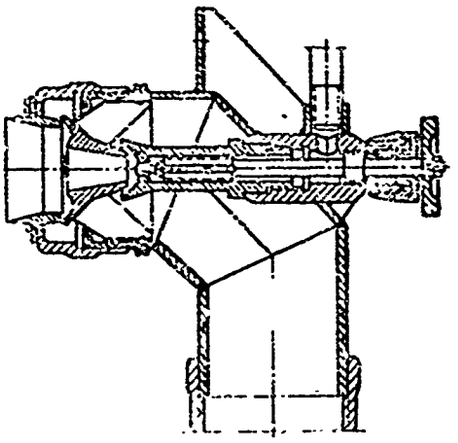

Fig. 99. FDM atomizer with two-stage air supply, developed by the authors.

In order to improve the interaction between the airflow and the fuel jet, vortex flows can be produced, for example, by means of a paddle wheel, worm guides, tangential impact, etc. Among the vortex-type, or, as they are sometimes termed, turbulence atomizers, the atomizers of A. I. Karabin (Fig. 101) are widely used. In these designs, the fuel is supplied via a straight central duct, and a paddle wheel is installed in the path of motion of the air in front of the atomizer outlet. Imparting thus a tangential velocity to the air promotes the atomization of the fuel since the air then not only has a velocity difference along the axis of the jet but also acts tangentially to the jet which gives a more efficient energy transfer.

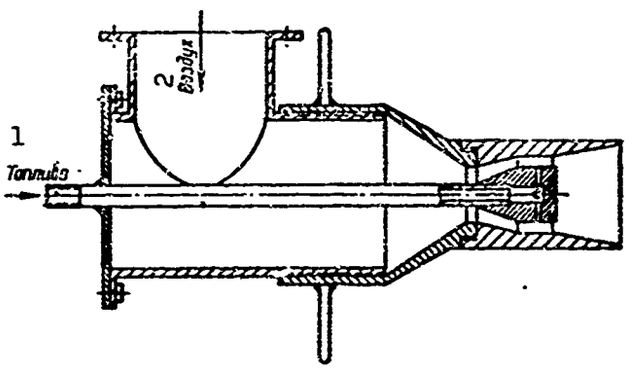

Fig. 100. Atomizer with supply of the fuel at a right angle to the air flow. 1) Fuel; 2) Air.

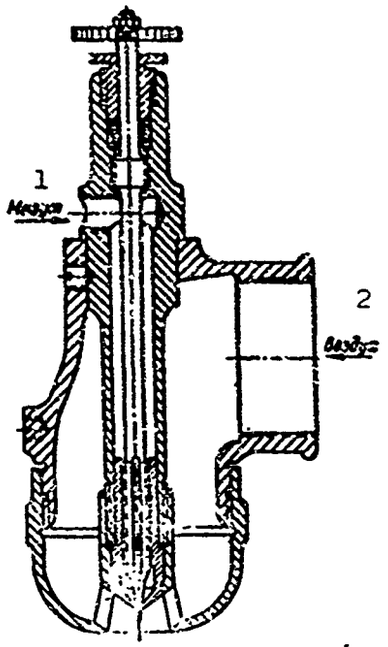

Fig. 101. Atomizer of A. I. Karabin. 1) Fuel; 2) Air.

A further design development of pneumatic atomization were the atomizers with two-way air supply in which the air is supplied to the fuel jet from within and without. This provides a maximum surface contact between the fuel and the atomizing agent. The atomizer installed in the gas turbine locomotive engine of the firm "General Electric" [187] operates in accordance with this principle. The output nozzle of this atomizer (Fig. 102,b) has the form of an annular slit, formed by the body and the rod with disc located in the center. The air is introduced along the rod and the periphery and the fuel arrives in the vortex chamber via six tangential orifices. Based on an analogous principle is the atomizer of Deissler, which consists of three cylinders (see Fig. 102,a) and a cone located at the output end. By this way three annular outlets are formed. The air entering the atomizer is divided into two flows: one passes along a central channel and discharges through the ring formed by the cone and the inner cylinder, the second one passes between the two cylinders (outer and middle). The fuel enters through tangential channels into the cavity between the inner and middle cylinder.

The atomizer of Katin consists of four cylinders (Fig. 103). The atomizing agent is steam which enters on either side of the fuel jet. Moreover, air is supplied through the central (fourth) channel.

As the most perfect atomizer design, which provides the optimum conditions for the energy transfer from the atomizing agent to the fuel, must be considered the atomizer in which two-way supply of atomizing agent and vortex formation in all three fluids is provided. Depending on the degree of vortex formation, such an atomizer can furnish the fuel at any flame angle. The two-way air supply promotes the mixing the increases the atomization efficiency. This atomizer can be designed for high- and low-pressure air.

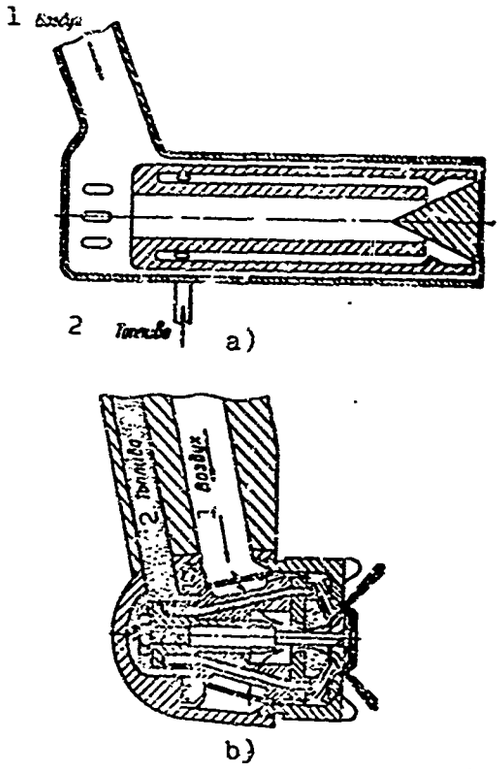

Fig. 102. Atomizer with two-way atomization: a) of Deissler, b) of the firm "General Electric." 1) Air; 2) Fuel.

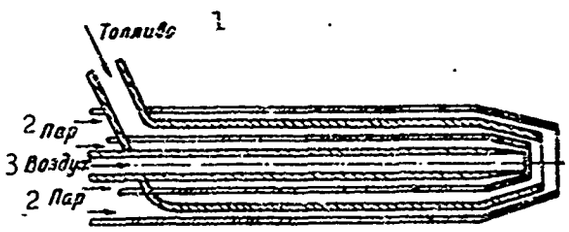

Fig. 103. Atomizer of Katin. 1) Fuel; 2) Steam; 3) Air.

The pneumatic atomizers provide better control possibilities than the mechanical atomizers because the parameters of both flows (fuel and air) affect the shape and dispersion condition of the flame. The air throughput is also usually varied by throttling, by installing a valve or choke in the air duct. Such a control system reduces the air throughput by variation of the output velocity which affects the fineness of dispersion and the flame distance.

In order to produce supercritical flow velocities of the fuel-air mixture, atomizers are equipped with a Laval nozzle. However, this nozzle is suitable only for a certain range of throughputs. An atomizer design has recently been proposed with a variable-cross section nozzle [?17] which has a rectangular profile in one projection and in the other, the shape of a Laval nozzle with movable walls,

which can be moved by means of levers to vary the cross section of the duct within wide limits (Fig. 104). The installation of rotary blades in the Karabin atomizers enables the flame angle to be varied. However, such universal atomizers are complex to make. As a rule, there is no need to regulate the flame with respect to all parameters (throughput, angle, degree of dispersion, range). For the operating conditions of an atomizer in furnaces it is normally sufficient to be able to regulate the fuel consumption at unchanged air throughput and velocity, corresponding to the optimum fineness of atomization of the fuel. Reducing the fuel consumption at unchanged parameters and throughput of the atomizing air (or other atomizing agent) improves the atomization efficiency.

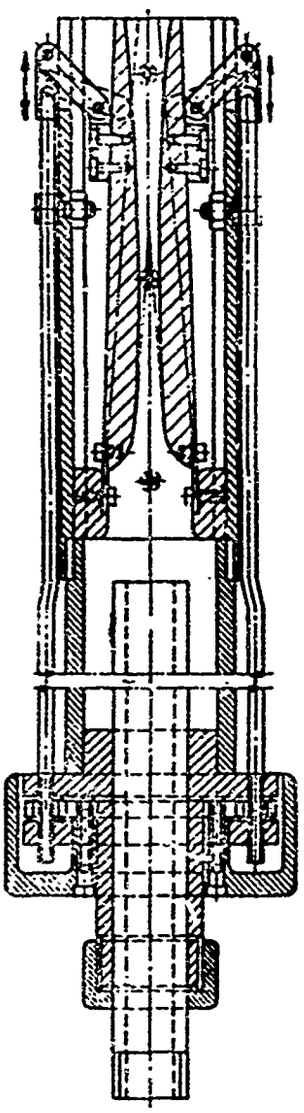

Fig. 104. Atomizer with variable cross section nozzle.

In some designs of pneumatic atomizers the air is necessary not so much for improving the atomization efficiency as for better preparation of the mixture and the creation of a suitable flame shape as is done in many rotating atomizers in which an annular air jet is provided along the periphery of the fuel cone.

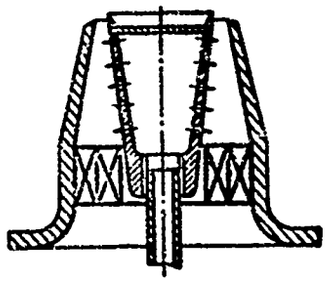

Fig. 105. Rotational atomizer with fuel introduced at right angles to the airstream.

A combination of all possible variants is used in pneumatic atomizer designs, hence it is difficult to classify them on the basis of single characteristics. For example, an atomizer design has been developed [218] in which the centrifugal effect is used by means of rotation of the atomizing cone to achieve a transverse delivery of the fuel and air and, moreover, where guiding vanes impart a vortex motion to the airstream (Fig. 105).

21. THEORY OF THE CALCULATION OF PNEUMATIC ATOMIZERS

The pneumatic atomizers were used for the atomization of fuel even before the mechanical atomizers but the mode of operation of these atomizers has been much less investigated. Whereas there is a rich experimental material available for centrifugal atomizers, various calculation methods exists and different theories have been proposed, only experimental data have been collected for the pneumatic atomizers and some general criterion relations have been proposed. The cause for the lag in the research on pneumatic atomizers is in the more complex physical pattern of the operation of these atomizers where one has to take into account the flow of two fluids with different properties and the interaction of these two flows with each other and the ambient medium.

The calculation of the fuel duct is normally limited to the determination of the output cross section for the maximum throughput. The flow rate of the fuel is determined by the system of fuel supply. If the fuel arrives in the atomizer from the fuel tank by gravity flow, the velocity will be

$$w = \sqrt{2g(H - \Delta H)}, \tag{5.91}$$

where H is the difference between the level of the fuel tank and the atomizer; δH is the pressure loss in the fuel system.

When a fuel pump is used, the velocity is determined as a function of the pressure in the fuel duct

$$w = \sqrt{\frac{2}{\varrho}(p - \Delta p)}. \tag{5.92}$$

The velocity of the fuel in pneumatic atomizers normally does not exceed 4 m/s.

The flow speed of the air for cylindrical and converging nozzles, considering the process as adiabatic when the pressure ratio is greater than critical

$$\frac{p_2}{p_1} > \left(\frac{2}{k+1}\right)^{\frac{k}{k-1}}; \tag{5.93}$$

can be determined by means of the equation

$$w_2 = \sqrt{2g\frac{k}{k-1}\left[1 - \left(\frac{p_2}{p_1}\right)^{\frac{k-1}{k}}\right]p_1 v_1}, \tag{5.94}$$

where p_1 is the absolute pressure before the discharge; p_2 is the absolute pressure in the medium into which the discharge takes place; v_1 is the specific volume of the gas before the discharge; k is the adiabatic index for air (k = 1.4).

In discharge of air, the critical ratio is 0.528, consequently, for high-pressure atomizers the ratio of pressures is usually less than critical, and, for low-pressure atomizers, greater than critical and in the last case

$$w_2 = \sqrt{2g\frac{k}{k-1}p_1 v_1}. \tag{5.95}$$

The theoretical air throughput for each of the flow conditions, respectively, is

$$Q = F\sqrt{2g\frac{k}{k-1}\left[\left(\frac{p_2}{p_1}\right)^{\frac{2}{k}} - \left(\frac{p_2}{p_1}\right)^{\frac{k+1}{k}}\right]p_1 v_1} \tag{5.96}$$

and

$$Q_{кр} = F\sqrt{2g\frac{k}{k-1}\left(\frac{2}{k+1}\right)^{\frac{2}{k-1}}\frac{p_1}{v_1}}. \tag{5.97}$$

In the equations (5.96) and (5.97), the area of the cross section of the air duct is unknown. The ratio of the geometrical dimensions of the air and fuel section, and, consequently, also the area of the air ducts, is determined by the condition of interaction between the air and fuel flow.

Let us examine the working principle of the pneumatic atomizer (see Fig. 97,a) in which the atomizing air is supplied within the fuel jet. Let us assume that up to the moment of interaction both flows have a uniform velocity distribution along the radius. When the air and fuel flow come into contact, the inner layer of the latter is subjected to a dynamic effect of the air flow in consequence of the velocity difference. As a result of this, the boundary layer of the fuel jet acquires additional energy from the air layer and is disintegrated. The fuel-air mixture thus formed exerts an analogous effect on the next layer (see Chapter 3, § 12).

According to the theory of turbulent flow [149], a boundary zone is formed during the interaction between the fuel and air flows, consisting of a fuel-air mixture. This zone is bounded on the outside by a fuel layer and on the inside, by an air layer which has the initial velocity. During their axial movement, the two boundaries form straight divergent lines (Fig. 106,a). We assume that the disintegration of the jet is terminated at the moment of disintegration of the last fuel layer, i.e., when the outer boundaries of the fuel jet and the fuel-air zone intersect. If the diameter of the air jet is very small, then the axial velocity begins to decrease rapidly after the disappearance of the core of the flow with the initial velocity. This reduces considerably the velocity of the layers remote from the axis and, consequently, reduces the interaction between the fuel and air flows. In the case of a very large diameter of the air flow, a core with the initial velocity will remain in its center after the disintegration of the fuel jet. The energy of this core is used only to increase the flight distance of the drops since the disintegration of the jet is already terminated. Hence this energy is superfluous with respect to atomization. The optimum ratio between the diameters of the fuel and air flows is the ratio at which the lines of the boundaries of the fuel-air zone intersect at equal distances from the atomizer nozzle from the outer boundary of the fuel jet and the axis of the flow.

The slope of the outer line of the boundary layer (Fig. 106,a, line 1) can be determined by using the corresponding equations for a gas jet propagating in a liquid [149]. The radius of the outer boundary in the transition section is equal to

$$r = 2.4r_0, \tag{5.98}$$

where r_0 is the initial radius of the air jet.

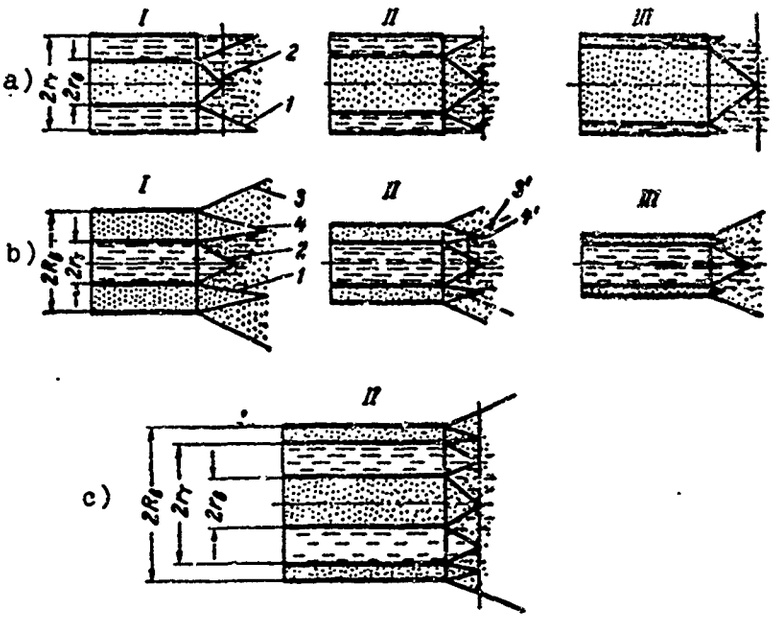

Fig. 106. Schematic representation of the interaction between the fuel and air streams: a) with external delivery of the fuel; b) with internal delivery of the fuel; c) with two-way delivery of the fuel; I) inadequate diameter of the air nozzle; II) optimum; III) too large; 1) outer and 2) inner boundary of fuel-air zone; 3 and 4) outer and inner boundary of the air zone.

The total length of the initial and transition section amounts to

$$x_н = 5r_{0.} \tag{5.99}$$

hence the slope of the outer line is determined as the ratio

$$\frac{r}{x} = 0{,}48. \tag{5.100}$$

The pole distance x_0 can be found by equating $r = r_0$:

$$x_0 = \frac{r_0}{0{,}48}. \tag{5.101}$$

The length of the initial section of the air jet, propagating within the fluid, is equal to

$$x_н = 6{,}5\left(\lg\frac{\alpha_т}{\alpha_0}\right)^{-1} r_{0.} \tag{5.102}$$

In atomization of petroleum residue with air, we have

$$x_n = 2{,}29r_0. \tag{5.103}$$

From (5.103) we find the slope of the line of equal velocity (Fig. 100,a, line 2)

$$\frac{r}{x} = 0{,}4366. \tag{5.104}$$

Using the equations (5.100) and (5.104), we can find the ratio of the radii of the fuel and air section

$$r_т = 2{,}1r_в. \tag{5.105}$$

Knowing the fuel throughput and the area of the fuel duct cross section, we can readily determine the two radii

$$F = \pi(r_т^2 - r_в^2), \tag{5.106}$$

then

$$r_т = 0{,}196\sqrt{F}; \tag{5.107}$$

$$r_в = 0{,}093\sqrt{F}. \tag{5.107,a}$$

The proposed equations can be used for an approximate determination of the atomizer dimensions because the distance at which the atomization process is assumed to be terminated has been somewhat arbitrarily assumed in the calculations.

During the atomization of the fuel in the atomizers of Shukhov, Rockwell and others (see Fig. 96), the airstream acts on the fuel jet from the surface, on the other side the airstream is in contact with the ambient air (see Fig. 106,b) and imparts to it part of its energy which can be considered as loss (because it does not contribute to the atomization of the jet).

The boundary region of the fuel-air and the homogeneous air jet is limited by the zero velocity lines and the core of the stream. We assume that the disintegration of the fuel is terminated in the initial section when the core of the flow disappears, i.e., when the whole fuel jet has been diffused by the air.

The line which limits the core of the flow for a two-phase jet during the atomization of liquid [149], can be found from the relation for flat jets

$$\frac{r}{\tau} = 0{,}31 \lg \frac{Q_r}{Q_n}. \qquad (5.108)$$

In atomization of petroleum residue with air, this relation is

$$\frac{r}{x} = 0{,}88. \qquad (5.109)$$

For the outer boundary we take the same slope as for the case of introduction of the air within the fuel (5.104). The boundary zone on the side of the ambient air lies between the straight lines (Fig. 106,b, line 3 and 4) of the internal boundary

$$\frac{R}{x} = 1{,}49a \qquad (5.110)$$

and the outer one

$$\frac{R}{x} = 3{,}4a, \qquad (5.111)$$

where a is a coefficient which characterizes the structure of the airflow.

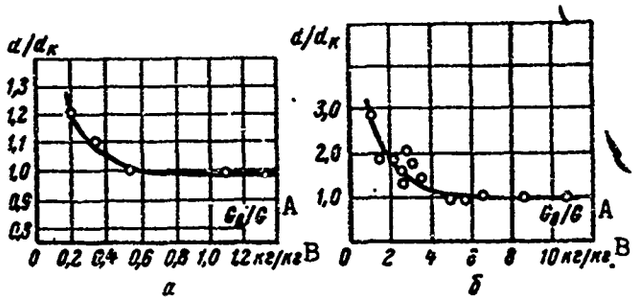

Fig. 107. Fineness of dispersion as a function of the specific air consumption. d_k drop diameter corresponding to optimum air consumption: a) according to [18]; b) according to [141]. A) G_v/g; B) kg/kg.

With increase in the ratio of the airstream diameter to the diameter of the fuel jet and, consequently, increase in the specific air consumption, the condition for energy transfer and fineness of dispersion improve. This is due to the fact that the deceleration of the jet as a result of the energy exchange with the ambient air has less effect on the transfer of energy to the fuel. However, once a complete disintegration of the fuel jet is attained, further increase in the mass of air has practically no effect on the atomization, merely increasing the flight distance of the drops. This assumption is confirmed by experiment (Fig. 107). The improvement of the atomization with increase in air throughput takes place up to a certain ratio and further increase in the air throughput does not affect the atomization efficiency.

By means of this diagram (see Fig. 106,b) it is possible to find the optimum ratio of the air and fuel jets. In this case the point of intersection of the line of the lower limit of the air boundary layer and the upper limit of the fuel-air layer should lie in an intermediate section (at the end of the initial section). Using Eqs. (5.104), (5.109) and (5.110), it is easy to show that this condition is met by a ratio of the radius of the air and fuel jet, determined by the equation

$$R_в = (1{,}5 + 1{,}7\,a)\,r_т. \tag{5.112}$$

According to experimental data obtained in studies of air jets, the coefficient a varies from 0.066 to 0.076. Using the average 0.07, we find $R_в = 1.61r_т$. In practice, the ratio $R_в/r_т$ varies within the range of 1.5 to 15 [18], increasing with decreasing pressure (velocity). In order to improve the interaction between the air and fuel flows, the air output sections are made in such a way that the airstream hits the fuel under a certain angle instead of being parallel to it. Furthermore, to reduce the air throughput and the unavoidable losses, due to the interaction with the ambient air, the fuel nozzle is slightly recessed so that it is inside the atomizer (see Fig. 106,b, lines 3 and 4).

If one examines the diagrams of the interaction between the air and the fuel jet (see Fig. 106) it can be seen that only part of the energy of the air is imparted to the fuel. In the simplest case, with delivery of the fuel and air in parallel directions, the equations derived on the basis of the theory of turbulent flow can be used to calculate the energy lost in atomization. Let us divide the fuel-air flow into several elementary rings. For each annular cross section with radius r and thickness dr, the kinetic energy of the flow can be calculated by means of the equation

$$dE = \frac{w^2\,dm}{2}, \tag{5.113}$$

where w is the velocity of the flow at a given point; dm the mass element of the moving flow passing through the chosen cross section

$$dm = 2\pi\rho w r\,dr. \tag{5.114}$$

Several relations have been proposed for characterizing the velocity variation in the boundary layer, of which the following gives the best agreement with the experimental data

$$\frac{w}{w_0} = F'(\varphi), \tag{5.115}$$

where w_0 is the initial flow velocity; ϕ a dimensionless radius

$$\varphi = \frac{r}{ax}, \tag{5.116}$$

where a is a coefficient to characterize the structure of the flow; r the distance from the axis of the flow; x the distance along the axis.

The function $F'(\phi)$ does not have a simple analytical expression and for this reason, tables have been compiled [149] for solving problems in which Eq. (5.115) is used. For a first approximation, we can use the simpler analytical relation of the form

$$\frac{w}{w_0} = (1 - \bar{r}^{1.5})^2, \tag{5.117}$$

$$\bar{r} = \frac{r}{r_x}, \tag{5.118}$$

where r is the distance from the jet axis; r_x, the radius of the jet in the cross section under consideration.

Having solved Eqs. (5.113), (5.114), (5.117) and (5.118), we obtain an analytical expression for the variation of the energy of the air boundary layer as a function of $\bar{r}$

$$E_в = \pi \rho_в w_0^3 r_x^{-3} \int_{r_k}^{r_1} (r_x^{1.5} - r^{1.5})^4 r\,dr. \tag{5.119}$$

The limits of integration of this equation, according to the condition of interaction of the flows at optimum ratio of the dimensions, will be: $r_1 = 1.9r_0$, and $r_2 = 1.5r_0$.

After solving Eq. (5.119), taking into account that $r_k = r_1$, we find

$$E_в = 8.08 \cdot 10^{-5} \pi \rho_в w_0^3 r_0^2. \tag{5.119,a}$$

The equation for determining the velocity profile in the zone of the fuel-air boundary layer will have the form

$$\frac{w}{w_0} = 1 - (1 - \bar{r}^{1.5})^2 = 2\bar{r}^{1.5} - \bar{r}^3. \tag{5.120}$$

The variation of the concentration of air and fuel in the fuel-air jet can be expressed by the equations

$$q_в = \bar{r}^{1.5}; \tag{5.121}$$

$$q_т = 1 - \bar{r}^{1.5}. \tag{5.122}$$

The variation of the density of the mixture over the jet cross section as a function of the concentration is characterized by the relation

$$\rho_{см} = \frac{\rho_в \rho_т}{\rho_т q_в + \rho_в (1 - q_в)}. \qquad (5.123)$$

Having solved Eqs. (5.113), (5.114), (5.120), and (5.123), we find the variation of the energy along the radius of the fuel-air zone

$$E_р = \pi \rho_в \omega_0^3 \int \frac{\rho_т (2\bar{r}^{1,5} - \bar{r}^3)^3}{\bar{r}^{1,5}\rho_т + (1 - \bar{r}^{1,5})\rho_в} r\,dr. \qquad (5.124)$$

The ratio ρ_v/ρ_t for the conditions of air atomization of fuels is of the order of 0.0014, and $(1 - \bar{r}^{1.5}) < 1$, hence the second term in the denominator can be neglected and Eq. (5.124) written in the form

$$E_р = \pi \rho_в \omega_0^3 r_x^{-7,5} \int_{r_1}^{r_2} (2r_x^{1,5} - r^{1,5})^3 r^4\,dr. \qquad (5.125)$$

Integrating Eq. (5.125) within the limits of variation of the radius of the fuel-air zone (from $r_1 = 0$ to $r_2 = 1.5r_0$), we obtain the total energy of the fuel-air mixture

$$E_р = 1{,}44\pi\rho_в \omega_0^3 r_0^2. \qquad (5.126)$$

In order to determine the energy transferred to the fuel, the right part of Eq. (5.125) must be multiplied with q_t (5.122), and then the integral taken in the limits $r_1 = 0$ to $r_2 = 1.5r_0$. As a result, we find the energy of the fuel, equal to

$$E_т = 0{,}97\pi\rho_в \omega_0^3 r_0^2, \qquad (5.127)$$

and the energy of the air

$$E_{в.з} = 0{,}47\pi\rho_в \omega_0^3 r_0^2. \qquad (5.128)$$

From the energy calculations (5.126), (5.127) and (5.128) it is possible to derive the utilization factor of the energy of the air for atomization as the ratio of the expended energy to the energy transferred to the fuel jet:

$$\beta = \frac{E_т}{E_в + E_{в.з} + E_т}. \qquad (5.129)$$

This value β is an optimum when the boundary line of the fuel-air zone corresponds to the diagram (see Fig. 106,b,II). With greater diameter of the air flow (see Fig. 106,b,III), the integration of Eq. (5.119) must be carried out within the range of variation of r from $r_2 = R_v + 0.27r_0$ to $r_1 = R_v - 0.12r_0$, and the denominator of the expression (5.129) must be increased by the energy of the core of the flow

$$E_z = \pi w_{0Q_z}^3 (R_z^2 - 2{,}59r_0^2). \tag{5.130}$$

which in this case will characterize the energy not expended in atomization and, in this sense, wasted. This air flow will affect the flight distance of the drops and the ratio of the mixture components, increasing the air content.

For nozzles with central air supply, the equation for the energy of the fuel is written thus

$$E_т = \pi Q_т w_0^3 r_x^{-9} \int_0^{r_2} (r_x^{1,5} - r^{1,5})^6 r^{1,5} dr, \tag{5.131}$$

for the air

$$E_в = \pi Q_в w_0^3 r_x^{-9} \int_0^{r_2} (r_x^{1,5} - r^{1,5})^6 r\, dr, \tag{5.132}$$

hence

$$\beta = \frac{E_т}{E_т + E_в}. \tag{5.133}$$

If the radius of the air flow is increased beyond the optimum, the denominator of the expression (5.133) is increased by

$$E_z = \pi Q_в w_0^3 (r_z^2 - 0{,}23r_т^2). \tag{5.134}$$

The above-presented method of calculating the two systems of pneumatic atomizers can be used for an approximate determination of the dimensions of the fuel and air cross section. The coefficient β enables the estimation of the atomizer efficiency with regard to the energy losses.

Examination of these two basic atomizer designs shows that the atomization efficiency can be improved within limits by increasing the specific air throughput. Hence, when the atomization must be further improved, the velocity of the air must be increased which can be achieved by a suitable increase in the parameters of the atomizing air. Another method of improving the atomization efficiency without altering the parameters of the air consists in increasing the surface

of interaction between the fuel and air flow. This method is realized, for example, in the atomizers with two-way air supply (within and outside the fuel jet). To determine the optimum ratios of the three cross sections (two for air and one for fuel), we assume that this corresponds to the condition of intersection of the lines of the boundary zones formed by the external and internal action of the air in one cross section (see Fig. 106,c).

Using the equation for the determination of the size of the output cross sections in the case of internal and external air supply (see Fig. 102 and 106,c), we determine the ratio of the dimensions of the three cross sections for the case of two-way air supply

$$r_v = 4{,}11 r_t, \tag{5.135}$$

$$R_v = 5{,}4 r_t, \tag{5.136}$$

where r_v and R_v, respectively, are the radius of the cross section of the inner and outer airflow; r_t is the outer radius of the fuel cross section.

The energy of the air and fuel flows at the end of the initial section has the following values:

$$E_t = 7{,}3\pi\varrho_a w_0^2 r_0^2 \tag{5.137}$$

$$E_a = 3{,}5\pi\varrho_a w_0^2 r_0^2 \tag{5.138}$$

$$\beta \simeq 0{,}7. \tag{5.139}$$

When the air is supplied under high pressure, it is not necessary in most cases to realize the maximum ratio of the throughput since the atomization efficiency depends more on the velocity than on the throughput. This is evident from the energy equation in which the velocity is present in the second and the throughput in the first power.

To estimate the fineness of dispersion of the fuel only as a function of the relative velocity, as is frequently proposed in the literature [18], is possible for atomizers in which the air throughput is considerable. The low-pressure atomizers usually operate with high throughput (above the optimum) and the throughput need not be contained in the formulas for the determination of the atomization efficiency. For all atomizers it is more correct to characterize the atomization by the specific energy, making allowance for the utilization factor.

The investigations carried out by the authors have shown that the dependence of the fineness of dispersion on the air velocity at different specific air throughputs is not uniform (Fig. 108). In these studies, the fuel throughput varied in accordance with the operating conditions of the furnace. If one plots a graph of the variation of the average drop size as a function of the specific

energy of the atomizing agent, the atomization efficiency is defined by a single curve for all operating conditions (Fig. 109). Hence, it is more correct to use in the equations for the calculation of the atomization efficiency the energy and not the velocity, and the equation then assumes the form

$$d_k = \frac{B}{e^5}. \qquad (5.140)$$

According to our experiments and those of several other investigators, the power exponent varies within the limits of 1.1 to 0.4.

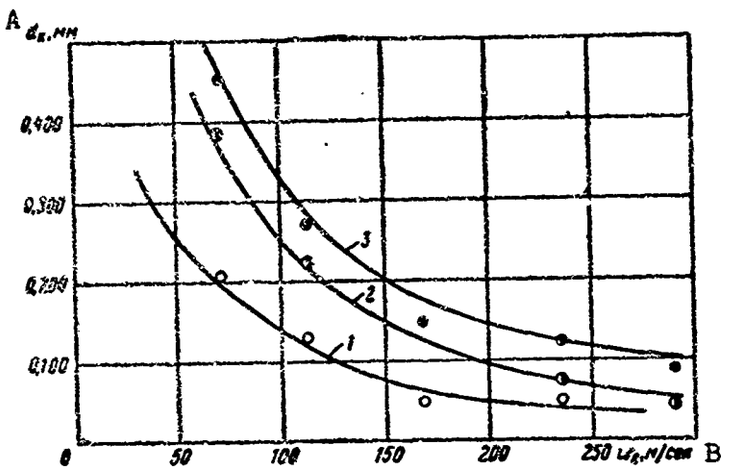

Fig. 108. Average (median) drop diameter as a function of the velocity of the air at the fuel throughput: 1) 74 kg/h; 2) 135 kg/h; 3) 205 kg/h. A) d_k, mm; B) w_v, m/s.

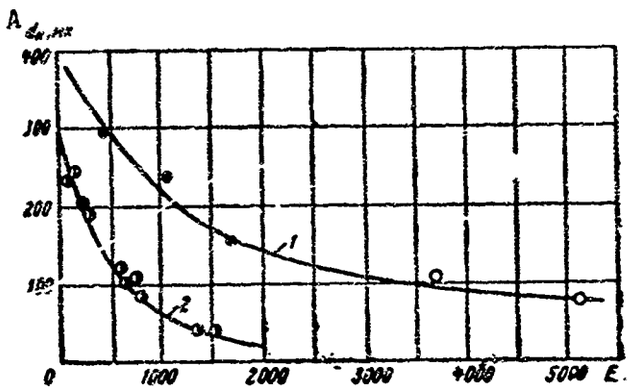

Fig. 109. Average (median) drop diameter as a function of the specific energy of the atomizing agent: 1) for atomizers with parallel flow; 2) for atomizers with transverse air supply. A) d_k, μ.

A comparison of the pneumatic atomizer designs leads to the conclusion that the improvement of the atomization process is achieved mainly by bringing about a closer interaction between the atomizing air and the fuel jet, i.e., by improving the process of energy transfer. Obviously, the more energy of the atomizing air or steam is transferred to the fuel jet, the better is the atomizer design and the required atomization efficiency can be attained with less expenditure of energy. Comparison of two atomizers with regard to the specific energy consumption showed that the atomization efficiency is considerably higher in the case of transverse supply of the fuel and airstream (see Fig. 109,2).

Tests of low-pressure atomizers, carried out by the authors under industrial conditions, enabled the following values of the utilization factor of the energy of the air for the atomization to be obtained: for straight-jet FOOM atomizers, 0.18-0.25; for opposed-flow FDM atomizers 0.35-0.40, and FDB 0.40-0.43; and for the turbulent atomizers of Karabin 0.55-0.66 [217].

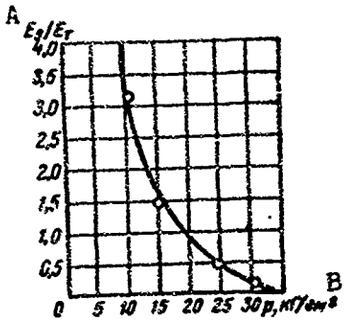

Fig. 110. Variation of the ratio of the energies of the atomizing air and fuel as a function of the fuel pressure for double-circuit atomizers with single output nozzle, operated in accordance with the principle of pneumatic atomization. A) E_v/E_t; B) p, kgf/cm^2.

It is essential to establish the boundaries of these principles of atomization in the atomizers operating at small throughputs like the pneumatic, and large throughputs like the mechanical atomizers. This can be determined on the basis of the ratio of the energies of the fuel and air flow. For example, to improve the atomization efficiency at low throughputs in an atomizer (see Fig. 78,b) investigated at the TsNII MPS, air was supplied to the second stage under a constant pressure of 5 kgf/cm^2. With increasing fuel throughput, the effect of the atomizing air decreases in consequence of the increasing pressure and energy of the fuel jet as well as a result of the decrease in the pressure drop of the air caused by the increased counter pressure of the fuel. The variation of the ratio of the energies of the air and fuel as a function of the throughput (pressure) of the fuel is given in Fig. 110. As follows from this relation, at fuel pressures above 20 kgf/cm^2 the kinetic energy of the air practically has no effect on the fineness of dispersion. The experimental results (Fig. 111) showed that the difference in the fineness of dispersion with and without supply of air at a fuel pressure of 20 kgf/cm^2 is within the limits of measurement error.

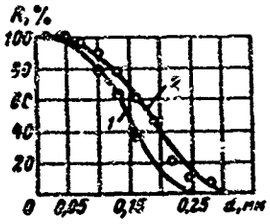

Fig. 111. Drop size distribution at the fuel pressures: 1) with air supply; 2) without air.

In atomization with air one has also to allow for the cooling of the air as a result of the expansion which has a double effect. On the one hand, the temperature of the petroleum residue is lowered and the viscosity increased which results in less efficienct atomization. On the other hand, the density of the air is increased which promotes the energy transfer to the fuel jet. The lowering of the fuel and air temperature increases the preheating time of the drops and their time of preparation for combustion.

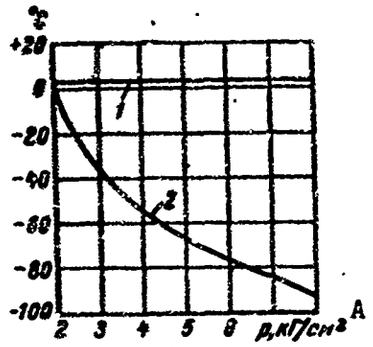

Fig. 112. Variation of the teperature of the atomizing air at critical 1, and supercritical 2 flow velocity. A) p, kgf/cm^2.

For adiabatic expansion of the air, the cooling can be calculated by means of the equation

$$\frac{T_2}{T_1} = \left(\frac{p_2}{p_1}\right)^{\frac{k-1}{k}}. \qquad (5.141)$$

In the case of critical pressure in outflow through a converging nozzle, the ratio of the absolute temperatures is 0.86, whereas for supercritical velocities the cooling is more intense (Fig. 112).

In order to reduce the negative effect of cooling, the air or fuel should be preheated to compensate for the temperature drop during expansion.

22. NEW ATOMIZATION METHODS AND ATOMIZER DESIGNS

In most industrial atomizers, the potential pressure energy of the fuel or the kinetic energy of air or steam are used for the atomization. However, as has been shown in Chapter 3, only a very small proportion of the pressure energy in the form of the energy of turbulent pulsations, wave fluctuations, aerodynamic resistance and cavitation is used for the disintegration of the fuel jet. One of the first attempts to intensify the wave fluctuations was made in diesel atomizers by means of so-called interrupted flow consisting in dividing a fuel injection cycle into a system of separate briefer squirts [219]. This idea was also used in continuous atomizers in which the injection of the fuel in brief successive squirts gave a better atomization. The improvement in the atomization by fractional injection is due to the sudden (shock) velocity increase which causes additional wave oscillations. This type of flow can be achieved by installing two throttle cross sections one of which is varied by means of a spring-operated valve. This design causes auto-oscillations in the hydromechanical system consisting of a pump, hydraulic accumulator and atomizer. The oscillation frequency in such atomizers attains 200-1000 Hz.

Experiments were made in the Soviet Union and elsewhere to superpose artificial oscillations on the fuel jet by means of a mechanical pulsator inserted into the fuel injection system, which also improved the atomization of the fuel.

The effect of ultrasonic vibrations causes a more intense disintegration of the liquid. This process has been described in a work [220] carried out as far back as 1932.

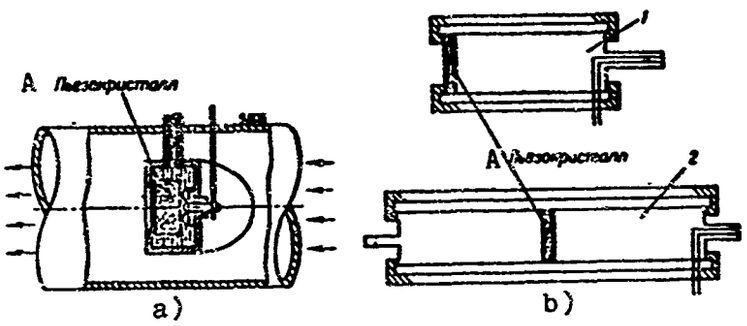

Fig. 113. Ultrasonic atomizer with piezoelectric vibration generator: a) for carburetor engines; b) schematic view of continuous atomizer with single (1) and double (2) resonator. A) piezocrystal.

For the automization of fuel with ultrasound, ultrasonic converters are used (piezoceramic and magnetostriction) with electrical generators and also hydro- and aerodynamic emitters. The fuel is subjected to ultrasonic vibrations by letting it impinge directly on the emitting surface of the converter [221] or via an intermediate part [222]. A fuel atomizer for carburetor engines (Fig. 113,a) based on the first principle has been proposed. The fuel impinging on the emitting surface of the vibrator is instantly transformed into fine

drops which mix with the airstream. An atomizer for any type of installation can be built on the basis of this principle.

The fineness of dispersion depends on the fuel throughput and the amplitude and frequency of the vibrations. The vibration amplitude of the piezocrystal itself is very small and is intensified by means of the resonating part with nozzle for atomization. The length of the resonators should be a multiple of 1/4 of the wavelength at the resonance frequency of the vibrations (see Fig. 113, b). Atomizers with piezoceramic converters have been made with throughputs of up to 6 liters/h. If the energy is increased to generate vibrations with higher energy, heating and disintegration of the piezoceramic occurs. According to a report [222], a burner with piezoelectric ultrasonic atomizer gave 5000 hours of continuous service in a furnace.

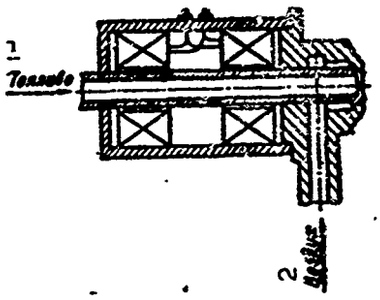

Fig. 114. Ultrasonic atomizer with magnetostriction vibration generator. 1) Fuel; 2) Air.

The use of magnetostriction converters for the atomization of fuel [223] was realized in an atomizer design (Fig. 114) which had a fuel pipe made of a ferromagnetic material giving a magnetostriction effect. Two electromagnetic coils were mounted on the tube, and supplied with an alternating voltage of high frequency. At certain frequencies, the magnetic flux in the ferromagnetic material causes a magnetostriction effect and every magnetic excitation pulse compresses or tensions the fuel tube. Since one end of the tube is fixed, the other, in consequence of the repeated extensions and compressions vibrates mechanically in the longitudinal direction. The frequency of the magnetic flux should be equal to the resonance frequency of the tube or its harmonic. A node forms at the point of attachment; in order to obtain maximum vibration of the free end, the length of the tube should be 1/4, 3/4 or 5/4, etc.. of the wavelength corresponding to the resonance frequency of the vibrations. The vibration of the tube promotes the development of wave perturbations in the fuel jet and leads to cavitation at certain frequencies.

The air flowing past outside the fuel tube is also subjected to the vibration effect which promotes the mixture formation and combustion. By varying the frequency and energy of the vibrations which can be done by corresponding variation of the parameters of the electric current supplied to the coils it is possible to control the fineness of atomization in a burner of this type.

The use of piezoceramic or magnetostriction converters in atomizers requires special generators of electric oscillations. Hydrodynamic sound emitters have recently been developed and have been widely used. Vortex and rotational sound sources and also emitters with plate or rod resonance vibration devices are used in the Soviet Union in many branches of industry. The acoustic atomizer [224] does not differ in principle from the centrifugal two-stage atomizer with single output nozzle (Fig. 115,a). Suitable choice of the geometrical dimensions ensured the production of vibrations with a frequency of 4-7 kHz and fine dispersion of the fuel. The pressure of the air and fuel in this atomizer was 6 kgf/cm^2. A study of an acoustic atomizer with sound generator made in the form of a hollow rod with a wedge slit (Fig. 115,b) showed that the atomization efficiency is better at low air throughputs (5% of the fuel throughput). At an air pressure of 1 kgf/cm^2, the average drop diameter was 92 μ, and at a pressure of 4 kgf/cm^2, 87 μ [225]. The fuel enters the atomizer and is delivered to the combustion zone in the form of a film through an annular gap.

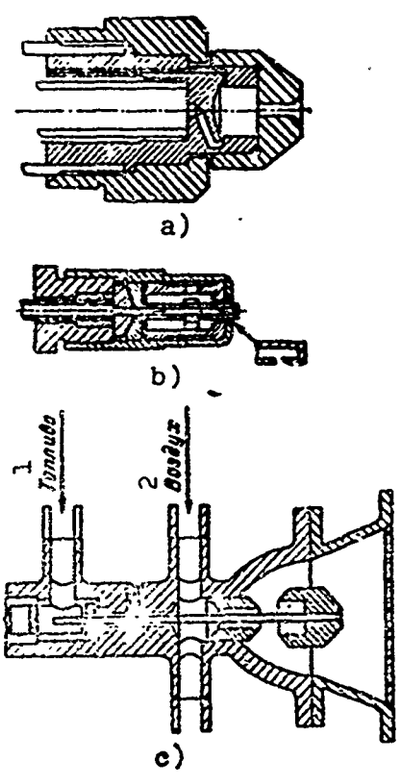

Fig. 115. Ultrasonic atomizer with acoustic emitter: a) of the vortex type; b) with vibrating rod; c) with resonance plate. 1) Fuel; 2) Air.

Another variant of acoustic atomizer (see Fig. 115,c) incorporates a vibrating device in the form of a resonator which is connected with a rod through which the fuel is injected. Air with a pressure of 2.8 kgf/cm^2 which flows along the tube, forms vortices when it impinges on the resonator, thus producing vibrations with a frequency of 6.5 kHz. The intensity of the ultrasonic vibrations in the acoustic atomizers depends on the flow velocity of the air and the counter pressure of the medium. Tests with an ultrasonic whistle, carried out at the TsNII MPS in collaboration with NIIkhimmash, showed that the dependence of the intensity of the ultrasonic vibrations on the velocity of the air has a maximum which is shifted in the direction of higher velocities by increase in the counterpressure. The vibration intensity corresponding to the maximum then increases markedly. Consequently, better atomization conditions can be achieved by the use of ultrasonic atomizers with such emitters in furnaces operated under pressure.

It was observed during atomization of fuels that the drops acquire an electric charge [228]. A fuel drop with an electric charge is subjected to the action of forces opposed to the forces of surface tension. If these forces exceed the surface tension forces, a disintegration of the drop takes place.

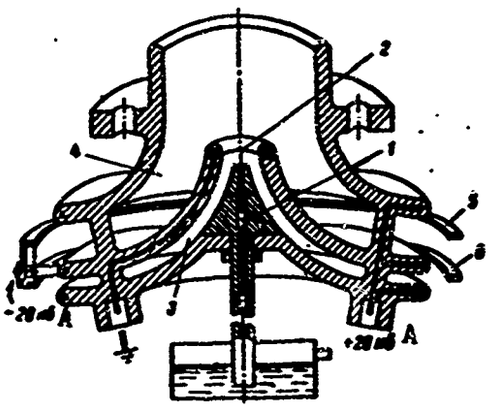

Fig. 116. Burner with electrical atomization. A) kV.

Tests made with different liquids showed that the fineness of dispersion at equal strength of the electric field [229] produced by a ring electrode with a voltage of 1400 V, depends on the ratio of the dipole moment to the surface tension coefficient. During atomization of curde oil by the electrical method, drops with a diameter of 50 to 200 μ were produced. In a burner with electrostatic atomization [230], the air and fuel are ionized by means of an electric field and are accelerated to the required velocity. The fuel throughput in such a burner (Fig. 116) amounted to 10 kg/h, and the air consumption to 200 m^3/h. The fuel arriving through the central tube 1 together with the air, the ionized molecules of which are accelerated in the electric field, is directed through the annular gap 2. The ring 3, together with the fuel nozzle, forms a pair of zone electrodes. Secondary air enters through the two sections 3 and

4, having first passed the spark electrodes 5 and 6. Owing to the high field density at the spark electrodes (10^7 V/cm), the air molecules are set into motion and the air issues from the annular channels 3 and 4 with a velocity of up to 20 m/s.

23. HYDRAULIC CALCULATION OF THE DEFLECTORS

Intense vortex formation in the air delivered to the heating space is currently the main method of achieving a practical application of the principle of vortex combustion of liquid fuel. Among the numerous inlet devices to achieve vortex formation in the flow, the blade deflectors have found the most widespread application (cylindrical, conical, semiconical, with straight and profile blades, with constant and varying cross section, etc.) The most widely used blade deflectors are flat cylindrical deflectors with straight and profile blades (Fig. 117). Upon emerging from the deflector, the airstream has a rotational-translational motion and, forms a divergent jet as it enters the strongly enlarged furnace volume. In the furnace volume, a hollow hyperboloid of rotation is created, on the outer and inner surfaces of which annular vortices are formed which give rise to counter current zones. The internal circulation zone formed in the region of the high temperature combustion products, transfers heat to the root of the flame, thus achieving continuous ignition of the fuel flame. The annular vortex arising on the outer surface of the rotating jet can play a double part, depending on external conditions. If the furnace volume accommodates several burners, the zones of the counter currents at the outer surface of each jet arise in the region of the hot combustion products of the adjacent jets, in consequence of which an additional quantity of heat is supplied to the root of the flame, which helps to ignite the fuel and to stabilize the combustion zone. In a furnace with a single inlet device, the external circulation zone may be the source of supply of large masses of relatively cold air to the root of the flame and thus may have a negative effect on the development of the ignition process. Furthermore, the external countercurrent zone is very frequently the cause of the removal of relatively small fuel drops from the flame and their deposition on the inlet device.

The cylindrical blade deflector is characterized by two basic design quantities which determine its aerodynamic properties: the blade angle and the sleeve ratio. The sleeve ratio determines in first approximation the air throughput through the deflector (at a given pressure) and the blade angle the degree of vorticity of the airflow and the size of the reverse currents.

The air throughput through the blade deflector is calculated by means of the equation

$$G_в = F_3 \mu_3 \sqrt{2g\gamma \Delta p}, \qquad (5.142)$$

where F_3 is the area of the aperture cross section of the deflector; μ_3 is the throughput coefficient; Δp is the pressure drop in the deflector.

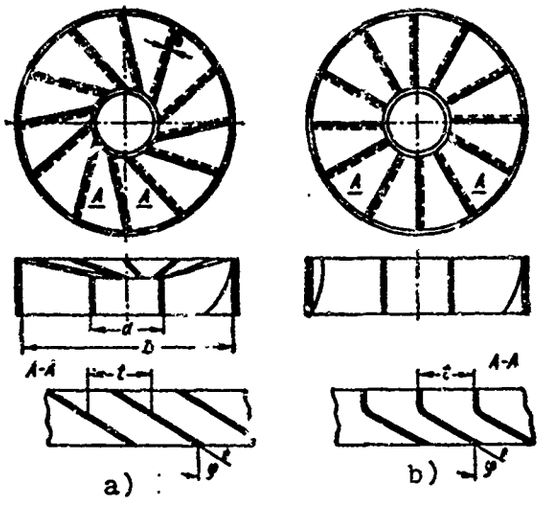

Fig. 117. Cylindrical blade deflector: a) with straight blades; b) with profile blades.

For a deflector with straight blades, the quantity F_3 is calculated as

$$F_3 = \frac{\pi \cos \varphi}{4}(D^2 - d^2) - \frac{D-d}{2} n\delta, \qquad (5.142a)$$

where D and d are, respectively, the outer and inner diameter of the deflector; n, δ, respectively, the number and thickness of the blades; φ, the blade angle.

The internal diameter d of the deflector is normally determined by the diameter of the atomizer. The number of blades and their thickness, as a rule, are fairly constant for the most diverse deflector designs. The second term of Eq. (5.142,a) can generally be neglected since it is considerably smaller than the first term.

The dependence of the throughput coefficient on the resistance coefficient [231] can be used for approximate calculations:

$$\mu_3 = \frac{1}{1+\sqrt{\varepsilon}}. \qquad (5.143)$$

The resistance coefficient ε is connected with the pressure drop Δp in the deflector by a relation of the form

$$\Delta p = (1+\varepsilon)\gamma \frac{w^2}{2g}, \qquad (5.144)$$

where γ and w, respectively, are the specific gravity and velocity of the airflow in front of the deflector.

Substituting (5.143) and (5.144) into the initial throughput equation, we obtain after some simple transformations

$$G_в = F_3 \gamma w \frac{\sqrt{1+\varepsilon}}{1+\sqrt{\varepsilon}} = \frac{\pi \cos\varphi}{4}(D^2 - d^2)\gamma w \frac{\sqrt{1+\varepsilon}}{1+\sqrt{\varepsilon}}. \qquad (5.145)$$

In most cases, the diameter of the air supply duct is equal to the outer diameter of the deflector so that the velocity of the inflowing airstream can be determined by means of the equation

$$w = \frac{4G_в}{\pi D^2 \gamma}. \qquad (5.146)$$

After substitution of (5.146) into (5.145), we find

$$1 = \cos\varphi\left(1 - \frac{d^2}{D^2}\right)\frac{\sqrt{1+\varepsilon}}{1+\sqrt{\varepsilon}}. \qquad (5.147)$$

The resistance coefficient ε is not an independent variable but is determined by the combination of the blade angles and the sleeve ratio. To find ε, let us consider the energy losses in the deflector which can be divided into the following:

1) the shock losses at the entry in consequence of the sudden decrease of the cross section in the channel between the blades;

2) the friction losses at the side surfaces of the blades;

3) the energy losses due to the change in the direction of flow and the appearance of vortex zones in the channels between the blades;

4) the shock losses due to the sudden increase in cross section at the outlet from the deflector.

Assuming that the energy losses during the entry of the flow into the deflector and during its exit are the same, we can write the resistance coefficient in the form

$$\varepsilon = \varepsilon_т + \varepsilon_п + 2\varepsilon_{вх}. \qquad (5.148)$$

For a deflector with straight blades, the resistance coefficient $\varepsilon_т$, based on the geometrical relations, is determined as

$$\varepsilon_т = \lambda \frac{n}{\cos\varphi} \frac{4[n\cos\varphi(D+d) - 2\delta n + (D-d)n]}{\pi(D^2-d^2)\cos\varphi - \frac{D-d}{2}n\delta}. \qquad (5.149)$$

The friction coefficient λ during the motion of a fluid in channels with square cross section in its turn is a function of the parameter Re and for turbulent flow within the range of Reynold numbers from 3000 to 100,000 is determined by means of the equation

$$\lambda = \frac{0.3164}{Re^{0.25}}. \qquad (5.149,a)$$

According to the recommendations [232], λ for pure sheet metal can be assumed to be constant and equal to $\lambda = 0.008$ for approximate calculations. The resistance coefficient during rapid variation of the passage cross section of a channel is a function of the ratio of the maximum cross sectional area to the area in the narrowest part of the deflector and is calculated by means of the formula

$$\varepsilon_n = \left(0{,}707\sqrt{1-\frac{F}{F_1}}+1-\frac{F}{F_2}\right)^2, \qquad (5.150)$$

where F_1, F_2 are the areas of the passage cross sections in front of land behind the deflector, respectively; F is the minimum cross section of the deflector.

The resistance coefficient for flow reversal is usually given in the manuals [235] as a function of the curvature of the channel.

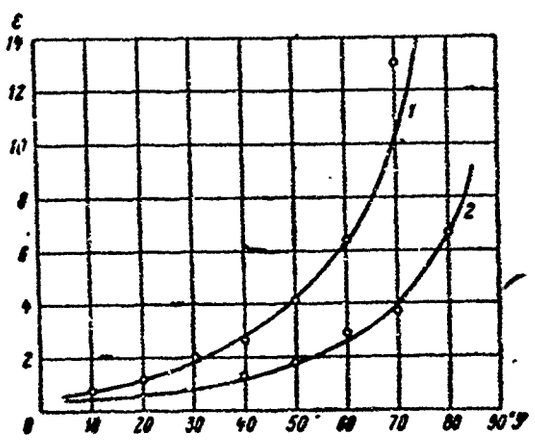

Fig. 118. Total resistance coefficient ε of a blade deflector with straight 1 and profile 2 blades as a function of the blade angle ϕ.

To simplify the calculations, one normally uses the experimental values of the total resistance coefficient ε, obtained for some deflector designs and published, for example, in [232]. In particular, the authors did some work to determine the characteristics of cylindrical deflectors with straight and profile blades, the results of which are presented in Fig. 118. It can be inferred from Fig. 118 that the total resistance coefficient of a blade deflector increases markedly with increase in the blade angle. The installation of profile (curved) blades greatly improves the entry conditions into the deflector for the airstream, in consequence of which the hydraulic losses are greatly reduced (see Fig. 118,2). The variation of the sleeve ratio within the range of 0.2-0.55, as experiments have shown, has relatively little effect on ε and on the entry velocity. Variation of the velocity of the inflowing air within the range of 20-100 m/s

left the total resistance coefficient practically constant for a deflector with straight blades as well as one with profile blades.

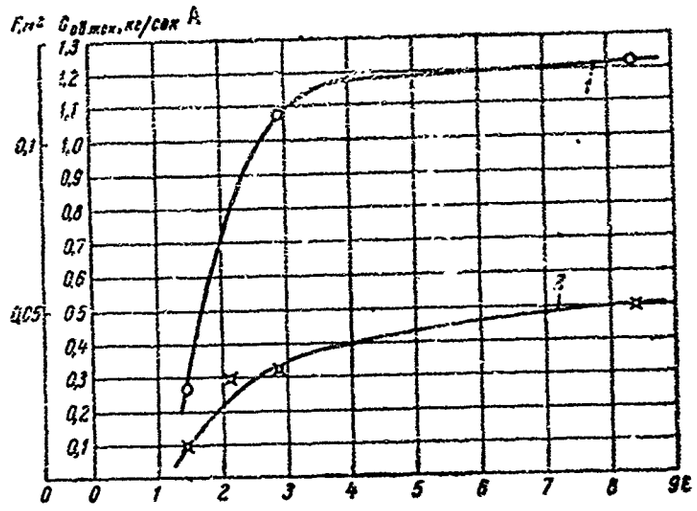

Fig. 119. Total surface of the ignition zone 1 and the quantity of combustion products 2 returning to the root of the flame, as a function of the resistance coefficient of a cylindrical deflector with profiel blades. A) $G_{ob.tok}$, kg/s.

Thus, the main independent variable for approximate calculations is the blade angle. By assigning a value to ϕ and determining the value of ε for it in accordance with Fig. 118, the ratio of the geometrical dimensions of the deflector can be determined from Eq. (5.147). The choice of the blade angle is a very difficult task since this requires an allowance to be made, not only for the peculiarities of the aerodynamic structure of the rotating flow but also for a large number of additional factors, for example, the correspondence between the angle of the fuel cone emerging from the atomizer and the dimensions of the zone of reverse flow. The main condition governing the choice of the blade angle is the achievement of a stable ignition of the fuel arriving in the furnace volume. It can be inferred from Fig. 119 [234] that the dimensions of the ignition zone and the quantity of combustion products which are returned to the root of the flame, increase sharply with increase in the resistance coefficient of the deflector. However, from values of $\varepsilon \geq 0.4$ upwards, the rate of growth of these values drops greatly which makes it economically feasible to use deflectors with very high resistance coefficients. By comparing Figs. 118 and 119, it can be concluded that the most rational blade angles in cylindrical deflectors are angles in the range of 40-70°. At these angles, acceptable resistance coefficients are obtained (ε = 2-4.0) for blade deflectors with profile blades. In practice, the range of variation of the blade angles is slightly more narrow and amounts to 45-60°.

For stationary power installations in which the combustion process develops in fairly large volumes, smaller angles are normally used (ϕ = 45-55°). Higher values (ϕ = 60-70°) are normally chosen for the

deflectors of highly boosted combustion chambers in which the high flow velocity makes the requirements with regard to the stability of the combustion process very stringent.

As indicated in the foregoing, external zones of reverse flows arise during the breakaway of the flow which reduce the diameter of the central zone. The main method currently used to prevent breakaway of the flow is the installation of a transition cone between the blade deflector and the combustion chamber proper. In this cade, the condition for breakwasy-free flow is written in the form of the following empirical formula

$$\operatorname{tg} \beta/2 < a + b \sin^2 \varphi, \tag{5.151}$$

where β is the aperture angle of the transition cone; ϕ is the blade angle; a and b are empirical coefficients, the average values of which can be assumed to be a = 0.05 and b = 1.

When the vortex jet leaves the deflector without breakaway, the size of the zone of reverse flow in the direction of the flow axis is approximately

$$L = \frac{cD_{ts}}{l \sin \varphi}, \tag{5.152}$$

where D_{ts} is the diameter of the inner circulation zone; l, the distance from the deflector to the vertical axis of the annular vortex; c, an empirical coefficient, equal to ≈3.73; ϕ, the blade angle.

The geometrical parameters of the circulation zone (D_{ts} and l) in turn are determined by the following empirical formulas:

$$D_{ts} = D_t \sqrt{0{,}75 - (1{,}35 - \sin \varphi)^2} \tag{5.153}$$

and

$$l = 0{,}45 D_{ts}, \tag{5.154}$$

where D_t is the typical transverse dimension of the furnace (for GTU combustion chambers, the diameter of the fire tube).

In the choice of the number of blades, allowance must be made for the fact that a certain overlapping of the blades must be ensured to give each air jet emerging from the channel between the blades the optimum direction of motion. According to the recommendations of [243], the overlapping coefficient of the blades for a cylindrical de lector can be assumed as

$$k = \frac{\pi d_{sr}}{th} = 1{,}1 - 1{,}3, \qquad (5.155)$$

where d_{sr} is the average diameter of the deflector; t the pitch of the blades with regard to the mean diameter; h, the number of blades.

The overlapping of the blades increases with increase in the blade angle.

Thus, the initial data for the calculation of a blade deflector are the throughput of air and its parameters and the diameter of the inner sleeve and the blade angle. Following the determination of the total resistance coefficient according to (5.149)-(5.150) or by means of the curves of Fig. 118, the diameter of the outer sleeve of the deflector is determined by means of Eq. (5.147). The hydraulic losses thus determined are then taken into account (after determination of all other losses) in the choice of the fan requirements.

Manuscript Page No.

Transliterated Symbols

163 т = t = tangentsial'nyy = tangential

163 т = t = toplivo = fuel

163 с = s = soplo = nozzle

163 э = e = ekvivalentnyy = equivalent

164 в = v = vozdukh = air

167 т = t = treniye = friction

168 ЦНИИ МПС = TsNII MPS = Tsentralnyy nauchno-issledovatel'skiy institut ministerstva putey soobshcheniya = Central Scientific Research Institute of the Ministry of Railways

169 г = g = gidravliduskiy = hydraulic

170 ЦККВ = TsKKV = Tsentral'noye kotel'no-konstruktorskoye byuro = Central Boiler Design Office

172 ф = f = fakel = flame

177 экст = ekst = ekstrem = extreme

181 с = s = summarnyy = total

183 п = p = privedennyyu = reduced

185 пр = pr = protivodavleniye = counterpressure

185 т = t = teoreticheskiy = theoretical

185 о = o = opytnyy = experimental

188 к = k = kaplya = drop

189 н = n = naruzhnyy = external

192 ср = sr = sredniy = average

192 д = d = deystvitel'nyy = real

205 кр = kr = kriticheskoye = critical

212 см = sm = smes' = mixture

212 р = r = radius = radius

213 я = ya = yadra = core

221 НИИхиммаш = NIIkhimmash = Nauchno-issledovatel'skiy i konstruktorskiy institut khimicheskogo mashinostroeniya = Design, Planning and Scientific Research Institute of Chemical Machinery

224 вх = vkh = vkhod = entry

225 п = p = prokhod = passage

226 об.ток = ob.tok = obratnykhtok = reverse flow

227 ц = ts = tsirkulyatsiya = circulation

227 т = t = topka = furnace

227 ГТУ = GTU = gazoturbinnaya ustanovka = gas-turbine power plant

Chapter 6

METHODS OF CONTROL OF THE ATOMIZATION AND COMBUSTION PROCESSES

24. CONTROL OF THE EXTERNAL PARAMETERS OF THE FUEL FLAME DURING AUTOMIZATION

The external control parameters of the fuel flame include the fuel throughput, the aperture angle of the flame and the fuel distribution over the jet section. Furthermore, it is expedient in some cases to measure the maximum flight distance and velocity of the drops.

A simple and accurate method of determining the fuel throughput is the gravimetric method in which the throughput is determined as the ratio of fuel weight to the interval of time during which it has been consumed. Under industrial conditions, the determination of the weight of fuel consumed within a certain period is replaced by the measurement of the volume of the fuel. The volume meters, samplers with stopwatch or counter, operate on this principle. For heavy (black) oils, however, the use of these devices involves difficulties because the fuel sticks to the walls and it is not possible to determine exactly the beginning and end of the time mark for the outflow from the calibrated volume. In the simplest case, the fuel consumption within a large time interval can be determined by measuring the fuel level in the fuel tank. The fuel supplied to the tank can be measured by means of a simple device [235] with dumping tanks (Fig. 120). With a low fuel level in the tank, a cock is opened by a float and the fuel flows into a small tank which is mounted on an axis. The small tank is divided into two halves by a partition. The position of the axis and the form of the small tank are such that the center of gravity of the system is shifted, the system turns over the fuel flows into the fuel tank.

The disc crude oil meters (Fig. 121) work on the same principle. The liquid fills repeatedly a chamber with a certain volume which then dumps the contents. This causes the disc to carry out an oscillating motion; each oscillation of the disc is recorded by a counter. The volume flow meters make it possible to determine the average fuel consumption over large periods and can be used only as control devices.

In modern furnaces with automatic control of the process, continuous throughout measurement is essential. For this purpose, as follows from the throughput equation (5.10), the velocity of the fuel during its passage through a calibrated orifice can be measured. The velocity is determined on the basis of the revolutions of a fan wheel installed in the pathway of the liquid. Mechanical, magnetic, radioactive, optical and electrical methods can be used to measure

the rate of rotation of the fan wheel (Fig. 122). Several types of flow meters are now known which do not contain moving elements in the measuring channel. They make use of the electrical properties of the fuel (in the induction flow meters), the thermal (in the calorimetric flow meters), ionization, ultrasonic, etc. properties [236].

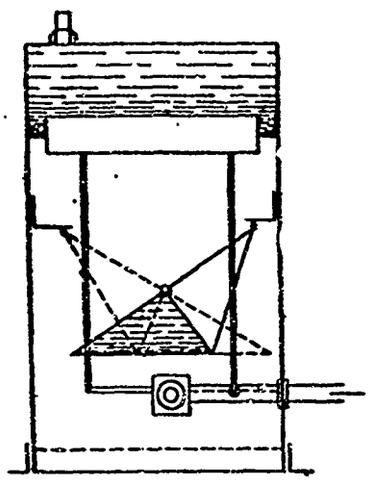

Fig. 120.

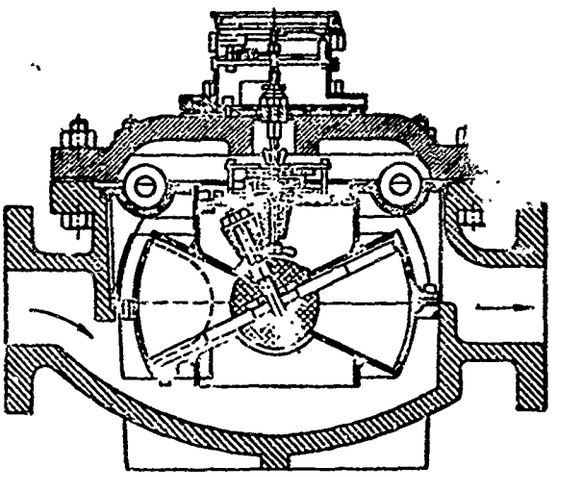

Fig. 121.

Fig. 120. Schematic view of flow meter with dumping tanks.

Fig. 121. Schematic view of disc crude oil meter.

Float devices, rotameters and piston flow meters are also used under industrial conditions. The principle of operation of all these devices is based on the equilibrium between the force of gravity of the float and the dynamic pressure of the flowing liquid. The float which is enclosed in a conical tube is lifted in proportion to the increasing throughput which causes an increase in the dynamic pressure. The piston flow meter PPE (Fig. 123) can be used for continuous measurement of the throughput of petroleum residue. As the throughput increases, the piston 1, which is connected by the special rod 2 with the iron plunger 3, is lifted. By moving within the electromagnetic coil 4, this plunger modifies the inductance of the latter, which is measured with another apparatus. The measurement range of this flow meter can be regulated by inserting the additional weight 5.

Diaphragm devices are widely used in practice to measure fuel throughput. The measurement of the throughput with these devices consists in a measurement of the pressure drop on the diaphragm. The pressure drop depends on the throughput. The same principle is used in the installation of calibrated nozzles. Since the output nozzle in atomizers has known dimensions, the fuel throughput can be calculated from the pressure in front of the nozzle. For this, it is necessary to calibrate first the atomizer and to determine the

physical properties of the liquid, above all the viscosity. Several viscosimeter designs with automatic maintenance of constant viscosity by variation of the fuel temperature have been proposed for the direct measurement of the viscosity.

The flame angle can be most accurately measured by means of photographs taken of two cross sections which must be at right angles to each other. Under industrial conditions devices are sometimes used for the measurement of these angles (Fig. 124) consisting of an angle scale and a movable lath, connected with an indicator.

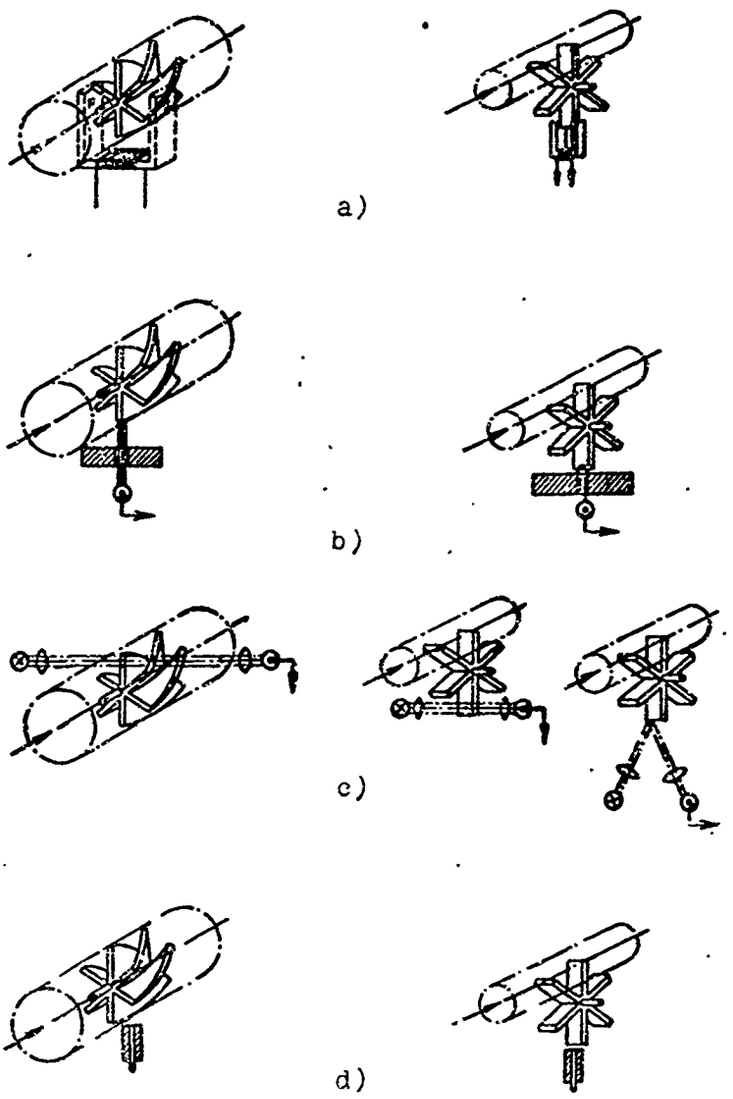

Fig. 122. Methods of measuring the rate of rotation of the fan wheel: a) magnetic; b) radioactive; c) optical: d) electrical.

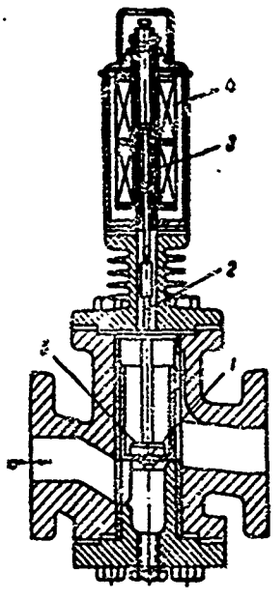

Fig. 123. Piston flow meter.

In pneumatic atomizers it is difficult to determine the boundaries of the flame because the bulk of the fuel is surrounded by a mist of fine drops. In this case, the flame angle can be approximately determined on the basis of the fuel distribution in a radial direction. The fuel is atomized into a tank which is divided into annular sections and the diameter of the outermost section into which fuel has been deposited, is measured. The ratio of the radius of this section to the distance between the atomizer and the tank is assumed to be equal to the tangent of half the flame angle. Instead of a tank with annular sections one can install a device containing test tubes or measuring cylinders.

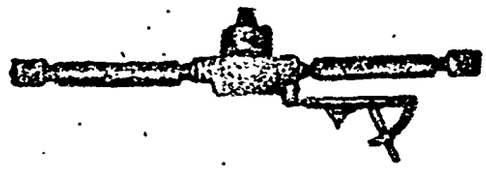

Fig. 124. Device for the measurement of the flame angle.

By means of measuring cylinders or annular sections it is also possible to determine the radial distribution of the fuel. By measuring the quantity of fuel falling into each measuring cylinder or annular section, one can determine the density of the fuel flame at any distance from the center by means of the following relation:

$$q_i = \frac{Q_i (r_{i+1}^2 - r_i^2)}{\sum_{i=1}^{i=n} Q_i (r_{i+1}^2 - r_i^2)}, \qquad (6.1)$$

where Q_i is the weight of fuel in the measuring cylinder (or section) at a distance r_i from the center.

Serious attention must also be given in the control of atomizer performance to the uniform distribution of the fuel among the annular sections. During the manufacture of the atomizers, the nonuniformity in the distribution of the fuel is measured by atomizing into a tank, divided into several sectors (Fig. 125). Each sector is connected with a measuring cylinder. After weighing of the cylinders, the nonuniformity of atomization is estimated on the basis of the ratio of the difference of the maximum weights to the average weight

$$e = \frac{q_{max} - q_{min}}{q_{cp}}, \tag{6.2}$$

$$q_{cp} = \frac{\sum_{i=1}^{i=n} q_i}{n}. \tag{6.3}$$

The throwing power of the fuel flame is most simply determined as the maximum flight distance of the drops with horizontal position of the atomizer.

The apparatus shown in Fig. 126a, can be used for determining the kinetic energy of the jet. A surface connected with a frame mounted on flat springs which connect it with a second, immovable frame, is placed in the path of motion of the fuel jet. The surface is displaced by the fuel and compresses the spring to a distance at which the force of the jet and the resistance of the spring are equal. By measuring the linear displacement of the surface, it is possible to determine the work, equal to the kinetic energy of the flying drops, on the basis of the spring characteristics:

$$A = \int_{s=0}^{s=s_1} F(s)\,ds = \frac{\sum_{i=1}^{i=n} mw^2}{2}. \tag{6.4}$$

By measuring the kinetic energy of the jet at different distances from the atomizer nozzle it is possible to determine the law according to which this energy or the average drop size decreases since the mass of drops in the section of the jet remains constant. The above-described method can be used for measuring the energy of the drops in different zones of the flame. In this case, the area should be reduced to a few square millimeters. At the same time, more sensitive measurement means must be used on account of the small deformations of the system.

Fig. 125. Device for the measurement of the uniformity of distribution of the fuel over the flame cross section.

The velocity of individual drops can also be determined by means of highspeed microkinematography or by means of the tracks of the drops on normal photomicrographs.

An apparatus working in accordance with the following principle, is used to measure the velocity of the drops (see Fig. 126b). In the path of motion of the fuel drops, two rotating discs are located, with a gap of H between them. Each disc has a small orifice at the distance R from the axis. The orifice in the disc which is further away from the jet, is shifted by the distance h against the direction of rotation. Behind the discs, a collecting plate coated with soot is placed. Only drops, the time of flight of which in the gap between the discs is equal to the time of rotation of the disc by the amount h hit the plate

$$\tau = \frac{h}{\omega} = \frac{H}{\omega R}, \tag{6.5}$$

hence

$$\omega = \frac{\omega R h}{H}. \tag{6.6}$$

By varying the speed of rotation ω of the discs or the displacement of the orifice, drops with the velocity ω can be collected. By measuring the size of the drops trapped on the plate, the velocity of the drops of all sizes in any section of the flame can be measured. In order to exclude the effect of air currents produced by the rotation of the discs, the latter are shielded by stationary walls.

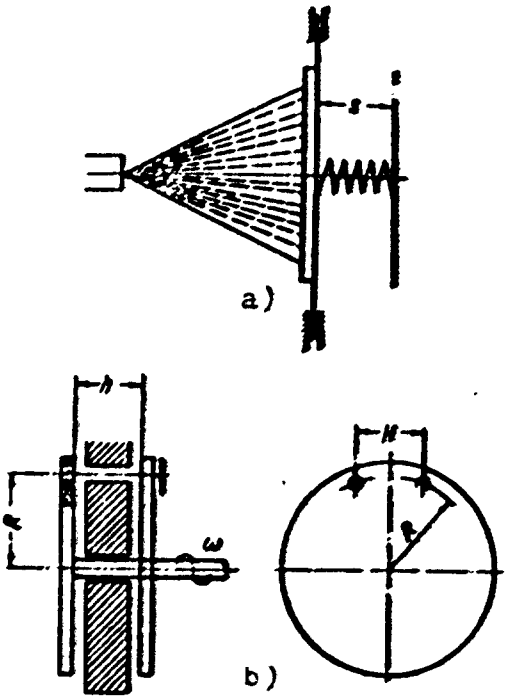

Fig. 126. Principles of the measurement apparatus: a) for the kinetic energy of the jet; b) for the drop velocity.

25. CONTROL OF ATOMIZATION EFFICIENCY

Tens of different methods of determining the drop diameter of a fuel flame have been proposed and utilized for studies of atomizer performance. The methods of collection, microphotography, modelling, and aerodynamic, optical and electrical methods are most widely used [237].

The collection methods are used in four variants: 1) collection on a plate which is coated with a thin layer of a substance which does not mix or react with the atomized liquid; 2) collection in a liquid-filled vessel; 3) collection on a mesh of organic glass; 4) collection on a plate coated with a layer of soot.

The plate, vessel with liquid or mesh are exposed to the jet for a short interval of time (from 1/500 to several seconds) to obtain a sample of the atomized fuel. Then the diameters of the drops are measured under the microscope and their number calculated.

The collecting plates can be coated with castor oil, glycerol with compressor oil (for water) and other compositions depending on the atomized liquid. The drop measurements must be carried out immediately after sampling or the samples must be stored under conditions which exclude the possibility of any substantial change in the drop size due to evaporation. The drops are collected on the plate at a considerable distance from the atomizer in order to avoid sharp impacts and disintegration of the drops.

Collection in a liquid reduces the impact effect on the drop and preserves the drop size. If the liquid is correctly selected, the drops collected in it can be kept for long periods without essential changes, without evaporating or changing shape which makes it possible to measure them some time after sampling. However, catching in a liquid does not eliminate the possibility of coalescence of nearby drops and of change in their arrangement pattern when the containers are moved.

When the drops are collected on a mesh made of thin fibers (~1 μ) of organic glass [238-239] they are retained on it by surface tension forces. The range of applicability of these nets is limited by the strength of the fibers which decreases considerably at higher temperatures as well as by the possibility that drops can pass through the mesh. Hence, this method of measurement is used only for drops with a velocity of not more than 10 m/s and a temperature not over 60°C.

Collection on a smoked plate makes it possible to determine the real size and relative positions of the drops.

However, the results of measurement of the imprints can be used for characterizing the fineness of dispersion only if an unequivocal correlation has been established between the size of the imprint and the drop diameter and if the number of imprints on the section to be measured corresponds to the number of drops. Tests carried out at the G. M. Krzhizhanovsky Power Engineering Institute [240] have shown that when the thickness of the soot layer is less than the drop diameter, the Stoker relation applies

$$\frac{d_0}{d_к} = 0{,}77\,We^{0{,}2},$$

where d_0 is the diameter of the imprint; $d_к$ the drop diameter; We the Weber parameter.

If the thickness of the soot layer is greater than 1.5-2 times the drop diameter, then, according to the studies of N. N. Strulevich and Yu. F. Dityakin, the imprints in the soot coincided with the drop size with an accuracy of 2-3%.

With high impact velocities of large drops, double imprints are sometimes obtained and the quality of the imprints is insufficient to allow determination of the drop size. The drop diameter can be considered to be equal to the imprints if the imprints show up under the microscope as deep and with smooth edges.

The method of collection on soot cannot be used for large drops (500 μ) since this would require a thick soot layer (0.65-0.75 mm) which can flake off after impact of the drop [240]. To obtain clearer imprints, a thin film of magnesia is applied over the soot (0.01-0.02 mm). The smoked plate is inserted into the apparatus shown in Fig. 127.

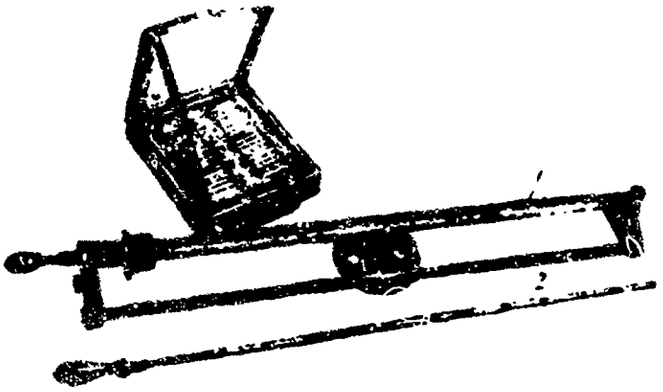

Fig. 127. Apparatus for collection of drops: 1) mobile tube with notch; 2) rod with smoked plates.

The main deficiency of all variants of the collection method is the arbitrary choice of the place and time of measurement and the relatively small number of measured drops compared with the total number of drops in the jet. In one test, 3 to 9 thousand drops are usually collected, which amounts to 0.01-1.0 weight-% of the fuel throughput per second.

Automation of the counting and measurement of the drops enables the time for processing the measurement data to be considerably shortened to subjective errors to be eliminated. One of the devices for the automatic processing of the test data [241] works in accordance with the following principle. A beam of light is directed on to the plate with the drop imprints, is reflected from it and falls on a photo element. The beam of light passes successively through the entire area of the collection plate in the manner of photoelectric telegraph transmitters. The sensor (photoelement), depending on the brightness of the beam reflected from the plate, sends signals to the converter which transforms them into pulses with amplitudes, proportional to the length of the signal. The use of a more complex setup [242] makes it possible to determine the drop distribution on the basis of the sizes of the imprints and not the lines which are accidentally selected by the scanning beam. For this purpose, there are seven sensors and the system works only when the drop imprints are in the focus of the apparatus. The devices for automatic drop counting are very complex and are used only for experimental research work in laboratories.

The main advantage of the microphotography method compared with collection is the fact that photography gives a true idea of the shape, size and mutual arrangement of the drops in the jet. The photographic apparatus has an objective with high resolving power and a large focal length. To give accurate pictures of the fast-flying drops, the illumination source must provide a brief (about 10^{-8} s) light pulse. The use of photography with a moving film made it possible to "arrest" part of the drops relative to the photographic film and to increase the exposure time to 10^{-6} to 10^{-5} s [243]. However, owing to the different speed of individual drops it was not

possible to obtain a "standstill" and clear photographic pictures of all the drops within the field of view of the apparatus.

The main deficiency of the microphotographic method is that only a very small part of the jet comes into the field of view of the microscope of the photographic apparatus and that a large number of exposures is required for an objective estimate of the drop sizes composing the jet. Their processing is laborious and the automatic measurement and counting of the drop images is difficult because of the inaccurate reproduction.

The modelling method consists in using instead of the fuel a substance which is solid at normal temperature (20°C) and is then heated until the physical constants correspond to those of the fuel to be investigated. As such a substance to replace kerosene and diesel fuel, paraffin can be used which has a viscosity and surface tension at 91°C which is close to that of kerosene and at 70°C, to that of diesel oil.

Ceresin grade 57 with addition of an isobutylene polymer is recommended as a model substance for the study of the atomization of petroleum residues [244]. By varying the proportions of these substances and the temperature of the mixture it is possible to model different grades of petroleum residue. Figure 128 shows a stand, used by the authors for the measurement of the fineness of dispersion by the method of modelling with paraffin.

The atomized paraffin drops are collected during a certain period of time (10-20 s) in a tank divided into sectors and filled with alcohol, which rotates at uniform velocity during the collection of the drops around an axis which coincides with the atomizer axis. The distance between the atomizer and the tank should be such that the drops are partly solidified during their flight (superficially) to prevent them from sticking together.

The collection of the paraffin in ethanol or methanol ensures rapid cooling and solidification of the drops. This is also necessary for wet sieving since with dry sieving, the paraffin drops stick to each other and clog the meshes of the sieve.

The solid drops collected in the tank are passed through a series of sieves with gradually increasing fineness and through filter paper. The oversize drops for each sieve are determined by weighing the paraffin residue on each sieve.

The grading of the drops by means of sieves gives satisfactory results and drops of approximately equal diameter remain on the sieves (Fig. 129).

The modelling method makes it possible to process (sieve) several grams of paraffin which corresponds to some ten million drops. This is an entirely sufficient sample. Based on its analysis it is possible to indicate the drop size distribution over the entire jet with a high degree of reliability.

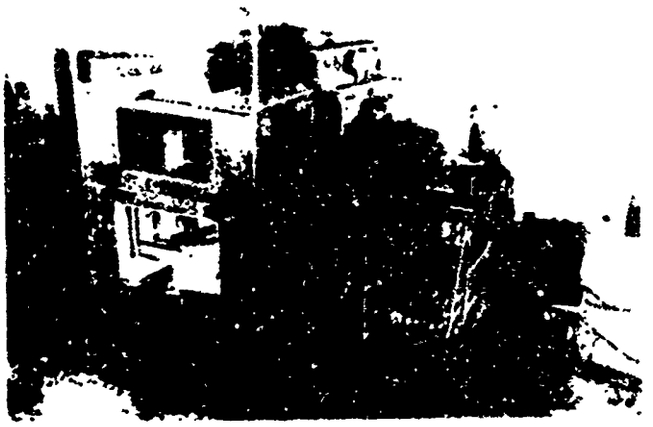

Fig. 128. Photographic view of the stand for the measurement of the drop sizes by the modelling method.

When the atomizer is in a horizontal position, the fuel drops will have a different flight distance depending on their size. If receiving tanks are located along the jet axis, only drops of a certain size fall into each tank. Hence, the finer drops will fall into the tanks which are closer to the atomizer and the larger drops into those which are more remote. By measuring all these drops it is possible to plot a distribution curve.

Owing to the different angles at which the fuel leaves the atomizer, it is not possible to carry out the measurement over the whole jet at once. One has to isolate a narrow fuel cone with small angle by means of special cut-offs and to carry out the measurement on individual cross sections. Since the difference in the flight distance of the drops is very slight in the case of fine atomization, this method is used only for atomizers operating at low fuel pressures (up to 16 kg/cm^2). With vertical position of the atomizer, the velocity of free fall of the drops in a viscous medium, according to Stokes law, beginning at a certain moment of time, becomes constant and equal to [245]

$$w = \frac{g d_k^2}{18\eta}(\rho_k - \rho_v), \qquad (6.7)$$

where g is the gravitational acceleration; d_k the drop diameter; η the viscosity of the medium in which the drops are falling; ρ_k, ρ_v is the density difference between the drops and the medium.

When a mixed beam of drops falls into a tall vessel, each drop size has its own velocity of motion which is higher for large than for small particles. By measuring the dropping velocity of the drops and the density of each layer, the sizes of the drops and their group size distribution can be determined.

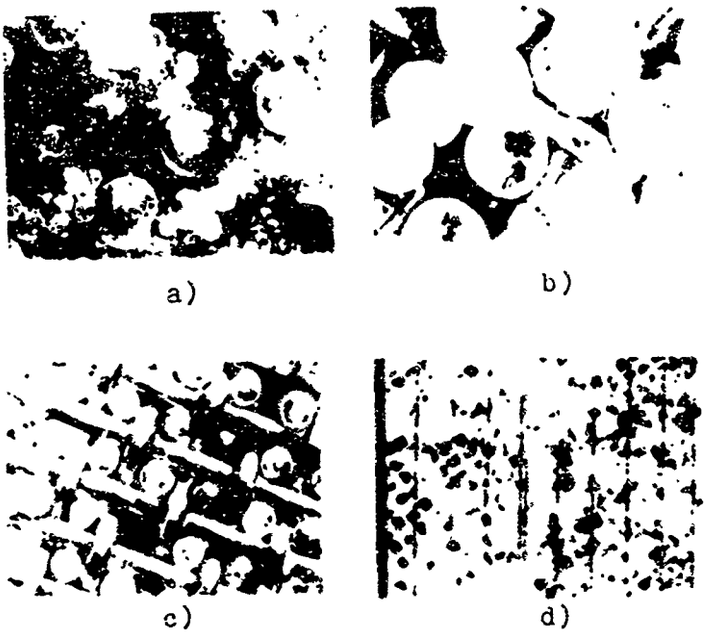

Fig. 129. Microphotograph of paraffin drops: a) before sieving; b) oversize on a sieve with 400 μ mesh; c) oversize on a sieve with 160 μ mesh; d) on a sieve with 40 μ mesh.

The chief disadvantages of the method of measurement of the drop velocity are the following. Firstly, the large number of drops of different size in the jet makes it difficult to observe the free fall of individual drops. Secondly, to obtain objective data on the drop sizes in the jet it is necessary to carry out a large number of measurements, including for drops moving within the jet, which requires the use of special cut-off devices. Thirdly, drops with a size of 5-10 μ can be observed only by means of a microscope and in this case the velocity of the drops is determined only for the time during which they move within the field of vision of the microscope which is insufficiently accurate.

The height H where all drops begin to fall at constant velocity, is the same, then it follows from equation (6.7) that

$$w = \frac{H}{\tau}, \tag{6.8}$$

hence

$$d_k = \frac{\sqrt{\frac{18\nu H}{g(\rho_k - \rho_a)}}}{\sqrt{\tau}} = \frac{k_1}{\sqrt{\tau}}. \tag{6.9}$$

All the quantities entering into the numerator k_1 remain constant during the measurement process, thus drops with the diameter $d_k + \Delta d_k$ fall on the balance within the time $\tau + \Delta\tau$. By measuring their weight during certain time intervals and determining by means of (6.9) the diameters of the drops falling on the balance during this

time, it is possible to obtain a weight curve of the drop size distributions. An analogous method in dispersion analysis has been termed sedimentometric method [245, 246, 247].

The main deficiency of this method is the difficulty of obtaining a uniform deposition velocity when the fuel is atomized under high pressure. However, by combination of the sedimentometric method with drop collection it is possible to measure the fineness of dispersion at nonuniform deposition velocities. A schematic of such an apparatus, used by the authors, is given in Fig. 130. The atomizer with shutter which allowed atomization of the fuel for a brief period, was installed on top of a high column. Microbalances and a device for collecting the drops were located below the column.

The fuel, by means of a gate operated by an electromagnet, is diverted into an overflow tank and only during the experiment, for a period of 0.2-0.6 seconds, the gate allows the fuel access to the column. The large drops arrive first on microbalance and the collecting device, then the smaller drops follow. Thus, the weight of fuel falling on the microbalance will increase gradually which makes it possible to plot a curve of drop weight versus time. By measuring the diameters of the drops falling on the collection device it is possible to plot the relation between the diameter of the collected drops and the time. Knowing the weight and diameter of the drops, corresponding to a certain period, it is easy to find the weight curve.

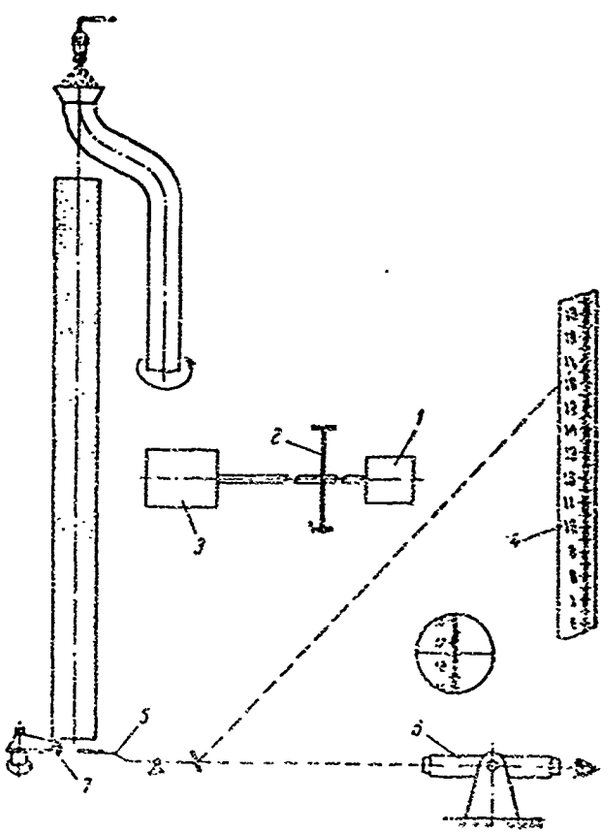

Fig. 130. Principle of the sedimentometric apparatus for the measurement of drop sizes: 1) mirror; 2) silken thread; 3) platform for the deposition of the drops; 4) balance, 5) microbalance; 6) sighting tube; 7) smoked plate.

The optical measurement methods are based on the utilization of phenomena such as scattering, reflection, absorption of light, interference and diffraction, observed during the passage of a light beam through a fog of drops. As a result of the passage of a beam of light through the jet of atomized fuel, the brightness of these beams is reduced [148-247]. The drops can be regarded as opaque spheres since they have a short focal distance and parallel rays falling on them are strongly scattered. Since the area of the photometer screen is small compared with the surface on which the light dispersed by the drop falls it can be assumed that the decrease in the illumination of the photometer is proportional to the total surface of the diametric drop cross sections

$$\frac{\Delta I}{I} = \frac{F_к}{F_ф}, \tag{6.10}$$

where ΔI is the quantity of light lost due to the opaque objects (drops) in its path; I is the quantity of light emanating from the source; F_k is the total area of the drops; F_f is the area of the photosensitive layer of the photoresistance or photocell.

This relation is correct only for a thin layer of jet in which the possibility is excluded that several particles are in line in the direction of the light beams to the light-sensitive cell (Fig. 131a), i.e., for a layer with the thickness Δx:

$$\frac{\Delta j}{j} = \frac{F_к \Delta x}{l F_ф}, \tag{6.11}$$

where l is the distance from the jet in the line of measurement; if the jet is symmetrical, then $l = D_f$; D_f is the jet diameter at the measurement point.

Going over to the limits and solving the equation with the limiting conditions $x = 0$, $j = j_0$, $x = l$, $j = j_0 - \Delta j$, we find

$$\ln(j_0 - \Delta j) - \ln j_0 = \frac{F_к}{F_ф}. \tag{6.12}$$

This equation makes it possible to determine the total drop surface on the basis of the decrease in illumination

$$F_к = \pi \sum_{i=1}^{i=n} d_i^2 N = \pi \overline{d_{ср}^2} N. \tag{6.13}$$

To determine the average drop diameter, we must exclude N which can be done if the volume of the drops in the measurement zone is known

$$V = \frac{\pi}{6} \sum_{i=1}^{i=n} d_i^3 N = \frac{\pi}{6} \overline{d_{ср}^3} N. \tag{6.14}$$

If the drops are uniformly distributed in the jet, their volume will be proportional to the volume of the jet $F_f D$ and the fuel throughput Q within the time τ will be proportional to the $\pi D_f^2 w\tau$. It follows from these relations that

$$V = \frac{QF_\phi}{\pi D_f w \gamma}, \qquad (6.15)$$

where Q is the fuel throughput per second in kg/s; w is the drop velocity in m/s; γ is the specific gravity in kg/cm^3.

The average drop diameter is determined by means of the relation

$$d_{cp} = \frac{\sum d^3 N}{\sum d^2 N} = \frac{6V}{F_\kappa}. \qquad (6.16)$$

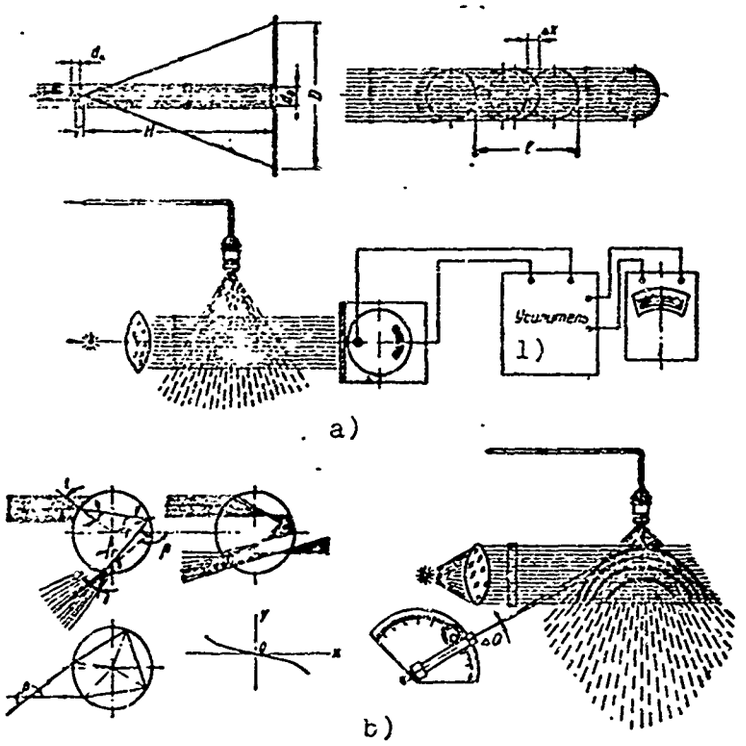

Fig. 131. Principle of the optical measurement methods: a) photometric method; b) rainbow method. 1) counter.

Solving equations (6.12)-(6.16), we obtain

$$d_{cp} = \frac{6Q}{\pi\gamma D w \ln \frac{I - I_0}{I_0}}. \qquad (6.17)$$

Thus, by measuring the decrease in illumination with a photometer, the fuel throughput, the velocity and jet diameter, we can find the average drop size.

When a plane light wave falls on a drop, the rays, being subject to diffraction and internal reflection, form a new wave surface which, interacting with the incident wave, gives an interference pattern. With monochromatic light this pattern is a series of concentric arcs. The angular distance $\Delta\theta$ between these arcs is determined by the wavelength λ of the incident light, the diameter d_k, the diffraction coefficient n of the drops and the difference of the two values of Herault's coefficient corresponding to the first and second bands of the arc $\Delta z = z_1 - z_2$ (the values of z are taken from Tables [248]).

The equation which connects all these quantities, when solved relative to d_k, assumes the form

$$d_k = 0{,}433 \frac{\Delta z \lambda}{\Delta\theta} \left[\frac{4-n}{(n^2-1)^2}\right]^{1/4}. \qquad (6.18)$$

The principle of drop size measurement by this method (the rainbow method) is shown in Fig. 113b.

The rainbow method gives good results when the drops at the point of measurement (of incidence of the beam) are of equal diameter.

When there are large differences in drop size, the interference bands obtained from the different diameters, overlap and do not give individual bands which could be used for measurement of the angles. This method cannot be used for excessively small drops either (less than 5 μ) because the wavelength of the light becomes comparable with the drop diameter and an interference pattern is not observed.

When the rays pass through a small orifice in an opaque screen, diffraction rings are formed. The relation between the diameter d_k of the orifice, the wavelength of the light λ, the angular distance θ of any ring with maximum illumination and the order of this ring m from the center is expressed by the equation

$$d_k = \frac{\lambda}{2\sin\theta}(m + 0{,}22). \qquad (6.19)$$

By considering the drops as randomly arranged opaque discs and measuring the angular distance of the rings formed when light passes through a layer of drops, we find the drop diameter by means of formula (6.19).

This method has a great deficiency: the observation of the diffraction rings, formed around the light source when it is viewed through a layer of fine drops, is very difficult because the light source is much brighter than the rings and the eye, adapted to it, has difficulty in distinguishing the darker system of rings.

The above described optical methods enable the average drop size to be determined and give good results when the scatter of drop sizes is small, but are unsuitable for the measurement of the size of individual drops. An important advantage of the optical methods is the fact that they do not affect the jet and do not interfere with the atomization process. The devices for the optical measurement of drop size are extremely simple in design, incorporating mainly standard apparatus (photometer, goniometer, projection apparatus, etc.). The drops can be measured during the atomization of fuel in atomizers operated at any pressure and with atomization in an airstream.

Fig. 132. Sensor for the measurement of drops by the electronic method.

The electrical methods of measuring the drop size are based on the utilization of the property of the drops to act as capacitances, capable of transporting electrical charges. The measurement consists in the following. The drops, passing through an electric field, receive a charge, the magnitude of which is equal to the capacitance of all the drops in the jet. By measuring the quantity of electricity transported by the atomized fuel it is possible to determine the average drop diameter.

The electronic method is used for the determination of the entire spectrum of drop sizes [249]. A special sensor (Fig. 132) is inserted into the jet which is a probe of fine wire. The probe is connected with the grid of an electronic tube in which a constant electrical potential is maintained. When a drop comes into contact with the probe, a pulse appears in the circuit, the amplitude of which is proportional to the capacitance and, consequently, to the drop size. The pulses are amplified and are delivered to a counter via a classifier (discriminator). When the classifier is tuned to different voltages, the number of pulses is counted within a certain range of drop sizes only. The results do not require complex processing and a drop size distribution curve can be plotted by means of them without additional calculations.

In addition to the above described methods, other methods for the measurement of the drop diameter [154] are known but they have not found practical application and will not be discussed here for this reason. Combined methods are sometimes used in practice for the measurement of drops. A combination of two methods makes it possible to eliminate certain deficiencies of each. For example, one can use a combination of collection and sedimentometric methods with weighing

of drops or collection and an electrical, sedimentometrical and photometrical, etc.

The authors have determined the relative and maximum error of the collection method by repeated measurement of the fineness of dispersion of diesel fuel. For a fineness of dispersion, characterized by a median diameter of 0.235 mm, they amount to 23.2 and 24.4%, respectively, of the average value of the median diameter for all tests. These values correspond [245-246] to the accuracy (20%) of the microscopic method of dispersion analysis.

Most of the total error of the collection method is due to the small sample of drops for measurement. The subjective errors, which according to the result of processing of a single measurement by 10 operators amounts to 17-18%, also contributes greatly to the error of the method. The errors resulting from the fact that the diameters of the drop imprints are not identical with the diameters of the drops, although they increase the measurement results, do not greatly affect the accuracy of the method.

During repeated atomization of paraffin with the same atomizer under conditions corresponding to a fineness of dispersion with a median diameter of 0.171 mm, a relative error of 17.9% and a maximum error of the average median dimensions of 17.5% for all tests was found.

When a sample taken at one time in 10 different containers arranged in the sectors of a circle and rotating uniformly around the atomizer axis was sieved, the relative deviation from the average results was 16.9% and the maximum 15.9%. The measurement error in the two cases differs only slightly, consequently, the main error of the modelling method is the inaccurate sieving.

An analysis of the measurement results of the sedimentometric method showed that the relative error is 14.9% and the maximum error 16.1% of the average of several measurements.

These errors include the errors in weighing of the drops due to the dynamic impact of the drops on the weighing platform; the errors due to insufficiently accurate separation since the fuel is atomized during a certain time interval and the large drops, emerging from the atomizer, also reach the balance simultaneously with the smaller drops, which leave the nozzle during the open interval; the errors in the determination of the drop diameters on the basis of imprints on a soot-coated disc; the errors resulting from evaporation of the drops during their deposition and weighing and other, less important errors.

The relative error of the microphotographic method due to innaccurate photographic recording, according to the data of the French Petroleum Institute [250] amounts to ±6%, not taking into account the accuracy of counting and measuring of the drops.

Thus, the testing of atomizers is preferably carried out with optical or electrical methods which give the average drop size without the need for a laborious processing of the measurement results. One can also use the collection method with estimation of the fineness of dispersion on the basis of the largest drops.

The microphotographic or electronic method is most suitable for tests of atomizer performance in furnaces. At the laboratories, where a greater accuracy in the measurement of the entire spectrum of drop sizes is required, it is most expedient to use the modelling or sedimentometric methods.

26. CONTROL OF THE COMPLETENESS OF THE COMBUSTION PROCESS

The process of combustion of a fuel, like any other process of transformation of one form of energy into another, involves unavoidable losses, the total value of which is usually determined by means of the following relation:

$$q_{\text{топ}} = 1 - \eta_{\text{гор}}, \qquad (6.20)$$

where q_{top} are the total losses in the furnace process; η_{gor} is the completeness of combustion of the fuel in the furnace.

Equation (6.20) relates directly to the process of heat evolution in the furnace and does not therefore include terms characterizing the process of heat transfer from the combustion products to the working fluid or the ambient medium. Since the efficiency of the process of heat evolution in the furnace is unequivocally defined by the furnace losses, the control of the combustion efficiency is reduced to the determination of the nature and magnitude of these losses. According to the terminology of G. F. Knorre [156], these losses are those from the chemical and mechanical incompleteness of combustion.

By losses due to chemical incompleteness of combustion is meant the quantity of heat energy per unit weight of consumed fuel which has remained chemically bound in the unburned gases, mainly in the form of CO; H_2; CH_4; C_mH_n.

The total loss due to chemical incompleteness of the combustion is defined by means of the relation

$$q_{\text{х.н}} = \frac{Q_{\text{х.н}}}{Q_{\text{н}}^{\text{р}}} \cdot 100\%, \qquad (6.21)$$

where $Q_{kh.n}$ is the quantity of heat energy which is not liberated within the furnace.

The quantity $Q_{kh.n}$, in its turn, is determined by means of the equation

$$Q_{\text{х.н}} = 56{,}7 \frac{C^{\text{р}}}{CO_2^{\text{полн}}} (CO + 0{,}85H_2 + 2{,}8CH_4), \qquad (6.22)$$

where C^p; CO; H_2; CH_4 are, respectively, the percentage content of carbon in the fuel, and that of carbon monoxide, hydrogen and methane in the flue gases; CO_2^{poln} is the total percentage content of carbon dioxide, carbon monoxide and methane in the combustion products

$$CO_2^{полн} = CO_2 + CO + CH_4. \qquad (6.23)$$

Thus, the determination of the losses due to chemical incompleteness of combustion is reduced to determination of the percentage concentration of the individual combustion products.

The magnitude of the loss due to mechanically incomplete combustion is determined as the specific chemically bound energy, contained in the unburned fuel. The experimental data obtained in the study of different thermal power installations, attest to the fact that the products of the mechanical incompleteness of combustion are present in the flue gases in the form of foglike fuel, soot and resin-coke particles. The presence of these substances in the gas stream even when the losses due to mechanically incomplete combustion are small, causes serious interference with the performance of the whole installation or its individual parts. The total amount of these losses, related to unit weight of introduced fuel, can be written in the form

$$q_{мех}^{\Sigma} = \frac{\delta_т Q_н^т + 8100(\delta_с + \delta_к)}{Q_н^р}, \qquad (6.24)$$

where q_{mekh}^{Σ} is the total relative loss due to mechanically incomplete combustion; Q_n^t is the lower heat of combustion of the fuel aerosol (fuel vapor which has gone beyond the individual combustion zone of the drop in the flame); δ_t; δ_s; δ_k, respectively, are the specific weight concentrations (per unit weight of fuel) in the combustion products of fuel aerosol, soot and coke.

Thus, the determination of the quantity q_{mekh}^{Σ} is reduced to determination of the specific (per unit weight of fuel) concentrations of these components.

The methods currently used for determining the gaseous components of the combustion products are very diverse but the method of absorption analysis of a gas sample with the gas analyzers GKhPZ (GOST 6329-52) and VTI-2 (GOST 7013-54) has found the widest application in field testing and research practice. The widespread use of the chemical method of analysis of the combustion products is mainly due to the fact that it allows a simple isolation of the principal components (CO_2, O_2, CO), which is sometimes sufficient for gaging the completeness of combustion.

In most cases, this type of analysis of the combustion products is insufficient because of the large error in the determination of q_{khim} when components such as H_2, CH_4, C_mH_n are contained in the flue gases. Because of this, the improved gas analysis devices (VTI-1; 2) were developed which allow the determination of these components by combustion and subsequent absorption of the combustion products. However, to obtain complete information on the composition of the combustion products on the basis of their chemical analysis involves a great loss of time. The duration of a complete gas analysis with the VTI-2 is 3.5-4 hours. This naturally reduces the practical value of chemical analysis considerably and prevents its widespread use.

Table 19
Magnetic Susceptibility at t = 20°C and Relative Thermal Conductivity at 0°C and 760 mm Hg of the Main Gaseous Components of the Combustion Products [251]

1 Газ	$\lambda_r/\lambda_в$	$\chi \cdot 10^6$
2 Воздух	1,000	-
3 Водород	7,130	—0,164
4 Водяные пары при 100° С	0,973	—0,58
5 Двуокись серы	0,344	—
6 Двуокись углерода	0,84	
7 Метан	1,318	+1
8 Окись углерода	0,964	—
9 Азот	0,998	—0,55
10 Кислород	1,015	+142

1) gas; 2) air; 3) hydrogen; 4) steam at 100°C; 5) sulfur dioxide; 6) carbon dioxide; 7) methane; 8) carbon monoxide; 9) nitrogen; 10) oxygen.

Various schemes and designs of automatic gas analyzers have been proposed to date, which make use of differences in the physical or chemical properties of the combustion product components (thermal conductivity, magnetic susceptibility, infrared absorption, etc.), of which the data presented in Table 19 may give an idea.

The creation of a gas analyzer for the determination of the main gaseous components in the combustion products on the basis of differences in the numerical values of the thermal conductivity or magnetic susceptibility is practically impossible. Hence, different kinds of devices using this principle are designed, as a rule, only for the determination of a single component (usually H_2, CO_2, O_2). Thus, for example, in the automatic gas analyzer GEUK-21 which is intended for the determination of CO_2 in furnace gases, the principle of continuous comparison of the thermal conductivity of the gas mixture to be analyzed and the air by means of a measuring bridge is used.

Since the thermal conductivities of the other components of the flue gases (with the exception of hydrogen) differ relatively little from the thermal conductivity of air and their concentrations are low, the variation of the CO_2 concentration will be the main factor responsible for any unbalance of the bridge. Even a low hydrogen concentration in the test mixture causes large errors in the CO_2 measurement. In order to eliminate this source of error, the hydrogen contained in the mixture is eliminated by combustion in an electrical furnace. The same principle of comparing thermal conductivities is used in the electrical gas analyzer TP-1110 which was designed for continuous measurement of hydrogen concentration. The main difference is the fact that here one compares the thermal conductivities of the analysis and standard mixture in which the hydrogen concentration corresponds to the upper limit of the reading of the gas analyzer.

As follows from the data of Table 19, the magnetic properties of oxygen and other gaseous components of the combustion products differ quite considerably. Different gas analyzer schemes for determining the oxygen concentration in gas mixtures are based on the utilization of these peculiarities of oxygen.

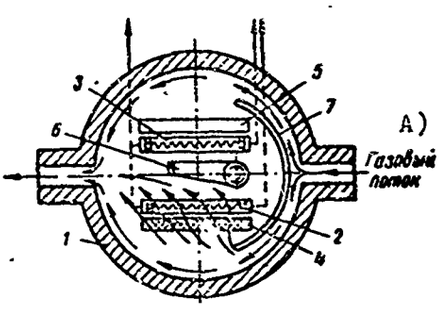

Fig. 133. Principle of the sensor of the magnetic gas analyzer for oxygen determination MGK-348: 1) body; 2), 3) heating elements; 4) magnet pole; 5) phantom pole; 6) control lug; 7) partition. A) gas flow.

Figure 133 shows schematically the gas flow in the measuring chamber of the gas analyzer MGK-348, in which the phenomenon of thermomagnetic convection is utilized.

If oxygen is contained in the mixture, it interacts with the magnetic field of the poles in consequence of which a flow of cool gas appears above the thermocouple.

The oxygen, in its turn, loses most of its magnetic properties as it is heated and is displaced by a new "cold" portion. Thus, a continuous gas flow arises above the thermocouple, the intensity of which is determined by the oxygen concentration in the mixture. Accordingly, the degree of cooling of the thermocouple is also

determined by the oxygen concentration. The different temperature and, consequently, different resistance of the arms of the measuring bridge causes an unbalance. The unbalance voltage which is proportional to the oxygen concentration in the test mixture, is delivered to a secondary recording device. The main permissible measurement error of this gas analyzer is estimated to be 0.5% for the range of 0-21% O_2. The gas analyzer MN-5106 operates on an analogous principle.

Much more complex in principle are the gas analyzers based on the different absorption of infrared by the different components of a gas mixture. The principle of operation of this gas analyzer (optico-acoustical) is that a discontinuous flux of infrared which passes through the test mixture, loses part of its energy in it. The magnitude of this loss is proportional to the concentration of the element to be determined. The remainder of the energy arrives in the optico-acoustic receiver which is filled with the test mixture. In consequence of the discontinuous energy supply to the gas in the receiver, temperature fluctuations are produced accompanied by pressure fluctuations at audio-frequencies. These sound oscillations are received by means of a condenser microphone connected with the corresponding measuring circuit. The gas analyzers of this type are also used for the measurement of the concentration of a single one of the components of the gas mixture (CO_2, CO or CH_4).

Thus, a brief review of the basic methods of gas analysis allows us to conclude that the practical efficiency of their application is greatly reduced by the deficiencies inherent in all these methods: the extremely long duration of the analysis for the chemical gas analyzers and the impossibility of determining all the components of the flue gases with automatic gas analyzers. Hence, the principles used for the automatic continuous determination of any of the main components of the combustion but also and mainly for designing different schemes of automatic control and monitoring of the combustion process. In these schemes, the concentration, for example, of CO_2 or O_2 is used as the main or correcting pulse [252-254] since the physical methods of determination of these components make it possible to record very small variations in their concentration in two-component mixtures. The possibility of determining with great accuracy one of the two components of a mixture by means of some physical method was the prerequisite for the development of the chromatographic method of analysis of combustion products.

In principle, this method is a combination of the chemical method of separation of gaseous components by adsorption and the physical method of determination of the concentration of the component in question.

The adsorption separation of a gas mixture is based on the different rate of adsorption and desorption of the components in the test mixture. If a small quantity of the test mixture (a few cubic centimeters) is quickly introduced into the carrier gas (nitrogen, atmospheric air, etc.) flowing through a column with a special adsorbent, a gas mixture consisting of the carrier gas and the flue gas components dissolved in it (H_2, CO, CH_4) arrives in the separating column. During their passage through the column, these components are

determined by the oxygen concentration. The different temperature and, consequently, different resistance of the arms of the measuring bridge causes an unbalance. The unbalance voltage which is proportional to the oxygen concentration in the test mixture, is delivered to a secondary recording device. The main permissible measurement error of this gas analyzer is estimated to be 0.5% for the range of 0-21% O_2. The gas analyzer MN-5106 operates on an analogous principle.

Much more complex in principle are the gas analyzers based on the different absorption of infrared by the different components of a gas mixture. The principle of operation of this gas analyzer (optico-acoustical) is that a discontinuous flux of infrared which passes through the test mixture, loses part of its energy in it. The magnitude of this loss is proportional to the concentration of the element to be determined. The remainder of the energy arrives in the optico-acoustic receiver which is filled with the test mixture. In consequence of the discontinuous energy supply to the gas in the receiver, temperature fluctuations are produced accompanied by pressure fluctuations at audio-frequencies. These sound oscillations are received by means of a condenser microphone connected with the corresponding measuring circuit. The gas analyzers of this type are also used for the measurement of the concentration of a single one of the components of the gas mixture (CO_2, CO or CH_4).

Thus, a brief review of the basic methods of gas analysis allows us to conclude that the practical efficiency of their application is greatly reduced by the deficiencies inherent in all these methods: the extremely long duration of the analysis for the chemical gas analyzers and the impossibility of determining all the components of the flue gases with automatic gas analyzers. Hence, the principles used for the automatic continuous determination of any of the main components of the combustion but also and mainly for designing different schemes of automatic control and monitoring of the combustion process. In these schemes, the concentration, for example, of CO_2 or O_2 is used as the main or correcting pulse [252-254] since the physical methods of determination of these components make it possible to record very small variations in their concentration in two-component mixtures. The possibility of determining with great accuracy one of the two components of a mixture by means of some physical method was the prerequisite for the development of the chromatographic method of analysis of combustion products.

In principle, this method is a combination of the chemical method of separation of gaseous components by adsorption and the physical method of determination of the concentration of the component in question.

The adsorption separation of a gas mixture is based on the different rate of adsorption and desorption of the components in the test mixture. If a small quantity of the test mixture (a few cubic centimeters) is quickly introduced into the carrier gas (nitrogen, atmospheric air, etc.) flowing through a column with a special adsorbent, a gas mixture consisting of the carrier gas and the flue gas components dissolved in it (H_2, CO, CH_4) arrives in the separating column. During their passage through the column, these components are

subjected to continuous processes of adsorption and desorption which takes place at a strictly determined velocity for each component. No irreversible adsorption of gases on the adsorbent takes place. As a result the gas flowing out of the column is not longer the multi-component mixture, but a two-component mixture which successively changes in composition because the components of the original mixture pass through the column at different velocities. Thus, for example, the rate of motion of hydrogen through the separation column, owing to the low degree of adsorption, is practically the same as that of the carrier gas. The accordingly increased adsorption of the carbon monoxide and methane gives rise to a certain time lag in the appearance of these components at the outflow end of the separation column. The determination of the concentrations of the components in the successively formed binary mixtures can be carried out with very high accuracy by one of the physical methods. For example, in the chromatographic gas analyzer GSTL, this is done by measuring the resistance of a platinum wire during the catalytic combustion of H_2, CO or CH_4 on it. The resistance variation of the platinum wire is recorded by a secondary self-recording device of the type of electronic potentiometer EPP-09 in the form of a trace with clearly visible peaks, the relative position of which characterizes the content of a certain component and the magnitude of the peak indicates its volume concentration on a certain scale.

The analysis of a gas sample requires very little time because when the flow velocity of the carrier gas and the length of the column are chosen correctly, the successive outflow of the components can be completed within 10-20 seconds.

The short duration of the analysis, the absence of subjective errors, the possibility of determining components present in low concentration and the high accuracy are all advantages of the gas-chromatographic method of analysis, responsible for its rapid adoption not only in research but, which is the most important, directly under industrial conditions.

All the methods of determining the losses due to mechanically incomplete combustion can be conventionally divided into two main groups: indirect methods, involving the measurement of some quantities in some way connected with the mechanical incompleteness of combustion and the direct methods, i.e., sampling of the combustion products and subsequent analysis.

The optical method, based on the measurements of the optical density of the combustion products, the calorimetric method, based on the measurement of the thermal conductivity coefficient of a layer of soot and coke, which has been deposited on the walls of the calorimeter, etc., belong to the first group.

To the second group belong all mechanical or chemical methods of analysis of the combustion products. By mechanical methods are meant those in which the solid products of incomplete combustion are separated from the flue gases and then analyzed. The chemical analysis methods presuppose the use of various chemical reagents.

To the mechanical methods of determination of the losses due to incomplete combustion belongs the collection of soot and coke particles on a cold surface with subsequent analysis under the microscope and calculation of their concentration in the gas flow on the basis of the known sedimentation law and also the sampling of combustion products with subsequent filtration and direct weighing of the collected unburnt fuel.

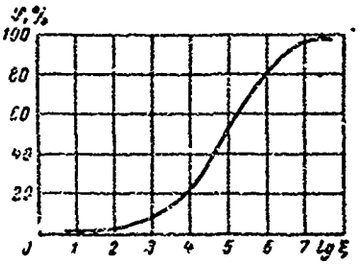

Fig. 134. Sedimentation coefficient ϕ of the particles as a function of the parameter ξ.

The collection method makes it possible to determine the quantity and dimensions of the coke and soot particles in the gas flow through the furnace. In this case, use is made of the dependence of the sedimentation coefficient ϕ of a particle with a certain diameter on the external flow conditions which is described by the following equation [255]:

$$\varphi = f(\xi); \quad \xi = \frac{w\delta^{4.7}\rho^{2.5}\rho_p^{0.5}g}{\mu^3 D}, \tag{6.25}$$

where w is the flow velocity of the gas in m/s; δ is the diameter of the particle in m; ρ_p is the density of the gas in kg/m^3; ρ is the density of the particle in kg/m^3; μ is the kinematic viscosity of the gas in kg/s/m^2; D is the diameter of the cylinder on which the sedimentation takes place in m; g is the gravitational acceleration in m/s^2; ϕ is the sedimentation coefficient for a particle with a given diameter.

The form of the relation $\phi = f(\xi)$ is given in Fig. 134 for the condition of flow of a gas containing anthracite and metal particles ($\delta \approx 10$ μ) around a cylinder. The experimental data differed from those calculated by means of equation (6.25) by ±4.0% [255].

The method of bubbling the combustion products through a liqui. in a vessel (Fig. 135) can also be counted among the mechanical methods.

Among the chemical methods of determining the losses due to mechanically incomplete combustion are the method of gas analysis and separate combustion.

By the gas analysis method, the losses are determined as the difference between the weight of the supplied and burnt fuel. The equation for calculating the loss due to mechanically incomplete combustion has the form

$$q_{mex}^{\Sigma} = Q_c C^p \left(1 - \frac{\beta_{топл}}{\beta_{газ}}\right), \qquad (6.26)$$

where Q_s is the calorific value of carbon in the original fuel in %; C^p is the percentage of carbon in the original fuel; β_{topl} is the characteristic of the original fuel; β_{gas} is the characteristic of the combustion products

$$\beta_{топл} = 3(1 - O_{o.k}) \frac{0{,}1250^p + 0{,}039N^p}{C^p - 0{,}375mS^p}, \qquad (6.27)$$

$$\beta_{газ} = \frac{21 - (CO_2 + 0{,}605CO + O_2)}{CO_2 + CO}, \qquad (6.28)$$

where $O_{o.k}$ is the volume proportion of oxygen in the oxidizer; H^p, O^p, N^p, S^p are the contents of hydrogen, oxygen, nitrogen and sulfur, respectively, in the original fuel in %; CO_2, CO, O_2 are the carbon dioxide, carbon monoxide and hydrogen contents in the combustion products; m is a correction factor; for organic sulfur, m = 1.

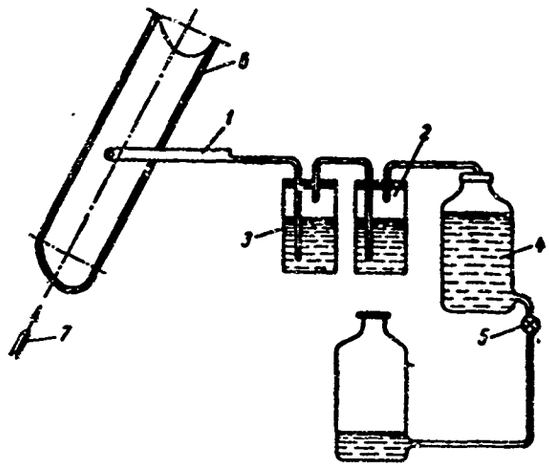

Fig. 135. Principle of measurement of the losses due to mechanically incomplete combustion according to [256]: 1) sampling tube; 2) container with kerosene; 3) container with water; 4) measuring cylinder; 5) cock; 6) gas conduit; 7) direction of flow of the combustion products.

For preliminary calculations, taking into account the low sulfur and nitrogen content of the fuel

$$\beta_{топл} = 2{,}37 \frac{H^p - 0{,}1250^p}{C^p}. \qquad (6.29)$$

Analysis of the errors in the determination of the combustion product characteristic β_{gas} shows that

$$\Delta\beta_{газ} \simeq 0{,}0405\frac{1}{CO_2}. \tag{6.30}$$

This error increases considerably with increase in the excess air and at α = 3-5, which is the case in power furnaces, it becomes equal to the measured value and when the losses due to mechanical incompleteness of combustion are small, it exceeds β_{gas}. For approximate calculations in the absence of air aspiration and with adequate accuracy of determination of the main components of the flue gases, the loss due to mechanically incomplete combustion can be approximately determined by means of the relation

$$q_{мех}^{ч} \approx 1 - \frac{\alpha_0}{\alpha_{газ}}, \tag{6.31}$$

where α_0 is the excess air, calculated from the ratio of air and fuel throughput in the furnace; α_{gas} is the excess air, determined on the basis of the composition of the combustion products.

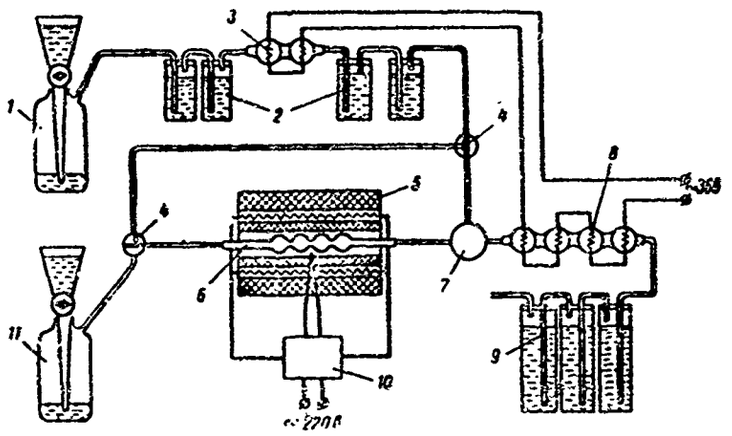

Fig. 136. Schematic view of apparatus for determining the losses due to mechanical incompleteness of combustion by the method of successive combustion: 1) gasometer with oxygen; 2) absorption vessels; 3) two-bulb combustion pipet with platinum spirals; 4) three-way cock; 5) Mars transformer furnace; 6) quartz sampler; 7) mixer; 8) four-bulb combustion tube; 9) absorption vessels with $Ba(OH)_2$; 10) temperature control; 11) gasometer with nitrogen.

The method of separate combustion (Fig. 136) is based on the fact that part of the combustion products, containing an aerosol of fuel and soot, is sucked through a quartz filter tube filled with calcined asbestos. A condensation of the fuel vapor and precipitation of the soot particles then take place. The filter tube is then placed in an electric furnace with a temperature of 400-450°C where a stream of nitrogen evaporates the fuel again and displaces it into a mixer to which pure oxygen is supplied at the same time. The mixture thus formed flows into a combustion chamber where it burns, forming CO_2 and water. The CO_2 in turn reacts with $Ba(OH)_2$ which is backtitrated to give the quantity of carbon contained in the fuel aerosol.

To determine the soot content, the temperature of the furnace is increased to 1000-1200°C and pure oxygen is supplied to the filter tube where the combustion of the soot takes place. The subsequent quantitative determination of the carbon dioxide formed is analogous to the above described method. Strictly speaking, this method does not allow the entire heat loss of the furnace due to mechanical incompleteness of combustion to be determined but only that due to unburned carbon.

During the sampling of the combustion products, their volume throughput, temperature and pressure must be measured, which enables the specific weight concentration of the components to be determined in accordance with the following relations:

$$\delta_т' = \frac{0{,}06kI_1}{C^p I_{п.г}}, \tag{6.32}$$

$$\delta_с' = \frac{0{,}0006kI_2}{I_{п.г}}, \tag{6.33}$$

where k is a correction factor for the 0.1 N solution of $Ba(OH)_2$; I_1 and I_2 are the quantities of 0.1 N $Ba(OH)_2$ solution corresponding to the absorbed carbon dioxide, formed during the combustion of the fuel aerosol (I_1) and soot (I_2), respectively; $I_{p.g}$ is the quantity of combustion products, passed through the filter tube; C^p is the percentage of carbon in the original fuel; 0.06 and 0.0006 respectively, are the titers of the $Ba(OH)_2$ solution for the carbon calculation.

Recalculated per unit of fuel weight, the specific concentrations of the fuel aerosol and soot respectively will be determined as

$$\delta_т = \delta_т'(1 + \alpha L_0), \tag{6.34}$$

$$\delta_с = \delta_с'(1 + \alpha L_0). \tag{6.35}$$

It must be pointed out, however, that the accuracy of determination of the losses due to chemical as well as mechanical incompleteness of combustion is determined not only by the perfection of the methods but equally so by the methods of sampling. The great heterogeneity of the temperature, velocity and concentration fields in the gas conduits of a furnace makes the problem of obtaining a "representative" sample of the combustion products a very difficult task, even for the determination of the gaseous components. This task is further complicated in the determination of the losses due to mechanically incomplete combustion since the liquid and vapor products of incomplete combustion are condensed and precipitated on the walls of the sampling device which assumes special significance when heavy fuels are used. It must be stated that sampling devices which fully satisfy all requirements for the accurate determination of the losses due to mechanically incomplete combustion have not yet been designed; the method of selecting an average sample in furnaces of different types itself has not yet been developed. This makes it sometimes necessary to collect a large number of local samples at different points of the furnace volume or flame which in turn makes the determination of the total efficiency of the combustion process hig_ inconvenient. It is to be hoped that the further development of the existing methods of controlling combustion efficiency, above all the chromatographic method, in addition to the development of entirely new methods of analysis of combustion products, will make it possible not only to greatly simplify and accelerate the determination of the composition of furnace gases but also to obtain new data on the nature of the development of the combustion process of atomized fuel in a turbulent airstream.

Manuscript Page No.	Transliterated Symbols
234	ср = sr = srednyy = average
237	к = k = kaplya = drop
243	ф = f = fotoelement = photocell
243	ф = f = fakel = jet
248	топ = top = toplivo = fuel
248	гор = gor = goreniye = combustion
248	х.н = kh.n = khimicheskaya nedozhoga = chemically incomplete combustion
249	полн = poln = polnyy = total
249	мех = mekh = mekhanicheskyy = mechanical

249 ГОСТ = GOST = gosudarstvennyy obshchesoyuznyy standart = All-Union State Standard

249 ВТИ = VTI = Vsesoyuznyy ordena trudovogo krasnogo znameni teplotekhnicheskiy institut imeni F. E. Dzerzhinskogo = All-Union Red Banner of Labor F. E. Dzerzhinskiy Institute of Heat Engineering

250 хим = khim = khimicheski = chemical

254 п = p = potok = flow

255 газ = gas = gas

257 п.г = p.g. = produkty goreniya = combustion products

REFERENCES

1. Greber, Erk, and Grigul'. Oxnovy ucheniya o teploobmen (Fundamentals of Heat Exchange). IL., 1958.

2. Shorin, S. N. Teploperedacha (Heat Transfer). Stroyizdat, 1952.

3. Rauschenbakh, B. V., S. A. Belyy, et al. Fizicheskiye osnovy rabochego protsessa v kamerakh sgoraniya vozdushno-reaktivnykh dvigateley (Physical Basis of the Processes in the Combustion Chambers of Ramjet Engines). Mashinostroyeniye, 1964.

4. Mikheyev, M. A. Osnovy teploperedachi (Fundamentals of Heat Transfer). Gosenergoizdat, 1949.

5. Godsave, G. Studies of the Combustion of Drops in a Fuel Spray – the Burning of Single Drops of Fuel. Fourth Symposium (International) on Combustion (Combustion and Detonation Wave), Baltimore, 1953.

6. Lewis, B., T. Elbe. Goreniye, plamya i vzryvy v gazakh (Combustion, Flame and Detonations in Gases). IL., 1948.

7. Jost, V. Vzryvy i goreniye v gazakh (Detonations and Combustion in Gases). IL., 1952.

8. Irisov, A. S. Isparyayemost topliv dlya porshnevykh dvigateley i methody eye ispol'zovaniya (Evaporation of Fuels for Piston Engines and Methods of its Utilization). Gostoptekhizdat, 1955.

9. Klyachko, L. A., and A. V. Kudryavtsev. Goreniye kapel' topliva v potoke nagretogo vozdukha (Combustion of Fuel Drops in a Stream of Hot Air). Prikladnaya mekhanika i tekhnicheskaya fizika, No. 6, AN SSSR, 1963.

10. Bellos, Svett. Zazhiganiye i vosplameneniye uglevodorodnykh topliv (Combustion and Ignition of Hydrocarbons Fuels). Collection: Osnovy goreni,a uglevodorodnykh topliv (Fundamentals of the Combustion of Hydrocarbon Fuels). IL., 1960.

11. Varshavskiy, G. A. Goreniye zhidkogo topliva (diffuzionnaya teoriya) (Combustion of Liquid Fuel (Diffusion Theory)). BNT NKAP, 1945.

12. Spaulding, D. Sgoraniye v zhidkostnykh reaktivnykh dvigatelyakh (Combustion in Liquid-Fuel Rocket Engines). Voprosy raketnoy tekhinki, No. 11, 1959.

13. Goldsmith, Penner. O gorenii individual'nykh kapel' topliva v okislitel'noy atmosfere (On the Combustion of Individual Drops of Fuel in an Oxidizing Atmosphere). Voprosy raketnoy tekhniki, No. 2, (26), 1955.

14. Spalding, D. The Combustion of Liquid Fuels. Ch. 5.

15. Izoda, Kumagan. Goreniye kapel' (Combustion of Drops). Collection: Voprosy goreniya (Problems of Combustion). Metallurgizdat, 1963.

16. Brysov, S. I., L. A. Klyachko, and A. B. Ezrokhi. Goreniye kapel' topliva nepodvizhnykh otnositel'no okruzhayushchego vozdukha (Combustion of Fuel Drops Stationary Relative to the Ambient Air). Tr. In-ta im. Baranova, No. 275, 1955.

17. Paleyev, I. I., F. A. Agafonova. Issledovaniye goreniya kapel' zhidkogo topliva (Study of the Combustion of Liquid Fuel Drops). Collection: Voprosy aerodinamiki i teploperedacni v kotel'no-topochnykh protsessakh (Problems of Aerodynamics and Heat Transfer in Boiler and Furnace Processes). Edited by G. F. Knorre. Gosenergoizdat, 1959.

18. Vitman, L. A., B D. Katsnel'son, and I. I. Paleyev. Raspylivaniye zhidkosti forsunkami (Atomization of Liquids in Burners), Gosenergoizdat, 1962.

19. Kobayasi, K. The Engineer Digest, Vol. XVI, No. 1, 1955.

20. Kobayasi, K. An Experimental Study on the Combustion of a Fuel Droplet. Fifth Symposium (International) on Combustion in Engineer and Combustion Kinetics, London, 1955.

21. Novyye metody szhiganiya topliv i voprosy teorii goreniya (New Methods of Ignition of Fuels and Problems of Combustion Theory). Tr. In-ta goryuchikh iskopayemykh AN SSSR, Vol. 19, 1962.

22. Zharkov, B. L. Rezul'taty eksperimental'nykh issledovaniy protsessa sgoraniya odinochnykh kapel' tyazhelykh zhidkikh topliv (Results of Experimental Studies of the Process of Combustion of Single Drops of Heavy Fuels). Collection: Perevod kotel'nykh ustanovok i proizvodstvennykh pechey na gas i zhidkoye toplivo (Conversion of Boiler Installations and Industrial Furnaces to Gas and Liquid Fuel Operation). Tr. Vses. n.-i. in-ta zhel.-dor. transporta, No. 228, Transzheldorizdat, 1961

23. Spolding, D. Eksperimental'noye issledovaniye goreniya i zatukhaniya zhidkogo topliva na sfericheskoy poverkhnosti (Experimental Study of the Combustion and Extinction of Liquid Fuel on a Spherical Surface). Voprosy raketnoy tekhniki, No. 3 (21), 1954.

24. Goldsmith, Opyty po goreniyu otdel'nykh kapel' topliva (Experiments on the Combustion of Single Fuel Drops). Voprosy raketnoy tekhniki, No. 2 (38), 1957.

25. Gurevich, M. A., and V. B. Shteynberg. Temperatura plameni odinochnoy kapli zhidkogo topliva (Flame Temperature of Single Drops of Liquid Fuel). ZhTF, Vol. XXVIII, No. 2, 1958.

26. Masdin, E., and M. Thring. Combustion of Single Droplets of Liquid Fuel. J. Inst. Fuel., No. 35, 1962.

27. Agafonova, F. A., M. A. Gurevich, and E. F. Tarasova. Usloviya ustoychivogo goreniya yedinichnykh kapel' zhidkogo topliva (Conditions of Stable Combustion of Single Drops of Liquid Fuel). Tr. III Vsesoyuznogo soveshchaniya po teorii goreniya, AN SSSR, 1960.

28. Holl, A., and J. Diderichsen. An Experimental Study of the Burning of Single Drops of Fuel in Air of Pressures up to Twenty Atmospheres. Cm. 5.

29. Agafonova, F. A., M. N. Gurevich, and I. I. Paleyev. K teorii goreniya kapli zhidkogo topliva (On the Theory of Combustion of Liquid Fuel Drops). ZhTF, Vol. XXVII, No. 6, 1957.

30. Vyrubov, D. N. Smeseobrazovaniye v dvigatelyakh dizelya (Mixture Formation in Diesel Engines). Collection: Rabochiye protsessy dvigateley vnutrennego sgoraniya (Processes in Internal Combustion Engines). Mashgiz, 1946.

31. Klyachko, L. A., and Z. V. Istratova. K teorii nizhnego predela rasprostraneniya plameni v dvukhfaznoy smesi (Contribution to the Theory of the Lower Limit of Flame Propagation in a Binary Mixture). Tr. III. Vsesoyuznogo soveshchaniya po teorii goreniya, AN SSSR, 1960.

32. Kumagai. Goreniye raspylennogo topliva (Combustion of Atomized Fuel). Collection: Voprosy goreniya (Problems of Combustion). Metallurgizdat, 1963.

33. Glinkov, M. A. Osnovy obshchey teorii pechey (Fundamentals of the General Theory of Furnaces). Metallurgizdat, 1962.

34. Spolding, D. B. Osnovy teorii goreniya (Fundamentals of Combustion Theory). Gosenergoizdat, 1959.

35. Probert, R. Philosophical Magazine, Vo. 37, 1946.

36. Sodkha. Vnutrennaya ballistika zhidkostnykh reaktivnykh dvigateley (Internal Ballistics of Liquid Fuel Rocket Engines), Voprosy raketnoy tekhniki, No. 3, 1959.

37. Goreniye dvukhfaznykh smesey (Combustion of Binary Mixtures). Izd. Energeticheskogo in-ta AN SSSR, 1958.

38. Basevich, V. Ya., and S. M. Kagarko. O nekotorykh osobennostyakh goreniya raspylennogo topliva (Some Peculiarities of Combustion of Atomized Fuel). Tr. III. Vsesoyuznogo sobeshchaniya po teorii goreniya AN SSSR, 1960.

39. Kling, R. Mikrofotografische Untersuchungen von Brennstoffnebeln in Brennkammern (Microphotographic Studies on Fuel Aerosols in Combustion Chambers), BWK, Vol. 10, No. 6, 1958.

40. Inozemtsev, N. V., and V. K. Koshkin. Protsessy sgoraniya v dvigatelyakh (Combustion Processes in Engines). Mashgiz, 1949.

41. Kinbara, Ikegami. O polozhitel'nykh i otritsatel'nykh ionakh v diffuzionnykh plamenakh (On Positive and Negative Ions in Diffusion Flames), see 5.

42. Marsden, R. The Electrical Noise of Turbulent Flames. See 5.

43. Calcot. Protsessy obrazovaniya ionov v plamenakh (Processes of Formation of Ions in Flames), Voprosy raketnoy tekhniki, No. 4 (46), 1958.

44. Mikhaylov, A. I., et al. Rabochiy protsess i raschet kamer sgoraniya gazoturbinnykh dvigateley (Working Process and Calculation of the Combustion Chambers of Gas Turbine Engines). Oborongiz, 1959.

45. Vyrubov, D. N O metodike rascheta isparenlya topliva (On the Method of Calculat of Fuel Evaporation). Collection: Dvigateli vnutrennego sgoraniya (Internal Combustion Engines). Tr. MVTU, No. 25, 1965.

46. Protsessy goreniya (Combustion Processes). Fizmatgiz, 1961.

47. Sletscher and Churchill. Radiatsionnyy nagrev chastits aerovzvesi (Radiative Heating of Aerosol Particles). Voprosy raketnoy tekhniki, No. 6 (42), 1957.

48. Kanevsky, J. Jet Propulsion, No. 26, 1956.

49. Bolt, Boyle and Arbor. Sgoraniye zhidkogo raspylennogo topliva (Combustion of Atomized Liquid Fuel). Voprosy raketnoy tekhniki, No. 5 (41), 1957.

50. Basevich, V. Ya. O skorosti goreniya raspylennogo topliva (On the Rate of Combustion of Atomized Fuel). Collection: Sgoraniye i smeseobrazovaniye v dizelyakh, AN SSSR, 1960.

51. Tesner, P. A. Obrazovaniye sazhi pri razlozhenii i gorenii uglevodorodov (Formation of Soot During the Decomposition and Combustion of Hydrocarbons). Gazovaya promyshlennost', No. 5, 1961.

52. Fenimore, Jones, Moore. Obrazovaniye ugleroda v ploskikh plamenakh pri 1600°K (Carbon Formation in Flat Flames at 1600°K). See 15.

53. Zinger, Grummer. Obrazovaniye ugleroda v ochen bogatykh uglevodorodo-vozdushnykh plamenakh. I-sledovaniye khimicheskogo sostava produktov reaktsii, temperatury, ionizatsii i struktury uglerodistykh chastits (Formation of Carbon in Rich Hydrocarbon-Air Flames. Study of the Chemical Composition of the Reaction Products, and the Temperature, Ionization and Structure of the Carbon Particles), see 15.

54. Van der Held. Obrazovaniye i gazifikatsiya ugleroda v atmosfere produktov sgoraniya (Formation and Gasification of Carbon in the Combustion Product Atmosphere), see 15.

55. Porter, G. Carbon Formation in the Combustion Wave. See 5.

56. Shtelin, Freyzi, Anderson. Obrazovaniye ugleroda iz atsetilena (Carbon Formation from Acetylene), see 43.

57. Sokolin, A. S. Kineticheskaya interpretatsiya M-protsessa (Kinetic Interpretation of the M-Process). Collection: Goreniye i smeseobrazovaniye v dizelyakh, AN SSSR, 1960.

58. Kireyev, V. A. Kurs fizicheskoy khimii (Course of Physical Chemistry). Goskhimizdat, 1955.

59. Problemy okisleniya uglevodorodov (Problems of the Oxidation of Hydrocarbons), AN SSSR, 1957.

60. Shalla, Clarke, MacDonald. Issledovaniye dymoobrazovaniya i dozhiganiya dymn v laminarnykh plamenakh (Study of Smoke Formation and Afterburning of the Smoke in Laminar Flames). Voprosy raketnoy tekhniki, No. 5 (35), 1956.

61. Obrazovaniye dyma i nagara pri gorenii uglevodorodo-vozdushnykh smesey (Formation of Smoke and Deposits During the Combustion of Hydrocarbon-Air Mixtures). Collection: Osnovy goreniya uglevodorodnykh topliv (Fundamentals of the Combustion of Hydrocarbon Fuels), IL., 1960.

62. Tamura, Tanasawa. Isparenive i goreniye kapli, soprikashyushcheysya s goryachey poverkhnost'yu (Evaporation and Combustion of a Drop in Contact with a Hot Surface), see 15.

63. Pavlov, S. F., and S. S. Okhotnikov. Osobennosti szhiganiya nizkosortnykh zhidkikh topliv v pryamotochnykh kamerakh sgoraniya (Peculiarities of the Combustion of Lowgrade Liquid Fuels in Ramjet Combustion Chambers). Collection: Voprosy gazoturbinnoy tyagi (Problems of Gas Turbine Thrust). Transzheldorizdat, 1962.

64. Paleyev, I. I. Opovedenii yedinichnykh kapel' tyazhelogo topliva v kamerakh s zakruchennym potokom (On the Behavior of Single Drops of Heavy Fuel in Vortex Chambers). Tr. III. Vsesoyuzhogo soveshchaniya po teorii goreniya, AN SSSR, 1960.

65. Chlenov, A. G. Bezdymnoye szhiganiye mazutov (Smokeless Combustion of Petroleum Residues). Promyshlennaya energetika, No. 4, 1963.

66. Speranskiy, B. A. Szhiganiye mazuta v topkakh parovykh kotlov FRG (Combustion of Petroleum Residue in the Furnaces of Steam Boilers in the FRG). Energokhozyaystov za rubezhom, No. 4, 1960.

67. Gvozdetskiy, L. A., A. D. Gorbanenko, V. V. Karpov, and L. M. Tsiryulnikov. Szhiganiye orlanskoy nefti povyshennoy stabilizatsii v topkakh parovykh kotlov (Combustion of Orlansk Highly Stabilized Crude Oil in Steam Boiler Furnaces). Elektricheskiye stantsii, No. 10, 1962.

68. Kruk, M. T., P. I. Yanko, and L. A. Stepanov. Osobennosti puska i osvoyeniya kotla TGM-84 pri szhiganii sernistogo topliva (Pecularities of the Startup and Operation of the Boiler TGM-84 with Combustion of Sulfur-Containing Fuel). Elektricheskiye stantsii, No. 5, 1964.

69. Gvozdetskiy, L. A., A. D. Gorbanenko, G. K. Krasil'nikov, A. V. Martynov, and L. I. Tsiryul'nikov. Opyt szhiganiya stabilizirovannoy vysokosernistoy nefti v topkakh parovykh kotlov elektrostantsii (Experimental Combustion of Stabilized High Sulfur Crude Oil in the Boiler Furnaces of Electrical Power Stations). Edited by the Doctor of Techn. Sciences, Prof. Z. I. Geller. Izd. BTI, Orgres, 1964.

70. Dzhekin, K., D. Anderson, and R. Thompson. Issledovaniye nagara v kotlakh rabotayushchikh na mazutakh (Study of Deposits in Boilers Operated on Petroleum Residues). Collection: Prisadki k motornym i toplivan (Additives for Motor and Boiler Fuels). Edited by A. L. Feygin. Izd. TsNIITEneft, 1957.

71. Knyazev, N. M., A. V. Sinyavskiy, and M. G. Starkov. Izmeneniye prisadkami svoystv otlozheniy na poverkhnostyakh nagreva mazutnykh kotlov (Modification of the Properties of Deposits on the Heating Surfaces of Boilers Operated on Petroleum Residue by Means of Additives), Elektricheskiye stantsii, No. 1, 1957.

72. Fat'yanov, A. D. Zola mazutov i obrazovaniye otlozheniy pri ikh szhiganii (Ash of Petroleum Residue and Formation of Deposits During Their Combustion). Collection: Fiziko-khimicheskiye i ekspluatatsionnyye svoystva sernistykh kotel'nykh i dizel'nykh topliv (Physicochemical and Operational Properties of Sulfur Bearing Boiler and Diesel Fuels). Izd. GOSINTI, 1958.

73. Jones, C., and R. Hardy. Petroleum Ash Components and Their Effect on Refractories. Jnd. Eng. Chem., Vol. 44, No. 11, 1952.

74. Kuznetsov, N. V., L. I. Luzhkov, and F. M. Beloborodov. Ochistka chugunnoy drob'yu konvektivnykh poverkhnostey kotel'nykh agregatov (Cleaning of the Convection Surfaces of Boiler Installations with Cast-Iron Shot). Teploenergetika, No. 12, 1957.

75. Kuznetsov, N. V., and G. I. Luzhkov. Voprosy proyektirovaniya ustroystv dl a drobevoy ochistki konvektivnykh poverkhnostey kotel'nykh agregatov (Problems of Designing of Equipment for Shotblasting of the Convection Surfaces of Boiler Installations). Teploenergetika, No. 1, 1958.

76. Rudakov, Ya. D., A. V. Martyinov, and V. V. Kuznetsova. Prisadka kaustitcheskogo magnezita pri szhiganii mazutov (Additives of Calcined Magnesia for the Combuation of Petroleum Residue). Elektricheskiye stantsie, No. 9, 1961.

77. Krasnoselov, G. K., and V. K. Myasnikov. Stendovyye izmereniya effektivnosti vvoda magnezita v dymovyye gazy kotloagregata, rabotayushchego na vysokosernistom mazute (Stand Measurements of the Effectiveness of Magnesite Addition to the Flue Gases of a Boiler Installation, Operated with High Sulfur Petroleum Residue). Elektricheskiye stantsii, No. 3, 1964.

78. Gorin, V. I., and A. P. Kovalenko. O sovmestnom szhiganii neftepromyslogo gaza i sernistogo mazuta (Simultaneous Combustion of Natural Gas and Sulfurbearing Petroleum Residue). Elektricheskiye stantsii, No. 3, 1964.

79. Grumley, P., and A. Fletcher. The Formation of Sulphur Trioxide in Flue Gases. J. of the Inst. of Fuel., Vol. 29, No. 187, 1956.

80. Gumz, W. Rauchgastaupunkt udn Rauchgaskorrosion (Dew Point of Flue Gas and Flue Gas Corrosion). BWK., Vol. No. 3, 1957.

81. Maslennikov, M. S. Kontrol' vlazhnosti topliva, dymovykh gazov i tochki rosy (Control of the Moisture Content of Fuel, Flue Gases and Dew Point). Gosenergoizdat, 1951.

82. Shitsman, S. E. Tochka rosy dymovykh gazov (Dew Points of Flue Gases). Teploenergetika, No. 6, 1954.

83. Geller, Z. I., and F. A. Lipinskiy. Ob effektivnosti szhiganiya mazuta (diskussiya s A. K. Vnukovym) (On the Efficiency of Combustion of Petroleum Residue (Discussion with A. K. Vnukov)). Elektricheskiye stantsii, No. 1, 1964.

84. Glaubitz, F. The Economic Combustion of Sulphur-Containing Heating Oil. Combustion, No. 1, 1963.

85. Glaubitz, F. The Economic Combustion of Sulphur-Containing Heating Oil. Combustion, No. 3, 1963.

86. Cooper, D. K. Low Excess Air Firing Heat Rate at Large Unfility. Combustion, No. 2, 1964.

87. Reley, D. V. Teoriya zvuka (Theory of Sound), Vol. 2, Gosenergoizdat, 1955.

88. Henlein, A. Raspad strui zhidkosti (Disintegration of a Liquid Jet), Coll.: "Dvigateli vnutrennego sgoraniya" (Internal Combustion Engines), Vol. 1, ONTI [Department of Scientific and Technical Information], 1936.

89. Weber, K. Raspad strui zhidkosti (Disintegration of Liquid Jet), Coll.: "Dvigateli vnutrennego sgoraniya," Vol. 1, ONTI, 1936.

90. Lyshevskiy, A. S. Raspad strui vyazkoy zhidkosti pod vozdeystviem nesimmetrichnykh bozmushcheniy (Disintegration of a Jet of a High-Viscosity Liquid under the Influence of Asymmetrical Perturbations), Izvestiya VUZov, seriya "Energetika," No. 3, 1959.

91. Lyshevskiy, A. S. Osesimmetrichnyy raspad krugloy strui vyazkoy zhidkosti (Axially-Symmetrical Disintegration of High-Viscosity Liquid Jet with Circular Cross Section), Izvestiya VUZov, seriya "Energetika," No. 7, 1960.

92. Lyshevskiy, A. S. O granitsakh perekhoda mezhdu otdel'nymi vidami raspada zhidkoy struy (On the Transitions Between Different Forms of Disintegration of a Liquid Jet), Izvestiya VUZov, seriya 'Energetika," No. 1, 1961.

93. Lyshevskiy, A. S. Ob ustoychivosti i raspade poloy strui vyazkoy zhidkosti, dvizhushcheysya s malymi skorostyami (On the Stability and Disintegration of a Hollow Jet of a High-Viscosity Liquid, Moving at Low Velocities), Izvestiya VUZov, seriya "Energetika," No. 3, 1958.

94. Dityakin, Yu. F., and R. I. Yagodkin. Vliyaniye periodicheskikh kolebaniy skorosti i plotnosti sredy na raspad zhidkikh struy (Effect of Periodic Fluctuations of the Velocity and Density of the Medium on the Disintegration of a Liquid Jet), Izv. AN SSSR, No. 4, 1957.

95. Borodin, V. A., Yu. F. Dityakin, and V. I. Yagodkin. O droblenii sfericheskoy kapli v gazovom potoke (On the Breakdown of a Spherical Drop in a Gas Stream), Zhurnal prikladnoy mekhaniki i tekhnicheskoy fiziki, No. 1, 1962.

96. Borodin, V. A., and Yu. F. Dityakin. Neustoychivyye kapillyarnyye vol'nyna poverkhnosti razdela dvukh vyazkikh zhidkostey (Unstable Capillary Waves on the Phase Boundary of two Liquids), Prikladnaya matematika i mekhanika, Vol. 23, No. 3, 1949.

97. Ramzin, L. K., G. Yu. Kozlinskiy, and Yu. O. Novi. Primeneniye parafinistogo mazuta v kotel'nykh ustanovkakh (Utilization of Paraffin-Containing Petroleum Residue in Boiler Installations), Izvestiya teplotekhnicheskogo instituta, No. 2 (25), 1927.

98. Triebning, H. Der Einblase und Einspritzvorgang bei Dieselmaschinen (The Air and Fuel Injection Process in Diesel Engines), Vienna, 1925.

99. Kalish, G. G. Issledovaniye forsunok beskompressornykh dizeley (Study of the Atomizers of Compressorless Diesels), Izv. NATI, Nos. 3-4, 1932.

100. Belokon', N. I. Ispytaniye forsunok na parokhode "Grazhdanin" (Testing of Burners on the Steamer "Grazhdanin" (citizen)), Transpechat' NKPS, 1939.

101. Klyuzner. Protsess vpryskivaniya v beskompressornykh dizelyakh (Atomization Process in Compressorless Diesels), Coll.: "Dvigateli vnutrennego sgoraniya," Vol. 1, 1936.

102. Buzukov, A. A. Razrusheniye kapel' i struy zhidkosti vozdushnoy udarnoy vol'noy (Disintegration of Drops and Jets of Liquid by an Air Shock Wave), Zhurnal prikladnoy mechaniki i tekhnicheskoy fiziki, No. 2, 1963.

103. Volynskiy, M. S. O droblenii kapel' v potoke vozdukha (On the Disintegration of Drops in an Airstream), Dokl. AN SSSR, Vol. 62, No. 3, 1948.

104. Degtev, O. N. Skhema deformatsii kapel' v potoke gaza i granitsy ustoychivosti kapel' (Scheme of Drop Deformation in a Gas Stream and Stability Limits of the Drops), Coll.: "Ratsional'noye ispol'zovaniye energeticheskikh resursov promyshlennosti," Tr. Ural'skogo politekhnicheskogo instituta im. S. M. Kirova, No. 61. Metallurgizdat, 1956.

105. Volynskiy, M. S. Izucheniye drobleniya kapel' v gazovom potoke (Study of the Disintegration of Drops in a Gas Stream), Doklady AN SSSR, Vol. 68, No. 2, 1949.

106. Bukhman, S. V. Eksperimental'noye issledovaniye raspada kapel' (Experimental Study of Drop Disintegration), Vestnik AN Kazakhskoy SSSR, No. 11, 1954.

107. Volynskiy, M. S., and L. I. Chernoshchekov. Issledovaniye ispareniya kapel' zhidkostey v potoke vozdukha (Study of the Evaporation of Liquid Drops in an Airstream), Tr. III Vsesoyuznogo soveshchaniya po teorii goreniya, Vol. 2, AN SSSR, 1960.

108. Wölfjen. Über die Feinheit der Brennstoffzerstaubung in Ölmaschinen (On the Fineness of Fuel Atomization in Oil Burning Engines), Darmstadt, 1925.

109. Kuhen, R. Über die Zerstaubung flüssiger Brennstoffe (On the Atomization of Liquid Fuels), Motorwagen, No. 19, 1925-1925.

110. Strazhevskiy, L. M. O dal'noboynosti strui zhidkogo topliva v vstrechnom potoke vozdukha (On the Range of a Jet of Liquid Fuel in an Oncoming Airstream), Tekhnika vozdushnogo flota, No. 1, 1938.

111. Natanzon, O. Ya. O raspylivanii topliva v dvigatelyakh dizelya (Atomization of Fuel in Diesel Engines), Dizelestroeniye, Nos. 3-5, 1938.

112. Fuks, N. A. Uspekhi mekhaniki aerozoley (Successes of the Mechanics of Aerosols), AN SSSR, 1961.

113. Dunskiy, V. F. O koagulyatsii pri raspylivanii zhidkosti (On Coalescence During Atomization of Liquids), Zhurnal tekhnicheskoy fiziki, Vol. 26, No. 6, 1956.

114. Ul'yanov, I. E. O vnutrikanal'nom raspade pri raspylivaniya topliva (On the Disintegration of Fuel Inside Channels During Atomization), Izv. AN SSSR, otdeleniye tekhnicheskikh nauk, No. 8, 1954.

115. Hunsaker, J. Mech. Eng., 57, 1935.

116. Shal'nev, K. K. Kavitatsiya nerovnostey poverkhnosti (Cavitation on Surface Irregularities), Zhurnal tekhnicheskoy fiziki, Vol. 21, No. 2, 1951.

117. Brauer, H. Strömung und Wärmeubergang bei Rieselfilmen (Flow and Heat Transfer in Dripping Films), VDI - Forschungsheft, No. 457, 1956.

118. Feind, R. Strömungsuntersuchungen bei Gegenstrom von Rieselfilmen und Gas in lotrechten Rohren (Flow Studies with Counter-Currents on Dripping Films and Gas in Vertical Tubes), VDI - Forschungsheft, No. 481, 1960.

119. Vereshchagin, L. F., A. A. Semerchan, and S. S. Sekoyan. K voprosu o raspade vysokoskorostnoy vodyanoy strui (On the Problem of the Disintegration of a High-Velocity Water Jet), Zhurnal tekhicheskoy fiziki, Vol. 29, No. 1, 1959.

120. Kornfel'd, M. Uprugost' i prochnost' zhidkostey (Elasticity and Strength of Liquids), GITTL, 1951.

121. Kutovoy, V. A. Raspylivaniye topliva dizel'nymi forsunkami (Fuel Atomization in Diesel Atomizers), Oborongiz, 1959.

122. Oschatz, Werner. Düsen und Strahluntersuchungen (Nozzle and Jet Studies), Dresden, 1940.

123. Strauber, H. Die elektrostatische Zerstäubung von Flüssigkeiten (Electrostatic Atomization of Liquids), Zeitschrift für angewandte Physik, No. 6, 1954.

124. Minskiy, E. M. O pul'satsiyakh skorosti pri vpolne ustanovivshemsya turbulentnom techenii (On the Velocity Pulsations in Steady-State Turbulent Flow), Zhurnal tekhnicheskoy fiziki, Vol. 10, No. 19, 1940.

125. Chernov, A. P. Dvizheniye melkikh tverdykh chastits v svobodnom vozdushnom potoke (Motion of Fine Solid Particles in a Free Airstream), Doklady AN SSSR, Vol. 105, No. 6, 1955.

126. Kukharev, M. N. Issledovaniye raspylivaniya topliva primenitel'no k bystrokhodnym dizelyam (Study of Fuel Atomization in High-Speed Diesels), Coll.: "Issledovaniye raspylivaniya i goreniya dizel'nogo topliva," Tr. Tsentral'nogo nauchno-issledovatel'skogo avtomobilnogo i avtomotornogo instituta, No. 87, Mashgiz, 1959.

127. Lyshevskiy, A. S. K voprosu ob opredelenii parametrov, kharakterizuyushchikh kachestvo raspylivaniya zhidkogo topliva (On the Problem of the Determination of the Parameters Characterizing the Atomization Efficiency of Liquid Fuel), Izvestiya VUZov, seriya "Mashinostroeniye," No. 7, 1959.

128. Pigford, R. J., and C. Pulz. Performance Characteristics of Spray-Type Absorption Equipment, Ind. and Eng. Chem., Vol. 43, No. 7, 1951.

129. Geller, Z. I., and M. Ya. Moroshkin. Metodika rascheta i konstruktsiya tsentrobezhnykh forsunok dlya raspylivaniya topochnykh mazutov (Method of Calculation and Design of Centrifugal Atomizers for Petroleum Residue Fuels), Teploenergetika, No. 4, 1963.

130. Blokh, A. G., and Ye. S. Kichkina. Srednly diametr kapel' pri raspylivanii zhidkogo topliva tsentrobezhnymi forsunkami (Average Drop Diameter during Atomization of Liquid Fuel with Centrifugal Atomizers), Teploenergetika, No. 9, 1955.

131. Plitt, I. G., I. N. Polyanchikov, and S. M. Ivanov. O nekotorykh predvaitel'nykh rezul'tatakh issledovaniya raspyla mekhanicheskimi forsunkami (On Some Preliminary Results of the Study of Atomization with Mechanical Atomizers), Tr. Dnepropetrovskogo khimikotekhnologicheskogo instituta im. Dzerzhinskogo, No. 16, Part 2, "Khimiya i khimicheskaya tekhnologiya" (Chemistry and Chemical Technology), Dnepropetrovsk, 1963.

132. Degtev, O. N. O raspylivaniye vyazkikh zhidkostey (On the Atomization of High-Viscosity Liquids, Coll.: "Ratsional'noye ispol'zovaniye energeticheskokh resursov promyshlennosti, Tr. Ural'skogo politekhnicheskogo instituta im. Kirova, No. 61, 1956.

133. Dyatlov, I. P. Vozdushno-mekhanicheskoye raspylivaniye topliva v gazoturbinnykh dvigatelyakh (Pneumatic-Mechanical Atomization of Fuel in Gas Turbine Engines), Coll.: "Aviatsionnyye dvigatel," Tr. Kazanskogo aviatsionnogo instituta, No. 55, Kazan', 1960.

134. Vitman, L. A., B. D. Katsnel'son, and M. M. Efros. Raspylivaniye zhidkogo topliva pnevmaticheskimi forsunkami (Atomizations of Liquid Fuel with Pneumatic Atomizers), Coll.: "Voprosy aerodinamiki i teploperedachi v kotel'no-topochnykh protsessakh, Gosenergoizdat, 1958.

135. Zel'dovich, Ya. B. K teorii obrazovaniya novoy fazy, kavitatsiya (On the Theory of Formation of a New Phase and Cavitation), Zhurnal eksperimental'noy i teoreticheskoy fiziki, Vol. 12, Nos. 11-12, 1942.

136. Treng, G., and P. Grossman. K zakonu raspredeleniya razmerov kapel' pri rapylivanii (On the Distribution Law of the Drops in Atomization), Voprosy raketnoy tekhniki, No. 4 (22), 1954.

137. Li, D. U. Vliyaniye konstruktsiy sopla i usloviy raboty na raspylivaniye i raspredeleniye toplivnykh struy (Effect of Nozzle Design and Operating Conditions on the Atomization and Distribution of the Fuel Jets), Coll. "Dvigateli vnutrennego sgoraniya," Part 1, ONTI, 1936.

138. Astakhov, I. V. Vliyaniye vyazkosti i drugikh faktorov na mel'kost' raspyla (Effect of Viscosity and Other Factors on the Fineness of Dispersion in Atomization), Dizelstroeniye, No. 2, 1938.

139. Gebhardt, H., Die Tropfeugrösen bei Drüllzerstöubung (The Drop Sizes in Atomization), B.W.K., Vol. 10, No. 8, 1958.

140. Sauter, J. V.D.I., Heft 312, 1926.

141. Nikigama, S., and J. Tanasava. Experiments on the Atomization of Liquids in Airstream, Trans. of ASME, Rep. 4 (Japan), No. 18, 5, 1938.

142. Baytron. Raspylivaniye zhidkostey sverkhzvukovymi vozdushnymi struyami (Liquid Atomization with Supersonic Airflows), Voprosy raketnoy tekhniki, No. 5 (29), 1955.

143. Mugele, R., and H. Evans. Droplet Size Distribution in Sprays, Ind. Enol. Chem., Vol. 43, No. 6, 1951.

144. Blinov, V. I. O dispersnosti mekhanicheski raspylennoy vody (On the State of Dispersion of Mechanically Atomized Water), Tr. Vsesoyuznogo teplotekhnicheskogo instituta, 1930.

145. Feind, R. Strömungsuntersuchungen bei Gegenstrom von Rieselfilmen und Gas in lotrechten Rohren (Flow Studies on Counter Currents of Dripping Films and Gas in Vertical Tubes), VDI Forschungsheft, No. 481, 1960.

146. Brauer, H. Widerstandsgesetzte für innen berieselte und gasdurchströmte senkrechte Rohre (Laws of Resistance for Vertical Tubes with Dripping Liquids and Counter-Current Gas Flow), Chem. Ind. Techn., No. 11, 1960.

147. Vulis, L. A., and N. N. Terekhina. Rasprostraneniye turbulentnoy strui gaza v srede inoy plotnosti (Propagation of a Turbulent Gas Jet in a Medium with Different Density), Zhurnal tekhnicheskoy fiziki, Vol. 29, No. 6, 1956.

148. Ershin, Sh. A., and Z. B. Sakipov. Issledovaniye nachal'nogo uchastka turbulentnykh struy szhimaemogo gaza (Study of the Initial Section of a Turbulent Jet of a Compressed Gas), Zhurnal tekhnicheksoy fiziki, Vol. 29, No. 1, 1959.

149. Abramovich, G. N. Teoriya turbulentnykh struy (Theory of Turbulent Flow), Fizmatgiz, 1960.

150. Kulagin, L. V. Kharateristiki dlya otsenki tonkosti raspylivaniya topliva (Characteristics for Estimating the Fineness of Dispersion of Fuel), Coll. "Issledovaniye lokomotivnykh gazoturbinnykh dvigateley," Tr. vsesoyuznogo nauchno-issledovatel'skogo instituta zheleznodorozhogo transporta, No. 214, Transzheldorizdat, 1961.

151. Spravochnik teplotekhnika (Manual of Heat Engineering), Vol. 2, Gosenergoizdat, 1949.

152. Dityakin, Yu. F., and A. N. Britneva. Obobshcheniye s pomoshch'yu bezrazmernykh kriteriev rezul'tatov izmereniy razmerov kapel' pri raspylivanii zhidkostey tsentrobezhnymi forsunkami (Generalization by Means of Dimensionless Criteria of the Measurement Results on Drops During Atomization of Liquids with Centrifugal Atomizers), Teploenergetika, No. 11, 1959.

153. Osnovy preyektirovaniya i kharakteristiki gazoturbinnykh dvigateley (Fundamentals of the Design and Characteristics of Gas Turbine Engines), Mashinostroeniye, 1964.

154. Sauter, J. Die Grossenbestimmung der in Gemischnebeln von Verbrennungskraftmaschinen vorhandenen Brennstoffteilchen (Size Determination of Fuel Particles Present in the Aerosols of Internal Combustion Engines), VDI, Heft 279, 1926.

155. Yeltyshev, B. N. Primeneniye vysokovyazkikh kreking-mazutov dlya otopleniya promyshlennykh pechey (Utilization of High-Viscosity Cracking Residues for Firing Industrial Furnaces), AN SSSR, 1954.

156. Knorre, F. G. Topochnyye protsessy (Furnace Processes), Gosenergoizdat, 1958.

157. Kutateladze, S. S., and R. V. Tsukerman. Ocherk rabot russkikh uchenykh i inzherenov v oblasti kontel'noy tekhniki (Synopsis of Works of Russian Scientists and Engineers in the Field of Boiler Engineering), Gosenergoizdat, 1951.

158. Ustroystvo dlya vvoda vtorichnogo vozdukha v zonu sgoraniya mazuta (Device for Introducing Secondary Air into the Combustion Zone of Petroleum Residue), French Patent, cl. 23, I, 23, II, No. 1274920, 25 Sept. 1961 (1), 110 (3), No. 888113, 24 Jan. 1962.

159. Teplovoy raschet kotel'nykh agregatov (Heat Calculation of Boiler Installations), Standard method, Gosenergoizdat, 1957.

160. Panasenko, M. D., and S. G. Agababov. Vliyaniye velichiny topochnoy kamery na dopustimoye po usloviyam goreniya teplovoye napryazheniye (Effect of the Furnace Chamber Size on the Heat Stress Permissible in Connection with the Combustion Conditions), Teploenergetika, No. 4, 1961.

161. Miller, H., and E. Beargsley. Spray Penetration with a Simple Fuel Injection Nozzle, NACA, No. 222, 1926.

162. Astakhov, I. V. Priblizhennyy metod otsenki konusa raspyla, dal'noboynosti i melkosti raspyla strui topliva beskompressornogo dizelya (Approximate Method of Estimating the Atomization Cone, the Range and Fineness of Dispersion of the Fuel Jet of a Compressorless Diesel), Dizelestroeniye, Nos. 10-11, 1939.

163. Mehlig, H. Zur Physik der Brennstoffstrahlen in Dieselmaschinen (On the Physics of the Fuel Jets in Diesel Engines), ATZ, Nos. 10-11, 1939.

164. Lyshevskiy, A. S. Primeneniye zakonov turbulentnoy diffuzii k issledovaniyu rasseivaniya zhidkikh struy, vytekayushchikh iz malykh otverstiy (Application of the Laws of Turbulent Diffusion to the Study of the Scattering of a Liquid Jet Emerging from Small Orifices), Tr. Novocherkasskogo politekhnicheskogo instituta, Vol. 39/53, Yerevan, 1957.

165. Gurvits, A. A. K voprosu o dvizhenii tverdoy chastitsy v potoke gaza, Izvestiya VUZov, seriya "Energetika," No. 8, 1963.

166. Skvortsov, G. E. O dvizhenii chastitsy v svobodnoy strue (On the Motion of a Particle in a Free Jet), Inzhenerno-fizicheskiy zhurnal, No. 8, 1964.

167. Litvinov, A. T. Ob otnositel'nom dvizhenii chastitsy (ili kapli zhidkosti) v skorostnom gazovom potoke (On the Relative Motion of a Particle (or Fuel Drop) in a Fast Gas Stream), Teploenergetika, No. 5, 1964.

168. Khudyakov, G. P. O gorenii kapli zhidkogo topliva, nakhodyashcheysya v polete (On the Combustion of a Drop of Luquid Fuel during the Flight Trajectory), Izvestiya AN SSSR, OTN, No. 4, 1949.

169. Penner, S. S., and T. T. Datner. Problemy goreniya v zhidkostnykh raketnykh dvigatelyakh (Combustion Problems in Liquid Rocket Engines), Coll. "Zhidkiye i tverdyye raketnyye topliva," IL, 1960.

170. Vyrubov, D. N. O metodike rascheta isparenlya topliva (On the Method of Calculation of Fuel Evaporation), Coll. "Dvigateli vnutrennego sgoraniya," Mashgiz, 1954.

171. Zuev, V. S., and L. S. Skubachevskiy. Kamery sgoraniya vozdushnoreaktivnykh dvigateley (Combustion Chambers of Turbojet Engines), Oborongiz, 1958.

172. Gershman, I. I. Vosplameneniye i goreniye dizel'nogo topliva v savisimosti ot kachestva ego raspylivaniya (Ignition and Combustion of Diesel Fuel as a Function of the Atomization Efficiency), Coll. "Sgoraniye i smeseobrazovaniye v dizelyakh," AN SSSR, 1960.

173. Gulin, Ye. I. Vliyaniye stepeni i odnorodnosti raspylivaniya topliva na protsessy vosplameneniya i goreniya v dizele (Effect of the Degree of Uniformity of Atomization of the Fuel on the Processes of Ignition and Combustion in a Diesel), Coll. "Sgoraniye i smeseobrazovaniye v dizelyakh," AN SSSR, 1960.

174. Browning, Taylor, and Kroll. Vliyaniye razmera chastitsy na goreniye odnorodnykh aerozoley (Effect of Particle Size on the Combustion of Homogeneous Aerosols), Voprosy raketnoy tekhniki, No. 5, (14), 1957.

175. Lebedev, B. P. O modelirovanii kamer sgoraniya (Modelling of Combustion Chambers), Coll. "Problemy gazoturbostroeniya," Tr. Mezhvuzovskoy nauchno-tekhnicheskoy konferentsii, MVTU, 1958.

176. Vinogradov, Ye. S. Analiz podobiya protekaniya protsessa goreniya zhidkogo topliva v kamerakh gazoturbinnykh dvigateley i rezul'taty issledovaniya rezhimnykh i konstruktivnykh faktorov na protsess (Similarity Analysis of the Combustion Process of Luquid Fuel in the Chambers of Gas-Turbine Engines and Results of the Study of the Operating and Design Factors on the Process), IL, 1960.

177. Doroshenko, V. Ye. O protsesse goreniya v kamere gazoturbinnogo dvigatelya (On the Combustion Process in the Chamber of a Gas-Turbine Engine), Tr. III Vsesoyuznogo soveshchaniya po teorii goreniya, AN SSSR, 1960.

178. Kulagin, L. V., and S. S. Okhotnikov. Vliyaniye kachestva raspylivaniya tyazhelykh zhidkikh topliv na rabotu kamer sgoraniya transportnykh GTU (Effect of Atomization Efficiency of Heavy Liquid Fuels on the Performance of the Combustion Chambers of Transport Gas-Turbine Engines), Coll. "Kotloturbostroeniye," Tr. TsKTI, No. 50, "Gazovyye turbiny," L., 1964.

179. Kulagin, L. V., and S. S. Okhotnikov. Obosnovaniye trebovaniy k kachestvu raspylivaniya zhidkogo topliva v vysokoforsirovannykh topochnykh ustroystvakh (Basis of the Requirements on the Fineness of Dispersion of Liquid Fuel in Highly Boosted Furnace Devices), Coll. "Ratsional'nyye metody szhiganiya zhidkogo topliva i gaza," Transport, 1964.

180. Grigor'ev, P. I. Usovershenstvovannaya besparovaya forsunka "Atom" (Improved Steamless Atomizer "Atom"), Nizhniy Novgorod (year not mentioned).

181. Semenenko, N. A., L. N. Sidel'kovskiy, and V. K. Yurenev. Kotel'nyye ustanovki promyshlennykh predpriyatiy (Boiler Installations of Industrial Enterprises), Gosenergoizdat, 1960.

182. Karabin, A. I. Sovremennyye podgotovki i szhiganiya mazuta v promyshlennykh ustanovkakh (Modern Preparation and Combustion of Petroleum Residue in Industrial Installations), Izd. Kievskogo universiteta, 1962.

183. Andreev, I. K. Mnogosopel'nyye i kombinirovannyye mazutnyye mekhanicheksiye forsunki bol'shoy proizvoditel'nosti (Multi-nozzle and Combined Mechanical Petroleum Residue Atomizers with High Output), Energetik, No. 4, 1962.

184. Energetika za rubezhom. Pyleugolnyye i mazutnyye topki (Power Engineering Abroad. Coaldust and Petroleum Type Furnaces), Gosenergoizdat, 1961.

185. Alekseyev, A. V., and N. M. Kondak. Tsentrobezhnyye forsunki gazoturbinnykh dvigateley (Centrifugal Atomizers of Gas-Turbine Engines), Kiev, 1958.

186. Hildebrandt, F. Entwicklungsarbeit am rucklaufregelbaren Öldruckbaren, Freiburger Forschungsheft, A N 215, 1962.

187. Kurochkin, N. N. Kamery goreniya gazoturbinnykh dvigateley (Combustion Chambers of Gas-Turbine Engines), Gosenergoizdat, 1955.

188. Appareil pulverisateur, selecteur de synchronisation des pressions avalamount et des vitesses, lineaire-centrifuge pour bruleur a combustible liguide (G. Goffaem). Belgian Patent, cl. F. 23d, No. 569856.3, 30 June 1961

189. Prakhov, A. M. Issledovaniye raboty kombinirovannoy perepusknoy forsunki (Performance Study on a Combined Bypass Atomizer), Coll. st. No. 20 po regulirovaniyu aviadvigateley, Oborongiz, 1955.

190. Henry, Lanois. Gazovyye turbiny maloy moshchnosti (Low-Power Gas Turbines), Mashgiz, 1958.

191. Gorbatov, A. F. Opyt sozdaniya forsunki dlya kamer ogranichennogo ob'ema (Experience in the Design of Atomizers for Combustion Chambers with Small Volume), Kotloturbostroyeniye, No. 6, 1948.

192. Abramovich, G. N. Prikladnaya gazovaya dinamika, Gostekhizdat, 1953.

193. Berman, L. D. K issledovaniyu raboty tsentrobezhnykh sopel (On the Study of the Performance of Centrifugal Nozzles), Teploenergetika, No. 3, 1955.

194. Klyachko, L. A. K teorii tsentrobezhnoy forsunki (On the Theory of the Centrifugal Atomizer), Teploenergetika, No. 3, 1962.

195. Doumas, M., and R. Laster. Liquid-Film Properties for Centrifugal Spray Nozzles, Chem. End. Rr., Vol. 49, No. 10, 1953.

196. Binnie, A. The Passage of a Perfect Fluid Through a Critical Cross Section or Throat, Proc. Roy. Soc., Vol. 197, No. 1051, 1949.

197. Marschall, W. Atomization and Spray Drying, Chem. Eng. Prog. Monograph., series No. 2, 1954.

198. Zenger, Ye. Smeseobrazovaniye v kamerakh sgoraniya (Mixture Formation in Combustion Chambers), Voprosy raketnoy tekhniki, No. 3, 1953.

199. Tikhonov, V. B. K raschetu tsentrobezhnoy forsunki (On the Calculation of the Centrifugal Atomizer), Izvestiya VUZov, seriya "Aviatsionnaya tekhnika," No. 3, 1958.

200. Talakvadze, V. V. Teoriya i raschet tsentrobezhnoy forsunki (Theory and Calculation of the Centrifugal Atomizer), Teploenergetika, No. 2, 1961.

201. Prakhov, A. M. Issledovaniye i raschet tsentrobenzhnoy forsunki (Research and Calculation of Centrifugal Atomizers), Coll. "Avtomaticheskoye regulirovaniye aviadvigateley," No. 1, Oborongiz, 1959.

202. Blok, A. G., and Ye. S. Kichkina. O koeffitsientakh raskhoda i uglakh konusnosti fakela (On the Throughput Coefficients and Cone Angle of Flames), Teploenergetika, No. 10, 1957.

203. Geller, Z. A., V. I. Ashikhmin, and N. V. Shevchenko. Ispol'zovaniye raspolagaemogo napora v tsentrobezhnykh forsunkakh (Utilization of the Applied Pressure in Centrifugal Atomizers), Teploenergetika, No. 4, 1964.

204. Tsiryul'nikov, L. M., A. D. Gorbanenko, and B. L. Zharkov. O stabil'nosti raskhodnykh kharakteristik tsentrobezhnykh forsunok bol'shoy proizvoditel'nosti (Stability of the Throughput Characteristics of Centrifugal Atomizers with Large Capacity), Teploenergetika, No. 2, 1964.

205. Kulagin, L. V. Opredeleniye ugla fakela pri istechenii topliva iz tsentrobezhnoy forsunki (Determination of the Flame Angle for the Flow of Fuel from a Centrifugal Atomizer), Vestnik Vsesoyuznogo nauchno-issledovatel'skogo instituta zheleznodorozhnogo transporta, No. 2, 1959.

206. Kulagin, L. V. Vliyaniye izmeneniya geometricheskikh razmerov forsunki na tonkost' raspylivaniya (Effect of Variation of the Geometrical Dimensions of an Atomizer on the Fineness of Dispersion of the Fuel), Vestnik Vsesoyuznogo nauchno-issledovatel'skogo instituta zhelezodorozhnogo transporta, No. 7, 1960.

207. Longwell, J. Goreniye zhidkikh i tverdykh topliv (Combustion of Luquid and Solid Fuels), Coll. "Protsessy goreniya," Vol. 2, seriya "Aerodinamika bol'shikh skorostey i reaktivnaya tekhnika," Fizmatgiz, 1961.

208. Kulagin, L. V. Funktsional'naya vzaimozamenyaemost' tsentrobezhnykh forsunok (Functional Interchangeability of Atomizers), Coll. "Vzaimozamenyaemost' i tekhnicheskiye izmereniya v mashinostroeniye," No. 4, Mashinostroeniye, 1964.

209. Kulagin, L. V. Opredeleniye dopuskov na osnovnyye razmery tsentrobezhnykh forsunok (Determination of the Tolerances for the Basic Dimensions of Centrifugal Atomizers), Coll. "Voprosy gazoturbovozostroeniya i transportnoy teploenergetiki," Tr. Vsesoyuznogo nauchno-issledovatel'skogo instituta zheleznodorozhnogo transporta, No. 187, Transzheldorizdat, 1960.

210. Kulagin, L. V. Issledovaniye raboty dvukhonturnykh forsunok (Study of Two-Circuit Atomizer Performance), Teploenergetika, No. 10, 1963.

211. Kulagin, L. V. Issledovaniye raboty dvukhsoplovykh dvukhstupenchatykh forsunik (Study of the Performance of Two-Nozzle, Two-Stage Atomizers), Coll. "Voprosy gazoturbinnoy tyagi," Transzheldorizdat, 1962.

212. Hinre, J., and H. Milborn. Atomization of Lignits by Means of a Rotating Creep, J. Appl. Mech., Vol. 17, No. 2, 1950.

213. Kulagin, L. V., S. S. Okhotnikov, and B. M. Morozov. Vybor ratsional'noy skhemy pneumaticheskoy forsunki (Selection of Efficient Designs of Pneumatic Atomizers), Coll. "Ratsional'nyye metody szhiganiya zhidkogo topliva i prirodnogo gaza," Tr. Vsesoyuznogo nauchno-issledovatel'skogo instituta zhelezodorozhnogo transporta, No. 264, Transport, 1964.

214. Baboshin, V. M. Issledovaniye vliyania coeffitsienta izbytka bezdukha na dlinu fakla emul'sionnykh gorelok (Study of the Effect of the Excess Air Coefficient on the Flame Length of Emulsion Burners), Teploenergetika, No. 10, 1963.

215. Levchenko, P. B. Gorelka dlya szhiganiya mazuta (Burner for Combustion of Petroleum Residue), Coll. "Ogneupory, keramika, kamennoye lit'ye," Tr. Ural'skogo politekhnicheskogo instituta im. Kirova, No. 117, Sverdlovsk, 1962.

216. Kist'yants, L. K., A. N. Poplavskiy, S. S. Okhotnikov, and B. M. Morozov. Konstruktsii forsunok i gorelok dlya nagrevatel'nykh pechey (Designs of Atomizers and Burners for Heating Furnaces), Transzheldorizdat, 1961.

217. Durrant, A. The BJSRA Variable-Throat Burner, J. of the Inst. of Fuel, Vol. 35, No. 259, 1962.

218. Kuhlmann, A. Eine neue Brennform fur Heizol und Kohlenstaub-Feuerungen (A New Burner Nozzle for Fuel Oil and Coal Dust Furnaces), VDI, 93, No. 5, 1956.

219. Kalish, G. G. K voprosu ob ustoychivosti rezhima raboty forsunka (On the Problem of Stable Atomizer Performance), Tr. NATI, No. 40, Mashgiz, 1941.

220. Newton, G. Magnetostriction Oscillator Producing Intense Audible Sounds and Some Effects Obtained, Physis., 3, No. 5, 1932.

221. Mataushek, I. Ultrazvukovaya tekhnika (Ultrasonic Engineering), Metallurgizdat, 1962.

222. Ölfeuerung, No. 10, 1962.

223. Rosenthal, A. Device for Dispensing Liquid Fuel into Combustion Air of Furnaces (US Patent No. 2481620, N'yu-York).

224. Bender, R. Associate Editor Industrial Acoustic Burners Power, The Magazine of Energy Systems Engineering, No. 4, 1963.

225. Lamekin, N. S. Osnovy teorii forsunki dlya zhidkogo topliva s gazovym generatorom (Fundamentals of the Theory of the Atomizer for Liquid Fuel with Gas Generator), Izvestiya VUZov, seriya "Mashinostroyeniye," No. 11, 1960.

226. Popov, A. G. Vliyaniye zvukovykh kolebaniy na goreniye ugleroda (Effect of Sonic Vibrations on the Combustion of Carbon), Teploenergetika, No. 3, 1961.

227. Kubanskiy, P. N. K voprosu o vliyanii ul'trazvuka na protsess goreniya (On the Problem of the Effect of Ultrasound on the Combustion Process), Teploenergetika, No. 1, 1962.

228. Lenard, P. Über Wasserfallelektrizität (On Water Fall Electricity), Ann. Phys., No. 47, 1915.

229. Forschungskonferenz über Verbrennung von destilliertem Heizöl (Research Conference on the Combustion of Distilled Fuel Oil), Die Ölfeuerung, 7, No. 8, 1962.

230. Wobig, A. Brenner für gasförmige oder flüssige Brennstoffe (Burner for Gaseous or Liquid Fuels), (French Patent cl. 24c (F23f), No. 1121762, 9 August 1962).

231. Prandtl, L. Gidroaerodinamika (Hydroaerodynamics), IL, 1949.

232. Mikhaylov, A. I., G. M. Gorbunov, V. V. Borisov, A. A. Kvasnikov, and N. I. Markov. Rabochiy protsess i raschet kamer sgoraniya gazoturbinnykh dvigateley (Performance and Calculation of the Combustion Chambers of Gas-Turbine Engines), Oborongiz, 1959.

233. Idel'chik, I. E. Gidravlicheskiye soprotivleniya (Hydraulic Resistance), Gosenergoizdat, 1954.

234. Kamery sgoraniya gazoturbinnykh ustanovok (Combustion Chambers of Gas-Turbine Power Plants), TsBNTI po avtomatizatsii i mashinostroyeniyu, M., 1963.

235. Kremlevskiy, P. P. Pribory teplovogo kontrolya otechestvennogo porizvodstva (Devices for Temperature Control of Soviet Production), Vol. 1, Raskhodomery (Flowmeters), Narkomtyazhprom (People's Commissariat of Heavy Industry), 1938.

247. Kutovoy, V. A. Issledovaniye melkosti raspylivaniya toplivnoy strui (Study of the Fineness of Dispersion of a Fuel Jet), Symposium No. 2 on Design of Aviation Diesels, Oborongiz, 1949.

248. Gemfris, V. Fizika vozdukha (Physics of Air), ONTI, 1936.

249. Zhitkovskiy, Yu. Yu. Elektronnoye ustroystvo dlya issledovaniya dispersnosti raspylennykh zhidkostey (Electronic Device for the Study of the Degree of Dispersion of Atomized Liquids), Inzhenerno-fizicheskiy zhurnal, Vol. 1, No. 6, 1958.

250. Manson, Benerdzhi, and Etti. Mikrofotograficheskoye issledovaniye raspylivaniya zhidkikh topliv (Microphotographic Study of the Atomization of Liquid Fuels), Voprosy raketnoy tekhniki, No. 4 (34), 1956.

251. Mironov, K. A., and L. I. Shipetin. Teplotekhnicheskiye izmeritel'nyye pribory (Heat Engineering Measuring Devices), Gosenergoizdat, 1961.

252. Sinyakevich, B. G. Pribor dlya avtomaticheskogo opredeleniya khimicheskogo nedozhoga i korrektsiya sootnosheniya toplivo-vozdukh (Device for Automatic Determination of Chemically Incomplete Combustion and for the Correction of the Fuel-Air Ratio), Elektricheskiye stantsii, No. 3, 1963.

253. Saburov, V. I. Opyt ekspluatatsii avtomatiki protsessa goreniya s impul'som O_2 (Experimental Experience in the Operation of Automatic Combustion with O_2 Pulses), Teploenergetika, No. 3, 1964.

254. Vidkov, A. K. Upravleniye rezhimom goreniya gaza i mazuta v krupnykh parovykh kotlyakh (Control of the Combustion Conditions of Gas and Petroleum Residue in Large Steam Boiler Furnaces), Elektricheskiye stantsii, No. 3, 1964.

255. Ignat'ev, V. I., and I. I. Zverev. Osazhdeniye chastits aerozolya na tsilindre (Precipitation of Aerosol Particles on a Cylinder), Inzhenerno-fizicheskiy zhurnal, No. 12, 1960.

256. Gorbanenko, A. D., L. M. Tsiryul'nikov, and G. K. Krasnoselov. O mekhanicheskom nedozhoge zhidkogo topliva v topochnykh kamerakh (On the Mechanically Incomplete Combustion of Liquid Fuel in Furnace Chambers), Elektricheskiye stantsii, No. 10, 1964.

257. Knorre, G. F. Teplovyye raschety po gazovomu analizu (Heat Calculations Based on Gas Analysis), Gosenergoizdat, 1947.

UNCLASSIFIED

Security Classification

DOCUMENT CONTROL DATA - R & D

(Security classification of title, body of abstract and indexing annotation must be entered when the overall report is classified)

ORIGINATING ACTIVITY (Corporate author)	2a. REPORT SECURITY CLASSIFICATION
Foreign Technology Division Air Force Systems Command U. S. Air Force	UNCLASSIFIED
	2b. GROUP

REPORT TITLE

COMBUSTION OF HEAVY LIQUID FUELS

DESCRIPTIVE NOTES (Type of report and inclusive dates)

Translation

AUTHOR(S) (First name, middle initial, last name)

Kulagin, L. V. and Okhotnikov, S. S.

REPORT DATE	7a. TOTAL NO. OF PAGES	7b. NO. OF REFS
1967	279	257

8. CONTRACT OR GRANT NO.	9a. ORIGINATOR'S REPORT NUMBER(S)
F33657-68-D-0865 P002	
b. PROJECT NO. 60401	FTD-HT-23-927-68
c.	9b. OTHER REPORT NO(S) (Any other numbers that may be assigned this report)
d.	

10. DISTRIBUTION STATEMENT

Distribution of this document is unlimited. It may be released to the Clearinghouse, Department of Commerce, for sale to the general public.

11. SUPPLEMENTARY NOTES	12. SPONSORING MILITARY ACTIVITY
	Foreign Technology Division Wright-Patterson AFB, Ohio

13. ABSTRACT

This book is intended for the engineers working in the field of liquid-fuel combustion control and also for advance students in related courses of study. The fundamental laws governing liquid-fuel atomization and combustion are discussed and optimal combustion conditions are analyzed. The combustion characteristics of individual fuel droplets, as functions of the external conditions and fuel properties, the droplet combustion process in a flame length and the quality of atomization are examined. In addition, atomization quality is covered, and nozzle systems and the construction of nozzles are analyzed. Methods of designing centrifugal and pneumatic nozzles, and methods of controlling atomization fineness and the quality of the combustion process are also offered. N. I. Belokon', Ye. M. Yudayeva, B. M. Morozov, E. R. Tozha, N. D. Rybchnekov, A. P. Koroleva.

DD FORM 1 NOV 65 1473

UNCLASSIFIED

Security Classification

14. KEY WORDS	LINK A		LINK B		LINK C	
	ROLE	WT	ROLE	WT	ROLE	WT
Combustion Control Droplet Atomization Fuel Combustion Fuel Nozzle Liquid Fuel Nozzle Design						